Purdue University
Purdue e-Pubs

Open Access Dissertations | Theses and Dissertations

Spring 2015

A hydroclimatic assessment of the U.S. corn belt across spatial and temporal scales

Olivia B. Kellner
Purdue University

Follow this and additional works at: https://docs.lib.purdue.edu/open_access_dissertations

 Part of the Meteorology Commons

Recommended Citation
Kellner, Olivia B., "A hydroclimatic assessment of the U.S. corn belt across spatial and temporal scales" (2015). *Open Access Dissertations*. 483.
https://docs.lib.purdue.edu/open_access_dissertations/483

This document has been made available through Purdue e-Pubs, a service of the Purdue University Libraries. Please contact epubs@purdue.edu for additional information.

Graduate School Form 30
Updated 1/15/2015

PURDUE UNIVERSITY
GRADUATE SCHOOL
Thesis/Dissertation Acceptance

This is to certify that the thesis/dissertation prepared

By Olivia B. Kellner

Entitled

A HYDROCLIMATIC ASSESSMENT OF THE U.S. CORN BELT ACROSS SPATIAL AND TEMPORAL SCALES

For the degree of Doctor of Philosophy

Is approved by the final examining committee:

Ernest Agee

Dev Niyogi

Jonathan Harbor

Harshvardhan

To the best of my knowledge and as understood by the student in the Thesis/Dissertation Agreement, Publication Delay, and Certification Disclaimer (Graduate School Form 32), this thesis/dissertation adheres to the provisions of Purdue University's "Policy of Integrity in Research" and the use of copyright material.

Approved by Major Professor(s): Dev Niyogi

Approved by: Indrajeet Chaubey 4/7/2015

Head of the Departmental Graduate Program Date

A HYDROCLIMATIC ASSESSMENT OF THE U.S. CORN BELT ACROSS SPATIAL AND TEMPORAL SCALES

A Dissertation

Submitted to the Faculty

of

Purdue University

by

Olivia B. Kellner

In Partial Fulfillment of the

Requirements for the Degree

of

Doctor of Philosophy

May 2015

Purdue University

West Lafayette, Indiana

This dissertation is dedicated to my family: my father John, my mother Marcia, and my sister, Michelle. Additionally, I dedicate it to those who believed in me and my capabilities that I failed to see in myself through the years as I pursued my degrees in meteorology. The encouragement from these individuals, David L. Arnold and Daniel J. McMahon, kept me moving forward.

ACKNOWLEDGEMENTS

I would like to acknowledge the support of my committee members: Dev Niyogi, Ernest Agee, Jonathon Harbor, Daniel McCarthy, and Harshvardhan. Without their collaboration and encouragement this task would have been much more difficult and arduous. Further acknowledgement to supporting grants is provided at the end of each chapter.

TABLE OF CONTENTS

Page

Page

Page

Page

Page

Page

LIST OF TABLES

LIST OF FIGURES

Figure Page

Figure Page

Figure Page

ABSTRACT

Kellner, Olivia B. Ph.D., Purdue University, May 2015. A Hydroclimatic Assessment of the U.S. Corn Belt across Spatial and Temporal Scales. Major Professor: Dev Niyogi.

The term hydroclimate is used to describe the climate of a given location as determined by the incident radiant energy (temperature) and the existence of water in its various forms on Earth. Two types of climate comprise the science of hydroclimatology: the climate as established by general global circulation patterns at specific locations on Earth (large-scale climate) and the climate established at Earth's surface resulting from the daily fluxes of radiant energy and water in its various forms between the atmosphere, Earth's surface, and the subsurface (local-scale climate) (Shelton 2009). This dissertation investigates different spatial and temporal scales of the U.S. Corn Belt hydroclimate and includes analysis of large- and local-scale hydroclimatic feedbacks. Large-scale hydroclimate research in this assessment investigates how general circulation patterns and teleconnections, specifically the El Niño-Southern Oscillation and the Arctic Oscillation, influence climate variability in the form of temperature and precipitation patterns across the U.S. Corn Belt with findings applicable to agricultural decision making. A large- and local-scale hydroclimatic assessment examines the rainfall contribution of land-falling tropical cyclones to the Eastern U.S. Corn Belt. Locale-scale hydroclimate research considers the role of land-surface feedbacks in the life cycle of land-falling tropical cyclones. Results from the assessments that comprise this dissertation show that the spatial and temporal scales at which hydroclimatic feedbacks are examined are important to the understanding of hydroclimate system interactions. It is suggested from the results of this comprehensive assessment that the newly identified, large- and local-scale hydroclimatic feedbacks be given stronger consideration in

forecasts and climate projection models. Additionally, it is suggested that more hydroclimate assessments across spatial and temporal scales be completed to better prepare for and mitigate the effects of projected climate variability and climate change. A framework for climatological applications to agronomy is discussed in the first chapter, with the findings of the hydroclimatological assessments in subsequent chapters primarily applied to agronomic decision making.

CHAPTER 1. INTRODUCTION

Scientific investigation of the U.S. Corn Belt hydroclimate using historical, observed climate data, as well as use of numerical weather prediction models, allows for hydroclimatic relationships across spatial and temporal scales to be better understood by climate scientists. A deeper understanding of hydroclimatic relationships across the U.S. Corn Belt is identified in the following chapters and appendices through scientific investigation inclusive of climate variability, natural change, and anthropogenic influences. The deeper understanding of hydroclimatic relationships found by these studies provides climate scientist with better adaptive and mitigative strategies to intervene in the current course of history that looks to place Earth in a more hydroclimatologically volatile state. The goal of this hydroclimatic assessment of the U.S. Corn Belt is to obtain a better understanding of hydroclimatic relationships across spatial and temporal scales that primarily result from climate variability, and apply the findings to agronomic decision making. Additional results are found to be applicable to tropical cyclone forecasting with the goal to improve inland tropical cyclone forecasts.

Hydroclimatology is a complex science. It is the combination of weather, climate, and hydrology, and to understand the importance of hydroclimatological research and its applications, a brief summary of hydroclimatology is provided in the remaining sections of Chapter 1. Hydroclimatic assessments of different spatial and temporal scales across the U.S. Corn Belt are provided in subsequent chapters.

1.1 Weather and Climate

Each day at different locations around the world weather occurs. The “average” weather conditions the world experiences through time is defined as climate. Weather

and climate conditions determine the clothing people wear, agricultural production and food supplies, energy demand, ease of transportation, recreational activities, and ultimately influence the establishment of societies and economies. Weather is the immediate state of the atmosphere at a given time and place, and includes variables such as wind, temperature, precipitation, pressure, sky cover, and atmospheric phenomena. Weather is responsible for billions of dollars in damages to buildings and infrastructure each year often as the result of extreme climate events such as droughts, floods, record snowfall events, highly active hurricane or wildfire seasons, and tornado outbreaks (Smith and Katz 2013). Through time, weather and extreme weather events culminate to define a location or region's climate. The hydroclimatological analysis across spatial and temporal scales in this dissertation will investigate hydroclimatic relationships and interactions primarily affecting the agriculture industry, with a secondary focus on land-surface interactions driven by climatologically anomalous environments.

The most commonly observed weather variables that meteorologists and climatologists collect to monitor changes in weather and climate are precipitation: hourly, daily, and monthly; and temperature: daily average, maximum, and minimum for the 24-hour day, the month, season, and year (e.g. Georgakakos et al., 1995; Dessler 2012). Additional variables include insolent solar radiation, cloud cover, snowfall, snow depth, rain free days, sunshine hours, wind speed, and direction (Kellner and Niyogi 2014).

Climate is most commonly defined by a region's observed temperature and precipitation patterns across monthly, seasonal, and annual time scales (Dessler 2012) which are common climatological parameters of hydroclimate investigations (e.g. Grundstein and Bentley 2001). Climate classification systems (e.g. Köppen Climate Classification and Holdridge Life Zone System) have been developed over time and applied around the world to better understand weather and climate systems (Kellner and Niyogi 2014).

While primarily defined by temperature and precipitation, a climate system is highly complex. The phase change of water (precipitation in its varying forms) stores or releases heat energy obtained from solar radiation in the climate system and across subsystems. Temperature influences the rate of evapotranspiration by determining how

much water air can hold in vapor form. The relationship between temperature and saturation vapor pressure of water determines when the phase change of water vapor to water occurs, leading to precipitation in various forms (Oke 1987; Stull 1988; Shelton 2009). With a greater understanding of moisture and energy fluxes across spatial and temporal scales of climate systems having been obtained in recent decades with the use of remotely-sensed technologies (Kellner and Niyogi 2014), evapotranspiration and soil moisture values are considered additional primary variables in hydroclimatological analysis (e.g. Georgakakos et al., 1995, Cayan and Georgakakos 1995; and Grundstein and Bentley 2001).

1.2 Large and Local Scale Climate

Due to its complex physical and thermodynamic nature, climate is referred to as large-scale climate or local-scale climate. The two types of climate are sometimes referred to as climate of the first kind and climate of the second kind (e.g. Shelton 2009). Large-scale climate focuses on weather and temperature patterns as established by general atmospheric circulation (i.e. Hadley, Ferrel, and Polar cells and jet streams). General atmospheric circulation is driven by the transmission, absorption, and reflection of solar radiation through Earth's atmosphere that strikes Earth's surface at different angles and intensity depending on latitude. Due to uneven surface heating, temperature gradients develop within circulation cells leading to the generation of jet streams as defined by the hypsometric equation and thermal wind relationships (e.g. Holton 2004). Jet streams can be influenced by large-scale topographic features such as the Rocky Mountains (Holton 2004), and serve as steering currents for storm systems helping to further establish temperature and rainfall regimes around the globe. Large-scale energy and moisture fluxes such as those seen with airmass movement are further embedded within general atmospheric circulation cells and jet streams.

Local-scale climate is viewed separately from general atmospheric circulation patterns and primarily driven by the daily fluxes of heat and moisture between the overlying atmosphere (the planetary boundary layer), the land surface, and subsurface (i.e. surface and subsurface hydrology) (Shelton 2009). Local-scale serves as the foundation

of the science of hydroclimatology. Local-scale climate is a merger of meteorological and hydrological processes that govern climate at Earth's surface (e.g. Cayan and Georgakakos 1995; Georgakakos et al., 1995; Shelton 2009). While surface runoff/overland flow, streams, rivers, reservoirs, and lakes are a large component of hydrology, they are not reviewed or researched in detail in this dissertation. While local-scale climate is considered the foundation of hydroclimatology, it is large-scale climate that establishes local-scale climates around the world. Thus, local-scale climate cannot be reviewed without considering large-scale climatic influences on the local-climate system.

1.3 Climate, Climate Variability, and Climate Change

The weather patterns that defined a region's climate are relatively constant when observed across large time frames (e.g. hundreds of years), but a climate system does experience episodes of climate variability (Dessler 2012; Shelton 2009). A climate system can undergo a systematic change (i.e. climate change) which influences the base-state of the climate system and shifts the annual balance of temperature and precipitation (e.g. warmer/colder or wetter/drier) in a direction different than previously established (Glickman 2000a), or a climate system can experience episodes of climate variability. Climate variability and climate change result from different physical processes in the Earth-atmosphere system, but are most commonly caused by natural processes of the Earth-atmosphere system and anthropogenic drivers, respectively. Climate variability occurs in a given climate when higher than normal or lower than normal temperature or precipitation patterns occur as a result of variability in atmospheric circulation patterns (i.e. teleconnections), leading to climatologically anomalous conditions. However, despite the occurrence of these extreme conditions, when averaged through time, a systematic change in the climate system does not occur. Recalling the definition above, climate change is defined as a systematic shift in temperature or precipitation patterns established as normal by the previous climate system resulting in a new average base state (Dessler 2012; Glickman 2000a).

1.3.1 Causes of Climate Variability and Change

1.3.1.1 Climate "Normal"

To better track and understand the possible natural and anthropogenic drivers of climate variability and change, the variable "climate normal" was developed to serve as a metric to which current weather conditions and observations are compared. Climate normals are most commonly the average value of a given climate variable over a 30-year period of record. Thirty years is the time frame chosen for climate normal computation because it is considered long enough to capture systematic changes in the "noise" of the atmospheric system found across shorter time scales, but is not a long enough time frame to smooth out decadal changes in climate (WMO 2014). Quality control efforts in the form of algorithms to account for possible observational errors or to adjust for measurements being reported at different times during the day have been implemented in recent decades (Durre et al., 2010). The climate normal is used to determine whether climate variability or climate change is occurring, and once climate variability or climate change processes are identified, climate scientists seek to identify the drivers of climate variability or change.

1.3.1.2 Physical Drivers of a Climate System

Physical drivers of a climate system are natural processes occurring within the Earth-atmosphere system or result from human (i.e. anthropogenic) interactions with the climate system. Natural drivers of variability and change in a climate system include teleconnection patterns, solar cycles, eccentricity and tilt of the Earth on its axis, volcanic eruptions, natural aerosols such as seas spray from the ocean surface, pollens, or volcanic ash, and fluctuations in the amount of water vapor in the atmosphere. Anthropogenic drivers of climate variability and change include greenhouse gas (GHG) emissions, combustion of fossil fuels such as coal and oil for energy, land use change (e.g. urban sprawl, deforestation), aerosols resulting from factory emissions and vehicle exhaust, and socio-economic drivers such as governmental policy related to the burning of fossil fuels or deforestation for agriculture (Dessler 2012; Melillo et al., 2014; Robinson and Henderson-Sellers 1999; Shelton 2009).

1.3.2 The Climate System

A system is defined as a regularly interacting or interdependent group of items that form a unified whole (Merriam-Webster 2014). In this case, a climate system (the unified whole) is comprised of numerous geophysical spheres of science (components forming the unified whole): the hydrosphere (surface and subsurface hydrology), the atmosphere, the lithosphere (soils, rocks, and topography), the biosphere (vegetation, biota, and human life), and the cryosphere (frozen water/ice which impact surface albedo) (Shelton 2009). Each of these spheres is itself a separate physical system, but each system is linked to one or more of the others systems through the common molecule of water. Water passes through each of these subsystems in a climate system in its various physical forms: solid, liquid, or gas. As previously mentioned, the phase change of water through climate systems is a result of solar radiation. Solar radiation is the primary driver of the phase changes of water within and between these systems, and is the primary driver of convective transport across spatial and temporal scales (Shelton 2009; Dessler 2012).

1.3.2.1 Radiation and Earth's Energy Balance

The sun emits black body radiation in various wavelengths that strike Earth providing heat to the Earth's surface and atmosphere through visible and non-visible wavelengths of energy. The amount of solar radiation entering the Earth-atmosphere system has been relatively constant through time with observations of approximately 1367 W/m^2 at the top of the atmosphere and 287 W/m^2 on average at Earth's surface (Oke 1987; Stull 1988). However, values of incident solar radiation and the amount of it absorbed at the surface can vary at a given location based on cloud cover, latitude and longitude, land cover type, and surface albedo (Farmer and Cook, 2013; Oke 1987; Robinson and Henderson-Sellers 1999; Stull 1988). On a given day or even over a season, Earth's radiation budget is typically not balanced. This results in uneven heating of Earth's surface initiating and driving convective processes (Farmer and Cook, 2013; Oke 1987; Shelton 2009; Stull 1988). The study of radiation-driven water movement through the atmosphere and the hydrosphere (and its terrestrial components of overland

flow, runoff, rivers, streams, and subsurface water flow) comprises the study of hydroclimatology (Shelton 2009). Subsystems of the hydrosphere and atmosphere are further linked by energy exchanges and moisture fluxes through Earth's surface and subsurface (i.e. the lithosphere) (e.g. Georgakakos et al., 1995).

1.3.2.2 Climate System Interactions

While the term "climate system" is singular, hundreds of climate systems exist globally spanning different spatial and temporal scales (Farmer and Cook, 2013; Shelton 2009). A climate system(s) can be part of a larger climate system. The Earth's climate system is considered a closed system, but climate systems spanning different spatial and temporal scales on Earth are open systems that regularly interact with each other. An example of an open climate system is the local urban climate established by the city of Indianapolis. The urban climate of Indianapolis contributes towards the state of Indiana's overall climate because its daily temperature and precipitation are used in calculations for state seasonal and annual climate normals. Expanding to an even larger spatial extent, Indiana's climate contributes to the overall climate of the Midwest United States.

1.3.2.3 Spatial and Temporal Scales of Climate Systems

The spatial and temporal scales of meteorology readily apply to the field of hydroclimatology (Shelton 2009). Meteorological spatial and temporal scales include the microscale, the mesoscale, the synoptic scale, and the planetary scale (Orlanski 1975). The microscale ranges from less than one meter to one kilometer (km) and temporally encompasses phenomena that last seconds to minutes. Weather phenomena at the microscale include turbulent eddies and boundary layer phenomena. The mesoscale spatially ranges from one km to tens of kms (up to 100 km) and includes weather phenomena lasting several minutes to hours (thunderstorms and tornadoes). The synoptic scale includes weather systems such as low-pressure systems that span 100 km to 1000 kms and last several days to a week. The planetary scale includes those atmospheric processes that span spatial scales of 1000s of kms and last several weeks to months. The strength and orientation of the jet stream(s) as a series of troughs and waves are examples

of the planetary scale (Orlanski 1975). The translation of the spatial and temporal scales of meteorology to that of applied hydroclimatology is not overly complex.

Microclimates are climates such as those that exist on the surface of a leaf or around the body of an animal and changes in temperature and moisture are monitored over seconds to minutes. Mesoscale climates are typically captured by average daily maximum and minimum temperatures, precipitation, and hours of sunlight. Spatially, mesoscales climates would span several counties in a state (i.e. roughly 50-100 square miles). The mesoscale also includes the daily radiation balance of incoming (K↓) and outgoing shortwave (K↑) radiation (via scattering, reflection from clouds) and incoming (L↓) (via backscattering, reflection, or absorption and reemission from clouds) and outgoing (L↑) longwave radiation between the Earth's surface and the atmosphere (quantified by the equation: $R_n = K\downarrow - K\uparrow + L\downarrow - L\uparrow$). The daily radiation balance between the surface and the atmosphere is inclusive of energy and moisture fluxes such as latent heat (LE), sensible heat (H), and ground heat flux (G) and is quantified by the equation $R_n = LE + H + G$ (Farmer and Cook, 2013; Oke 1987; Stull 1988). In regards to the hydroclimate, atmospheric phenomena such as tornadoes, sea-breeze fronts, and atmospheric boundaries within the boundary layer (their return frequency, intensity, and duration) are part of mesoscale hydroclimate system (Shelton 2009).

Synoptic scale hydroclimatology encompasses weather and climatic processes across spatial scales of several hundred miles and includes high and low pressure systems, hurricanes, and monsoons and the associated climatological rainfall established by the recurrence of these atmospheric phenomena in a given area. Hydroclimatological averages of temperature and precipitation spanning several weeks to months and seasons bridges the gap between the synoptic and planetary scales in hydroclimatology. Drought resulting from prolonged atmospheric ridging results in warmer than normal surface temperatures because of minimal cloud cover, increased sensible heat flux, and little evapotranspiration. This scenario is a prime example of synoptic and planetary scale hydroclimatology interacting with each other.

The jet stream is the primary atmospheric component of the planetary scale of hydroclimatology, and it is the main driver of climate variability. The strength and

orientation of the jet stream results from global temperature gradients and from teleconnection patterns. Teleconnections further influence temperature and precipitation regimes of locations downstream (e.g. Cayan and Georgakakos 1995; Robinson and Henderson-Sellers 1999). Teleconnections are identified weather phenomena occurring in parts of the world separated by large distances that influence weather elsewhere (Glickman 2000b). Examples include the El Niño Southern Oscillation, Pacific North American pattern, the North Atlantic Oscillation, and the Madden-Julian Oscillation (Shelton 2009; Robinson and Henderson-Sellers 1999). Climate change will occur over the time span of years, thus is not part of the meteorological spatial and temporal classification scheme. However, how hydroclimatological parameters change at the different spatial and temporal scales through time helps determine if climate change is occurring (Dessler 2012; Shelton 2009).

1.3.3 Climate System Components and Interactions

Climate systems interact with each other across all five spheres through sub-system interactions that vary spatially and temporally (Shelton 2009). Because each of the five spheres encompasses the movement of energy, mass, and momentum through them via various processes, a climate system is a highly intricate. The lithosphere moderates the flow of water on and through the land surface, which either recharges ground water or is utilized by vegetation. Vegetation is a representation of the biosphere, which transpires, releasing water vapor back into the atmosphere. The flow of water over the land surface, through the land surface into the ground, and back into the atmosphere encompasses the hydrosphere. All of these cyclical processes are driven by solar radiation that in addition to those moderators of solar radiation previously discussed, is also impacted by the cryosphere. Ice and snow cover, glaciers, sea ice, and permafrost all play a large role in planetary albedo and Earth's radiation balance (Farmer and Cook, 2013; Shelton 2009).

1.3.3.1 Large-scale Climate: General Atmospheric Circulation

As previously discussed, climate systems and associated subsystems interact with each other across spatial and temporal scales. General atmospheric circulation is driven

by the Hadley, Ferrel, and Polar circulation cells, which result from the uneven distribution of solar radiation and subsequent heating of the atmosphere across Earth's surface. Landmass location (northern vs. southern hemisphere), landmass size, surrounding ocean size, and different angles at which solar radiation strikes Earth's surface result in convection currents that drive circulation from the tropics (regions of excess heat) to the poles (regions that are heat deficient). Between these convectively driven circulation cells, jet streams form due to the presence of baroclinicity (sharp contrasts in temperature and moisture between circulation cells) as described by the thermal wind and the hypsometric equation. Earth's rotation on its axis further contributes to the evolution of general atmospheric circulation patterns as it leads to the formation of planetary wave features embedded within jet streams.

1.3.3.2 Local-scale Climate: Land Surface Interactions

Land surface interactions are documented across spatial and temporal scales, with larger spatial scale land surface interactions being able to influence large-scale climate (i.e. atmospheric flow and circulation). Vegetated land surfaces are often cooler and more humid than a bare soil land surfaces. The different temperature and moisture properties of these land surface types impacts the structure of the planetary boundary layer (PBL) which can further impact atmospheric processes in the PBL (Oke 1987; Stull 1988). An example of land surface interactions at large spatial scales is the general understanding (as established through years of research) that sufficient rainfall (occurring on mesoscale to synoptic scales) over time and space results in cooler and wetter ambient conditions while drier conditions over time and space (mesoscale to synoptic scale) result in a feedback of drier, hotter conditions which can lead to drought (e.g. Wolfson et al., 1987; Georgakakos et al., 1995; Grundstein and Bentley 2001; Pal and Eltahir 2003). It has been recognized that prolonged drought of large spatial extent can contribute to intensified high pressure systems and shifts in the jet stream (planetary scale), manifesting into the established large-scale climate (e.g. Pal and Eltahir 2003). Detailed discussion of land surface interactions at more finite spatial and temporal scales is in the following sections.

1.3.3.3 Large- and Local-scale Climate Merger

In addition to land surface interactions at larger spatial scales, as just discussed, a simple example of how large-scale and local-scale climate merge is exemplified by coastal climates. Because land has a lower heat capacity than water, the land surface heats faster during the day (greater sensible heat flux) than ocean waters which results in a sea breeze (winds move from the ocean towards inland). At night, once the land surface cools (sensible heat flux becomes lower than that over the ocean), the ocean is now warmer than the land due to water's high heat capacity and a land breeze is generated. The moderation of ocean temperatures occurs over weeks to months, while the daily radiation balance impacts land temperature over several hours (Farmer and Cook, 2013; Robinson and Henderson-Sellers 1999; Shelton 2009). This relationship between land and water is why coastal climates are often described as moderate climates. Coastal climates experience variation in a 24-hour period but experience little variation over long time frames. Specific types of coastal climates, such as the Mediterranean climate, are a result of local scale coastal climates being influenced by the general circulation established by the Ferrell circulation cells and the Westerlies (large-scale climate).

1.3.3.4 Climate System Land Surface Components

The feedbacks between climate systems and sub-systems are determined by solar radiation and land surface properties that govern the surface radiation balance. Such land surface properties include vegetation type, height, and density, topography, soil type and associated hydraulic and thermodynamic properties, and albedo. All of these factors influence the transfer of heat, moisture, and momentum between the atmosphere, the land surface, and the sub surface (Farmer and Cook, 2013; Oke 1987; Shelton 2009; Stull 1988). The dynamic interactions of heat and moisture through the land surface are ultimately governed by the state of soils, making a soil's hydraulic and thermodynamic characteristics one of the primary hydroclimatological parameters driving local-scale climate (e.g. Georgakakos and et al., 1995), and at large enough spatial and temporal scales, large-scale climates as previously discussed.

1.3.3.4.1 Vegetation

Vegetation is part of the biosphere in the climate system model and is a characteristic and a component of the Earth's land surface. Vegetation is important to climate systems in that it absorbs radiation to use for photosynthesis and releases moisture in the form of water vapor as it transpires to prevent overheating. Transpiration releases water vapor into the overlying atmosphere, cooling temperatures and raising the moisture content of air. Vegetation is also reflective to certain wavelengths of radiation, and vegetation disturbs surface air flow, contributing to the evolution of turbulent eddies. Vegetation density (amount of vegetation per unit area) can affect how much water vapor is released in a given area, how much radiation is absorbed or reflected, and effects how much rainfall reaches the soil. Vegetation stands with a thick canopy will not allow rainfall to reach soils while a less dense canopy allows for rainfall to hit the surface, infiltrate and percolate through the soil to feed plants or recharge the ground water (Oke 1987; Noilhan and Planton 1989; Shelton 2009).

1.3.3.4.2 Topography

Topography is a word used to describe the height, shape, and slope of the land surface and is part of the lithosphere. Mountains and valleys are types of topography and all topography can influence climate. Mountains moderate airflow, result in orographic lift and subsequent rainfall and rain shadow regions, and depending on axial orientation, strongly influence the surface energy balance (Farmer and Cook 2013; Robinson and Henderson-Sellers 1999; Shelton 2009). A mountain range that runs north to south will heat up early in the morning on the east facing slopes driving convective over-turning in the boundary layer nearby. Valleys are typically cooler than mountains and hold larger amounts of moisture due to a decrease in direct solar radiation and subsequent evapotranspiration. Valleys also channel airflow and are common sources of valley winds.

1.3.3.4.3 Soils

Also part of the lithosphere, soils are a crucial component in understanding the behaviors of the hydrosphere and atmosphere. Soil properties such as texture, porosity,

permeability, thermal properties such as heat capacity, conductivity, and thermal diffusivity strongly influence how solar radiation and moisture are transferred between the land surface and atmosphere which influences evapotranspiration, conduction, and convection rates. Additionally, these properties influence the amount of soil moisture recharge, rate of water infiltration, and surface runoff (Oke 1987; Chow et al., 1988; Stull 1988).

Soil texture describes the size of the soil grain and is most commonly classified as sands (coarsest), silts, or clays (finest). Porosity describes the open space between soil particles which is determined by soil texture. Porosity determines the rate of water infiltration at the land surface and also determines ground water movement. Permeability describes how fast water moves through a type of soil. Those soils with high porosity (large pore spaces) are good hydraulic conductors.

Thermal properties of soil such as heat capacity, thermal conductivity, and thermal diffusivity determine how fast radiative heat is transferred through soil (Chow et al., 1988; Shelton 2009). Soil heat capacity is a function of the mineral organic content (what the soil particle is made of) and water content of the soil. Sand has the highest heat capacity while clay has the lowest heat capacity. Thermal conductivity of soils is a function of soil texture (particle size) and moisture. Thermal conductivity has different relationships for each soil type; however, most soils follow an exponential increase in thermal conductivity based on soil volumetric water content. Sand has the highest thermal conductivity and clay has the lowest. Thermal diffusivity of soils describes the rate of transfer of heat through the soil medium (or rate of ground heat flux) (Chow et al., 1988). How fast heat is transferred to and from the soil can impact vegetation growth (such as with corn), and if the land surface is bare, how fast the atmospheric boundary layer becomes unstable due to a high sensible heat flux. While hydraulic and thermal characteristics of soil can be considered a separate subsystem within the hydrologic cycle, soils have a large influence on vegetation (the biosphere) and the overlying atmospheric profile, and further interaction with the atmosphere and hydrosphere can occur (e.g. Grundstein and Bentley 2001).

1.3.3.4.4 Albedo

Albedo is the term used to describe the ratio of total incoming solar radiation to the amount of radiation that is reflected back the atmosphere (Dessler 2012; Oke 1987; Stull 1988). Simply stated albedo is essentially Earth's reflectivity. Albedo is largely determined by characteristics of the surface struck by solar radiation. Atmospheric radiation is transmitted through the atmosphere whereupon striking a cloud or the land surface, it can be further transmitted, reflected, scattered, or absorbed (Dessler 2012; Oke 1987; Stull 1988). Scattering and absorption are properties of albedo (reflection), as a surface with a high albedo will act to reflect and scatter the solar radiation further whereas surfaces with low albedo will absorb the solar radiation and retain that energy as heat. Albedo thus plays a direct role in the partitioning of heat fluxes at the land surface. Clouds can be highly reflective based on their composition or may absorb solar radiation (Dessler 2012; Oke 1987; Stull 1988). Land surface types such as concrete, granite, limestone, light-colored soils such as white sand, and water have a high albedo. Low albedo surfaces include asphalt, red and brown brick, and dark, wet soils with high organic content (Oke 1987; Lobell and Asner 2002). Vegetation primarily has lower albedos ranging from 10% to 30% because it absorbs solar radiation for photosynthetic processes (Oke 1987, Ahrens, 2006).

1.3.3.4.5 Land Surface Interactions

The intricate study of heat, moisture, and momentum fluxes between the subsurface, the land surface, and the atmosphere nearest to Earth's surface is local-scale climate. Focused study of local-scale climate is referred to land surface interactions, and is a crucial part of hydroclimatology (Shelton 2009). Land surface feedbacks related to meteorological processes such as convection and precipitation may result from discontinuities in land surface type. When the land surface changes from one type to another, such as a forest to open grassland, the differing radiative and moisture balances (sensible and latent heat fluxes) and momentum fluxes (resulting from changes in surface roughness and wind direction and speed) from these surfaces can generate different atmospheric environments above them (e.g. Mahmood et al. 2011) in the PBL that can

lead to the development of non-classical mesoscale circulations such as land-breezes (e.g. Mahfouf et al. 1987; Segal and Arritt 1992) and help trigger convection (Baidya and Avissar 2000; Clark and Arritt 1995; Desai et al. 2006; Pielke 2001). A change in the land surface type across a spatial area is referred to as land surface heterogeneity and is a topic of meteorological and hydroclimatological studies. Soil moisture and albedo can contribute to land surface heterogeneity as well. Large urban areas are often categorized as having their own climate due to high sensible heat fluxes from high albedo surfaces, high thermal conductivity, and low latent heat fluxes due to lack of vegetation (Oke 1987). An urban center in the middle of a vast expanse of agricultural farmland or relatively flat terrain could also serve as an example of land surface heterogeneity.

1.3.4 Hydroclimatology as a Comprehensive Science

Through the discussion of weather, climate, and water laid forth in previous sections, hydroclimatology can be more precisely defined as the science of the cycling of water through the climate system. It incorporates the disciplines of hydrology (surface and sub-surface) and meteorology/climatology into one science to understand the transfer of water between the atmosphere and the land surface as driven by solar radiation, land surface characteristics (vegetation cover and type, land use type, soils, topography, proximity to water bodies, etc.), and atmospheric circulation across spatial and temporal scales of millimeters to kilometers and seconds to weeks (Shelton 2009). Solar radiation drives atmospheric circulation which contributes to local weather patterns and the establishment of local climate systems through time (e.g. Farmer and Cook 2013; Shelton 2009).

1.3.4.1 History

While the earth is 4.6 billion years old, understanding Earth's hydroclimatological past is extremely difficult due to the vast temporal void of weather and climate records chronicled by humans with instrumentation. Efforts for standardized record keeping of weather and climate data began approximately in the last 150 years. This short time frame limits scientific ability to detect changes in hydroclimates. Even with paleoclimate and proxy data sources, human understanding of Earth's hydroclimatological history

remains limited (Farmer and Cook 2013; Shelton 2009). Despite having such a limited climatic dataset, recent scientific developments in instrumentation and computation have advanced understanding of weather and climate. Precision measurement of climate variables at microscale level, the development and use of satellite and remote sensing platforms for enhanced observation, measurement, and assimilation into forecast models, and improvements in numerical weather and climate prediction models has provided for a better understanding of Earth's hydroclimate and the possible future scenarios of Earth's hydroclimate(s) under climate change (Shelton 2009).

1.3.4.2 Future

Weather and climate models are computer programs comprised of numerous algorithms that execute mathematical diagnostic and prognostic differential equations when provided with input data (weather data). Models of this nature are deterministic modeling systems. While forecast accuracy of these systems has improved through time and are currently able to capture past cycles of climate variability (i.e. hind-casting) and forecast near real-time severe weather events, high accuracy of current weather and climate models remains a challenge because weather and climate systems are dynamical, chaotic systems. This leaves levels of uncertainty and unknowns, especially when forecasting future climate scenarios. Despite model uncertainty, global and regional climate models concede that under a warming climate scenario, changes will occur in the spatial and temporal distribution of rainfall. For the Midlatitudes, rainfall events are expected to become more intense, be of shorter duration, and have longer dry periods between events (IPCC 2014; Melillo et al., 2014). This shift in the hydroclimate has implications to water supplies, storm water runoff drainage systems, urban structures and development, agriculture, and recreation (IPCC 2014; Melillo et al., 2014).

Despite having an understanding of how large-scale and local-scale climate interact with each other, the projected shifts in temperature and precipitation under future climate change scenarios will further impact the environments and behaviors of currently established hydroclimates. Urban sprawl and changes to land use and land cover are additional anthropogenic sources of climate modification to consider in future hydroclimates (IPCC 2014). Urban sprawl and changes in land use or land cover will

introduce new land surfaces possessing different radiative/thermodynamic and hydrodynamic properties. This leads to changes in heat and moisture fluxes between the overlying atmosphere and land surface which can further influence rainfall and convection (IPCC 2014; Shelton 2009). Under such future circumstances/scenarios, climate scientists expect shifts in temperature and precipitation away from climate normals currently established around the world (IPCC 2014). Specifically focusing on the Midlatitudes, temperatures are expected to warm, with overnight low temperatures becoming warmer and daytime high temperatures becoming higher. Projections of precipitation are not as certain as temperatures. However, with warmer air temperatures the amount of water in the atmosphere is expected to increase (Melillo et al., 2014; IPCC 2014). This leads to the consensus of heavier rainfall events with longer dry periods between rainfall events (which have already been documented in parts of the U.S. – e.g. Kunkle et al., 2013).

1.4 Conclusion

Meteorology, climatology, and hydrology are sister sciences, which when analyzed as a comprehensive science, is known as hydroclimatology. Climatology is the science of collecting, analyzing, and interpreting past weather data through spatial and statistical analyses (Glickman 2000c; Shelton 2009) to understand what has occurred in the past, what is currently happening in relation to the past, and what may happen in the future if certain climatological parameters change in time. Meteorology is the science of observing current weather and predicting weather into the future. Hydrology is the science of studying water, which is input into the hydrologic system through weather. As commented by Adolf von Harnack, "We study history in order to intervene in the course of history." This is a statement that encapsulates the purpose of this hydroclimatological assessment of the U.S. Corn Belt across spatial and temporal scales. Through the scientific investigation of the hydroclimate system with historical, observed climate data discussed in the following chapters, thermodynamic and hydrodynamic climate system relationships are better understood across spatial and temporal scales. With a deeper understanding of past and current hydroclimate relationships through detailed

consideration of climate variability, natural change, and anthropogenic influences, climate scientist can provide better adaptive and mitigative strategies to intervene in the current course of history that looks to place Earth in a more hydroclimatologically volatile state.

The following seven chapters investigate hydroclimatological relationships present primarily in the agricultural and agronomic industries. Each chapter begins with an introduction to the hydroclimatological relationship(s), elements, and parameters discussed in that chapter, which is then followed by a comprehensive discussion of the hydroclimatological element at hand. A comprehensive discussion of agroclimatology comprises Chapter Two. Hydroclimatic variability resulting from teleconnections and the associated impacts to historic corn yields is discussed in Chapter Three. The extreme hydroclimate event of drought and its impacts to agricultural production systems in the context of the 2012 drought is examined in Chapter Four. Chapter Five investigates the role of land-falling tropical storm systems to warm season rainfall across the Midwest and the possible use of tropical cyclone forecasts in agricultural planning and mitigation of climate variability. Hydroclimate extremes in the form soil moisture surpluses (wettest seasons on record) and deficits (driest seasons on record or droughts), and the land surface interactions of these anomalous land surface conditions to land-falling tropical storm systems are investigated in Chapter Six using remotely sensed datasets, operational datasets, and numerical weather prediction datasets. A synthesis of findings with future research directions is provided in Chapter Seven.

1.5 References

Ahrens, C.D., 2006: Meteorology today: An introduction to weather, climate, and the environment. Eighth Edition. Belmont: Thompson Learning, Inc. Pp. 608.

Baidya R. S. and R. Avissar, 2000: Scales of response of the convective boundary layer to land-surface heterogeneity. *Geophysics Research Letters*, 27, 533–536.

Cayan, D.R. and K.P. Georgakakos, 1995: Hydroclimatology of continental watersheds: 2. Spatial analyses. *Water Res. Research*, 31.3 677-697.

Chow, V.T., D. Maidment, and L.W. Mays, (1988): Applied Hydrology. New York: McGraw-Hill International Editions. Pp 572.

Clark, C. and P. Arritt, 1995: Numerical simulations of the effect of soil moisture and vegetation cover on the development of deep convection. *Journal of Applied Meteorology,* 34, 2029-2045.

Desai, A. R., K. J. Davis, C. J. Senff, S. Ismail, E.V. Browell, D.R. Stauffer, and B.P. Reen, 2006: Case study on the effects of heterogeneous soil moisture on mesoscale boundary layer structure in the Southern Great Plains. Part I. *Boundary-Layer Meteorology*, 119. 195-238.

Dessler, A.E., 2012: Introduction to climate change. New York: Cambridge University Press. 252pp.

Durre, I., Menne, M.J., Gleason, B.E., Houston, T.G., and Vose, R.S., 2010: Comprehensive Automated Quality Assurance of Daily Surface Observations. *J. Appl. Meteor. Climatol.*, 49, 1615–1633. doi: http://dx.doi.org/10.1175/2010JAMC2375.1.

Farmer, G. and J. Cook, 2013: Climate change science: A modern synthesis. Vol. 1 – The physical climate. Dordrecht: Spring Science and Business Media. 564 pp.

Georgakakos, K.P., D.H. Bae, and D.R. Cayan, 1995: Hydroclimatology of continental watersheds: 1. Temporal analyses. *Water Res. Research*, 31 (3), 655-675.

Grundstein, A.J. and M.L. Bentley, 2001: A growing-season hydroclimatology, focusing on soil moisture deficits for the Ohio Valley region. *J. of Hydrometeor.*, 2, 345-355.

Glickman, T.S., 2000a. "Climate Change": Glossary of Meteorology, 2nd Edition. Boston: American Meteorological Society. 850pp.

Glickman, T.S., 2000b. "Teleconnection": Glossary of Meteorology, 2nd Edition. Boston: American Meteorological Society. 850pp.

Glickman, T.S., 2000c. "Climatology": Glossary of Meteorology, 2nd Edition. Boston: American Meteorological Society. 850pp

Holton, J.R., 2004: An introduction to dynamic meteorology. 4th Edition. Burlington: Elsevier Academic Press. 535pp.

IPCC, 2014: Climate Change 2014: Impacts, Adaptation, and Vulnerability. Part A: Global and Sectoral Aspects. Contribution of Working Group II to the Fifth Assessment Report of the Intergovernmental Panel on Climate Change. Field, C.B., V.R. Barros, D.J. Dokken, K.J. Mach, M.D. Mastrandrea, T.E. Bilir, M. Chatterjee, K.L. Ebi, Y.O. Estrada, R.C. Genova, B. Girma, E.S. Kissel, A.N. Levy, S. MacCracken, P.R. Mastrandrea, and L.L. White (eds.). Cambridge: Cambridge University Press, 1132 pp. http://ipcc-wg2.gov/AR5/images/uploads/WGIIAR5-PartA_FINAL.pdf. (Accessed 20 December 2014.)

Kunkel, K.E., T.R. Karl, H. Brooks, J. Kossin, J.H. Lawrimore, D. Arndt, L. Bosart, D. Changnon, S.L. Cutter, N. Doesken, K. Emanuel, P.Y. Groisman, R.W. Katz, T. Knutson, J. O'Brien, C.J. Paciorek, T.C. Peterson, K. Redmond, D. Robinson, J. Trapp, R. Vose, S. Weaver, M. Wehner, K. Wolter, and D. Wuebbles, 2013: Monitoring and Understanding Trends in Extreme Storms: State of Knowledge. *Bull. Amer. Meteor. Soc.*, 94, 499–514. doi: http://dx.doi.org/10.1175/BAMS-D-11-00262.1

Landsea, C.W., 2014: How many tropical cyclones have there been each year in the Atlantic basin? What years were the greatest and fewest seen? Hurricane Research Division. Atlantic Oceanographic and Meteorological Laboratory. National Oceanic and Atmospheric Administration. 2 May 2014. http://www.aoml.noaa.gov/hrd/tcfaq/E11.html (Accessed 25 September 2014.)

Lobell, D.B. and G.P. Asner, 2002: Moisture effects on soil reflectance. *Soil Science Society of American Journal*, 66, 722-727.

Mahmood, R. A.I. Quintanar, G. Conner, R. Leeper, S. Dobler, R.A. Pielke Sr., A. Beltran-Przekurat, K.G. Hubbard, D. Niyogi, G. Bonan, P. Lawrence, T. Chase, R. McNider, Y. Wu, C. McAlpine, R. Deo, A. Etter, S. Gameda, B. Qian, A.Carleton, J.O. Adegoke, S. Vezhapparambu, S. Asefi, U.S. Nair, E. Sertel, D.R. Legates, R. Hale, O.W. Frauenfeld, A. Watts, M. Shepherd, C. Mitra, V.G. Anantharaj, S. Fall, H.-I. Chang, R. Lund, A. Treviño, P. Blanken, J. Du, and J. Syktus, 2010: Impacts of land use/land cover change on climate and future research priorities. *Bull. Amer. Meteor. Soc.*, 91, 37–46. doi: http://dx.doi.org/10.1175/2009BAMS2769.1.

Melillo, J.M., T.C. Richmond, and G.W. Yohe, Eds., 2014: *Climate Change Impacts in the United States: The Third National Climate Assessment*. U.S. Global Change Research Program, 841 pp. doi:10.7930/J0Z31WJ2.

Merriam-Webster Dictionary, 2014: System. Encyclopedia Britannica Company. http://www.merriam-webster.com/dictionary/system (Accessed 19 September 2014.).

Noilhan, J. and S. Planton, 1989: A simple parameterization of land surface processes for meteorological models. *Mon. Wea. Rev.*, 117, 536-549. doi: http://dx.doi.org/10.1175/1520-0493(1989)117<0536:ASPOLS>2.0.CO;2.

Oke, T.R., 1987: Boundary layer climates. Second Edition. New York: Routledge Press. Pp 435.

Orlanski, I., 1975: A rational subdivision of scales for atmospheric processes. *Bull. Amer. Meteor. Soc.*, 56, 527-530.

Pal, J. and E.A.B. Eltahir, 2003: A feedback mechanism between soil moisture distribution and storm tracks. *Quarterly Journal of the Royale Meteorological Society*, 129, 2279-2297.

Pielke, R.A. Sr., 2001: Influence of the spatial distribution of vegetation and soils on the prediction of cumulus convective rainfall. *Reviews of Geophysics*, 39, 151–177.

Robinson, P.J. and A. Henderson-Sellers, 1999: Contemporary climatology. London: Pearson Education Limited. Pp 352.

Segal, M. and R.W. Arritt, 1992: Non-classical mesoscale circulations caused by surface sensible heat flux gradients. *Bulletin of the American Meteorological Society*, 73, 1593-1604.

Shelton, M.L., 2009: Hydroclimatology: Perspectives and applications. New York: Cambridge University Press. Pp 426.

Smith, A.B. and R.W. Katz, 2013: U.S. billion-dollar weather and climate disasters: data sources, trends, accuracy, and biases

Stull, R., 1988: An introduction to boundary layer meteorology. Kluwer Academic, Pp 666.

Wolfson, N., R. Atlas, and X. Bian, 1987: Numerical experiments related to the summer 1980 heat wave. *Mon. Wea. Rev.*, 115, 1345-1357.

World Meteorological Organization (WMO), 2014: Climate data and data related products. *World Meteorological Organization*, Geneva, Switzerland. http://www.wmo.int/pages/themes/climate/climate_data_and_products.php (Accessed 19 September 2014.)

CHAPTER 2. AGROCLIMATOLOGY

2.1 Introduction

Agriculture is a fundamental component of human societies and economies. The domestication of wild flora and fauna over thousands of years provided a pathway for the development of societies, development of technology, industrialization, and tremendous growth in human population. Agriculture around the world sustains lives and drives global economies. Domesticated plants and animals that comprise agriculture depend on water and temperature for sustainment, to reproduce, and to survive in different climates around the world. Agronomy is the science and technology developed over centuries that is used to produce food (plants and livestock), fuel, and clothing. Agroclimatology is the combined sciences of weather and climate (large-scale and local-scale climates) with agronomy. The research and developed technologies revolving around improved agricultural production in regards to weather (severe storms, blizzards, and hurricanes), climate (changes in the return frequency of severe storms, blizzards, hurricanes), climate variability (increased/decreased magnitude of floods, drought, blizzards and hurricanes), and climate change (shift in the frequency of occurrence in the climate system) are the founding drivers of agroclimatology and its applications. This chapter discusses the history, advancement, and application of agroclimatology over the last approximately 100 years.

2.2 Agroclimatology

Agroclimatology – As Published in Encyclopedia of Natural Resources: Air. Doi: 10.1081-ENRA-120047622**.**

Full Citation: O. Kellner and D. Niyogi, 2014: Agroclimatology. Encyclopedia of Natural Resources: Air. Doi: 10.1081-ENRA-120047622 <http://www.tandfonline.com/doi/full/10.1081/E-ENRA-120047622#.VFKEn_ldXTo>. 2014.

Abstract

This chapter provides a broad introduction to agroclimatology. Agricultural productivity is intricately related to climate and a region's soil types, hydrologic cycle, and meteorology. Because of this, agronomy and climate are disciplines that are linked together in the science of agroclimatology: the applied science of water, soil, and crop management incorporating the knowledge of regional weather and climate information such as precipitation and temperature with an aim to improve crop yields. The interlinked roles of the disciplines of soil science, surface hydrology and the hydrologic cycle, agronomy (i.e., crop management and biomass), and meteorology and climatology on agroclimatology are introduced. A brief history of agroclimatology, discussion of agroclimatology and technologies associated with it today, the importance of agroclimatology, along with the projected path of agroclimatology into the future is discussed.

2.3 Introduction

Agroclimatology can be considered as the study of local climate (determined by water, soil, and radiation in a given area, along with biomass and daily weather) and that local climate's interaction with agriculture and crop production for food, fiber, fuel, and availability of feed for livestock. Agroclimatology can help answer questions such as: how do temperature and precipitation patterns affect agricultural productivity? Agroclimatology can have many foci: climatic influences on crop production, availability of feed for livestock, crop modification to help plants withstand climate extremes, resilience of pests, and sustaining yields in the face of an increasing world population, the

influence of the microscale environment on crop yield, and agroclimatic modeling [1, 2]. An emerging feature of the agroclimatic sciences has seen studies completed to understand the effect of climate change on agriculture, as well as the impact of agriculture on regional climates [3, 4, 5, 6].

2.3.1 Agroclimatology in the Beginning

The relation between world agricultural regions and global climatic patterns is well appreciated. It is also linked to a region's culture with seasonal festivals and events which celebrate the beginning and end of growing seasons. Agroclimatology is a relatively young science rooted in systematic weather observations of temperature and precipitation undertaken by many regional and national weather agencies such as, but not limited to, the United States' National Weather Service, the Met Office of the United Kingdom, and the India Meteorological Department. Large-scale weather and climate events such as the Dust Bowl (~1920s, 1930s, and 1950s) that struck the United States have also contributed to the growth and evolution of agroclimatology as a practical science [1, 2, 7]. Agroclimatology, can however, be traced back to the domestication of native plants in societies that began thousands of years ago with a series of trial and error with local flora. This primitive science of plant domestication sometimes led to the collapse of societies due to weather and climate shifts that led to prolonged drought and crop failures (i.e., Anasazi of North America, the collapse of Polynesian society on Easter Island, and Mesopotamia that spanned modern day Turkey, Syria, Iran, and Iraq) [8] showing the need for a detailed understanding of weather, climate, and food production. Successes in crop domestication through recognition of weather and climate patterns led to the establishment of distinctive crop growing regions such as the Fertile Crescent in the Mediterranean region due to its mild climate, and the U.S. Corn Belt due to its suitable glacial till soils and adequate rains. These two locations are examples of the many suitable crop growing regions around the world where agricultural economies are well rooted.

Regular weather observations began with the development of the telegraph and railroad networks around the world during the Industrial Revolution (mid to late 1800s)

which eventually led to the development of the national weather observation organizations across developed countries that kept record of daily weather data across the country. Daily weather observations were then shared via telegraph allowing for the development of daily weather maps that have grown through the century into the modern weather maps meteorologists and climatologists use today [9]. As meteorology grew in the late 1800s, the development of regional weather climatologies from archived weather data of observed temperature and precipitation around the world began as well [2, 10]. Building from these climatic data sets, climate systems were developed as a practical guide for sustaining flora and fauna. The Köppen Climate System (1918) and the Holdridge Life Zones System (1947) are examples of two climate classification systems that characterize specified regions/climate zones based on temperature and precipitation (Köppen) or on precipitation, potential evapotranspiration, and humidity (Holdridge). These climate systems provide a quick overview of the region's agricultural potential.

2.3.2 Agroclimatology Today

In the early 1920s, the initial step of implementing agroclimatology as a practicing science was made by the United Kingdom Royal Meteorological Society with an expression of the need to study the effect of weather phenomena on crop growth and total yield [7]. Research investigating the impacts between climatic variables and crop yields began with simple regression analysis. These analyses eventually expanded over subsequent decades to simple statistical and empirical crop models by the 1970s and 1980s [1, 2, 7]. The development of remote-sensing technologies after World War II and into the 1970s and 1980s resulted in research programs and instruments capable of direct measurements of soil and moisture fluxes in the field (in situ) without human interference (remotely-sensed data). Microsensors, automated weather stations, and remote-sensing technologies opened up a new dimension of detail in agroclimatology. The collection of meteorological, biophysical, and biogeochemical variables is now available in an unprecedented manner and this data is used to study and develop plant/climatic relationships. Some examples include assessing the effect of nitrogen levels on plant productivity or the effect of leaf area index on evapotranspiration and water demand in

local areas, each of which is used to understand crop sustenance. This has allowed for much more detailed research and discoveries between crops and locally observed weather/climate patterns to take place [1, 2, 11]. Through the 1980s, crop modification, decision support systems and tools, and more detailed research have energized the development of crop models. Availability of observed weather patterns and observed surface data at micro to county-level scales has led to a broader understanding of hydrologic cycles within crop-climate analysis. Today's crop production models can simulate crop physiology and productivity reasonably well and have advanced to incorporate climate change scenarios providing insight to the possible impacts of varying weather and climate conditions on crop yields. In other words, while simple and statistical relations between climatic patterns and crop response continue to be important, there is a growing ability to develop more sophisticated, predictive tools that appear to adequately mimic complex agroclimatic interactions at multiple scales.

Current efforts to improve crop production amidst shifting climate patterns and dynamic economies include the efforts of international research scientists and crop models working in sync on projects such as the Agricultural Model Intercomparison and Improvement Project (AgMIP) and the Decision Support System for Agrotechnology Transfer (DSSAT) [12,13]. Community efforts such as AgMIP consist of specialized teams comprised of experts in agronomy, economics, and climate, devoted to the detailed study of specific crops, collaborating and comparing more than multiple crop-specific (such as maize, wheat, rice, and sugarcane) models for crop response to carbon dioxide (CO_2), temperature, and other environmental factors. The research framework model for such collaborative assessments is to conduct studies at different locations to represent variation in crop production around the world and seek to find answers to questions such as: are models similar when responding to climate forcing parameters such as increased CO_2; is the accuracy of ensemble model prediction better than individual model prediction; and does the detail of input data into the model affect how the model responds? The end goals of such efforts are to increase capacity through new adaptation strategies and methods for major agricultural regions in the developing and developed world. A number of crop models such as DSSAT, which is a compilation of crop simulation

models founded on soil-plant-atmosphere dynamics for more than 28 crops, are now routinely available. The models simulate crop growth when given soil and meteorological input parameters to help assess the impacts of climate variability and change from farm-level to regional agricultural areas (Figure 2.1).

2.3.3 Importance of Agroclimatology

Agroclimatology is important for numerous reasons. Understanding weather and climatic impacts to crops and soils is important in order to feed increasing world populations. It is also important in turn to economic/commodity markets, livestock production (a large majority of livestock feed is developed from corn), and to climatic risk assessment. Agroclimatology also becomes important in cost-benefit analysis when considering irrigation, fertilizers, tile drainage systems, cropping systems, and yield [14].

The United States is the world's largest producer of corn. Extreme climatic events such as the 2012 drought can greatly influence crop production/yield, drastically impact commodity prices, and impact the agricultural sector of the economy. The 2012 drought across a large portion of the United States is a recent example of an extreme climatic event that dropped yield estimates of corn to 123.4 bushels per acre, the lowest since 1995. While not immediately felt in food prices by consumers, the effect of low yields can take a year to trickle through production and increase the cost of consumables. Feedlots paid lower prices for feed cattle in 2013 as a result of the higher cost of feed in 2013 caused by reduced availability of pasture and decreased yield from the 2012 drought. The decrease in available pasture results in cattle being fed over a longer term with feed, but at lower weights because of the higher cost of feed in 2013. It is speculated that this will lead to greater production declines by 2014 which will increase cattle prices for almost two years after the drought occurred [15].

Climatic risk assessment determines the risk (i.e., potential) of crop failure or success due to weather and climate variability over a growing season or over several growing seasons. Risk is often determined from analysis of past growing seasons and potential future weather and/or climate scenarios as computed by crop models and expert projections. Usually once a climatic risk assessment has been completed, a cost-benefit

analysis is undertaken by producers based on the assessment of global vulnerabilities. Decisions include choice of when to plant amidst balance of late frost risk at the beginning of the season, pest issues during the growing season, and having enough radiation/temperature (degree days) to complete maturity through harvest. Decisions related to crop insurance, fertilizers, and pesticide purchases are agronomically as well as economically important, and weather plays a dominant role in ensuring profitability. Thus agroclimatology plays an important role in helping manage weather and climate risks for producers and stakeholders, and in turn better mitigating and adapting to climate change and variability.

2.4 Agroclimatology Today: Some Important Variables

2.4.1 Agroclimatology in the 21st Century

Agroclimatology today focus more readily on providing guidance in the form of weather and climate products, aiming to develop resilience in crops to climatic extremes, pests, diseases, and weeds to improve crop growth and production at local and regional scales [1]. Although agroclimatology is specifically focused on studying the impacts of weather/climate patterns on crop production and soils, it is a multidisciplinary field comprised of, but not limited to knowledge from agronomists, soil scientists, biologists, hydrologists, meteorologists, climatologists, physical geographers, human geographers, sociologists, and economists [2]. Embedded within the agroclimatic notion is the societal need to provide decision support for current agriculture practices and weather catastrophes such as droughts or late frosts [16].

Agroclimatology is connected to several sub-sciences: soils, hydrology, weather and climate, and agronomy. Different soil types possess distinctive hydraulic and thermodynamic properties that influence the growth rate of plants and the movement of water and nutrients through the soil and on the land surface. Surface and subsurface hydrology are affected not only by the type of soil but the type and amount of vegetation present over that soil. The density of a plant biomass on the surface influences the amount of rainfall reaching soils and the amount of radiation reaching the land surface. Plant roots can also affect infiltration and runoff rates. Weather and climate affect

agronomic productivity mainly through precipitation, temperature, and radiation for plant photosynthesis and growth.

Multi-scale coupled soil-vegetation-atmosphere transfer (SVAT) processes regulate the hydrologic, energy, and nutrient transfer balance in agricultural landscapes (Figure 2.2). These transfer processes cascade across different scales that ultimately impact the crop yield and profitability. Crop transpiration and photosynthesis regulates the nutrients used by the plant via the gross primary production (GPP) and the net primary productivity (NPP) of the agroclimatic system. The NPP, or yield, is linked with transpiration through the plant canopy and evaporation from the soil surface. The soil surface is the fundamental level where the carbon/nutrient and water link is established, but can be scaled beyond the leaf, plant, and to larger regional scales of total biomass/vegetation in a field. Thus, a detailed understanding of SVAT processes often becomes essential in providing agroclimatic guidance [17].

Changes in regional agricultural crop cover and greenness / phenology lead to changes in regional dewpoints and temperatures from the evapotranspiration from plants and/or irrigation. The spatial extent and greenness of crop cover can result in increased moisture in the atmosphere and lowering of the surface air temperature [18, 19]. This in turn can lead to changes in regional convective potential, cloud cover, and in some cases rainfall (Figure 2.3). Understanding these linkages is difficult, yet this is where agroclimatological assessments tend to help by providing a framework and understanding how a particular region would be expected to behave in a statistical/climatological sense. The fundamentals of such statistical/climatological relationships lie in the understanding of variables that are important for agricultural principles. Some of the climatic variables that are analyzed include temperature (maximum, minimum, average), rainfall characteristics (distribution, intensity), and solar radiation. Additional variables such as sunshine hours, humidity, winds, soil temperature, soil moisture, and evaporation are also needed, but generally difficult to measure with high spatio-temporal resolution or fidelity and are estimated from different models [20, 21].

2.4.2 Primary Agroclimatological Parameters

2.4.2.1 Weather and Climate

Weather can be defined by daily precipitation, temperature, and other dynamic (wind) and thermodynamic (humidity) weather patterns. Weather characterization ranges from temporal and spatial scales of seconds to decades and millimeters to thousands of kilometers. The most common temporal and spatial scales for daily weather are: microscale (areas less than 1 km, seconds to minutes), mesoscale (1-100 km, several hours to a day), synoptic scale (100-1000 s km, days to a week), and planetary scale (1000 s km and lasts up to several weeks) [22, 23]. The average weather and its variability over a period of time delineate a specific area's climate [10]. The climate of a region is typically defined by the average and variance of temperature and precipitation, which is influenced by topography, proximity to water bodies, size of the given landmass, or any geographical feature including urban areas. Mountain ranges can lead to regional climate zones with higher precipitation climates on the windward side, while more arid and temperate climates are found downwind [10, 24]. Coastal climates are moderated daily and seasonally by ocean waters and currents due to the higher specific heat capacity of water and resulting land/sea breezes [10, 22]. Urban climates impact local temperatures, wind patterns, and boundary layer depths because of differences in surface layer energy and heat balances. A lack of vegetation and prolific extent of impervious, highly reflective and/or highly absorbent land-cover types generate this type of localized climate [22, 23, 25].

The average (and variation) over 30 years of recorded weather patterns such as daily rainfall, high and low temperature, and mean temperature is generally used to define a region's (climate zone, state, or multi-state region) set of climate "normals" [26]. These climate normals are used extensively in agriculture to determine the baseline and the ensuing anomaly for any given season. In the United States, climate divisions (typically nine per state) are determined to help the broader applications community be aware of temperature and precipitation patterns/and shifts at regional and state scales. Sometimes additional information on frost depth, soil temperatures, and average soil

moisture are available through the 30-year climatological summaries (Figure 2.4). For many regions within the United States, the climate divisions are also aligned with the United States Department of Agriculture's crop reporting districts and assist climate – crop yield assessments.

2.4.2.2 Soils

The basic soil classifications are based on particle size. Soils are typically classified as gravel (greater than 2.00 mm), sand (0.05-2.00 mm), silt (0.002 to 0.05 mm), or clay (less than 0.002 mm). The amount of quartz and carbon content of a given soil type is also included as a characteristic in some models to clarify the surface layer soil type from the underlying soil layers. Each basic soil type has specific thermal and hydraulic characteristics that influence temperature and moisture content of that specific soil. Soil heat capacity (amount of heat required to produce a given change of the temperature of the body which is largely influenced by the presence of water), thermal conductivity (how fast heat is transferred through soil), and hydraulic conductivity (how fast water is transferred through soil), are just a few of many parameters that govern how suitable a subsurface climate may be for a specific crop [27].

The land-surface (soil and vegetative surface) response is governed by solar radiation. Shortwave radiation is absorbed and continually reemitted by the land surface, with a peak of absorption and emission during the afternoon, and a dominant outward flux of longwave radiation in the form of sensible and ground heat flux back to space in the night [20, 22, 23]. Land surface radiation absorption or reflection characterized by a ratio of absorbed to emitted shortwave radiation called albedo (α). Typical values of albedo are 0.05-0.40 for dark and wet to light and dry soils, 0.18-0.25 for agricultural crops, 0.15-0.20 for deciduous forests, 0.05-0.15 for coniferous forests, 0.0.-0.10 (small zenith angle) to 0.10-1.0 (large zenith angle) for water, and 0.40 (old) to 0.95 (fresh) for snow [23].

The values of incident net radiation (NR) are quantified through the radiation balance equation which is the sum of incoming shortwave radiation ($SW\downarrow$), outgoing longwave radiation ($LW\uparrow$), sensible heat (H) (thermal heat transfer from the ground to overlying air via conduction and convection), latent heat (E) (heat released into the air as

water vapor condenses back into water), and ground heat (G) (thermal heat energy transferred from the ground) [20, 22, 23]. All together, these variables help quantify the surface radiation budget in relation to surface albedo that is primarily governed by surface characteristics:

$$\mathbf{SW\downarrow (1-\alpha) + LW\uparrow = NR}$$

$$\mathbf{H + E + G = NR}$$

Data to understand energy fluxes is typically available from research field sites (e.g., Fluxnet, fluxnet.ornl.gov [28]). Data availability is limited because specialized measurements of surface sensible heat flux, latent heat flux, ground heat flux, carbon dioxide flux, moisture flux, evaporation/transpiration, surface temperature, soil moisture, and soil temperatures are challenging to obtain and require sophisticated equipment that needs ample care and maintenance. These data are typically used to develop and test newer plant-yield, environmental response relationships. Crop modelers develop empirical equations that can be applied in models and regional-scale analysis. In recent years, satellite platforms such as the NASA Moderate Resolution Imaging Spectroradiometer (MODIS) aboard Terra and Aqua, Atmospheric Infrared Sounder (AIRS), and the Advanced Microwave Scanning Radiometer-Earth Observing System (AMSR-E) have also greatly contributed to the understanding of the Earth's surface and atmospheric radiation balances [29, 30, 31]. Near real-time analysis of leaf area index (LAI), normalized difference vegetation index (NDVI), enhanced vegetation index, evapotranspiration, surface temperature, and moisture stress index are some of the measurements these satellite platforms provide for research and application into crop models, along with near real-time information pertinent to irrigation and harvest (e.g., [32]). Surface flux data along with satellite data has been assimilated into weather forecast, climate, and crop growth models, achieving a higher level of understanding of weather/climate and crop production forecasts [33, 34].

2.4.2.3 Water

Agroclimatic decisions are acutely linked to hydroclimatology. Surface and ground water are readily coupled with the Earth's surface because they impact crop growth and evapotranspiration into the overlying atmosphere (which determines surface

moisture flux). Moisture flux of the land surface is controlled by the saturation and temperature of the overlying air, wind speeds, turbulent eddies, and intensity of sunlight reaching the surface in the form of shortwave radiation [8, 11, 20, 21, 22, 35]. Radiation reaching the Earth's soil surface contributes to the evaporation rate of water from the soil and is further impacted by vegetation. Plant physiology plays a large role in surface moisture flux: stomata (microscopic pores or openings on the leaves of plants) opens and closes based on environmental conditions such as carbon dioxide availability, soil moisture, atmospheric saturation, wind, and sunlight, releasing moisture into the atmosphere along with water vapor and oxygen exchange [20, 22, 35]. Moisture flux is a quantitative measure of soil moisture that moves up through the soil, through the plant, and evaporates out of the soil and transpires from the plant [22, 23, 27, 35]. Soil moisture excess or deficits in the form of floods or droughts (along with temperature) have a direct impact on plant health and yield. The timing of water stress is also important in determining the crop response to the impact of stress. Crops two to three weeks after planting are typically more vulnerable than two months into the growing season.

2.4.2.4 Crop Management (Vegetation/Biomass)

Climate variables such as base temperature, growing degree days, average frost days, first frost day, and last frost day help determine crop progress. Temperature becomes an important driver of crop development and is typically used as a resource available to the plant. This is quantified as growing degree days (GDDs) which are used to determine phenology such as when the seeds of row crops will germinate and grow in conjunction with determining pest development rates within the soil.

$$\mathbf{GDD = ((T_{max} - T_{min})/2) - T_{base}}$$

The base temperature for corn is commonly 10°C, and typically after 10 consecutive GDDs (base time for corn), seeds germinate and grow [20, 35]. Base temperature will vary by crop.

The last spring frost consideration is also crucial to seed germination and plant growth. If a seed is planted before the last frost, farmers risk plant loss because the seed will fail to germinate. As a result, climatologies of important crop management variables

have been developed: 1) the first and last frost dates (e.g., in the Midwest U.S. in states such as Indiana, temperatures below 32° and 28°F are used as the baseline temperatures), 2) snowfall amounts, 3) temperatures above 95°F, 4) rainfall, 5) evapotranspiration loss, etc. Climatologies also exist for high impact weather events such as high winds that can impact spray operations, hail that can cause crop losses, and heavy rain that can result in erosion and/or flood and surface ponding in fields. Developing a climatology of a specific variable includes taking the actual values and anomalies and averaging them with quality control procedures such as duration of measurement, time of day the measurement is observed, and site specific location information such as proximity to trees, buildings, concrete, and elevation to develop the desired climatology. These climatologies are taken either at a station level (like the U.S. Cooperative Observer Network) if observations exist, or at climate division levels over a 30 year period (e.g., 1981-2010). Additional weather networks exist across different spatial and temporal scales that contribute to the development of climatologies and provide real-time weather data to producers and forecasters. Many states have what are called "mesonetworks" that are comprised of weather observation stations in counties across a given state. These stations can provide hourly readings of temperature, precipitation, winds, evapotranspiration estimates, and pressure in addition to daily maximum and minimum temperatures, and 24 hour rainfall/precipitation totals. In the United States, these data are typically available from respective state climate offices.

Extreme climatic events such as floods or droughts during the 1930s, 1950s, 1980s, and most recently 2012 contribute greatly to reduced yield, crop profitability, and world market stability. Forecasting climate extremes such as floods and drought still remains highly uncertain despite advancements in weather and climate modeling. Global features such as the El Niño Southern Oscillation (ENSO) are a large determining factor in North American weather regimes [10]. When compounded across seasons or even years, ENSO related weather patterns can manifest and lead to anomalous events such as the 2012 drought [36].

Current agroclimatic research is aligned towards characterizing droughts and their impacts on crop yields, including linking the interplay between agriculture – droughts –

economic decisions and impacts. Drought is more than a lack of rainfall, and a number of indices have been applied to assess it. Drought impacts are characterized on the basis of timing (e.g., middle of the growing season well after planting), intensity, duration, spatial extent, and location (e.g., urban versus rural regions). Drought indices include basic analysis such as percentage of normal and quantitative meteorological measures such as the Standardized Precipitation Index (SPI) and Palmer Drought Severity Index (PDSI) [37].

Development of climatologies include weather and climate variables such as evapotranspiration, annual precipitation, total sunshine hours, plant hardiness zones, and mean freeze-free period for agricultural applications (Figure 4). These climatologies provide a baseline value to compare to current weather and climate patterns, letting agricultural producers and stakeholders know if seasonal weather patterns are trending above or below normal. This could allow producers to better prepare for a change in their projected yield for the season, and hopefully mitigate loss if sufficient time is still present to act accordingly. For example, the Useful to Usable (U2U) climate information project sponsored by the USDA is developing an agricultural climatology for the U.S. Corn Belt region that includes the ENSO phase at the climate division level for cereal crop producers [38]. This climatology can provide guidance to farmers related to irrigation, fertilizer application, planting, and harvest-reducing crop vulnerability to changing weather patterns [14].

2.4.3 Agroclimatology in the Future

An important question going forward is how can societies, economies, and countries sustain and continue to expand food supplies for a continually growing world population. This problem is further compounded with shifts in climate patterns, particularly temperature and precipitation across the world [1, 2, 39, 40]. Agronomic decisions and productivity is thus linked to environmental and economic sustainability. Climate projections indicate a high probability of the subtropics becoming drier while the midlatitudes will have continued shifts in temperature, rainfall, cloud cover, and related climatic patterns [41]. The agricultural community has been working with adaptation

approaches which at a macroscale will need to address the current distribution of arable land for agriculture and the increased demand for more hybrid crops to withstand wetter/drier climates. New soil diseases can pose a threat in regions experiencing changes in seasonal temperatures as growing seasons become longer and the time a field lays fallow shortens [42, 43]. Understanding these climate-pathogen relationships in a changing climate regime will likely become increasingly important.

In addition to the demand for hardier crops to surpass the challenges of a changing climate, the demand for biofuels will likely continue to rise as governments continue to mandate reduction of greenhouse gas emissions. Current research in this area includes determining the best crop rotation cycles to protect soil nutrients while also maximizing the use of crops and crop waste such as corn and corn stalks, oil seeds, crop residue, and woody biomass for the production of bioenergy and ethanol. However, growing crops for bioenergy and ethanol instead of food for populations, leads to societal questions that are also at the forefront of the climate change debate. In essence, future challenges facing agroclimatology include better decision-making tools, data acquisition, availability and uniformity (spatial and temporal), links between economic and regional decision makers, the development of more accurate and detailed crop and forecast models, and a more detailed understanding of climate change. These challenges require collaboration between different disciplines.

2.5 Conclusion

Agroclimatology is at an interesting juncture, becoming central to today's most challenging questions in a world of continued population growth, increasing food demand, and climate change. Technological advancements such as multiscale remote-sensing data, vegetation and moisture stress mapping, land data assimilation systems linked with crop models, and high resolution crop, weather and climate datasets and models will likely play an important role in the understanding and evolution of agroclimatology. Weather and climate data collection, assessment and mitigation of extremes such as floods and droughts, and climate and crop modeling will continue into the future as agroclimatology grows as a science. In addition, feedbacks of agricultural climates at field and regional

scales need to be further researched to grasp the full understanding of heat and moisture fluxes between soils, the overlying boundary layer, vegetation, and the feedback into crop yields.

Despite large technological advancements in data collection and analysis, and a more detailed understanding of the agroclimatic system than ever before, questions regarding the future vulnerability of agro-climate systems still remain unanswered. Collaborative research and efforts to mitigate the effects of climate change need to be aggressively supported and addressed to allow for continued food production, development of bioenergies, and human survival in a world currently experiencing climate variability and change [2]. Changes in temperature and precipitation as projected using climate change studies will impact crops and non-crop species. As summarized by a recent USDA synthesis report [43], the projected variability in precipitation and location shifts will require changes in water management practices (which will further feedback into the local climate system). Projected changes in temperature indicate the northward advance of frost-free days, opening the doors to additional regions for crop growth but also creating an environment that would be potentially conducive for invasive weeds and pests [43].

There are at least two enduring challenges that impact current monitoring and modeling efforts in agroclimate. The first is due to scale disparity: 1) field measurements are often "point" data while effects are often regional scale in nature and not well captured, and 2) if remotely-sensed/satellite data are used for assessing the regional view, the dominant impact of local-scale decisions and micro features which can influence crop yields are not captured. Combination approaches involving assimilation of multiscale products into a gridded assessment are currently underway and may likely alleviate the uncertainty due to this problem [44, 45]. The second challenge can be linked to capturing the diversity in agronomic practices. For example, most studies consider the relationship between climate and crop patterns for a "typical" crop and the variations between hybrids are poorly assessed. Similarly, variability in farm-scale practices such as planting date, presence of tilling, crop cover, and distances between crop rows, fertilizer use, and pest risk are also poorly captured and cause uncertainty in current assessments. Additional

challenges due to socioeconomic choices and economic tradeoffs are also difficult to capture.

Acknowledgements: NIFA/USDA - Useful to Usable (U2U): Transforming Climate Variability and Change Information for Crop Producers: Agriculture and Food Research Initiative Competitive Grant no. 2011-68002-30220, NSF INTEROP driNET, USDA NIFA Drought Trigger projects at Purdue through Texas A&M, and NSF COSIEN project at Purdue through UC Berkeley.

2.6 References

1. Decker, W.L. Developments in Agricultural Meteorology as a Guide to Its Potential for the Twenty-first Century. Agricultural and Forest Meteorology, Vol.69 (1), 1994, 9-25.

2. Steiner, J.L.; J.L. Hatfield. Winds of change: A Century of Agroclimate Research. Agronomy Journal, 100: S-132 - S-152, doi: 10.2134/agronj2006.0372c, 2008.

3. Pielke Sr., R.A.; Pitman, A.; Niyogi, D.; Mahmood, R.; McAlpine, C.; Hossain, F.; Goldewijk, K. K.; Nair, U.; Betts, R.; Fall, S.; Reichstein, M.; Kabat, P.; de Noblet-Ducoudré, N. Land Use/Land Cover Changes and Climate: Modeling Analysis and Observational Evidence. WIREs Climate Change 2011, doi: 10.1002/wcc.144, 2011.

4. Dirmeyer, P.A.; Niyogi, D.; de Noblet-Ducoudré, N.; Dickinson, R.E.; Snyder, P.K. Impacts of Land Use Change on Climate. International Journal of Climatology, 30, doi: 10.1002/joc.2157, 2010, 1905–1907.

5. Niyogi, D.; Kishtawal, C.; Tripathi, S.; Govindaraju, R.S. Observational Evidence that Agricultural Intensification and Land Use Change may be Reducing the Indian Summer Monsoon Rainfall. Water Resour. Res., 46, W03533, doi: 10.1029/2008WR007082, 2010.

6. Mishra, V.; Cherkauer, K.A.; Niyogi, D.; Lei, M.; Pijanowski, B.C.; Ray, D.K.; Bowling, L. C.;Yang, G. A Regional Scale Assessment of Land use/Land cover and Climatic Changes on Water and Energy Cycle in the Upper Midwest United States. International Journal of Climatology, 30, doi: 10.1002/joc.2095, 2010, 2025–2044.

7. Monteith, J.L. Agricultural Meteorology: Evolution and Application. Agricultural and Forest Meteorology, 103, 2000, 5-9.

8. Diamond, J.M. Collapse: How Societies Choose to Fail or Succeed. New York: The Viking Press (Penguin Group USA), 2004, 592pp.

9. Cox, J. D. Storm Watchers: The Turbulent History of Weather Prediction from Franklin's Kite to El Nino. Hoboken: Wiley & Sons, 2002, 252pp.

10. Robinson, P.J.; Henderson-Sellers, A. Contemporary Climatology. Essex: Pearson Prentice Hall, 1999, 317pp.

11. Lenschow, D.H. Handbook of Weather, Climate, and Water: Atmospheric Chemistry, Hydrology, and Societal Impacts: Boundary Layer Processes and Flux Measurements. Hoboken: John Wiley & Sons, Inc., 2003, 966pp.

12. Rosenzweig, C.; Jones, J.W.; Hatfield, J.L.; Mutter, C.Z.; Adiku, S.G.K.; Ahmad, A.; Beletse, Y.; Gangwar, B.; Guntuku, D.; Kihara, J.; Masikati, P.; Paramasivan, P.; Rao, K.P.C.; Zubair, L.. The Agricultural Model Intercomparison and Improvement Project (AgMIP): Integrated regional assessment projects. In D. Hillel and C. Rosenzweig (Ed.), Handbook of Climate Change and Agroecosystems: Global and Regional Aspects and Implications, 2, 263–280pp, 2012.

13. Jones, J.W.; Hoogenboom, G.; Porter, C.H.; Boote, K.J.; Batchelor, W.D.; Hunt, L.A.; Wilkens, P.W.; Singh, U.; Gijsman, A.J.; Ritchie, J.T.. DSSAT Cropping System Model. European Journal of Agronomy, 18, 235-265pp, 2003.

14. Takle, E.S.; C.J. Anderson; J. Anderson; J. Angel; R. Elmore; B.M. Gramig; P. Guinan; S. Hilberg; D. Kluck; R. Massey; D. Niyogi; J. Schneider; M. Shulski; D. Todey; M. Widhalm. Climate forecasts for corn producer decision-making. Earth Interactions, In Review, 2013.

15. Crutchfield, S. U.S. Drought 2012: Farm and Food Impacts. United States Department of Agriculture, Economic Research Service. 26 July 2013, < http://www.ers.usda.gov/topics/in-the-news/us-drought-2012-farm-and-food-impacts.aspx#.UnEd8HDqhyI>, 2013.

16. Prokopy, L.S.; Haigh, T.; Mase, A.S.; Angel, J.; Hart, C.; Knutson, C.; Lemus, M.C.; Lo, Y.; McGuire, J.; Morton, L.W.; Perron, J.; Todey, D.; Widhalm, M. Agricultural Advisors: A Receptive Audience for Weather and Climate Information? Weather, Climate, and Society, 5, 2013, 162-167pp.

17. Campbell, G.S.; Norman, J.M. An Introduction to Environmental Biophysics. 2nd Ed. New York: Springer Science + Business Media, 1998, 286pp.

18. Fall, S.; Niyogi, D.; Gluhovsky, A.; Pielke Sr., R.A.; Kalnay, E.; Rochon, G. Impacts of Land Use Land Cover on Temperature Trends over the Continental United States: Assessment using the North American Regional Reanalysis. International Journal of Climatology, 30, doi: 10.1002/joc.1996, 2010, 1980–1993.

19. Niyogi D.; Mahmood, R.; Adegoke, J.O. Land-Use/Land-Cover Change and Its Impacts on Weather and Climate. Boundary- Layer Meteorology, 133, doi 10.1007/s10546-009-9437-8 (Editorial), 2009, 297-298.

20. Griffiths, J.F., Editor. Handbook of Agricultural Meteorology. New York: Oxford University Press, 1994, 320pp.

21. Noilhan, J.; Planton, S. A Simple Parameterization of Land Surface Processes for Meteorological Models. Monthly Weather Review, 117, 1989, 536-549.

22. Stull, R.B. An Introduction to Boundary Layer Meteorology. New York: Springer LLC, 1988, 683pp.

23. Oke, T.R. Boundary Layer Climates, 2nd Ed. New York: Routledge, 1988, 464pp.

24. Holton, J.R. An Introduction to Dynamic Meteorology, 4th Ed. Waltham: Elsevier Academic Press, 2004, 535pp.

25. Landsberg, H.E. The Urban Climate. New York: Academic Press, 1981, 275pp.

26. Arguez, A. NOAA's 1980-2010 Climate Normals. 14 February 2012, < http://lwf.ncdc.noaa.gov/oa/climate/normals/usnormals.html>, 2011.

27. Houser, P.R. Handbook of Weather, Climate, and Water: Atmospheric Chemistry, Hydrology, and Societal impacts: Infiltration and Soil Moisture Processes. Hoboken: John Wiley & Sons, Inc. 2003, 966pp.

28. Baldocchi, D.; Falge, E.; Gu, L.; Olson, R.; Hollinger, D.; Running, S.; Anthoni, P.; Bernhofer, C.; Davis, K.; Evans, R.; Fuentes, J.; Goldstein, A.; Katul, G.; Law, B.; Lee, X.; Malhi, Y.; Meyers, T.; Munger, W.; Oechel, W.; Paw, K.T.; Pilegaard, K.; Schmid, H.P.; Valentini, R.; Verma, S.; Vesala, T.; Wilson, K.; Wofsy, S. FLUXNET: A New Tool to Study the Temporal and Spatial Variability of Ecosystem-Scale Carbon Dioxide, Water Vapor, and Energy Flux Densities. Bulletin of the American Meteorological Society, 82:11, 2001, 2415-2434pp.

29. Maccherone, B.; S. Frazier. About MODIS. < http://modis.gsfc.nasa.gov/about/>, 2013.

30. Graham, S.; C. Parkinson. AMSR-E. <http://aqua.nasa.gov/about/instrument_amsr.php>, 2011.

31. Ray, S. How AIRS Works. <http://airs.jpl.nasa.gov/instrument/how_AIRS_works/>, 2013.

32. Frolking, S.; Xiao, X.; Zhuang, Y.; Salas, W.; Li, C. Agricultural Land-use in China. A Comparison of Area Estimates from Ground-based Census and Satellite-borne Remote Sensing. Global Ecology and Biogeography, 8:5, 1999, 407-416pp.

33. Olioso, A.; Chauki, H.; Courault, K.; Wingeron, J. Estimation of Evapotranspiration and Photosynthesis by Assimilation of Remote Sensing Data into SVAT Models. Remote Sensing of Environment, 68:3, 1999, 341-356.

34. Kumar, A.; Niyogi, D.; Chen, F.; Barlage, M.; Ek, M.B. Assessing Impacts of Integrating MODIS Vegetation Data in the Weather Research Forecasting (WRF) Model Coupled to Two Different Canopy- resistance Approaches. Journal of Applied Meteorology and Climatology, 2013.

35. Monteith, J.L. Climatic Variation and the Growth of Crops. Quarterly Journal of the Royal Meteorological Society, 107: 454, 1981, 749-774.

36. Hoerling, M.; Schumert, S.; Mo, K. An Interpretation of the Origins of the 2012 Central Great Plains Drought. NOAA Drought Task Force, Narrative Team, <http://www.drought.gov/media/pgfiles/2012-Drought-Interpretation-final.web-041013_V4.0.pdf>, 2013, 1-50pp.

37. Guttman, N.B. Comparing the Palmer Drought Index and the Standardized Precipitation Index. Journal of American Water Resources Association, 34, 1998, 113-121pp.

38. Useful to Useable: Transforming Climate Variability and Change Information for Cereal Crop Producers. Agriculture and Food Research Initiative Competitive Grant no. 2011-68002-30220, <https://drinet.hubzero.org/groups/u2u>, 2013.

39. Downing, T.E.; Stowell, Y. Handbook of Weather, Climate, and Water: Atmospheric Chemistry, Hydrology, and Societal Impacts: Household Food Security and Coping with Climatic Variability in Developing Countries. Hoboken: John Wiley & Sons, Inc., 2003, 966pp.

40. Glantz, M.H. Currents of Change El Nino Impact on Climate and Society. Cambridge: Cambridge University Press, 1996, 194pp.

41. Bates, B.C.; Kundzewicz, Z.W.; Wu, S.; Palutikof, J.P., Editors. Climate Change and Water. IPCC Secretariat, Geneva, 2008, 210pp.

42. Southworth, J.; Pfeifer, R.A.; Habeck, M.; Randolph, J.C.; Doering, O.C.; Gangadhar Rao, D. United States to Future Changes in Climate, Climate Variability and CO2 Fertilization. Climate Research, 22, 2002, 73-86.

43. Walthall, C.L.; Hatfield, J.; Backlund, P.; Lengnick, L; Marshall, E.; Walsh, M.; Adkins, S.; Aillery, M.; Ainsworth, E.A.; Ammann, C.; Anderson, C.J.; Bartomeus, I.; Baumgard, L.H.; Booker, F.; Bradley, B.; Blumenthal, D.M.; Bunce, J.; Burkey, K.; Dabney, S.M.; Delgado, J.A.; Dukes, J.; Funk, A.; Garrett, K.; Glenn, M.; Grantz, D.A.; Goodrich, D.; Hu, S.; Izaurralde, R.C.; Jones, R.A.C.; Kim, S-H.; Leaky, A.D.B.; Lewers, K.; Mader, T.L.; McClung, A.; Morgan, J.; Muth, D.J.; Nearing, M.; Oosterhuis, D.M.; Ort, D.; Parmesan, C.; Pettigrew, W.T.; Polley, W.; Rader, R.; Rice, C.; Rivington, M.; Rosskopf, E.; Salas, W.A.; Sollenberger, L.E.; Srygley, R.; Stöckle, C.; Takle, E.S.; Timlin, D.; White, J.W.; Winfree, R.; Wright-Morton, L.; Ziska, L.H. Climate Change and Agriculture in the United States: Effects and Adaptation, USDA Technical Bulletin. Washington, DC, <http://www.usda.gov/oce/climate_change/effects_2012/CC%20and%20Agriculture%20Report%20(02-04-2013)b.pdf>, 2013.

44. Liu, X.; Niyogi, D.; Charusombat, U. Estimating Corn Yields Regionally Across Midwest Using the Hybrid Maize Model with a Land Data Assimilation System. Presentation, American Geophysical Union Fall Meeting 2012, San Francisco, California, <http://198.61.161.98/abstracts/meetings/2012/FM/sections/GC/sessions/GC21H/abstracts/GC21H-07.html >, 2012.

45. Niyogi, D.; Liu, X. Adaptability of the Hybrid-Maize Model and the Development of a Gridded Crop Modeling System for the Midwest US. Presentation, ASA, CSSA, and SSSA International Annual Meetings, Cincinnati, Ohio, <https://scisoc.confex.com/crops/2012am/webprogram/Paper70435.html>, 2012.

2.7 Tables

Table 2.1: Common soil and vegetation parameters in land surface models embedded within some crop models and weather/climate models (Adapted from Noilhan and Planton, 1989 [21]).

Primary Parameters: **Dominant types of vegetation and/or land cover (USGS/NLCD classifications):**

1) Vegetation type: cultivated or hay/pasture land (more detailed in crop models), forest type: deciduous, evergreen, mixed, shrubs

2) Dominant type of soil texture (USDA textural classification):

Sand	Loamy sand
Sandy loam	Loam
Sandy clay loam	Silty clay loam
Clay loam	Sandy clay
Silty clay	Clay

3) Meteorological parameters:

Daily T_{max} and T_{min}	Net solar radiation
Precipitation	Relative Humidity
Evapotranspiration	Soil Moisture

Secondary Parameters (estimated or prescribed)**:**

Saturated volumetric moisture content	Wilting point volumetric water content
Soil thermal coefficient at saturation	Depth of the soil column
Fraction of vegetation	Minimum surface resistance
Leaf Area Index (LAI)	Roughness length
Albedo	Emissivity
Soil thermal conductivity	Soil thermal diffusivity
Soil hydraulic conductivity	Soil hydraulic diffusivity
Soil heat capacity	Soil bulk density
Moisture flux resistance	

2.8 Figures

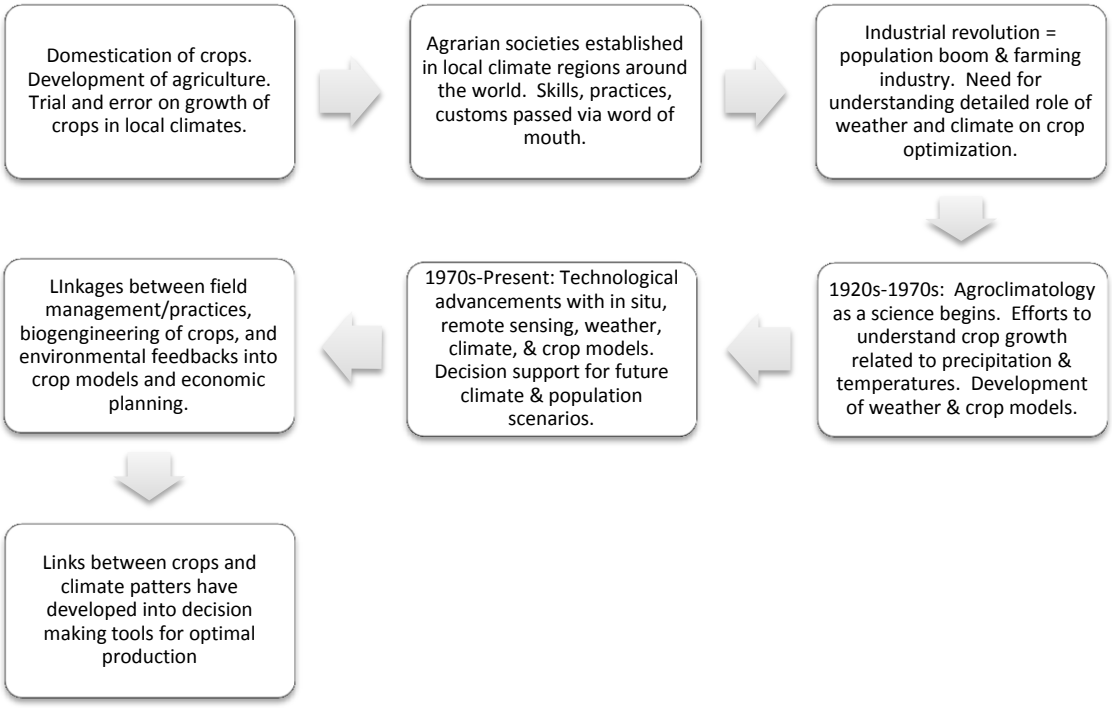

Figure 2.1**:** General narrative chart of the growth of agroclimatology.

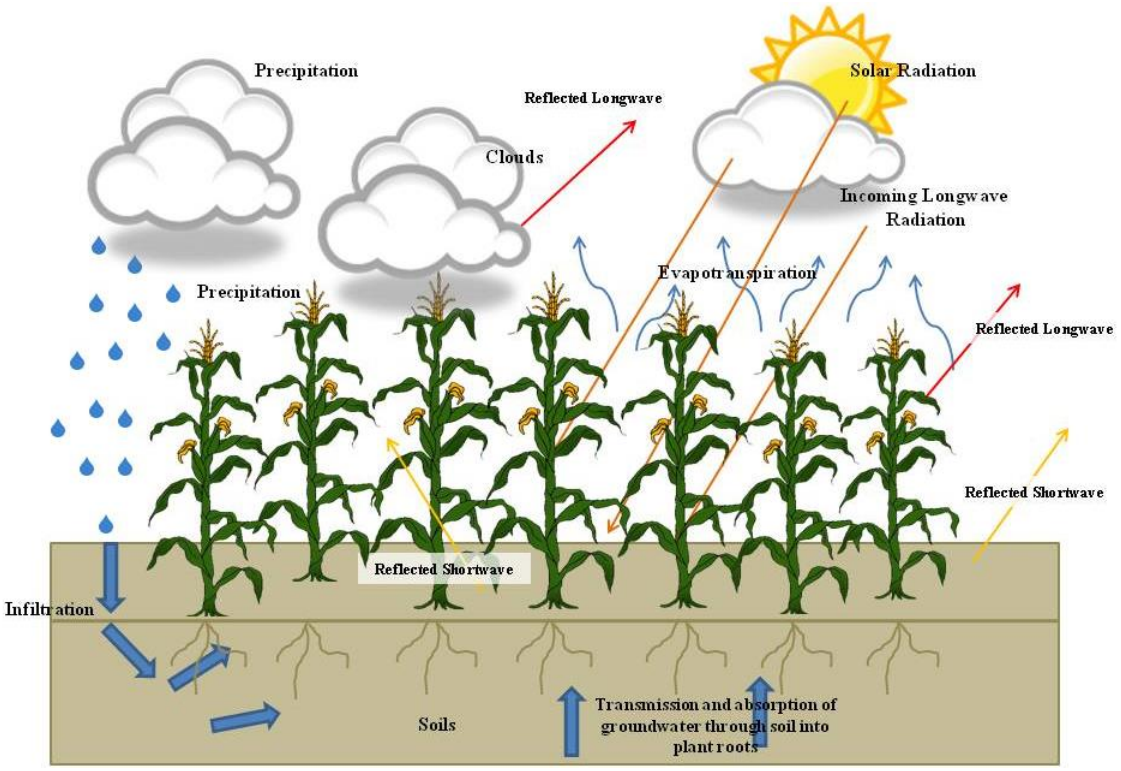

Figure 2.2: The soil-vegetation-atmosphere-transfer model (SVAT) represents the continuous feedback of radiative energy between the atmosphere, biosphere (crop), lithosphere (soil/land surface), and water in all its physical states: solid – ice crystals of clouds; liquid – raindrops; and gas – water vapor/evapotranspiration. Primary components and associated parameters include 1) soil: water retention, soil hydraulic conductivity, bulk density, water content, water potential, temperatures, infiltration, and evaporation; 2) canopy (vegetation/biomass): Leaf Area Index (LAI), physiology of the plant, leaf and plant density, seasonality, and evapotranspiration; 3) atmosphere: air temperature, humidity, wind speed, and solar radiation; and 4) hydrological cycle: evaporation, condensation, precipitation, infiltration, ground water flow, surface runoff, and ponding.

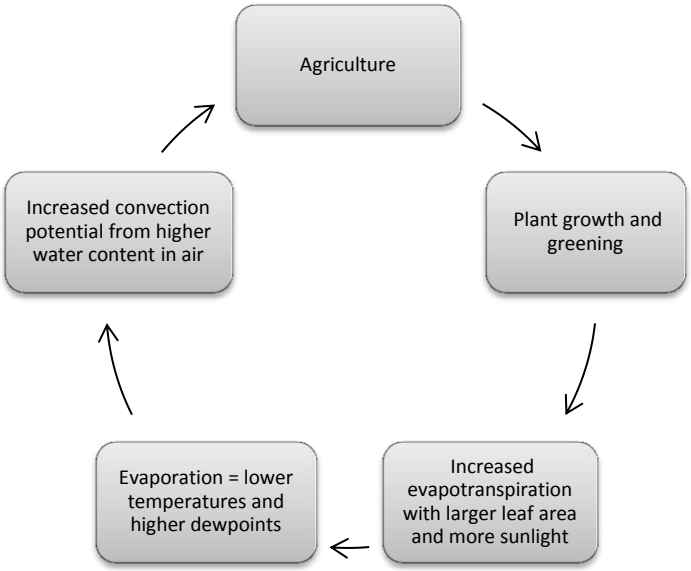

Figure 2.3: Examples of agricultural impacts on physical climate.

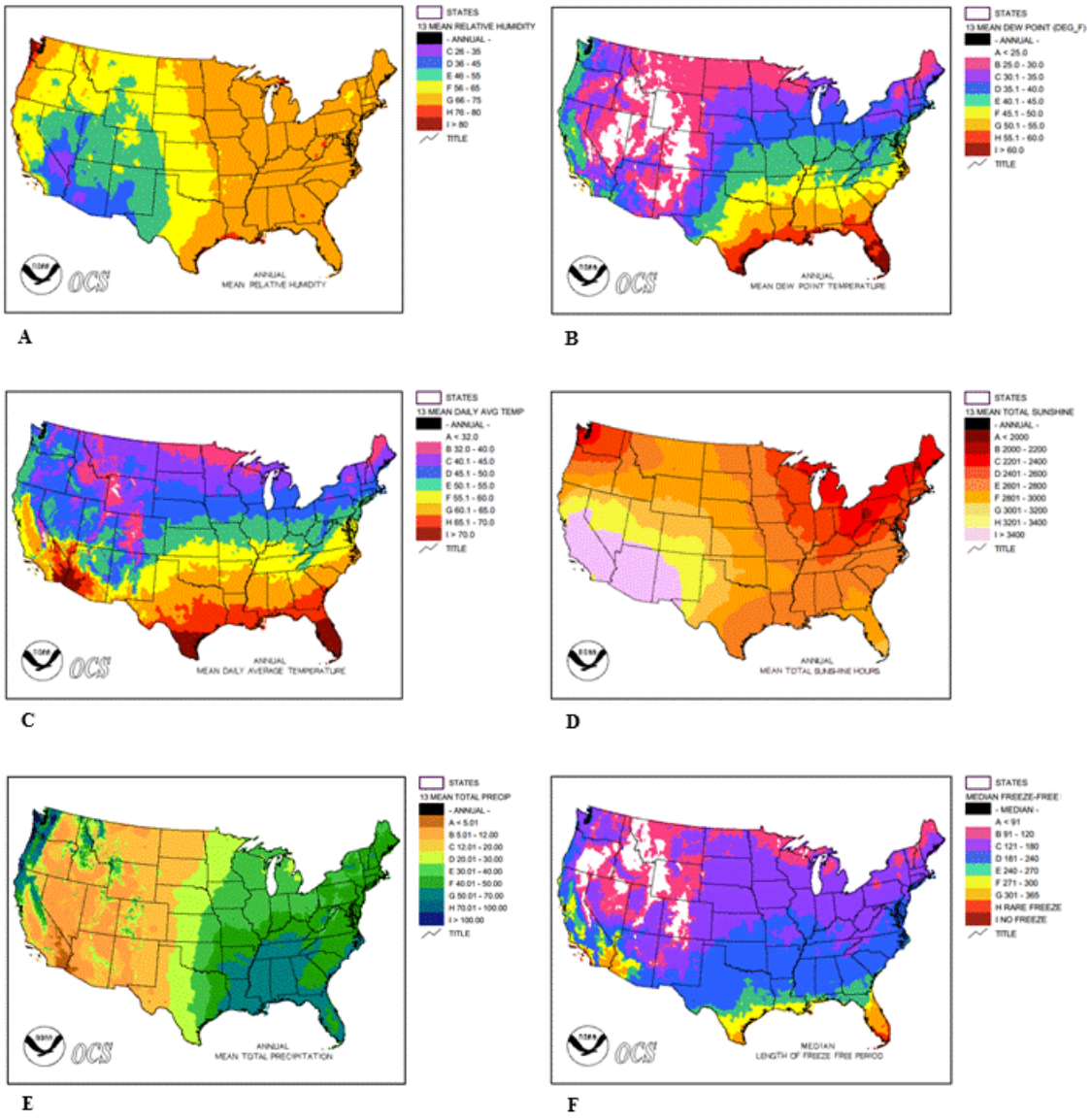

Figure 2.4: Examples of climatology maps collected from the National Climatic Data Center's Climate Maps of the United States database (CLIMAPS). Maps are developed from the 1961-1990 period of record from official weather and climate station sites unless otherwise noted. (A) Annual mean relative humidity in percent, (B) annual mean dewpoint temperature in degrees Fahrenheit, (C) annual mean daily average temperature in degrees Fahrenheit, (D) annual mean total sunshine hours, (E) annual mean total precipitation in inches, and (F) median length of freeze-free period in days.

CHAPTER 3. CLIMATE VARIABILITY AND THE U.S. CORN BELT: ENSO AND AO EPISODE-DEPENDENT HYDROCLIMATIC FEEDBACKS TO CORN PRODUCTION AT REGIONAL AND LOCAL SCALES

3.1 Introduction

Climate variability is an intrinsic part of global circulation and regional climates. Temperature and precipitation events representative of climate variability are captured in the extreme values of temperature and precipitation that primarily reside in the tails of a normal distribution. The range of values present in the tails of the distribution may increase or decrease through time but not actually effect the mean value of the sample distribution. Climate variability is driven by natural atmospheric circulation processes and anthropogenic drivers. Variability can occur on time frames of several weeks to several months and even over several decades. It is, however, much different that climate change. Climate change is a systematic change in the climate system through natural and/or anthropogenic causes that shift the mean of the sample distribution, and in turn shift/change the extreme values that comprise climate variability.

As discussed in Chapter 2, weather and climate are innate to agricultural production. Understanding the variability of temperature and precipitation as related to teleconnections (natural global and regional circulation features that affect the occurrence of weather in regions downstream of the teleconnection feature) helps agricultural produces (i.e. farmers) better prepare for extreme weather events associated with climate variability that can negatively impact yields. The research described in the following chapter serves to improve producers' understanding of the weather and climate system allowing them to make more informed decisions and improve profitability in light of climate variability and change.

3.2 Climate Variability and the U.S. Corn Belt: ENSO and AO Episode-dependent Hydroclimatic Feedbacks to Corn Production at Regional and Local Scales

Full Citation: Kellner, Olivia, and D. Niyogi, 2015: Climate variability and the U.S. Corn Belt: ENSO and AO episode-dependent hydroclimatic feedbacks to corn production at regional and local scales. Accepted April 2015, *Earth Interactions*.

Abstract

An El Niño Southern Oscillation (ENSO) and Arctic Oscillation (AO) climatology (1980-2010) is developed and analyzed across the U.S. Corn Belt using state climate division weather and historic corn yield data using ANOVA and correlation analysis. Findings provide insight to agro-climatic conditions under different ENSO and AO episodes and are analyzed with a perspective for potential impacts to agricultural production and planning, with findings being developed into a web-based tool for the US Corn Belt.

This study is unique in that it utilizes the Oceanic Niño Index and explores two teleconnection patterns that influence weather across different spatio-temporal scales. It is found that the AO has a more frequent weak to moderate correlation to historic yields than ENSO when correlated by average sub-growing season index values. Yield anomaly and ENSO/AO episode analysis affirms the overall positive impact of El Niño events on yields compared to La Niña events, with neutral ENSO events in between as found in previous studies. Yields when binned by AO episode present more uncertainty. While significant temperature and precipitation impacts from ENSO and AO are felt outside of the primary growing season, correlation between threshold variables of episode-specific temperature and precipitation and historic yields suggests that relationships between ENSO and AO and yield are present during specific months of the growing season, particularly August. Overall, spatial climatic variability resulting from ENSO and AO episodes contributes to yield potential at regional to sub-regional scales, making generalization of impacts difficult - highlighting a continued need for fine-scale resolution analysis of ENSO and AO signal impacts on corn production.

3.3 Introduction

Agricultural production in the United States contributes to 40% of the world's supply of corn (USDA 2013). Crop yield potential for a given growing season is largely dependent on temperature and precipitation (Kellner and Niyogi 2014), stressing the importance of understanding climate variability and projected climate change impacts in order to continue successful agricultural production in the future (Rosenzweig 2001; Rosenzweig et al. 2013; Pielke 2013). Research efforts have led to a better understanding of crop production under climate variability and change through analysis using historic weather, climate, and crop data (e.g., Carlson et al. 1996; Hansen et al. 1998; Legler et al. 1999; Phillips et al. 1999; Niyogi et al. 2014). Efforts to disseminate this useful information in a usable manner have been implemented across the world (e.g., the Agricultural Model Intercomparison and Improvement Project (AgMIP), Rosenzweig et al., 2012), while others more specifically focus on production in a designated region, such as the Useful to Usable (U2U) [1] project for the North Central Region (i.e., U.S. Corn Belt) in the United States (Takle et al. 2014). The U2U project is comprised of teams of researchers that focus specifically on developing improved weather and climate tools (such as this ENSO/AO climatology) to address producers' needs for more usable and useful weather and climate information to make more informed decisions (e.g., Crane et al. 2010; Meza et al. 2008). The efforts of the U2U research group aim to improve current and future growing season profitability and to help farmers mitigate and adapt to future climate variability and change.

Climate variability can be broadly described as weather conditions a region experiences outside what is considered climatologically normal, but that does not result in a systematic change to the climate system mean state. Initial evidence suggests climate variability more readily impacts agricultural production than climate change since agricultural production moves at a pace greater than climate change (Riley 2002). Agricultural production practices last 6-12 months (depending on the crop) with climate

[1] Useful to Usable: Transforming Climate Variability and Change Information for Cereal Crop Producers. USDA - National Institute of Food and Agriculture (NIFA) Agriculture and Food Research Initiative Competitive Grant no. 2011-68002-30220. Aclimate4u.org

variability following a similar time period of several weeks, years, or decades (depending on the climate index/teleconnection). Climate change is projected to occur over a much longer period of time. Examples of key drivers of climate variability (Goddard et al. 2001) include the El Niño Southern Oscillation (ENSO), the Arctic Oscillation (AO), the North Atlantic Oscillation (NAO), and the Madden-Jullian Oscillation (MJO). Examples of climate change include the drying trends expected in the subtropics and the projected shifts in the intensity (heavier) and duration (over a shorter period of time) of rainfall events in the Midlatitudes over the next 50-80 years that are expected to produce longer dry spells of weather in between rainfall events (IPCC 2013).

This paper focuses specifically on the historic behavior of ENSO and AO in the United States Corn Belt for the years 1980-2010 and the impacts these teleconnections and their resulting climate variability have had on corn yield. ENSO and AO are chosen in that ENSO is a longer-range (months to years) teleconnection index with long-term predictability and the AO is a short-term teleconnection (several weeks) with greater forecast uncertainty. These two time frames encompass exploring the impacts of growing season variability (ENSO) and sub-growing season variability (several weeks – AO). The working hypothesis of this study is that both growing season and sub-season variability driven by ENSO and sub-growing season variability driven by AO impact corn yields through positive and negative relationships dependent on teleconnection and episode, and both temporal scales of teleconnections need to be considered in producer decision making during the growing season. The initial impetus for the development of this climatology is the expressed need from producers (or other applied users) for more usable and useful weather and climate data analyses and decision support tools (DSTs) for a given growing region (i.e., "my county") (e.g. Arbuckle et al. 2013; Takle et al. 2014). This also builds on the work of Mase and Prokopy (2014) who discuss current producers' understanding and viewpoints of weather and climate data in decision making. This climatology reviews and highlights the applicability of weather and climate data to agricultural decision making when an ENSO or AO outlook is issued.

While ENSO impacts to U.S. and global yields have been a topic of research for decades (e.g., Adams et al. 1999; Brunner 2002; Carlson et al. 1996; Hollinger et al. 2001;

Legler et al. 1999; Mauget and Upchurch 1999; Rosenzweig 2001) several variations exist among these studies that result in a further need for ENSO analysis and impact on agricultural production. Needs for further study are driven by the following reasons: 1) study domains of previous research have varied in scope (global, continental United States, North Central Region, Great Plains and Midwest) and are not local scale; 2) previous research has varied in temporal methodology (e.g., yearly signal, growing season signal, 3- month intervals of the growing season), and statistical analysis (e.g., regression, binning, quartile analysis, ANOVA, deviation inconsistency with random sampling) which can overwhelm producers unfamiliar with science and statistics; 3) published studies vary in ENSO classification such as using sea surface temperature (SST) anomalies, the Southern Oscillation (SO), the Southern Oscillation Index (SOI), or the Multivariate ENSO Index (MEI). This results in varying conclusions on teleconnection feedbacks and crops (e.g., Hollinger et al. 2001; Mauget and Upchurch 1999) causing confusion regarding the exact impact information to producers and crop advisors; 4) past research uses historic weather and crop data of various spatial resolution with a majority of the studies using state-level yield analysis and not yield at crop reporting district-level removing localized feedbacks; and 5) past research tends to focus on more than one crop such as corn and soybeans (e.g., Hollinger et al. 2001) or corn and winter wheat (e.g., Mauget and Upchurch 1999), instead of focusing on one crop specifically.

To alleviate the variations amongst prior studies as described, this study is developed to be comprehensive and simple for end-users in the following ways: the study domain is chosen specifically to be of service to the primary corn production region in the United States (North Central Region). The climatology herein will be developed into a map-based, visual online decision support tool for cereal producers in the region through the U2U project team so that the producers and crop advisers may apply the useful weather and climate information of this climatology into their decision making process. This study is unique in that multiple temporal resolutions of ENSO episode are investigated. These include the annual ENSO signal [event based on the Oceanic Niño Index (ONI) definition of consecutive three-month running mean of sea surface temperature (SST) in the Niño 3.4 region (5^{o}N-5^{o}S, 120^{o}-170^{o}W)], the growing season

ENSO signal (April-October), a sub-growing season ENSO signal [first three months of production (AMJ) and three months of summer important to yield potential (JJA)], and a monthly ENSO signal. This study also applies a more fine-scale spatial resolution of weather data by incorporating specific National Weather Service (NWS) Cooperative Observer Program (COOP) site locations and aggregated weather data at the climate division level to analyze with more finite historic crop data at the crop reporting district level (instead of state level data like some past studies). The use of historic corn yields at crop reporting district level provides more localized feedback analysis. The analysis of corn production alone provides a detailed investigation of the mostly widely produced and utilized crop in the United States. Regarding the AO climatology and impacts to agriculture, it has yet to be adequately researched. Thus, the following climatology of the two separate teleconnections adds further analysis to ENSO/yield research and brings forth new findings of AO relationships to yield suggesting it may have more influence on yield production than ENSO.

3.4 Data and Methodology

3.4.1 Data

The data for this climatological analysis is retrieved from the Applied Climate Information System (ACIS) through the Midwest Regional Climate Center (MRCC) cli-MATE user interface[2]. Climate division data for the North Central Region (domain of the U2U research project: North Dakota, South Dakota, Nebraska, Kansas, Missouri, Iowa, Minnesota, Wisconsin, Illinois, Indiana, Michigan, and Ohio) is retrieved and analyzed for the years 1980-2010. Observed weather data is used in an effort to maintain the true integrity of observed weather datasets, as reanalysis data is subjected to data algorithms for automated quality control processes and development of spatial homogeneity that by design may reduce the impact of meso- and microclimates resulting from local features shown to influence production (e.g., Kravchenko and Bullock 2000).

[2] Data is from the DRD964x climate observations dataset as it was collected prior to the dataset (nClimDiv) currently available and in use in ACIS (NCDC 2014). The ACIS system is inclusive of in-situ observations reported to federal, regional, state, and local weather networks and can be found at: http://rcc-acis.unl.edu/index.php

Observed weather data is also used rather than gridded reanalysis because of producers mentioning having high confidence in observed weather data and a stronger connection to observed weather data.

While the time frame of 1980-2010 seems short for statistical analysis and raises the issue of uncertainty in results, 30 years of temperature and precipitation data have been deemed by the World Meteorological Organization (WMO) as a sufficient amount of time to capture longer climatic trends while simultaneous filtering out variability and anomalies (e.g. Trewin 2007; Wright 2012). This suggests that climate variability and anomalies can be detected across shorter time frames, as discussed in the results section. It is recognized that the process of categorizing years by ENSO or AO episode for analysis further reduces the number of years (*n*) in each group (a breakdown of categorization for each analysis is provided for each teleconnection in supplemental materials); however, since variability is expressed as being detectable in the 31 years of data reviewed, it is felt that the sizes of the subgroups are sufficient to capture statistical significance. It is further noted that statistical significance and sample size are interlinked (Ellis and Steyn 2003). With a small *n* for subgroups of ENSO and AO, significance is kept high at a 90% CI. Furthermore, the number of climate divisions reviewed (106) and the number of climate divisions showing statistically significant relationships of temperature or precipitation by month due to ENSO or AO episode agrees with previous findings spanning longer time frames (highlighted in previous section) suggesting that 30 years is sufficient for variability detection from teleconnections. Loikith and Broccoli (2014) use a similar time fame to investigate modes of climate variability as well finding significant results in the 30-year data set. In the context of agronomic processes there is also a tradeoff between climatic time period and the agronomic crop yield which have technological influences. It is felt that because of this, the 30 year time period provides a good compromise of time to include both the climatic time period and use of more recent technology.

Historic yield data is obtained for the same years from the USDA's National Agricultural Statistics Service by crop reporting district level. The years 1980-2010 are selected for the following purposes: 1) The latest climatic normal period for comparison

is 1981-2010 and 2) the time frame is mostly post-Green Revolution (e.g., Fuglie 2012; Pingali 2012) with gains in production attributable to increases in total factor productivity allowing for easier detection of climate variability signals in crop production. Note that the crop yield data (reported in bushels per acre) showed significant autocorrelation (tested using the Durbin-Watson Statistic (Montgomery et al., 2006)). Therefore, the crop yields are detrended with a one year lag linear regression analysis to account for autocorrelation in this time series dataset. The regression model used to detrend the crop yield data uses the 2010 predicted yield as the benchmark yield. This accounts for technological improvements in agriculture that have positively influenced yield and makes any weather or climate impacts on annual yields more apparent.

ENSO and AO data are obtained from the National Oceanic Atmospheric Administration (NOAA)'s Climate Prediction Center (CPC). ENSO data can be found at: http://www.cpc.ncep.noaa.gov/products/analysis_monitoring/ensostuff/ensoyears.shtml and AO data can be found at: (http://www.cpc.ncep.noaa.gov/products/precip/CWlink/daily_ao_index/monthly.ao.index.b50.current.ascii.table). The Oceanic Niño Index (ONI) is used for ENSO events which is based on the three-month running mean of sea surface temperature (SST) in the Niño 3.4 region (5^{o}N-5^{o}S, 120^{o}-170^{o}W) centered on the 30-year base periods which are now updated every five years. Since the time of data collection for this project, some months and years classified as El Niño, La Niña, or neutral have changed due to efforts made to classify ENSO events on a moving 30-year base period (Lindsey 2013). The data is the representative of historic ONI episodes when collected in 2011/2012. Classification of months as El Niño, La Niña, or neutral episodes in this climatology are based on the three-month running mean of SSTs as classified in the historic ONI data using values of 0.5 or greater and -0.5 or less as warm (El Niño) and cold (La Niña) thresholds, respectively, with neutral events ranging from -0.4 to 0.4. Events are not further classified by -0.5 and +0.5 deviations into weak, moderate, or strong events for ease of use when product users are exploring the climatological data through the online tool interface. The same classification scheme is applied to the AO. The Arctic Oscillation is monitored through the application of an Empirical Orthogonal Function to

monthly mean sea level (1000-hPa) north of 20˚N and is characterized by the departure of atmospheric pressure from normal of one sign (positive or negative) in the Arctic to departure of atmospheric pressure of one sign (positive or negative) centered over the Midlatitudes (37-45˚). It is normalized through application of the standard deviation of the monthly index based period from 1979-2000 (Climate Prediction Center 2005). Seeing as the computational methodologies of ENSO and AO monthly values are departures from a base state and have been normalized through base-period centering (ENSO) and standard deviation of the monthly index from a base period (AO), the possibility of autocorrelation between consecutive months should be minimized and no further adjustments have been made to the dataset.

3.4.2 Methodology

3.4.2.1 ENSO/AO Climatology

To develop the ENSO/AO climatology, the monthly-averaged observed precipitation and monthly-averaged observed mean temperature by climate division is collected for the Corn Belt using cli-MATE. Separation of months into ENSO and AO by episode (warm, cold or neutral for ENSO and positive, negative, or neutral for AO) is completed manually based on historic data as classified through the ONI. The average value of monthly-observed mean temperature or monthly-observed precipitation by teleconnection and type of episode is determined to develop a general climatology of average observed monthly precipitation and monthly mean temperature by teleconnection episode classification. The data are analyzed using Analysis of Variance (ANOVA) approach at a 90% confidence interval (CI). Because ENSO and AO are each grouped into three different types of episode classifications, a simple t-test cannot be completed, as the population of each group is no longer equal. ANOVA analyzes the means of the three groups, determining through analysis of the each group's variance if the means of each group are equal or not. Simply stated, ANOVA is a generalization of the t-test to more than two groups (Devore 2003). Where ANOVA supports rejection of the null hypothesis (all means of the group are equal), the difference between the means among ENSO or AO episodes is large enough to suggest statistical significance between the

different mean temperatures and observed precipitation experienced during different ENSO and AO episodes. During months where ANOVA findings are found to be significant, the variable with significance (temperature or precipitation) is suggested to be considered with more weight during agroclimatic decision making. The average monthly mean temperature is investigated in this climatology instead of the average monthly maximum temperature and average monthly minimum temperature because growing degree day computation uses mean temperature in its formulation. While it is understood that mean temperature can fail to capture extreme maximum and minimum temperatures (e.g. Schlenker and Roberts 2009), keeping the climatology simple but still usable to agricultural decision making is the main goal of this project. Furthermore, since ANOVA compares groups of data creating discontinuous samples, autocorrelation of temperature and precipitation data is typically not a factor.

3.4.2.2 ENSO/AO Extremes Climatology

The monthly climatic summaries used for analysis of extreme data (number of days/month where $T_{max} \geq 90°F$, $T_{max} \leq 32°F$, $T_{min} \leq 32°F$, Prcp ≥ 0.1 inch, and Prcp ≥ 1.0 inch) are gathered from the National Climatic Data Center (NCDC) Image and Publication Center (IPC) Local Climatological Data (LCD) repository. All sites (specific locations, not CRDs) within the U2U 12-state domain with available data for the years 1980-2010 are queried. Spatially, the 62 cities span the Corn Belt in a broadly uniform manner, thus no spatial interpolation is undertaken. The annual summary for each year 1980-2010 is reviewed and data for the number of days per month is collected. These months are then further separated by ENSO/AO episodes and undergo ANOVA analysis at the 90% CI. While all sites have temperature data from 1980 onward, precipitation data broken down at number of days per month with observed precipitation greater than or equal to 0.10 and 1.0 inch are only available from 1993 (Kansas and Nebraska) or 1996 (all other states) onward. Thus, ENSO/AO monthly episode analysis had to be limited to a shorter number of years. The variables of $T_{max} \geq 90°F$, $T_{max} \leq 32°F$, and $T_{min} \leq 32°F$ are selected to assess teleconnection episode categorization (ENSO or AO) on heat stress, freeze, and frost damage, respectively, while Prcp ≥ 0.1 inch and Prcp ≥ 1.0 inch are selected to assess precipitation (0.10 inch has been deemed enough to break

through the vegetation canopy) and heavy precipitation events (1.0 inch breaks the vegetation canopy and provides sufficient soil moisture recharge in the top layer of soil), a similar approach to agroclimatic analysis in Negri et al. (2005).

3.4.2.3 ENSO/AO Climatology and Yield Analysis by Crop Reporting District

Teleconnections result in climate variability influencing weather patterns across the United States. The influence of climate variability teleconnections in the form of weather can influence the potential yield of planted crops for a given growing season because of the dependence of crop yields on temperature and precipitation during phenological development (Elmore 2013; Hanway 1963; Neilson 2012; Neilson 2013a). Instead of only analyzing the impact of teleconnection episode for an entire growing season, three separate time frames are assessed: 1) average ENSO and AO episode categorization for the growing season (April – October); 2) average ENSO/AO episode categorization during the beginning months of the growing season (April, May, and June); and 3) average ENSO/AO episode categorization during the months of crop silking, grain-fill, and beginning of maturity (June, July, and August) (Neilson 2013b). The average episode classification of each teleconnection for each year spanning the specified time period is correlated to the historic, detrended yield time series at crop district level for each state in the Corn Belt to test for potential teleconnection influence on crop yield. Two-tailed significance is tested at the 90%CI for each crop reporting district.

3.5 Results

3.5.1 Climatology

The results of ENSO and AO climatology development by the state climate division level is expected to provide information of monthly-averaged observed precipitation and monthly average observed mean temperature for forecasters and agriculture producers. ENSO and AO climatologies and spatial impacts are analyzed separately; however, it is known that the two teleconnections can act synergistically. The intent of this separated analysis is to highlight the impact of each teleconnection on climate and agricultural production. Most climate divisions show distinct differences

between teleconnection episodes. A composite analysis of the two teleconnections will be completed after initial testing of the online decision support tool and will be discussed in a future study. The developed climatology values are not represented as above or below climatological normal because the computation of climatological normal values includes all episodes of each teleconnection. The average values of the three possible episode classification are compared to each other (negative, neutral, or positive). Seasonal climatologies for winter (December, January, and February), spring (March, April, and May), summer (June, July, and August), and fall (September, October, and November) are developed as well and are provided as supplemental material for conciseness.

3.5.1.1 Teleconnection Impacts to Temperature and Precipitation - ANOVA

The spatial distribution of temperature and precipitation across the Corn Belt is impacted by the different ENSO and AO episodes as classified in this study. Some climate divisions in a state are impacted significantly (90% CI) while others are not. Impacts from each teleconnection are broadly similar, affecting temperature and precipitation patterns during the seasonal transition months of spring and early summer and the seasonal transition months of late summer into early fall except with ENSO which has a large impact on mean temperatures during the month of December. Findings show more detailed information on the spatial distribution of ENSO and AO impacts across the Corn Belt rather than a general state or regional application of findings that may be too broad in scope as found in prior work which has utilized more spatially coarse data sets (such as state-level data). This can potentially enhance smaller-scale spatial variability of weather and climate patterns that may be present with specific teleconnections being missed by larger-scale analysis. These findings provide more of a localized climatology instead of a regional climatology to end users.

The figures referred to in the following sections provide a map detailing ANOVA significance for one month of mean temperature or average observed precipitation data for simplicity. Each parameter analyzed and discussed results in numerous maps. A comprehensive review of maps showing the different teleconnection episodes and impacts to temperature and precipitation will be available through the online decision

support tool user interface (http://agclimate4u.org). The detailed development, usability, and applicability of this interface for improved agronomic decision making will be the focus of a future paper.

3.5.1.1.1 El Niño Southern Oscillation

Monthly mean temperatures are impacted by ENSO primarily in August, October, and December (fall and winter months). These impacts are concentrated in climate divisions in the states of Illinois (December), Indiana (August, October, December), Michigan (August, October, and December), Wisconsin (August, October, and December), Minnesota (August, October, and December), Iowa (August and December), North Dakota (December), South Dakota (December), Nebraska (December), and Missouri (October and December). July mean temperatures are also episode-dependent, but spatially do not impact a cohesive sub-region of the domain (Figure 3.1). These temperature relationships likely result from the shift of the Polar Jet Stream farther north of the U.S. Corn Belt during El Niño events allowing warmer air to advect northward into these regions. During a La Niña event, the Polar Jet Stream is more meridional due to blocking high pressure over the north-central Pacific Ocean, resulting in a trough over the eastern half of the United States (Climate Prediction Center 2005 and references therein).

The most notable precipitation impacts due to ENSO are during the month of September across the Ohio River Valley (parts of Illinois, Indiana, Ohio, and far southeast Michigan) which may share a link to the number of land-falling tropical cyclones that migrate across the region during different ENSO episodes. The probability of two or more hurricanes making landfall in the United States during an El Niño year is 28% where as in a neutral or La Niña year it is 48% and 66%, respectively (Bove et al. 1998). Furthermore, findings from Kellner et al. (2015, submitted) show that land-falling hurricanes that impact the Midwest occur most frequently in the month of September and occur most frequently during neutral ENSO events, followed by La Niña years. Precipitation is impacted as well in February across northern Michigan (CDs 1-6) along with northeast and central Indiana (CDs 3-6). March precipitation is episode-dependent across western Iowa (CD 1, 4, and 7) and much of Nebraska (minus CD 7), northwest Kansas (CDs 1 and 2), and CD 8 in South Dakota (Figure 3.2).

3.5.1.1.2 Arctic Oscillation

ANOVA results show significant ENSO related impacts on average monthly observed mean temperatures in the months of March, April, July, August, October, November, and December in climate divisions and states in the Corn Belt. The AO statistically influences March mean temperatures in Illinois, Indiana, Ohio, Michigan, southeast Wisconsin (CD 3, 5-9), western Kansas (CDs 1, 4, and 7), and southeast Missouri (CDs 2, 5, and 6). April mean temperatures are significantly influenced by the AO in northern Illinois, northeast Indiana, far northwest Ohio, Michigan, Wisconsin, Minnesota, Iowa, North Dakota, and most of South Dakota (CDs 1- 3 and 6 -9). Summer months appear to be impacted by the AO as well. The difference between the average mean temperatures by AO episode during the month of July is found to be statistically significant in the states of Ohio (CDs 2, 3, 6, 7, and 10) and Michigan (CDs 4-10). August mean temperatures are significantly impacted by the AO across the northern climate divisions of the Corn Belt: CDs 1-3 in Illinois, CDs 1-5, 7, and 8 in Wisconsin, all of Minnesota, CDs. 1, 2, and 4-7 in Iowa, all of North Dakota, CDs 1-3, 7, and 9 in South Dakota, and finally eastern Nebraska (CDs 3, 6, and 9). During fall months, October, by far, experiences the largest spatially different mean temperatures by AO episode, with a statistical significance in average observed mean temperature by episode impacting all or portions of states in the Corn Belt. November mean temperatures are impacted in Illinois (CDs 4, 5, and 7), Indiana, Ohio, and southern Michigan. December mean temperatures are impacted in Illinois, Indiana, Ohio, southern Michigan, and the southeast half of Missouri (Figure 3.3).

Precipitation patterns are also influenced by the AO, however not to the spatial and temporal scale of mean temperatures. The AO primarily impacts average observed precipitation during the spring and fall months of March, April, October, and December in states across the Corn Belt. March precipitation is significantly impacted across southwest Ohio (CDs 1, 4-8, and 10), southwest to northeast through central Wisconsin (CDs 3, 5, 7, and 8) and northeast Minnesota (CDs 3 and 6). April impacts skirt the northern climate divisions of Michigan (CD 1), Wisconsin (CD 2), and Minnesota (CDs 1, 2, and 5). October precipitation is found to be significantly impacted across southern

Indiana (CDs 5-9) and much of Ohio (minus CDs 3, 6, and 7). This southwest to northeast orientation of observed precipitation significance across Indiana and Ohio is suggestive of a possible shift in the Polar Jet Stream/mean storm track due to changes in AO pressure oscillations. States having precipitation significantly influenced by the AO during the month of December include Kansas (CDs 1-3, 5, 6, 8 and 9), northwest Missouri (CDs 1 & 3), Indiana (CDs 1, 2, 8 and 9), Ohio (CDs 5 and 8), and northeast-central Illinois (Figure 3.4).

3.5.1.2 Teleconnection Episodes and Historic Crop Yields - Correlation

Agroclimatology shows that temperature and precipitation are the primary meteorological variables that impact corn growth and phenological development, with the potential for temperatures having slightly more of an impact than precipitation over the length of the growing season (e.g., Kellner and Niyogi 2014). However, precipitation is highly important, especially during the grain-fill period, thus it cannot be considered less of a contributor to yield production compared to temperature (Niyogi and Mishra 2012). Knowing that teleconnections influence climate variability, it is important to review the impacts of ENSO and AO on historic corn yield. AO is found to have a stronger impact than ENSO on the detrended yield time series for the period 1981-2010. Because the detrending methodology introduces a one-year lag, the regression analysis is completed for the years 1981-2010, while ANOVA analysis and the climatology development includes the years 1980-2010.

3.5.1.2.1 El Niño Southern Oscillation

ENSO has minor impact on the one year lag detrended yield time series when analyzed through correlation analysis (90% CI) at the crop reporting district level (CRD) for the three different time frames considered across the growing season. A more detailed analysis of the ENSO impacts on the observed and agroclimatic model simulated crop yields for the study domain is reported in Niyogi et al. (2013 and 2014).

3.5.1.2.2 Arctic Oscillation

The AO is found to have a larger impact on the detrended yield time series using correlation analysis. Significance is found at 90%, CI across states, across several of the different time frames analyzed in this study, and across more than one CRD in a state. This highlights the role of the AO in short-term climate variability and its possible impacts on agricultural production across the US Corn Belt. For the months of April – October and June, July, and August, all relationships are negatively correlated. For the months of April, May, and June, the relationship is positively correlated. Table 3.1 provides all states, time frames, and statistically significant findings between the average AO episode for the specified time frame and detrended yield time series at the 90% CI. Relationships as presented in Table 3.1 indicate that the more positive the AO signal, the lower the yield and the more negative the AO signal, the higher the yield for late summer and the growing season. A positive relationship between AO and yield exists in spring meaning that a positive AO would result in higher yields and a negative AO would result in reduced yields. The negative relationship found during the months of June, July, and August suggest 1) a positive AO signal results in decreased yield or a negative AO results in increased yields. The work of Hu and Feng (2010) identify that a negative AO episode in summer results in more summer rainfall due to the stronger transverse circulation in the Polar Jet and that a positive AO episode in summer results in less rainfall in the Central United States. The findings of Hu and Feng (2010) and the June, July, and August AO episode relationship with crop yields identified by this climatology support each other in that increased rainfall during silking and grainfill periods could likely contribute to result in historically higher yields. Table 3.2 highlights those states with climate divisions that have the highest average amount of observed precipitation during warm season months while the AO is in a negative episode.

3.5.1.2.3 AO and ENSO Crop Anomaly Analysis

Detrended yield time series values are taken as an anomaly above or below the CRD mean for the 1981-2010 period to assess whether historic crop yields, when grouped into ENSO or AO episodes, are above or below mean historic trend similar to

Hansen et al. (1998). For simplicity, anomalies of the detrended yield time series are binned into annual ENSO events (either El Niño, La Niña, or neutral as previously defined), average ENSO episode by growing season (April – October), and average AO signal for the growing season. While ENSO events have been named as "years" (i.e., the 1997-1998 El Niño year/event), the AO is not classified as such because the teleconnection varies on a weekly to monthly timescale. Thus, the AO anomalies are only binned by the average AO signal for the growing season.

Results for ENSO years/episodes generally agree with those of previous findings (e.g., Carlson et al. 1996; Hollinger et al. 2001; Mauget and Upchurch 1999; Rosenzweig 2001 and those studies mentioned therein) in that El Niño years experience higher than average yields in much of Missouri, Kansas, Minnesota, the southern two-thirds of Ohio, Iowa, central Michigan, Wisconsin, Nebraska, North Dakota and South Dakota. However, Indiana and Illinois have seen larger yields during ENSO neutral episodes. During a La Niña episode, all of these states and/or regions of these states experience lower than average yields. A slight difference is present in the northern two-thirds of Michigan and Wisconsin, Minnesota, North Dakota and South Dakota. These states experience lowest yields during ENSO neutral episodes.

Analysis of detrended yield time series crop anomalies for the average *growing season* ENSO episode changes yield anomalies so that in Illinois, Indiana, and Ohio, yields are lowest during El Niño episodes and highest during ENSO neutral episodes. Michigan and Wisconsin do not shift much except in the northern two-thirds of the state which experiences lowest yields during an ENSO neutral or La Niña event. Minnesota shifts so that lowest yields to occur during La Niña episodes instead of during neutral episodes. Growing season analysis for Iowa changes so that higher yields occur during ENSO neutral events. Kansas reveals no favored ENSO phase for higher or lower than normal years. Missouri shows lowest yields occurring during El Niño episodes in most CRDs and highest yields occurring during La Niña or neutral episodes. Growing season yield anomalies in the Dakotas become more variable with no trend except that an ENSO neutral to El Niño episode predominantly reduces yield. The yield anomaly for Nebraska when reviewed by growing season shows that lowest yields occur during El Niño

episodes and highest yields occur while in an ENSO neutral episode during the growing season.

AO anomalies of detrended yield time series show much larger variability above or below trend. However, results remain inconclusive due to the AO signal being predominantly neutral through the time period (1 year AO negative and 2 years AO positive) and the fact that much larger than normal yields occurred during the two AO positive years and greatly reduced yields occurred during the one AO negative year. This creates a large bias towards neutral episode events and the anomalous yields in AO negative and positive years. Table 3.3 provides a summary by state and crop reporting district ENSO and AO yield anomalies by episode of each teleconnection for the growing season. Differences between crop anomalies when looking at annual AO episode values versus growing season values are that a positive or negative AO episode results in reduced yields and largest yields occur during AO neutral episodes.

It is seen in this analysis of growing season versus annual episode that the time frame in which the detrended yield time series is analyzed by ENSO and AO episodes determines detrended yield time series crop anomalies. The authors wish to express that these findings are not of magnitude to warrant making a prognostic decision of above or below normal yields based on the average growing season or average annual forecast of ENSO or AO episode. Rather, the general trends of above or below normal yields based on identified weather conditions could continue be considered more heavily in the decision making process. The quantitative yield anomalies will also be dictated by agronomic practices such as planting dates, seed characteristics, and technology. Therefore, while ENSO or AO signatures may not translate or often times not be the dominant drivers for the quantitative statistically significant anomaly, we assert the qualitative trends are still useful. One such example of a qualitative trend is the strong La Niña (warmer and drier conditions) that contributed to the anomalously warm spring of 2012 and earlier than normal planting dates.

3.5.2 Extremes Climatology

Takle et al. (2014) highlight climatic conditions throughout the year and the needed weather and seasonal forecast content that affects corn production. Among these weather conditions are soil moisture, extreme heat, frost damage, growing degree days, extreme weather, and early freezes before harvest [McKeown et al. (2006) and Elmore (2013) provide a general review of such conditions]. The goal of developing this 'extremes' climatology for ENSO and AO episodes is to investigate the occurrence of such events as related to a given episode so that producers can be better acquainted about the potential likelihood of occurrence of warmer day time maximum temperatures (heat stress), increased likelihood of experiencing a frost or freeze event (damage to newly planted crops), or increased/decreased frequency of heavy rainfall events (applications of nitrogen, irrigation). The variables $T_{max} \geq 90°F$, $T_{max} \leq 32°F$, $T_{min} \leq 32°F$, Prcp $\geq$ 0.10 inch, and Prcp $\geq$ 1.0 inch show statistically significant findings at the 90% CI with ANOVA across spatial scales spanning locations either broadly across the Corn Belt or impacting as few as one location in the Corn Belt. These extremes are impacted by both teleconnections with both similar and as well as different statistical relationships. Only those impacted CDs with neighboring impacted CDs (essentially a sub-region) are included in discussion for brevity.

3.5.2.1 EL Niño - Southern Oscillation

3.5.2.1.1 Extreme Event Frequency-ANOVA

El Niño Southern Oscillation episodes do appear to impact the average number of days per month of extreme precipitation amounts and temperatures occurring in the Corn Belt. Precipitation is impacted significantly (90% CI, ANOVA) during the months of April (Prcp $\geq$ 1.0 inch), July (Prcp $\geq$ 0.10 inch), September (Prcp $\geq$ 0.10 inch and Prcp $\geq$ 1.0 inch.), and November (Prcp $\geq$ 0.10 inch). Temperatures are impacted significantly in March ($T_{min} \leq 32°F$), September ($T_{max} \geq 90°F$), October ($T_{max} \leq 32°F$), and December ($T_{max} \leq 32°F$). Figures 3.5 and 3.6 show the regional, sub-domain-scale distribution of these variables.

3.5.2.1.2 Extreme Event Frequency Impacts to Historic Yield-Correlation

To determine if the average frequency of monthly extreme events during a given ENSO episode impacts detrended yield time series, correlation is completed between yields and the average number of days per month an extreme event occurs by ENSO episode. The number of days per month $T_{max} \geq 90°F$ shows a moderate, positive relationship during the month of May in an El Niño episode and a negative impact in during an El Niño August. March and October during all ENSO episodes are the primary months having moderate to strong negative relationships between detrended yield time series and the average number of days per month $T_{max} \leq 32°F$ (indicating reduction in yield the more days per month that experience freezing temperatures). This highlights the vulnerability of freezing temperatures impacting field conditions during early spring (delayed planting dates) and also potentially impact harvest in fall through frost or freeze damage. $T_{min} \leq 32°F$ results in moderate to strong negative relationships during all ENSO episodes.

Positive, moderate to strong correlations exist between the average number of days per month Prcp ≥ 0.10 inch during an El Niño June (less average observed precipitation compared to the other two episodes) and a neutral August when correlated to historic detrended yield time series. A neutral ENSO episode in August has the strongest correlation to yields having on average one more day per month Prcp ≥ 0.10 inch across the Corn Belt. The average number of days per month where Prcp ≥ 1.0 inch when correlated to detrended yield time series has weak, positive correlations to La Niña Aprils and weak to moderate positive correlations during La Niña Augusts.

3.5.2.2 Arctic Oscillation

3.5.2.2.1 Extreme Event Frequency-ANOVA

Statistically significant impacts of the Arctic Oscillation are seen at sub-regional scales across the Corn Belt as well. The number of months impacted by each type of extreme event is greater than ENSO. Precipitation is impacted significantly during the months of February, March, April, June, and September when analyzed for the number of days per month Prcp ≥ 0.10 inch and the month of March when analyzed for number of

days per month Prcp ≥1.0 inch. Extreme temperatures are impacted by the AO in months preceding planting dates or after crops begin maturing: $T_{max} \geq 90°F$ (September), $T_{max} \leq 32°F$ (January, April, October, November, and December), and $T_{min} \leq 32°F$ (March, April, October, November, and December). Figures 3.7 and 3.8 show maps of these findings.

3.5.2.2.2 Extreme Event Frequency Impacts to Historic Yield-Correlation

Like ENSO, correlation of extreme events by episode of each teleconnection to detrended yield time series is completed to see if a relationship is present between the average number of days per month a given parameter occurs and yield. Only statistically significant relationships (95% CI) are discussed. Correlation analysis shows that a negative AO in August and a neutral AO in May are important months to consider the number of days $T_{max} \geq 90°F$. A negative AO in August has a negative, weak correlation (less days $T_{max} \geq 90°F$, higher the yield), and a neutral May has a positive relationship in that more days with $T_{max} \geq 90°F$, the higher the yield. The months of April, May, and September all show moderate to strong negative correlations with $T_{min} \leq 32°F$ with no AO phase taking dominance over other episodes. However, May (all phases) has the strongest relationship with the number of days $T_{min} \leq 32°F$. The relationship apparent through analysis is that the larger the number of days in May $T_{min} \leq 32°F$, the lower the yield – or – the less number of days $T_{min} \leq 32°F$, the higher the yield.

Analysis of historic detrended yield time series and precipitation highlights no relationship between historic yields and the average number of days per month Prcp ≥ 0.10 inch. The average number of days per month Prcp ≥ 1.0 inch has the strongest, positive correlations during the months of April, May, and July. A neutral episode during the month of April has a moderate to strong positive relationship and a positive episode in May has a weak to moderate positive relationship between the number of days per month Prcp ≥ 1.0 inch and yield.

3.5.3 Relating Climatological Findings to Agronomic Decision Making and Yield Impacts

ANOVA for meteorological season is completed (spring: March, April, and May; summer: June, July, and August; fall: September, October, and November; and winter: December, January, and February) and briefly discussed in terms of teleconnection episodes (AO: positive, negative, or neutral; ENSO: El Niño, La Niña, or neutral) and which episode leads to the wettest or driest and warmest or coldest conditions during that season. Findings are then briefly discussed in terms of impacts to agronomic decision making. Specific climate divisions and data can be viewed in the supplemental material. A more detailed spatial and temporal analysis (maps and bar graphs by month and episode) of ENSO and AO influences to weather patterns and how these weather patterns may in turn affect agronomic decision making will be discussed in more detail in a follow up paper. This paper is intended to prepare and analyze the meteorology/climatological data that can be used for the development of an online tool to help agricultural stakeholders make more informed decisions.

The statistically significant spatial and temporal influence of the AO on mean temperatures and precipitation across the domain during the seasons of spring, summer, and fall are broad in scope for mean temperatures and more focused into sub-regions of the domain for precipitation. The difference of average mean temperatures and mean observed precipitation between episodes is also greater when binned into AO episodes than ENSO episodes.

3.5.3.1 ENSO Seasonal Impacts and Agronomic Decision Making

3.5.3.1.1 Mean Temperatures

Compared to AO, ENSO episodes impart less spatial and temporal influences to weather patterns across the U.S. Corn Belt. Spring shows no statistically significant relationships for mean temperatures through ANOVA analysis. Summer temperatures are warmest during La Niña summers across Minnesota, Wisconsin, Michigan, Iowa, northern Illinois, and the northern two-thirds of Indiana. This suggests that during

summer in these locations, crops may be more likely to experience heat stress, which may reduce yield (as discussed in previous studies). Provided rainfall is below normal during this time, evapotranspiration rates may be enhanced, putting crops under moisture stress which may be alleviated through irrigation scheduling. A few climate divisions in far east Nebraska, central and southeast Kansas, and Missouri (CDs 1 and 6) are on average warmest during neutral ENSO episodes in summer. However, average temperatures are within several tenths of a degree to the La Niña average temperature. During summer mean temperatures are coolest during an El Niño episode for the same locations. Cooler temperatures could be indicative of less heat stress on crops, likely boosting yield if adequate GDDs are met (as also discussed in previous studies). Fall, like spring, shows no statistically significant relationships between ENSO episodes and mean temperature.

3.5.3.1.2 Average Observed Precipitation

Statistically significant relationships for precipitation are not present during spring and are minimal during summer (3 of 106 climate divisions). Fall has statistically significant precipitation relationships focused around the Great Lakes region in northwest and central Indiana, southern Michigan, and north-central and northeast Ohio. During an ENSO neutral episode, these CDs are on average the wettest during the fall, and are driest during La Niña episodes. In this region, farmers may consider delayed harvest during ENSO neutral events due to wet fields and delayed dry-down of crops. A La Niña episode may allow a producer to plan for earlier harvest due to drier conditions. Figure 3.9 provides a flow chart example of how this climatology and embedded information may be used in a decision making process and the DST is being developed.

3.5.3.2 Arctic Oscillation Seasonal Impacts and Agronomic Decision Making

3.5.3.2.1 Mean Temperatures

As related to agricultural decision making, spring is warmest across the domain when the AO is in a neutral episode. The coldest mean temperatures in spring occur during a negative AO episode across the southern two-thirds of the domain and across the roughly northern one-third of the domain during a positive AO episode. Thus, a neutral AO episode would provide for possibly earlier planting dates while a negative AO in the

spring could delay planting by several weeks. Summer mean temperatures are coolest across the domain when the AO is in a negative episode, and predominantly warmest when the AO is neutral, except in the far northwest and western edge of the domain. An AO neutral episode in summer may provide greater chance of heat stress on crops (and possible need for compensative irrigation), while cooler temperatures with a negative AO during the summer may inhibit temperatures needed for full crop development potential. Fall temperatures are coldest across the domain except for North and South Dakota when the AO is negative (possibility for earlier frosts) and warmest when the AO is in a neutral episode (better dry down conditions with little delay in harvest dates).

3.5.3.2.2 Average Observed Precipitation

The AO results in statistically significant precipitation relationships predominantly located over the central portions of the domain during the spring and the periphery of the domain during the fall. During the spring, precipitation is highest during a neutral AO across the central part of the domain (roughly Minnesota, Wisconsin, west-central Michigan, Iowa, southeast Nebraska, and northwest Missouri) which may lead to delayed planting due to increased soil moisture and soil compaction that inhibits field work days. The least amount of precipitation occurs during a negative AO in the aforementioned states. ANOVA of summer precipitation by AO episode results in only two of 106 CDs having noteworthy relationships. Fall precipitation is influenced by the AO predominantly during positive AO episodes and negative AO episodes, with wettest and driest conditions nearly opposite of each other. Western North Dakota and the far north-central region of the domain are driest in fall when the AO is positive (more suitable for timely crop dry-down and harvest) and wettest when the AO is neutral (delayed dry-down and harvest). Those climate divisions in Indiana and Ohio near-to (Ohio CDs 4 and 5) and bordering the Ohio River are wettest during a positive AO episode (delayed dry-down and harvest) and driest in a neutral AO episode (timely crop dry-down and harvest).

3.6 Conclusions

Climate change projections indicate shifts in regional/global climate and increased climate variability. This ENSO and AO climatology explores the weather and climate information applicable to producers in the U.S. Corn Belt/ North Central region that will be implemented into a decision support tool for agricultural producers to make more informed agronomic decisions. Climate variability in the form of precipitation and mean temperature is analyzed for each teleconnection across the U.S. Corn Belt with analysis completed for historic detrended corn yield time series down to the climate division/crop reporting district level. ENSO and AO are studied because of the temporal impacts of each teleconnection. It has been noted that ENSO impacts weather over several months whereas AO impacts weather patterns for several weeks. No gridded or reanalysis datasets are used in this study to maintain the integrity of historically-observed weather data and the agricultural producers' preference to utilize station data rather than gridded products. Findings of significance occur from single climate divisions/crop reporting districts, to sub-regional (i.e., smaller regions within a 12-state domain), and near-regional spatial scales.

This climatology explores the common climatological variables of mean temperature and precipitation while also exploring extreme events. Analyzing two temporally different teleconnections and finding similar, yet unique feedbacks highlights the importance of understanding climatological feedbacks across the Corn Belt. ANOVA analysis of ENSO and AO episodes by climate division shows the significance (or non-significance) of shifts in temperature and precipitation patterns as associated with ENSO and AO with AO impacts emerging more frequently (e.g., by month) throughout the year in this analysis. Previously discussed studies tend to highlight seasonal changes. ANOVA of extreme events ($T_{max} \geq 90°F$, $T_{max} \leq 32°F$, $T_{min} \leq 32°F$, $Prcp \geq 0.1$ inch, and $Prcp \geq 1.0$ inch) by ENSO/AO episode provides similar results. These findings show a need for more detailed information on the sub-regional spatial distribution of ENSO and AO impacts across the Corn Belt rather than a general state or regional application of findings which appears too broad in scope or value for agronomic decision making.

The most significant impacts of ENSO and AO (according to ANOVA) occur during the spring, fall, and winter months which lie outside the primary months of the production/growing season (April – October) suggesting indirect impact to crop production/yield. Correlation of each teleconnection and episode across different time frames (April-June, June-August, and April-October) to historic detrended yield time series at Crop Reporting District level shows that the AO affects historic yield (either positively or negatively). The consistent relationship with AO is that a more positive the AO phase in spring the higher the yield. For summer and the growing season, the more positive the AO Phase, the lower the yield and the more negative the AO phase, the higher the yield. Evaluation of historic detrended yield time series above or below trend when grouped by ENSO episodes agree with prior studies in that yields are historically greater than average during El Niño years and less than average during La Niña years. Historic yields when binned by the average ENSO episodes during the growing season results in similar findings. The average AO episode during the growing season shows inconclusive results due to a majority of seasons being in a neutral episode. While the quantitative yield anomalies found in this climatology are also dictated by agronomic practices such as planting dates, seed characteristics, and technology, it is felt that the general trends of above or below normal yields based on identified weather conditions could be considered in the decision making process. Therefore, while ENSO or AO signatures may not translate or often times not standout as the dominant drivers for the quantitative statistically significant anomaly, we assert the qualitative trends could still be useful for the agronomic decision making at local scales. The monthly frequency of extreme temperatures and precipitation when correlated to historic detrended yield time series demonstrate that month-specific teleconnection episode and impacts to daily rainfall and temperature is important to production as well and can be of value in decision making.

As part of the U2U project, the goal of this climatology is to investigate the hydroclimate of the U.S. Corn Belt. The data herein is currently being developed into an online decision support tool for cereal producers and other applied users so that they will be able to make more informed production decisions in the light of climate variability and

change. The climatology by design is simple in scope (averaging of observed weather variables, using only 30 years of weather, climate, and crop data, and basic statistical analysis) so that applied users can understand and use the data. This climatology is also intended to convey the importance of understanding spatial and temporal relationships of teleconnections such as ENSO and AO and how they impact agro-climatic patterns affecting yield potential in a growing season. It is clear through the different spatial and temporal agro-climatic impacts of AO episodes (broad in scope for mean temperatures and more focused into sub-regions of the domain for precipitation) and ENSO episodes (impacts are more concentrated across the central portions of Corn Belt) on seasonal mean temperatures and precipitation that further investigation could benefit from analyzing additional teleconnections that influence Midlatitude weather regimes so that an optimal understanding of climate variability can be communicated to producers. Findings further show that the AO imparts greater variability (mean observed precipitation and average observed mean temperature) between episodes than ENSO. The findings herein and planned analysis with development into an online tool will allow for better mitigative and adaptive efforts by producers that will help maximize yield as the world shifts towards climate uncertainty. The primary goal of this paper is to develop the data and climatological framework that can be translated into useful information for stakeholders.

The sub-regional impacts found in the climatology show the need for higher-resolution analysis of ENSO and AO impacts in order to help provide a predictive potential at finer scales (i.e., county level) when the ENSO or AO episode is known in advance. ENSO forecasts and discussions are readily issued by agencies around the world (Zebiak et al. 2014) potentially providing sufficient lead time for users to make informed decisions provided the forecast is issued in a timely manner and verifies (Takle et al. 2014). Because the AO is a teleconnection influencing weather and climate variability across shorter time frames, its predictability is less certain and is only forecast about two weeks out. This limits applicability by users to make informed decisions for the longer term, but still provides applicability in short term decision making such as increased likelihood of a frost or freeze event or episodes of heat stress over the next 14

days. With the goal of this climatology and DST to result in more effective decision making by the user in light of climate variability and change by using existing data and models (agclimate4u.org), the uncertainty associated with timely forecast issuance for climate variability indices is not reduced or removed through this climatology and associated DST. Rather the climatology and DST is developed so that climate variability is better understood by users to make more informed decisions with current weather and climate data when it is made available.

Acknowledgements: We thank Jim Angel - Illinois State Climatologist and Doug Kluck - NOAA's Central Region Climate Services for review of this manuscript. Additional acknowledgment goes to the Climate Pattern Viewer decision support tool development team: Pat Guinan- Missouri State Climatologist, Dennis Todey- South Dakota State Climatologist, Chad Hart - Iowa State University Extension Specialist, Beth Hall – Midwest Regional Climate Center, Jeff Andresen – Michigan State Climatologist, Tapan Pathak – University of Nebraska at Lincoln, Carol Song, Larry Biehl, Lan Zhao, and Melissa Widhalm - Purdue University. Useful to Usable (U2U) Transforming Climate Variability and Change Information for Crop Producers and Development of a High-Resolution Drought Trigger Tool (HIRDTT) for the United States; Agriculture and Food Research Initiative Competitive Grants 2011-68002-30220 and 2011-67019-20042 from the USDA National Institute of Food and Agriculture (NIFA). Project website is http://www.AgClimate4U.org.

3.7 References

Adams, R., C. Chen, B. McCarl, and R. Weiher, 1999: The economic consequences of ENSO events for agriculture. Climate Research 13 (3), 165-172.

Arbuckle, J.G., L.S. Prokopy, T. Haigh, J. Hobbs, T. Knoot, C. L. Knutson, A. Loy, A.S. Mase, J. McGuire, L.W. Morton, J. Tyndall, and M. Widhalm, 2013: Corn Belt farmers and climate change: Beliefs, perceived risk, and support for action. Climatic Change Letters, 117(4), 943-950.

Bove, M.C., J.B. Elsner, C.W. Landsea, and X. Niu, 1998: Effect of El Niño on U.S. landfalling hurricanes, revisited. Bull. Amer. Meteor. Soc., 79 (11), 2477-2482.

Brunner, A., 2002: El Nino and world primary commodity prices: Warm water or hot air? Review of Economics and Statistics, 84 (1), 176-183.

Carlson, R., D. Todey, and S. Taylor, 1996: Midwestern corn yield and weather in relation to extremes of the Southern Oscillation. J. Production Agric., 9 (3), 347-352.

Climate Prediction Center Internet Team, 2005: The ENSO Cycle. National Weather Service Climate Prediction Center. College Park, Maryland, 19 December 2005 http://www.cpc.ncep.noaa.gov/products/analysis_monitoring/ensocycle/enso_cycle.shtml. (Accessed 14 November 2014.)

Climate Prediction Center Internet Team, 2005: Teleconnection pattern calculation procedures: Arctic/Antarctic Oscillation. National Weather Service Climate Prediction Center. College Park, Maryland, 12 December 2005 http://www.cpc.ncep.noaa.gov/products/precip/CWlink/daily_ao_index/history/method.shtml. (Accessed 27 October 2014.)

Crane, T. A., C. Roncoli, J. Paz, N. Breuer, K. Broad, K. T. Ingram, and G. Hoogenboom, 2010: Forecast skill and farmers' skills: Seasonal climate forecasts and agricultural risk management in the southeastern United States. Wea. Climate Soc., 2, 44–59.

Devore, J.L., 2003: Probability and statistics for engineering and the sciences. Sixth Ed. Pacific Grove: Duxbury Press, 816pp.

Ellis, S.M., and H.S. Steyn, 2003: Practical significance (effect sizes) versus or in combination with statistical significance (p-values): research note. Management Dynamics: Journal of the Southern African Institute for Management Scientists, 12.4 p-51.

Elmore, R.W., 2013: Advances, Vulnerabilities, and Opportunities for Corn: A Perspective from Iowa. In: D. Niyogi (Ed.) Climate Vulnerability: Understanding and Addressing Threats to Essential Resources. Elsevier Inc., Academic Press, 3–15.

Fuglie, K. 2012: Productivity growth and technology capital in the global agricultural economy in Productivity growth in agriculture: An international perspective, Fuglie et al. Eds. Oxfordshire, England: CAB International, 335-368.

Goddard, L., S.J. Mason, S.E. Zebiak, C.F. Ropelewski, R. Basher, and M.A. Cane, 2001: Current approaches to seasonal to interannual climate predictions. Int. J. Climatol., 21, no. 9, 1111-1152.

Hansen, J.W., A.W. Hodges, and J.W. Jones, 1998: ENSO influences on agriculture in the Southeast United States. J. Climate, 11(3), 404-411.

Hanway,J.J., 1963: Growth stages of corn. Agron. J., 55: 487-492.

Hollinger, S.E., E.J. Ehler, and R.E. Carlson, 2001: Midwestern United States corn and soybean yield response to changing El Niño-Southern Oscillation conditions during the growing season. Amer. Soc. Agron. Special Publication no. 63. 31-54.

Hu, Qi and S. Feng, 2010: Influence of the Arctic oscillation on central United States summer rainfall. J. Geophys. Res. D. Atmos. 115.D01.

IPCC 5th Assessment Report - Stocker, T.F., D. Qin, G. Plattner, M.M.B. Tignor, S.K. Allen, J. Boschung, A. Nauels, Y. Xia, V. Bex, and P.M. Midgley, Eds., 2013: Climate change 2013 the physical science basis: Working group I contribution to the fifth assessment report of the Intergovernmental Panel on Climate Change. New York: Cambridge University Press, 1522 pp.

Kellner, O. and D. Niyogi, 2014: Agroclimatology. Encyclopedia of Natural Resources: Air. Doi: 10.1081-ENRA-120047622. http://www.tandfonline.com/doi/full/10.1081/E-ENRA-120047622#.VFKEn_ldXTo.

Kellner, O., D. Niyogi, and F. Marks, 2015: Land-falling tropical system contribution to the hydroclimate of the Midwest 1981-2012. *Wea. and Cli. Extremes,* Submitted.

Kravchenko, A.N. and D.G. Bullock, 2000: Correlation of corn and soybean grain yield with topography and soil properties. Agronomy J., 92, 75-83.

Legler, D., K. Bryant, and J. O'Brien, 1999: Impact of ENSO-related climate anomalies on crop yields in the U.S. Climatic Change, 42 (2), 351-375.

Lindsey, R. 2013. In Watching for El Niño and La Niña, NOAA Adapts to Global Warming. National Oceanic and Atmospheric Administration. ClimateWatch Magazine.http://www.climate.gov/news-features/understanding-climate/watching-el-ni%C3%B1o- and-la-ni%C3%B1a-noaa-adapts-global-warming. (Accessed 21 May 2014.)

Loikith, P.C. and A.J. Broccoli, 2014: The influence of recurrent modes of climate variability on the occurrence of winter and summer extreme temperatures over North America. J. Climate, 27, 1600-1618. doi: http://dx.doi.org/10.1175/JCLI-D-13-00068.1

Mase, A.S. and L.S. Prokopy, 2014: Unrealized potential: A review of perceptions and use of weather and climate information in agricultural decisions making. Wea. Climate and Soc. 6, 47-61.

Mauget, S.A., and D.R. Upchurch, 1999: El Niño and La Niña related climate and agricultural impacts over the Great Plains and Midwest. J. Prod. Agric., 12, 2, 203-215.

McKeown, A.W., J. Warland, and M.R. McDonald, 2006: Long-term climate and weather patterns in relation to crop yield: a mini review. Canadian J. Botany, 84(7), 1031-1036. doi: 10.1139/b06-080.

Melillo, J.M., T.C. Richmond, and G.W. Yohe, Eds., 2014: Climate change impacts in the United States: The third national climate assessment. U.S. global change research program, 841 pp. doi:10.7930/J0Z31WJ2. http://nca2014.globalchange.gov/. (Accessed 5 June 2014.)

Meza, F. J., J. W. Hansen, and D. Osgood, 2008: Economic value of seasonal climate forecasts for agriculture: Review of ex-ante assessments and recommendations for future research. J. Appl. Meteor. Climatol, 47, 1269–1286.

Montgomery, D.C., E.A. Peck, and G.G. Vining, 2006: Introduction to linear regression analysis, 4th edition. Hoboken: John Wiley and Sons. 504pp.

National Climatic Data Center (NCDC), 2014: Transitioning to a gridded climate divisional dataset. National Oceanic and Atmospheric Administration, Silverspring, Maryland. http://www.ncdc.noaa.gov/news/transitioning-gridded-climate-divisional-dataset. (Accessed 4 June 2014.)

Negri D.H., N.R. Gollehon, and M.P. Aillery, 2005: The effects of climatic variability on U.S. irrigation adoption. Climatic Change, 69, 299-323.

Neilson, R.L., 2012: Corn management for extreme conditions. Corny News Network Articles, Purdue University. http://www.agry.purdue.edu/ext/corn/news/timeless/extremecornmgmt.html. (Accessed 7 July 2014.)

Neilson, R.L., 2013a: When will my corn crop mature? Corny News Network Articles, Purdue University. http://www.agry.purdue.edu/ext/corn/news/articles.13/EstCornMaturity-0801.html. (Accessed 7 July 2014.)

Neilson, R.L., 2013b: Effects of stress during grain filling in corn. Corny News Network Articles, Purdue University. http://www.agry.purdue.edu/ext/corn/news/timeless/GrainFillStress.html. (Accessed 7 July 2014.)

Niyogi, D. and V. Mishra, 2012: Climate-agriculture vulnerability assessment for the midwestern United States. Climate Change in the Midwest: Impacts, Risks, Vulnerability and Adaptation. S.C. Pryor Ed. Bloomington: Indiana University Press, 69-80.

Niyogi, D.S., X. Liu, J. Andresen, A. Jain, A. Kumar, O. Kellner, and A. Elias, 2013: Can crop models simulate the ENSO impacts on regional corn yield in US Corn Belt? American Geophysical Union, Fall Meeting 2013, abstract #GC33A-1096.

Niyogi, D., X. Liu, J. Andresen, Y. Song, A. Jain, O. Kellner, E.S. Takle, and O.C. Doering, 2014: Crop models can capture the impacts of climate variability on corn yield. Geophys. Res. Lett., Submitted Nov. 2014.

Phillips, J., B. Rajagoplan, M. Cane, and C. Rosenzweig, 1999: El Niño-Southern Oscillation event-climate relationships; Climatic effects of maize. Int. J. of Climatol., 19(8), 877-888.

Pielke Sr, R.A., 2013: Climate vulnerability: Understanding and addressing threats to essential resources. Amsterdam: Elsevier Academic Press, 1570 pp.

Pingali, P.L., 2012: Green Revolution: Impacts, limits, and the path ahead. Proc. Natl. Academy Sci., 109.31. 2302–12308, doi: 10.1073/pnas.0912953109.

Reilly, J.M., 2002: Agriculture: The potential consequences fo climate variability and change for the United States. New York: Cambridge University Press, 150 pp.

Rosenzweig, C., 2001: Impacts of the El Niño-Southern Oscillation on agriculture: Guidelines for regional reanalysis. Amer. Soc. Agron. Special Publication no. 63. 21-30.

Rosenzweig, C., J.W. Jones, J.L. Hatfield, A.C. Ruane, K..J. Boote, P. Thorburn, J.M. Antle, G.C. Nelson, C. Porter, S. Janssen, S. Asseng, B. Basso, F. Ewert, D. Wallach, G. Baigorria, and J.M. Winter, 2013: The agricultural model intercomparison improvement project (AgMIP): Protocols and pilot studies. Agric. Forest Meteor., 170, 166-182. DOI: 10.1016/j.agrformet.2012.09.011.

Rosenzweig, C., J.W., Jones, J.L. Hatfield, C.Z. Mutter, S.G.K. Adiku, A. Ahmad, Y. Beletse, B. Gangwar, D. Guntuku, J. Kihara, P. Masikati, P. Paramasivan, K.P.C. Rao, and L. Zubair, 2012: The Agricultural Model Intercomparison and Improvement Project (AgMIP): Integrated regional assessment projects. In Handbook of Climate Change and Agroecosystems: Global and Regional Aspects and Implications; Hillel, D.; Rosenzweig, C., Ed.; Imperial College Press, Vol. 2, 263–280.

Schlenker, W. and M.J. Robers, 2009: Nonliner temperature effects indicate severe damages to U.S. crop yields under climate change. Proc. Natl. Acad. Sci. United States, **106: 37**, 15594-15598. doi: 10.1073/pnas.0906865106.

Takle, E.S., C.J. Anderson, J. Andresen, J. Angel, R.W. Elmore, B.M. Gramig, P. Guinan, S. Hilberg, D. Kluck, R. Massey, D. Niyogi, J.M. Schneider, M.D. Shulski, D. Todey, and M. Widhalm, 2014: Climate forecasts for corn producer decision making. Earth Interactions, 18-05, 1-8.

Trewin, B., 2007: The role of climatological normals in a changing climate. World Climate Data and Monitoring Program No 61, WMO-TD No 1377. http://www.wmo.int/pages/prog/wcp/wcdmp/documents/WCDMPNo61.pdf. (Accessed 14 October 2014) 46pp.

USDA, 2013: Crop Production. National Agriculture Statistical Service. 8 March 2013 http://www.epa.gov/agriculture/ag101/cropmajor.html (Accessed 3 June 2013.)

Wright, W., 2012: Discussion paper on the calculation of the standard climate normals: a proposal for a dual system. World Climate Data and Monitoring Program. http://www.wmo.int/pages/prog/wcp/wcdmp/documents/Rev_discussion_paper_May2012.pdf . (Accessed 14 October 2014) 5pp.

Zebiak, S.E., B. Orlove, Á.G. Muñoz, C. Vaughan, J. Hansen, T. Troy, M.C. Thomson, A. Lustig, and S. Garvin, 2014: Investigating El Niño-Southern Oscillation and society relationships. Wley interdisciplinary Reviews: Climate Change. doi: 10.1002/wcc.294.

3.8 Tables

Table 3.1: Correlation (90% CI) of average teleconnection episode 1981-2010 to detrended historic yields by growing season and sub-growing season intervals. "+" denotes a positive correlation and "-"denotes a negative correlation. Correlation of average ENSO episode and historic yields for specified time frames resulted in no relationships of significance. "NA" refers to those climate divisions in which crop yield data was not complete for the 1981-2010 period.

90% CI: Average AO Episode April - June & Yield, 1980-2010									
CRD	**10**	**20**	**30**	**40**	**50**	**60**	**70**	**80**	**90**
ND	NA	+		+		+	NA		+
SD			+			+			
NE				NA	+			+	
KS									
MO		+							
IA	+	+	+	+	+	+	+	+	+
MN		NA	NA	+	+		+	+	+
WI			+		+	+	+	+	+
IL	+		+	+	+	+			
IN									
MI									
OH									

90% CI: Average AO Episode June - August & Yield, 1980-2010									
CRD	**10**	**20**	**30**	**40**	**50**	**60**	**70**	**80**	**90**
ND	NA						NA		+
SD					-		-	-	
NE									
KS								-	-
MO			-						
IA									
MN		NA	NA						
WI									
IL							-	-	
IN									
MI									
OH				-					

90% CI: Average AO Episode April - October & Yield, 1980-2010									
CRD	**10**	**20**	**30**	**40**	**50**	**60**	**70**	**80**	**90**
ND	NA						NA		
SD									
NE				NA					
KS					-		-	-	-
MO	-		-	-	-	-	-	-	-
IA									
MN		NA	NA						
WI									
IL						-	-	-	-
IN	-	-	-	-	-	-	-	-	-
MI									
OH				-			-		

Table 3.2: Difference between average warm season rainfall for each AO episode at state climate division level to the average observed warm season rainfall for the respective state climate division. Bold numbers denote those states and climate divisions having the highest average observed warm season precipitation shown as a positive departure from the mean during a negative AO episode. Negative values indicate that the average warm season rainfall for that AO episode is below the warm season normal.

Above/Below Normal Average Observed Warm Season Rainfall (Apr. - Sept.) by AO Episode (1980-2010)											
CD		1	2	3	4	5	6	7	8	9	10
ND	Positive	-0.15	-0.22	-0.23	-0.08	-0.18	-0.07	-0.15	-0.21	-0.12	
	Negative	-0.20	-0.25	-0.16	-0.05	-0.05	-0.16	***0.13***	***0.06***	-0.08	
	Neutral	0.11	0.16	0.13	0.04	0.08	0.07	0.02	0.05	0.07	
SD	Positive	-0.30	-0.25	-0.06	-0.17	-0.22	-0.28	0.14	-0.10	-0.14	
	Negative	***0.30***	0.04	-0.30	***0.37***	***0.24***	***0.26***	-0.13	***0.15***	***0.05***	
	Neutral	0.02	0.07	0.11	-0.05	0.00	0.02	-0.01	-0.01	0.04	
NE	Positive	-0.23	-0.05	0.09		-0.07	-0.34	-0.09	-0.17	-0.64	
	Negative	***0.20***	***0.10***	-0.22		-0.01	-0.06	***0.19***	-0.16	0.15	
	Neutral	0.02	-0.01	0.04		0.03	0.14	-0.03	0.11	0.18	
KS	Positive	-0.30	-0.36	-0.73	-0.05	-0.34	-0.61	0.01	-0.11	-0.50	
	Negative	***0.24***	0.02	0.29	***0.06***	***0.22***	***0.39***	***0.08***	***0.36***	***0.69***	
	Neutral	0.03	0.12	0.17	0.00	0.05	0.10	-0.03	-0.07	-0.03	
MO	Positive	-0.65	-0.30	-0.52	-0.29	-0.16	0.31				
	Negative	***0.23***	***0.17***	***0.54***	***0.63***	***0.30***	-0.19				
	Neutral	0.16	0.06	0.02	-0.09	-0.03	-0.05				
IA	Positive	0.03	-0.26	-0.31	-0.16	-0.26	-0.61	-0.64	-0.61	-0.61	
	Negative	-0.36	-0.48	-0.19	-0.17	-0.04	***0.47***	***0.25***	0.13	***0.39***	
	Neutral	0.10	0.24	0.17	0.11	0.11	0.07	0.15	0.18	0.10	
MN	Positive	-0.01	0.07	-0.06	0.03	0.11	-0.02	0.15	0.05	0.05	
	Negative	-0.28	-0.53	-0.45	-0.37	-0.59	-0.66	-0.15	-0.32	-0.42	
	Neutral	0.09	0.14	0.16	0.10	0.14	0.21	-0.01	0.08	0.11	
WI	Positive	-0.05	-0.05	-0.17	0.06	-0.02	-0.10	-0.24	-0.05	0.19	
	Negative	-0.62	-0.37	-0.24	-0.47	-0.36	-0.28	-0.24	-0.30	-0.27	
	Neutral	0.20	0.13	0.13	0.12	0.12	0.12	0.16	0.11	0.01	
IL	Positive	-0.31	-0.01	-0.35	-0.11	-0.10	-0.05	-0.05	-0.04	0.07	
	Negative	***0.40***	***0.16***	***0.10***	-0.13	-0.05	-0.12	-0.02	***0.52***	***0.28***	
	Neutral	-0.01	-0.05	0.09	0.08	0.05	0.05	0.02	-0.14	-0.11	
IN	Positive	-0.19	0.03	-0.04	0.03	0.06	-0.10	0.12	0.02	-0.02	
	Negative	0.01	-0.11	-0.04	-0.06	-0.03	-0.01	***0.20***	***0.46***	***0.32***	
	Neutral	0.06	0.02	0.03	0.01	-0.01	0.04	-0.10	-0.15	-0.09	
OH	Positive	0.01	0.00	0.02	0.05	0.02	-0.10	-0.04	0.03	0.10	0.12
	Negative	***0.10***	***0.22***	***0.12***	-0.20	-0.07	***0.09***	***0.18***	***0.23***	***0.18***	***0.14***
	Neutral	-0.04	-0.07	-0.04	0.04	0.02	0.01	-0.04	-0.08	-0.09	-0.08
MI	Positive	-0.25	-0.17	-0.14	-0.01	0.12	0.04	0.02	-0.07	0.14	0.04
	Negative	-0.15	***0.12***	-0.04	-0.11	-0.27	-0.27	-0.01	-0.13	-0.05	***0.19***
	Neutral	0.14	0.02	0.06	0.04	0.04	0.07	-0.01	0.06	-0.03	-0.07

Table 3.3: Tables of crop anomaly (detrended minus the detrended mean) values in bushels per acre by teleconnection and episode for the growing season (April-October). "ND" stands for no data. **(a)** For the Arctic Oscillation (AO) "N" denotes negative episode (≤-0.5), "P" denotes positive episode (≥0.5), and "Neu" denotes a neutral episode (-0.4 to 0.4). **(b)** For ENSO "L" denotes cold episode (≤-0.5), "E" denotes warm episode (≥0.5), and "N" denotes a neutral episode (-0.4 to 0.4). Positive values indicate yields greater than the mean and negative values indicate yields less than the mean at crop reporting district level.

Growing Season														
		ENSO			AO				ENSO			AO		
State	CRD	E	L	N	Pos.	Neg.	Neu.	State	E	L	N	Pos.	Neg.	Neu.
IL	10	-8.5	-9.1	7.7	-10.4	-27.8	1.8	MO	-1.9	-3.0	2.1	-49.1	-50.1	5.5
	20	-11.4	-1.2	6.1	-8.2	-18.9	1.3		-1.6	0.1	0.8	-33.9	-39.9	4.0
	30	-8.4	-7.1	6.9	-51.8	-25.5	4.8		0.4	-2.7	0.8	-49.5	-9.7	4.0
	40	-11.7	-4.1	7.4	-25.5	-12.5	2.3		-5.3	3.7	1.3	-29.0	-33.2	3.4
	50	-10.1	-3.3	6.3	-18.5	-16.6	2.0		-2.6	2.0	0.6	-32.4	-21.5	3.2
	60	-9.0	-2.7	5.5	-31.8	-7.2	2.6		-6.9	0.8	3.2	-30.2	-25.8	3.2
	70	-9.9	-1.0	5.3	-28.9	-1.1	2.2		1.3	-0.7	-0.4	-22.2	-23.2	2.5
	80	-8.7	-1.4	4.9	-32.0	-6.6	2.6		-7.3	-5.3	5.6	-33.3	-18.0	3.1
	90	-10.5	-0.1	5.3	-29.2	0.5	2.1		-9.2	0.3	4.5	-28.3	-26.8	3.1
State	CRD	E	L	N	Pos.	Neg.	Neu.	State	E	L	N	Pos.	Neg.	Neu.
IN	10	-6.8	-5.5	5.5	-16.1	-15.0	1.8	IA	-5.2	-2.7	3.6	-18.6	-78.8	4.3
	20	-8.7	-9.2	7.8	-13.7	-11.0	1.4		-2.9	-1.4	2.0	-21.4	-86.9	4.8
	30	-6.1	-8.3	6.2	-18.3	-13.1	1.8		-0.2	-10.5	4.1	-6.7	-72.4	3.2
	40	-11.7	-3.3	7.1	-19.4	-5.6	1.6		-0.7	-3.4	1.6	-25.5	-73.3	4.6
	50	-6.5	-5.4	5.3	-23.3	0.3	1.7		1.5	-7.9	2.2	-10.9	-74.4	3.6
	60	-7.9	-3.9	5.4	-27.8	-5.9	2.3		-6.6	-14.5	8.7	-12.3	-60.6	3.2
	70	-13.9	-0.3	7.0	-24.3	-7.7	2.1		1.9	-3.3	0.3	-26.3	-70.5	4.6
	80	-14.0	-2.4	7.9	-30.4	5.0	2.1		-1.1	-4.2	2.1	-37.7	-65.7	5.2
	90	-12.4	-0.8	6.5	-32.2	-0.9	2.4		-5.4	-11.1	6.9	-53.3	-57.1	6.1
State	CRD	E	L	N	Pos.	Neg.	Neu.	State	E	L	N	Pos.	Neg.	Neu.
OH	10	-8.6	-3.4	5.6	-13.8	-31.0	2.2	KS	-1.7	3.0	-0.3	-8.3	-13.7	1.1
	20	-9.7	1.4	4.4	-15.9	-37.9	2.6		-1.4	-7.5	3.5	-5.8	0.3	0.4
	30	-10.4	2.2	4.3	-18.9	-35.3	2.7		-3.1	2.4	0.6	-18.6	-22.6	2.2
	40	-10.9	2.3	4.6	-35.0	-13.5	3.1		-4.2	-2.4	3.0	1.4	-18.4	0.6
	50	-4.7	2.2	1.5	-30.2	-22.4	3.1		1.4	-3.1	0.5	-14.7	-12.7	1.6
	60	-8.7	-0.4	4.5	-16.1	-20.2	1.9		0.9	0.9	-0.8	-12.8	-17.7	1.6
	70	-4.2	-0.3	2.2	-29.8	-18.4	2.9		-7.8	0.3	3.8	-58.5	-43.3	5.9
	80	-3.3	-3.0	2.8	-21.6	-22.6	2.4		-3.7	1.2	1.4	-24.9	-30.8	3.0
	90	-6.3	1.6	2.5	-24.0	-13.6	2.3		-0.3	8.7	-3.1	-18.9	-25.1	2.3

Table 3.3 continued

Growing Season														
		ENSO			AO				ENSO			AO		
State	CRD	E	L	N	Pos.	Neg.	Neu.	State	E	L	N	Pos.	Neg.	Neu.
MI	10	0.5	11.7	-4.6	-10.1	-29.0	1.8	ND	ND	ND	ND	ND	ND	ND
	20	2.4	-3.0	-0.1	-10.9	-3.2	0.9		-8.1	3.2	2.8	-14.5	-49.1	2.9
	30	-1.8	4.1	-0.6	-15.1	-12.7	1.6		-4.5	-2.7	3.3	-29.5	-29.5	3.3
	40	7.1	3.0	-4.7	-3.0	12.3	-0.2		-6.7	4.5	1.6	-19.4	-47.1	3.2
	50	0.9	4.8	-2.2	-7.1	5.3	0.3		-8.8	-2.2	5.2	-13.9	-40.0	2.5
	60	4.0	-2.8	-1.0	4.4	6.9	-0.6		-5.5	-2.5	3.7	-18.3	-40.2	2.8
	70	5.9	-6.7	-0.4	11.5	-1.0	-0.8		ND	ND	ND	ND	ND	ND
	80	0.9	-2.8	0.6	12.3	-1.0	-0.9		-7.1	8.0	0.6	-1.6	-31.3	1.3
	90	-2.7	-3.7	2.7	15.0	-9.2	-0.8		-2.6	-2.9	2.4	4.1	-53.1	1.7
State	CRD	E	L	N	Pos.	Neg.	Neu.	State	E	L	N	Pos.	Neg.	Neu.
WI	10	7.5	-4.9	-1.9	8.0	-34.1	0.7	SD	-4.1	3.3	0.8	-13.0	-32.4	2.2
	20	5.6	-4.7	-1.0	-7.7	-61.5	2.8		-3.2	4.5	-0.1	-1.9	-14.6	0.7
	30	1.8	1.6	-1.5	-8.3	-36.7	2.0		-3.9	-4.8	3.7	5.4	-56.6	1.7
	40	6.4	-8.8	0.1	5.7	-28.0	0.6		3.2	-6.2	0.7	3.6	-9.9	0.1
	50	2.9	-1.0	-1.1	-1.7	-26.1	1.1		-0.8	1.4	-0.1	-23.5	-15.8	2.3
	60	4.2	0.2	-2.2	-8.1	-43.5	2.2		-6.8	-1.2	3.9	-29.1	-64.8	4.6
	70	3.2	-11.4	2.7	9.3	-24.4	0.2		2.4	-4.9	0.7	-16.1	-16.3	1.8
	80	-2.7	-9.6	5.0	0.5	-21.0	0.7		-5.0	-7.6	5.3	-15.2	-1.1	1.2
	90	-2.4	-5.4	3.2	4.9	-13.2	0.1		-12.3	-4.2	7.7	-27.2	-39.0	3.5
State	CRD	E	L	N	Pos.	Neg.	Neu.	State	E	L	N	Pos.	Neg.	Neu.
MN	10	-3.5	-2.8	2.8	-21.8	-47.8	3.4	NE	-2.1	-0.5	1.2	-21.0	-44.4	3.2
	20	ND	ND	ND	ND	ND	ND		-4.0	-4.4	3.6	-15.0	-3.9	1.3
	30	ND	ND	ND	ND	ND	ND		-10.7	-5.0	7.2	-30.5	-33.0	3.5
	40	-0.4	-9.9	3.9	3.8	-66.5	2.2		-5.5	-3.8	4.2	-19.7	-26.8	2.5
	50	1.9	-11.7	3.5	-6.4	-64.0	2.8		-2.7	-1.2	1.8	-24.0	-50.4	3.6
	60	7.5	-10.8	0.3	-0.7	-35.2	1.4		-0.3	1.1	-0.3	-16.3	-23.6	2.1
	70	-2.3	-7.2	3.9	-9.6	-90.8	4.1		-3.5	0.0	1.8	-16.9	-47.2	3.0
	80	-0.6	-9.7	3.9	-10.3	-73.7	3.5		-4.3	0.6	1.9	-21.8	-45.7	3.3
	90	2.6	-11.6	3.1	8.5	-60.2	1.6							

.

3.9 Figures

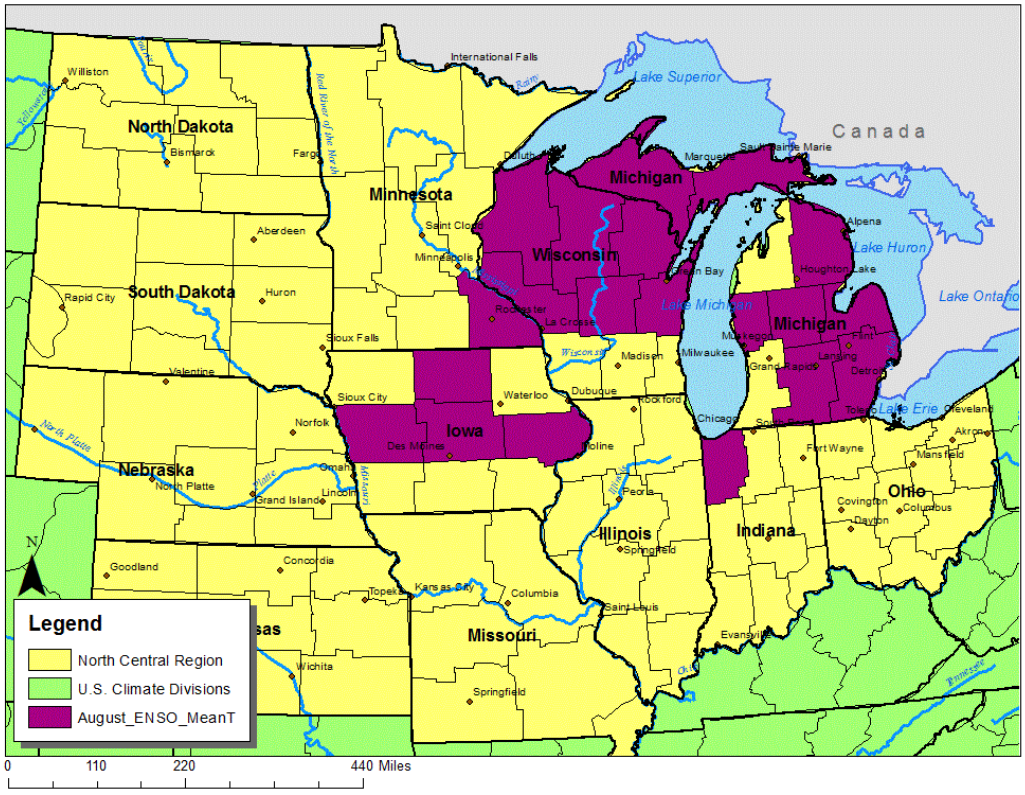

Figure 3.1: An example of a map highlighting climate divisions where average monthly mean temperatures in August are found to be significantly impacted (ANOVA, 90% CI) by ENSO episode 1980-2010.

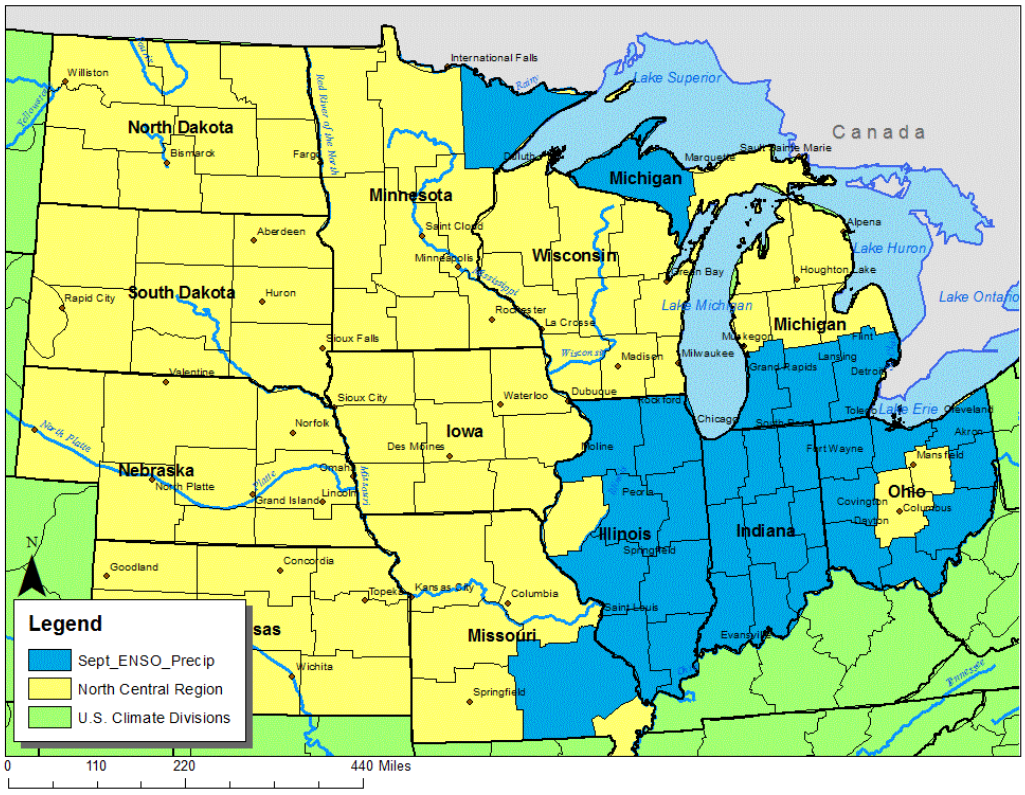

Figure 3.2: Same as Figure 1 except displaying average monthly observed precipitation for the month of September.

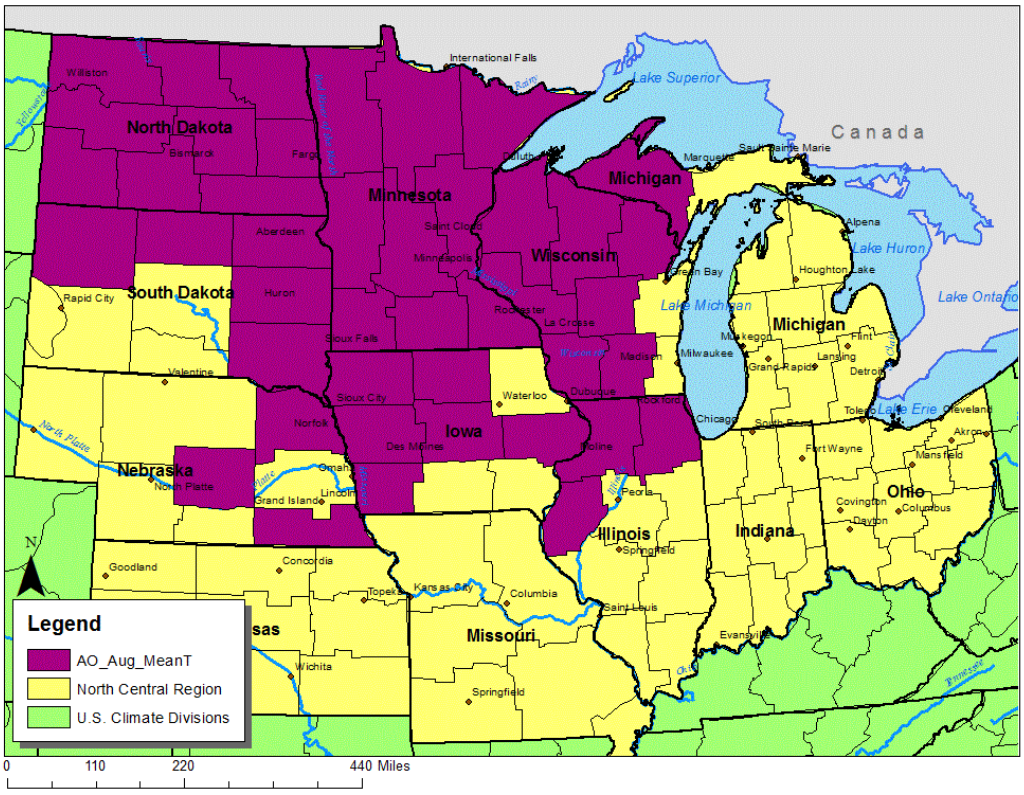

Figure 3.3: A map highlighting climate divisions where average monthly mean temperatures in August are found to be significantly impacted (ANOVA, 90% CI) by AO episode 1980-2010.

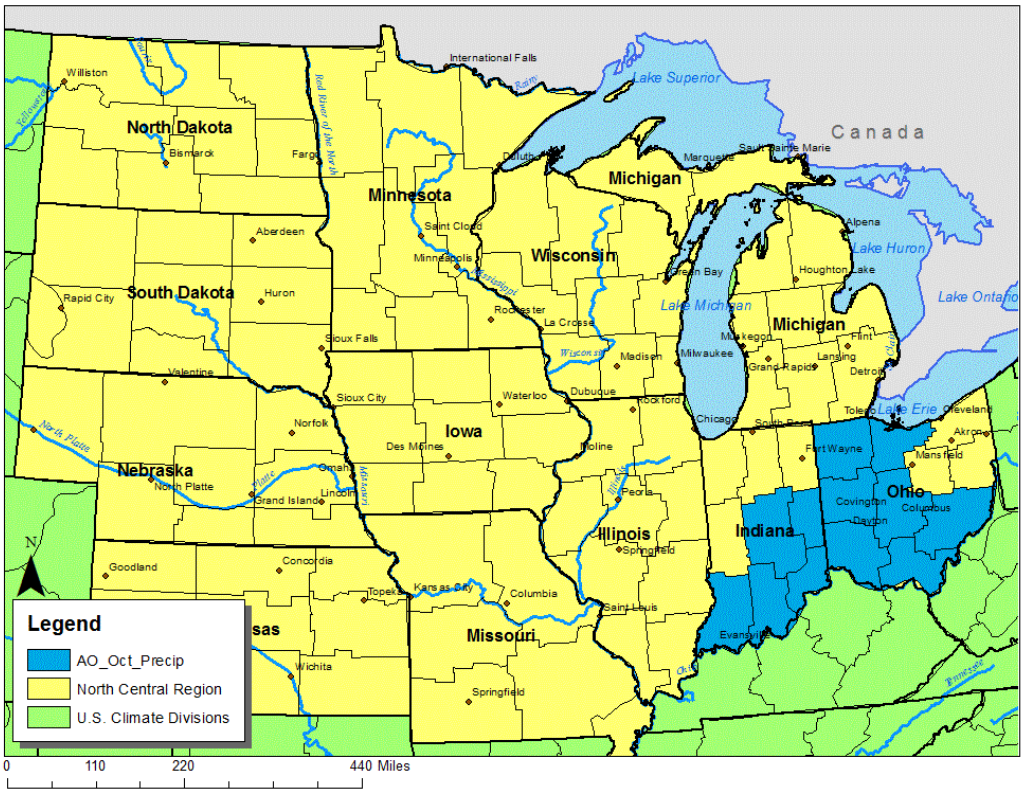

Figure 3.4: Same as Figure 3 except displaying average monthly observed precipitation for October.

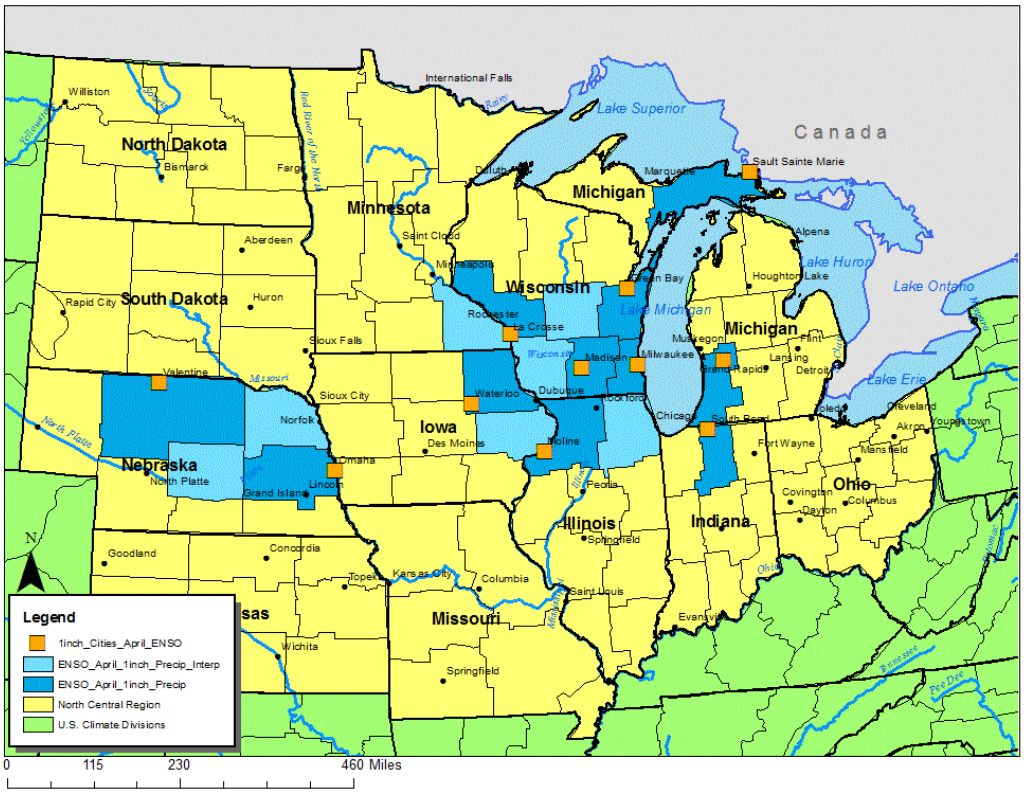

Figure 3.5: An example of a map highlighting climate locations and state climate divisions the cities reside in which the average number of days per month extreme precipitation event of Prcp ≥ 1.0 inch for the month of April is found to be significantly impacted (ANOVA, 90% CI) by ENSO episode 1996-2010. Orange squares denote the cities where findings are significant. Dark blue climate divisions house those cities. The light blue climate divisions are spatially interpolated (neighbored by two state climate divisions with noted significance) for aesthetics.

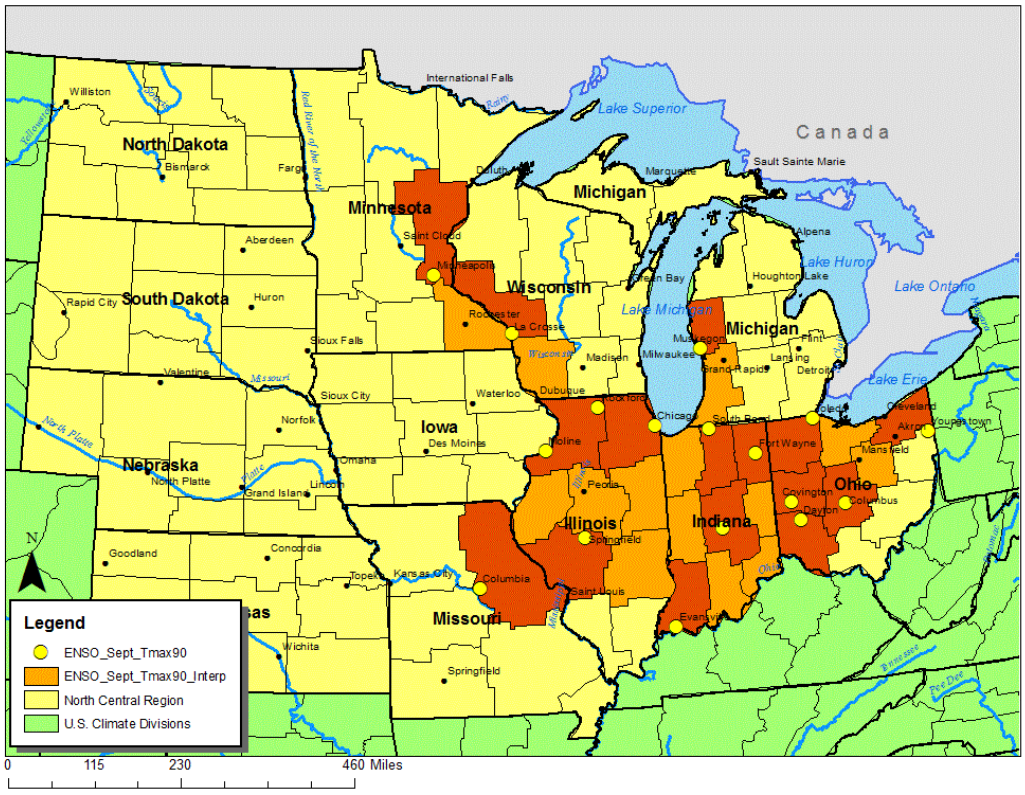

Figure 3.6: An example of a map highlighting climate locations where the average number of days per month the extreme temperature event of $T_{max} \geq 90°F$ is found to be significantly impacted (ANOVA, 90% CI) by ENSO episode 1980-2010. Yellow circles denote those cities where findings are significant. Dark red climate divisions house those cities. Orange climate divisions are spatially interpolated (neighbored by two state climate divisions with noted significance) for aesthetics.

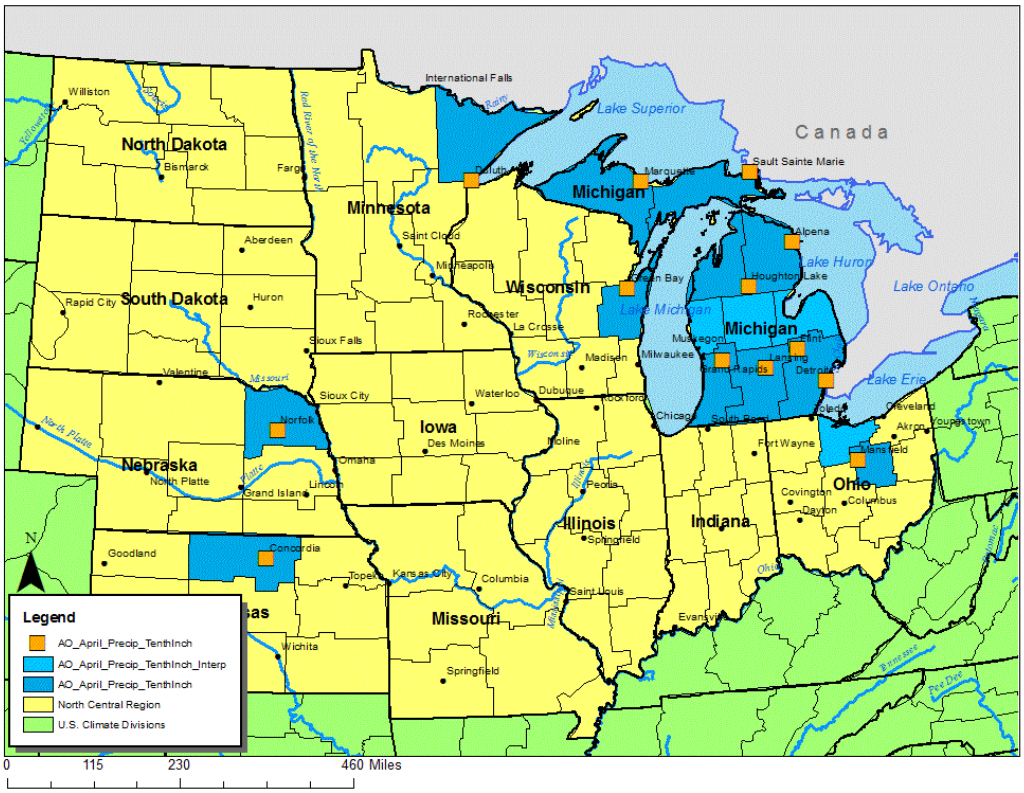

Figure 3.7: An example of a map highlighting climate locations where the average number of days per month in April that precipitation events of Prcp $\geq$ 0.10 inch are found to be significantly impacted (ANOVA, 90% CI) by AO episode 1996-2010. Orange squares denote the cities where findings are significant. Dark blue climate divisions house those cities. The light blue climate divisions are spatially interpolated (neighbored by two state climate divisions with noted significance) for aesthetics.

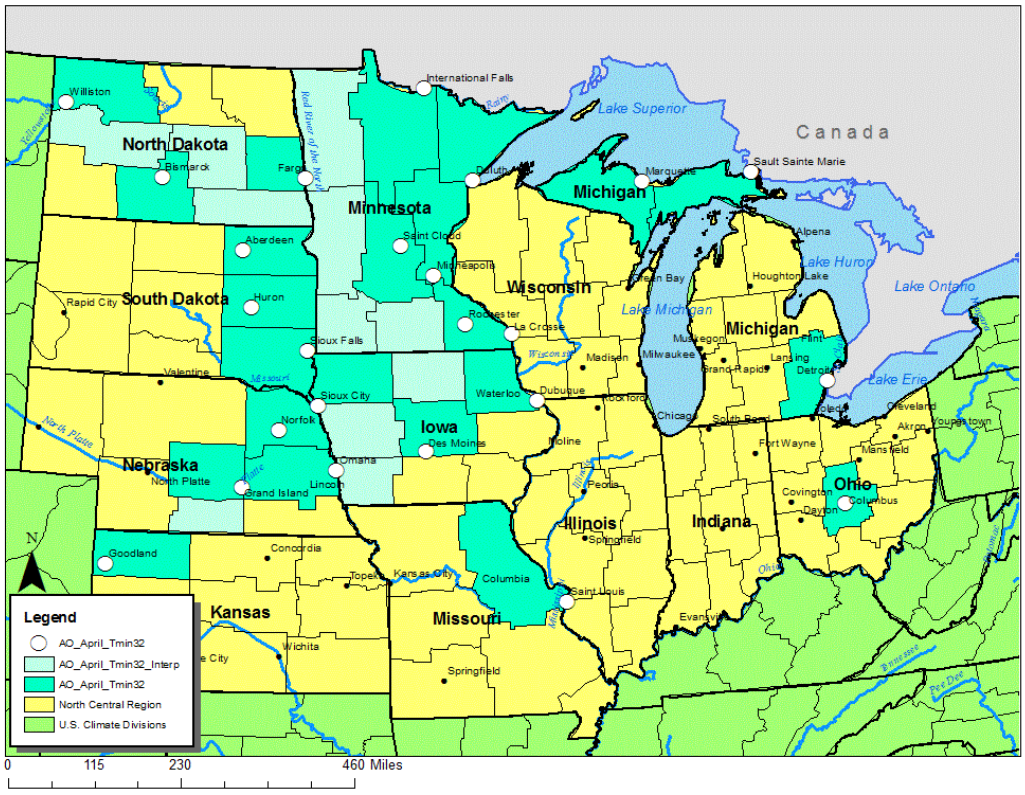

Figure 3.8: An example of a map highlighting climate locations where the average number of days per month the extreme temperature event of $T_{min} \leq 32°F$ (greater likelihood for frost/freeze events) is found to be significantly impacted (ANOVA, 90% CI) by AO episode 1980-2010. White circles denote the cities where findings are significant. Dark green/teal climate divisions house those cities. The light blue climate divisions are spatially interpolated (neighbored by two state climate divisions with noted significance) for aesthetics.

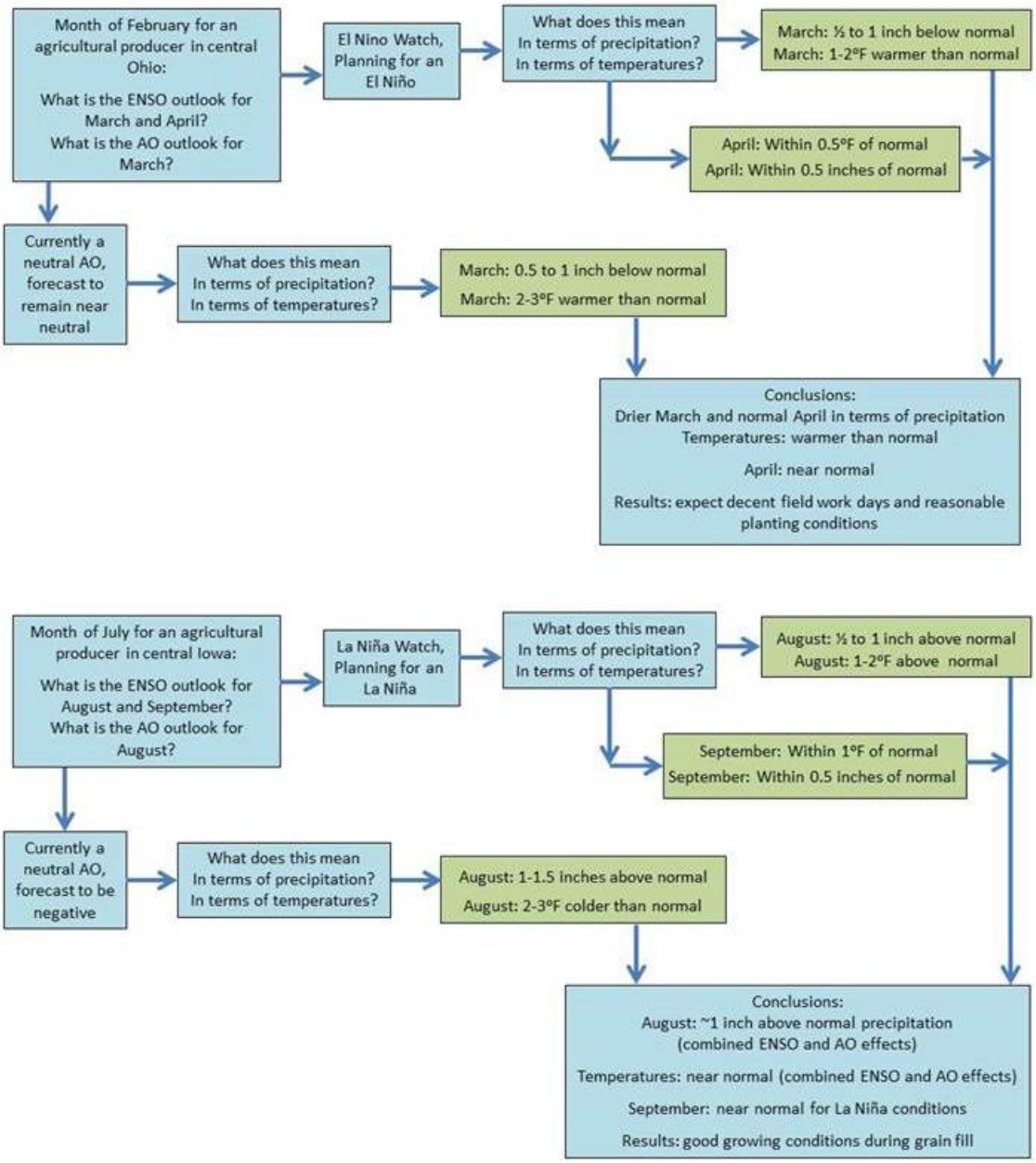

Figure 3.9: A flow chart presenting an example of the agro-climatic decision making process that can be adopted using the information available from the ENSO and AO climatology. The top chart highlights a springtime decision making scenario and the bottom chart highlights a mid-growing season scenario. Historic Oceanic Niño Index data can be found at http://www.cpc.ncep.noaa.gov/products/analysis_monitoring/ensostuff/ensoyears.shtml.

CHAPTER 4. ASSESSING DROUGHT VULNERABILITY OF AGRICULTURAL PRODUCTION SYSTEMS IN CONTEXT OF THE 2012 DROUGHT

4.1 Introduction

Climate variability lead to extreme weather and climate events when teleconnections, global circulation patterns, and high and low pressure systems align in such a way that anomalously dry (or wet) and/or warmer (colder) conditions occur in a given area for a prolonged period of time. Drought conditions at the land surface (local-scale climate) can evolve from a manifestation of teleconnections, global circulation patterns, and high and low pressure cells (large-scale climate). Drought is defined as a rainfall deficit in a given area based on that area's established climate as determined through its historic record. Drought type varies depending on the context in which one is viewing the water shortage: agricultural, hydrological, meteorological, and societal/economical. A lack of rainfall at the surface leads not only to a rainfall deficit, but leads to changes in vegetation, soil moisture, surface albedo, and surface temperatures (local-scale climate). Changes to these parameters cause changes in temperature and radiation fluxes between Earth's surface and the PBL. The lack of water and changes in temperature and radiation fluxes impart a large stress on agricultural systems. This chapter investigates feedbacks between the hydroclimatic state of drought, focusing more specifically on livestock forage and production and market impacts. The drought of 2012 is the most recent historical drought to have a significant impact on agricultural production in the United States and is used as an example to understand.

4.2 Assessing Drought Vulnerability of Agricultural Production Systems in the Context of the 2012 Drought

As Published in Forages and Pasture Symposium: Assessing drought vulnerability of agricultural production systems in context of the 2012 drought.

Full Citation: Kellner, Olivia and D. Niyogi, 2014: Assessing Drought Vulnerability in Agricultural Production Systems in the Context of the 2012 Drought. *Journal of Animal Science,* DOI:10.2527/jas.2013-7496. 2014.

Abstract

Weather and climate events and agronomic enterprise are coupled via crop phenology and yield, which is temperature and precipitation dependent. Additional coupling between weather and climate and agronomic enterprise occurs through agricultural practices such as tillage, irrigation, erosion, livestock management, and forage. Thus, the relationship between precipitation, temperature, and yield is coupled to the relationship between temperature, precipitation, and drought. Unraveling the different meteorological and climatological patterns by comparing different growing seasons provides insight into how drought conditions develop and what agricultural producers can do to mitigate and adapt to drought conditions. The 2012 drought in the United States greatly impacted the agricultural sector of the economy. With comparable severity and spatial extent of the droughts of the 1930s, 1950s, and 1980s, the 2012 drought impacted much of the U.S. crop and livestock producers via decreased forage and feed. This brief summary of drought impacts to agricultural production systems includes 1) the basics of drought; 2) the meteorology and climatology involved in forecasting, predicting, and monitoring drought with attribution of the 2012 drought explored in detail; and 3) comparative analysis completed between the 2011 and 2012 growing season. This synthesis highlights the complex nature of drought in agriculture production systems as producers prepare for future climate variability.

4.3 Introduction

This commentary synthesizes the meteorological conditions and impacts of the 2012 drought and the associated intricate relationship between weather, climate, and agriculture. While 2012 has a long list of significant weather events, arguably the most notable event was the drought of 2012. The 2012 drought peaked in July with over two-thirds of the United States experiencing drought conditions comparable to droughts of the 1930s, 1950s, and 1980s. The large loss in corn resulted in increased feed prices and increased prices for meats and animal-based products late in 2012, with further price increases felt into 2013 and likely 2014 (Crutchfield, 2013).

The magnitude, scope, and impact of the 2012 drought continue to be hard to define, predict, and assess. Drought occurs at different spatial, temporal, and socioeconomic scales depending on weather patterns and water demand for a given area. Drought can be far reaching and have indefinable impacts on economies, environments and ecosystems, and societies. Agricultural management decisions such as irrigation, planting dates, and cropping patterns can also affect drought intensity and evolution. The World Meteorological Organization (Geneva, Switzerland) recognizes hydrological, agricultural, and meteorological droughts, which are classified by 4 characteristics: intensity, duration, spatial extent, and timing. Each type of drought results from climate variability (i.e., departure from normal but within average climate) such as decreased precipitation, higher temperatures, lower relative humidity, and increased sunshine (Figure 4.1).

This paper analyzes the 2011 and 2012 growing seasons, as related to drought. The meteorology and climatology behind the differences in temperatures and rainfall between the seasons, along with the role of climate indices, is discussed. Atmospheric patterns, variability, and crop impacts are reviewed. A brief examination of future climate projections, with suggestions on planning for short and long term drought, is included.

4.4 Drought

4.4.1 Drought Indices

Drought is currently monitored through several indices developed over the last several decades. A common drought index is the Palmer Drought Severity Index (PDSI), which measures drought based on temperature and precipitation. The index considers precipitation as well as the state of the soil through ground water supply. The demand (or withdrawal) of water from the ground is dependent on the temperature of the overlying air, evapotranspiration, and requirement and demand of water from vegetation (if present). These variables are difficult to quantify due to the physical complexities of the hydraulic, radiative, and biologic processes involved. The PDSI is generally effective for assessing and monitoring long-term drought. A variant index focusing on hydrology, the Palmer Hydrological Drought Index (PHDI), is also used in some midwestern states. The PDSI and PHDI differ in that the PHDI more specifically focuses on long-term hydrological (versus long-term meteorological) conditions such as ground water, reservoir levels, lake levels, and river levels. For the short term (i.e., weeks to months), drought is better monitored through the Standardized Precipitation Index (SPI; McKee et al., 1993). This index uses precipitation anomaly as a metric for drought. Droughts can be classified as "flash droughts," which have rapid onset but only last for a short time span or droughts can be classified as slow onset, which almost seem to "creep" up on regions through time (Charusombat and Niyogi, 2011). The 2012 drought was complex in nature, with dry conditions and impacts accumulating through time to high levels by the end of summer 2012 (Figure 4.2). The U.S. Drought Monitor (USDM; http://droughtmonitor.unl.edu) collates a number of such drought indices (e.g., rainfall anomaly, SPI, PDSI), local impacts (on ground conditions and media reports), and community feedback to develop a blended drought map. The USDM drought map is considered the "gold standard" for drought status and is the basis for disaster declarations including becoming eligible for federal aid. Charusombat and Niyogi (2011) provide an overview of several drought indices with applicability for specific drought detection and drought prediction in the Midwest.

4.4.2 Understanding the Difference between the 2011 and 2012 Growing Seasons

Annual temperatures as a departure from normal for the year 2011 compared to 2012 are shown in Fig. 3. There is a high spatial correlation between warmer temperatures and drought (Figure 4.3). Across the Midwest and Ohio River Valley, temperatures in 2011 were mostly near normal or 0.5 to 1.1°C (i.e., 1 to 2°F) above normal. In 2012, the average departure from normal ranged from 0.5 to 2.8°C above normal (1 to >5°F above normal). Percentage of normal observed precipitation for each year shows a strikingly contrasting picture; 2011 shows 100% of normal precipitation or greater across much of Illinois, southeast Missouri, and all of Indiana, Ohio, Kentucky, and Michigan. In 2012, the U.S. Corn Belt was at 50 to 90% of normal precipitation for the year, with only regions in far northeastern Minnesota and those regions affected by lake effect snowfall events residing at or slightly above normal (Figure 4.4). While the annual summary provides a broader perspective in climatic context, reviewing the seasonal analysis highlights a dramatically dry and hotter 2012 growing season as compared with the cooler and wetter 2011 growing season.

The 2012 growing season fell subject to drought conditions because of a warmer than normal spring (i.e., March through May) with near-normal to normal rainfall across much of the central plains. March 2012 became the warmest March on record at 4.8°C (8.6°F) above average. April 2012 finished as the fourth warmest month of April on record and May 2012 as the second warmest month of May on record. For the continental United States, the average temperature for the season was 13.4°C (56.1°F), 2.9°C (5.2°F) above the 20th century average (NOAA National Climatic Data Center, 2012). These meteorological conditions resulted in significantly earlier planting dates across much of the region leading to earlier crop emergence (which led to increased evaporation and transpiration in the atmosphere), only to be affected by hot and dry weather a short while later during the meteorological summer months of June through August. The summer's average temperature for the continental United States was the second warmest on record at 23.2°C (73.8°F), 1.5°C (2.6°F) above the 20th century average. Alongside these record-breaking temperatures, normal precipitation nearly ceased east of the Rocky Mountains through the Great Plains and into the Midwest. Drought conditions peaked in

July when 61.8% of the spatial area of the continental United States was classified as experiencing moderate drought according to the PDSI, comparable to the size of the droughts during the 1950s. For the summer period, precipitation for the continental United States came 26.2 mm (approximately 1 inch) below average (14th driest summer on record; NOAA National Climatic Data Center, 2012). The hot, dry weather led quickly to high evaporation, transpiration, and dry soils impacting pasture lands and crop yields. The lack of rainfall and extreme heat during the crucial grain-fill period of July further exacerbated the decreased yield potential for the 2012 growing season. Hoerling et al. (2014) note that in a time series of crop yield from 1866 to the present, the 2012 growing season yield fell well below recent crop yield trends. Hoerling et al. (2014) further note that when coupled with the climatic impact of the 2012 drought, the yield impact is historic, with no year since 1866 experiencing such a large loss in crop yield.

Early planting and warm temperatures also created an environment suitable for the development of other biotic and abiotic stresses such as Aspergillus ear rot, which is associated with the mycotoxin aflatoxin. While concentrations of aflatoxin are acceptable in harvested yields, it is monitored by the USDA, which mandates that to prevent carryover into milk, silage and other feed components developed from a contaminated harvest should contain no more than 20 ppb of aflatoxin (Stewart, 2012; USDA, 2009). Milk coming from animals fed silage with aflatoxin must have aflatoxin residues less than 0.5 ppb to be considered safe for human consumption (Stewart, 2012). The possibility of early planting leading to a much more intense drought because of increased transpiration and soil moisture loss earlier in the season needs to be analyzed further and provides one more feature to the complexity of understanding the attributable factors and causal processes leading to droughts.

Normal weather patterns provide sufficient rainfall that will break through a crop plant canopy, infiltrate the soil, and keep the ground water supply adequately charged through the growing season. The 2012 drought resulted from a deficit in soaking rainfall and is classifiable as all 3 types of drought: hydrological, meteorological, and agricultural. This drought is not considered an extension of the southern Great Plains drought as

weather and climate regimes in the southern Great Plains are separate from those across the central Great Plains and the Midwest. The meteorological cause of the 2012 rainfall deficit was atmospheric blocking (i.e., the jet stream pushing too far north or weather system propagation slowing down and became stationary over several weeks) that led to high pressure being the predominant weather pattern resulting in minimal rain-producing weather systems. When rain did occur in the late spring and summer of 2012, rainfall was brief, heavy, and localized in nature resulting in some relief with "normal" rainfall amounts recorded. However, the majority of the Corn Belt did not receive sufficient rain for ground water recharge as shown in Figure 4.5 for the Midwest. The development of a high-resolution drought trigger tool (HIRDTT) by collaborators at Texas A&M University, North Carolina State University, and Purdue University with the use of the National Oceanic and Atmospheric Administration's National Weather Service's Multisensor Precipitation Estimation and SPI data provides detailed drought assessment of drought at sub-county scales. Figure 4.5 shows a HIRDTT map of with small areas of drought amelioration from brief convective thunderstorm events, although these storms did not provide sufficient rainfall to pull regions out of drought status. The spatial variability in the drought conditions at sub-county scale is apparent in this map.

4.4.3 Meteorological and Climatological Feedback for the 2012 Drought

Drought of the magnitude seen in 2012, 1988, 1950s, and 1930s has large impacts on crop yield that trickle down to silage production and animal feed and into other parts of the economy. Large-scale impacts such as these have led to intensive research by climatologists to determine if there is a climatic signal that can be identified ahead of time to predict droughts of such magnitude. Historical droughts have been studied by analysis of tree rings and sediment in lake beds across the United States. Findings by Cook et al. (2007), for example, show that over the last 1,000 yr., North America suffered from "mega droughts" (i.e., lasting several decades) during the drier CE 900 to 1300 period. Droughts then shifted to periods of shorter duration (i.e., several years to a decade) with the present time still experiencing shorter-term droughts. Therefore, compared with North America's past, CE 1300 to the present has been "wetter" in nature

despite the noted droughts of the 1930s and 1950s. Therefore, while the Cook et al. (2007) historical analysis helps understand climatology, it is important to note that short-term agricultural decisions are often dictated by short-term weather conditions. Thus, the 2012 drought caught farmers off guard because a warmer than normal March with near-average precipitation allowed for earlier planting dates; however, the atmosphere quickly transitioned to persistent drought conditions through the late spring and summer.

4.4.4 Causes of Drought

Drought can be a natural part of the Earth's climate. The role of climate variability or the role of climate change to a specific event, such as the 2012 drought, continues to be a difficult factor to address. Indeed, studies summarized in the recent Intergovernmental Panel on Climate Change (2013) assessment highlight a potential for larger rainfall variations in the future from global warming. These variations in rainfall can cause extended periods of dry weather that, depending on local and prevailing factors, can lead to drought conditions. Variability such as the dry signal associated with major La Niña events in the tropical Pacific may play a stronger role in drought development in some locales of North America, such as the West and the Great Plains (Cook et al., 2007). Niyogi and Mishra (2013), however, note that the current trend in the Midwest indicates low probability for large-scale droughts in general. However, that is not to say that farmers need not pay attention to extended periods of dry or wet weather that are projected to become more frequent with a warming climate. Amidst this variability, agricultural practices such as land management decisions, irrigation, planting dates, drainage systems, and tillage practices can impact local hydrologic cycles and either intensify dry conditions into drought conditions or help mitigate the impacts.

4.4.4.1 Climate Variability, Climate Change, and Teleconnections

Climate variability considers weather patterns on a smaller time scale, typically 10 yr. or less, and is often determined by teleconnection patterns such as the El Niño Southern Oscillation (ENSO), Arctic Oscillation (AO), North Atlantic Oscillation (NAO), Pacific North American pattern, Pacific Decadal Oscillation (PDO), and the Atlantic Multidecadal Oscillation (AMO). Climate change is the change in weather patterns over a

longer period of time, typically over several decades, with these weather patterns showing a systematic change in the state of the atmosphere. Climate variability is superimposed over broader climate change patterns. As a result, climate variability and associated impacts are often noticed first and climate change needs a longer period of record.

One of the most widely known global weather drivers that provide climate variability is ENSO (Philander, 1990). The ENSO describes the seesaw pattern of pressure between Darwin, Australia, and Tahiti in the eastern tropical Pacific (Southern Oscillation). The changes in atmospheric pressure between these locations feed back into rainfall patterns, ocean currents, and sea surface temperatures (SST) leading to changes in weather patterns downstream from these locations (e.g., over North America). An El Niño event describes a warm SST event, which weakens the atmospheric circulation known as the Southern Oscillation, and the La Niña event refers to cold SST and a stronger circulation. The "warm" or "cold" anomalies are typically 3- to 5-mo running means (length of running mean varies by index being used to monitor the Southern Oscillation) of SST 0.5°C greater than or less than the baseline temperature and that persist for at least 6 consecutive months. Changes in the intensity of the Southern Oscillation result in changes of energy transfers from the tropics to midlatitudes, which is why weather changes downstream over North America. While El Niño and La Niña events have a greater impact on winter precipitation, effects of each phase can be felt into the growing season. La Niña events have been found to result in drought conditions across the Southeast and wetter conditions across the Midwest during winters. El Niño events during winter months result in a dry, warm Midwest and a wet, cool South. A neutral phase results in a normal to wetter spring with normal temperatures. The departure from normal SST over the tropical pacific is important to the strength of the signals felt over North America. The effects of ENSO patterns are much more pronounced in coastal regions and our ongoing research indicates the Midwest shows a mixed signal between ENSO phases. During the spring and summer of 2012, the dominant ENSO pattern was a moderate to weak La Niña transitioning to ENSO neutral by the summer months.

4.4.4.2 2012 Teleconnections

Other teleconnections discussed previously contributed to the drought of 2012 as well. The AO is linked to the NAO, which contributes to short-term variability of weather patterns across the United States. For example, the 2013 growing season differed greatly from 2012 because during January, February and March of 2013, the AO was in a negative phase resulting in Midwest cold air outbreaks (periods of snow followed by rapid melt and milder temperatures). A positive AO is present when a lower-than-normal pressure is present over the polar region (leading to a stronger pressure gradient and jet stream), and a negative AO is present when a higher-than-normal pressure is present over the polar region (leading to a weaker pressure gradient and jet stream allowing for a greater likelihood of cold air outbreaks). Entering April and May, the AO shifted into a positive phase, which resulted in a stronger jet stream with less variation in temperatures and precipitation patterns. This, coupled with the ENSO neutral phase, contributed to near normal conditions across the U.S. Corn Belt, which was suitable for a good growing season. In contrast, the beginning of 2012 was influenced by a neutral AO in January and February followed by a positive AO in March. April and May transitioned back to a neutral AO with June changing signal to a strong negative AO. This allowed for warm air to surge farther north, which coincided with the La Niña and a blocking pattern helped to lock dry conditions into place across much of the United States. July, August, and September were predominantly AO neutral, with ENSO neutral conditions now prevailing but with blocking still occurring resulting in minimal rainfall for the United States.

The PDO is a Pacific Ocean SST index in the northern Pacific that is more directly coupled to ENSO but is more broadly variable when affecting weather regimes across the United States. From the 1940s to the 1970s, the PDO was in a positive phase resulting in warmer and wetter conditions in the Northwest and Alaska and cooler, wetter conditions in Mexico and the southern United States. Since the 1980s, the PDO has entered a negative phase resulting in colder and drier conditions in the Northwest and warmer, drier conditions in the Southeast (Wallace and Hobbs, 2006). Therefore, the PDO favored drier conditions across portions of the United States, adding to the dry

conditions of the La Niña, AO, and blocking pattern that established itself over the country in 2012.

The climate indices discussed are important to capture the interannual climate variability (i.e., temperature and precipitation pattern departures from normal) across the United States and provide guidance as to what seasonal weather patterns may be established. Climate indices are monitored by meteorologists and climatologists and serve as guidance tools in the long-term outlook; they are not intended to be predictors of short-term temperature and precipitation. The strength and covariability of teleconnections needs to be considered when determining seasonal and long-range weather outlooks. Typically a strong El Niño or La Niña can overpower the AO or PDO while weak or neutral ENSO conditions will be dominated by the other teleconnections. Examples of how teleconnections vary include the covariability of ENSO and PDO. When ENSO is positive (El Niño) and the PDO is positive, the central plains, southern portions of the southern United States, and the Eastern Seaboard are wetter than the Midwest. When ENSO is negative (La Niña) and the PDO is negative, the signal reverses; the Midwest is wetter and the central plains and Southeast United States are drier by comparison (Goodrich and Walker, 2011). McCabe et al. (2004) show that when assessing the PDO and AMO together, the AMO directs the spatial extent/broadness of potential drought and the PDO directs the location. Correlative relationships between temperature and precipitation have also been found (e.g., Trenberth, 2011) where increased temperatures lead to an increased risk of drought resulting from increased evaporation rates and surface drying.

4.4.5 The 2012 Drought and Impacts to Agriculture, Livestock, and Forage

4.4.5.1 Cause of the 2012 Drought

The assessment for the 2012 drought reported in Hoerling et al. (2014, p. 278) finds that the drought was a natural event with immediate causes linked to meteorology: "reduced Gulf moisture transport, cyclone activity, and frontal activity in late spring." Anomalous high pressure in the upper troposphere resulted in increased subsidence over the region decreasing natural processes of convection during the summer (Hoerling et al.,

2014). The likelihood of a drought of the magnitude experienced in 2012 to return in a following year or even in the next several years is considered rare. However, likelihood can depend on location in the United States. In regions such as the Midwest, droughts of the magnitude seen in 2012 are possible three to four times per century (Niyogi and Mishra, 2013).

4.4.5.2 Drought Frequency

Recent drought occurrences in North America show that agricultural drought is less frequent in the plains. This can be attributed to irrigation (for now, as ground water aquifers are being depleted at rapid rates) and the mean storm track. The decreased occurrence of drought in North America is also potentially due to the availability of technologies to mitigate drought in recent decades. The potential increase for drought today is more likely to be mitigated locally due to advancements in crop hybrids, increased irrigation, and field management efforts to conserve soil moisture. While there is currently no significant shift in total rainfall, heavy precipitation has been increasing over the last several decades (e.g., Kunkel et al., 2013). With this heavy rain, there is an increase in runoff because rainfall falls at a rate greater than soil infiltration. This can lead to an increased drought potential because the soil and ground water recharge cannot occur as needed. Uncertainty regarding the scale of increased heavy precipitation exists; therefore, definitive conclusions related to climate change and the frequency of drought associated with climate change cannot easily be made (Dai, 2011). Possible biases to increased heavy rainfall include more moisture content in regions with warmer air and the possible impact of local aerosols acting as cloud condensation nuclei and increasing rainfall (Alexander et al., 2006; Dai, 2011).

4.4.6 Future Climate Scenarios and Impacts to Livestock, Forage, and Feed

Most studies, assessments, observations, and projections of future climate change scenarios for the Great Plains and Midwest show warmer temperatures during the winter and during nighttime hours, along with heavier rains and longer dry periods. Specifics related to how much and why such changes will occur to the climate system continue to be debated by scientists. While large-scale global climate models capture global climate

projections, regional climate models still have difficulty forecasting the coupled feedbacks between large global-scale circulations and more localized climate change effects providing the aforementioned uncertainty (Mearns et al., 2012). Changing land use and land cover as well as adaptive practices will impact regional vulnerabilities and are difficult to account for in models (Pielke et al., 2013).

These uncertainties make preparing for drought and broader climate change and variability different for producers based on location, and impacts will be heterogeneous due the different components linked by climate change. For the United States, overall climate change analyses show that temperatures have been warming and will likely continue to warm at a small rate. Winters will be warming and nighttime temperatures will not get as cold. Precipitation is expected to become more intense (increased precipitation over a shorter amount of time) but is also expected to occur less often in some areas (e.g., Kunkel et al., 2013). To adapt, crop practices such as hybrid development, pesticide use, and irrigation must be adjusted to accommodate the changes in weather patterns. A shift in the growing season is likely to occur as well. An example of this is the shifting of planting dates to earlier in the year as seen with the anomalous warmth during March 2012. Because of this warmth, farmers began planting earlier than the normal time frame of mid to late April. May 2012 ushered in a period of little to no rainfall across the Great Plains with little to no moisture across the Great Plains and Ohio River Valley through June, July, and August, critical periods of phenological development for corn crops. Extreme heat in late June and early July acted to further harm crops (Hoerling et al., 2014). However, the drought of 2012 is considered a climatological anomalous event (e.g. Hoerling et al., 2014), and shifts in the growing season to earlier planting dates sometimes attributed to climate change may provide some positive impacts to the agricultural sector of the economy by allowing for double cropping.

Craine et al. (2010) find that the climatic changes discussed above can result in a decrease of forage quality. Analysis of over 21,000 fecal samples from cattle collected over 14 yr. across the continental United States shows that increasing temperatures and declining frequency of precipitation reduce dietary crude protein and digestible organic

matter in regions of a continental climate. Quality of forage in general was also found to decline. These findings indicate increased nutritional stress in the future for cattle, which results in a greater need for feed with nutritional supplements to offset a decrease in livestock growth (Craine et al., 2010). In addition to degradation in forage production and quality, climatic changes will affect livestock through 1) changes in feed-grain production, availability, and price; 2) overall animal health, growth, and reproduction through heat stress; and 3) disease and pest distributions that will shift as climate changes (Walthall et al., 2012).

4.4.7 Assessing Drought Risk: Adaptive and Mitigative Strategies

Climate change projections show an increase in occurrence of droughts (among other extreme climate events). To determine if a specific event such as the 2012 drought was exacerbated by climate change or if the 2012 drought was actually caused by climate change, the seasonality of weather patterns, climate variability, and climate change factors must be reviewed carefully to determine the cause of the drought. Often, further review of past weather observations, atmospheric patterns, and scale analysis must be completed to draw more definitive conclusions regarding the cause of a large drought such as the drought of 2012. Within the context of the multitude of factors contributing to the evolution of the 2012 drought and the local-scale practices contributing to impacts, it is difficult to ascertain the full 2012 drought impacts only by reviewing the rainfall/drought data and crop yield relationships. In general, it is difficult to predict drought with high confidence when dealing with different climatic scales (e.g., field, crop reporting district, state, or regional scale) and when not considering the impacts that may linger for several years after the drought event. Developing a broad if–then scenario analysis can help understand vulnerability and adaptation and mitigation strategies (Niyogi and Mishra, 2013).

4.5 Summary and Conclusions

The 2012 drought had a significant effect on the agricultural and nonagricultural sectors of the U.S. economy with effects of the 2012 drought currently impacting

consumers in the form of higher food prices (Dreibus et al., 2014). A promising, warmer-than-normal early spring weather pattern in 2012 led to early planting of crops, which quickly withered in the hot, dry weather that established itself over the Great Plains and Midwest late spring and summer 2012. The hot, dry weather that culminated in the 2012 drought resulted from a combination of weather patterns that led to the absence of precipitation systems either moving or forming over the majority of the eastern half of the United States. These patterns included a feedback of a negative PDO, a La Niña event, a negative to neutral AO, and strong blocking patterns. The effects of the 2012 drought impacted corn yields, which were further threatened by increased risk for pests (Stewart, 2012). The decreased corn yield and pasture in 2012 caused an increase in the cost of feed in 2013, further impacting prices for feeder cattle in 2013 (i.e., short-term price reduction). The decrease in available pasture resulted in cattle being fed over a longer term with feed but at lower weights because of the higher cost of feed in 2013. It is speculated that this will lead to greater production declines of cattle by 2014, which will increase cattle prices, especially for the consumer, almost 2 yr. after the drought occurred (Crutchfield, 2013).

The 2012 drought resulted from the evolution of the meteorological environment through the spring and summer of 2012 and shows the critical link between water resources (below normal rainfall and increased irrigation), ecosystem functions (plant production decreased and increased risk for ear rot), agriculture production (decreased yields and pasture), and food (decrease in feeder cattle due to price of corn and increase in cattle costs to consumers). Drought of the magnitude in 2012 is not common but not unlikely due to climate variability scenarios that arise from coupled teleconnection patterns. In addition to climate variability, agricultural practices can mitigate or aggravate a situation. Climate change projections are indicating a greater likelihood of increased dry spells between rainfall events in the future, making drought risk and vulnerability assessments more important to cereal and livestock producers in addition to nonagricultural sectors of the economy. Because drought impacts economic, environmental, and social realms, adaptation and mitigation to the effects of drought in agricultural and nonagricultural sectors of the economy is crucial to minimize loss in the

future (Ding et al., 2010; Wilhite and Glantz, 1985; Figure 4.6). The broader feedback of drought impacts across realms will need to be assessed from vulnerability perspectives for future drought mitigation (Niyogi and Mishra, 2013). The overall consensus for the 2012 drought can be summarized as a natural event that may have been abated by human actions such as later planting dates, crop choices, or availability to irrigation.

4.6 References

Alexander L. V., Zhang X., Peterson T. C., Caesar J., Gleason B., Klein Tank A. M. G., Haylock M., Collins D., Trewin B., Rahimzadeh F., Tagipour A., Rupa, Kumar K., Revadekar J., Griffiths G., Vincent L., Stephenson D.B., Burn J., Aguilar E., Brunet M., Taylor M., New M., Zhai P., Rusticucci M., Vazquz-Aguirre J. L.. 2006. Global observed changes in daily climate extremes of temperature and precipitation. Geophys. Res. Lett.**111**:D05109.

Charusombat U., Niyogi D. 2011. A hydroclimatological assessment of regional drought vulnerability: A case study of Indiana droughts. Earth Interact. **15**:1–65.

Cook E. R., Seager R., Cane M. A., Stahle D. W. 2007. North American drought: Reconstructions, causes, and consequences. Earth-Sci. Rev.**81**:93–134.

Craine J. M., Elmore A. J., Olson K. C., Tolleson D. 2010. Climate change and cattle nutritional stress. Glob. Change Biol. **16**:2901–2911.

Crutchfield S. 2013. U.S. drought 2012: Farm and food impacts. USDA Economic Research Service. www.ers.usda.gov/topics/in-the-news/us-drought-2012-farm-and-food-impacts.aspx#. UpN7rdLBN8E. (Accessed 4 November 2013.)

Dai A. 2011. Drought under global warming: A review. Wiley Interdiscip. Rev.: Clim. Change **2**(1):45–65.

Ding Y., Hayes M. J., Widhalm M.. 2010. Measuring economic impacts of drought: A review and discussion. Papers in Nat. Resourc. **196**:1–23.

Dreibus T. C., Josephs L., Jargon J. 2014. Food prices surge as drought exacts a high toll on crops. The Wall Street Journal. http://online.wsj.com/news/articles/SB10001424052702303287804579445311778530606. (Accessed 26 March 2014.)

Goodrich G. B., Walker J. M. 2011. The influence of the PDO on winter precipitation during high- and low-index ENSO conditions in the eastern United States. Phys. Geogr. **32**(4):295–312.

Hoerling M., Eischeid J., Kumar A., Leung R., Mariotti A., Mo K., Schubert S., Seager R. 2014. Causes and predictability of the 2012 Great Plains Drought.Bull. Am. Meteorol. Soc. **95**:269–282.

Intergovernmental Panel on Climate Change. 2013. Intergovernmental Panel on Climate Change 5th Assessment Report. Climate Change 2013 The Physical Science Basis: Working Group I Contribution to the Fifth Assessment Report of the Intergovernmental Panel on Climate Change. New York: Cambridge University Press. p. 1522.

Kunkel K. E., Stevens L. E., Stevens S. E., Sun L., Janssen E., Wuebbles D., Dobson J. G. 2013. Regional climate trends and scenarios for the U.S. national climate assessment. Part 9. Climate of the contiguous United States. NOAA Technical Report NESDIS 142–9. United States Department of Commerce, Washington, DC.www.nesdis.noaa.gov/technical_reports/NOAA_NESDIS_Tech_Report_142-9-Climate_of_the_Contiguous_United_States.pdf. (Accessed 11 December 2013.)

McCabe G. J., Palecki M. A., Betancourts J. L. 2004. Pacific and Atlantic Ocean influences on multidecadal drought frequent in the United States. Proc. Natl. Acad. Sci. USA **101**:4136–4141.

McKee T. B., Doesken N. J., Kleist J. 1993. The relationship of drought frequency and duration to time scales. In: *Proc. 8th Conf. on Applied Climatology*, American Meteorological Society, Boston, MA. p. 179–184.

Mearns L. O., Arritt R., Biner S., Bukovsky M. S., McGinnis S., Sain S., Caya D., Correia J. Jr., Flory D., Gutowski W., Takle E. S., Jones R., Leung R., Moufouma-Okia W., McDaniel L., Nunes A. M.
B., Qian Y., Roads J., Sloan L.,Snyder M. 2012. The North American Regional Climate Change Assessment Program: Overview of phase I results. Bull. Am. Meteorol. Soc. **93**:1337–1362.

National Oceanic and Atmospheric Administration (NOAA) National Climatic Data Center. 2012. State of the climate: National overview for annual 2012. www.ncdc.noaa.gov/sotc/national/2012/13. (Accessed 2 March 2014.)

Niyogi D., Mishra V. 2013. Climate-agriculture vulnerability assessment for the midwestern United States. In: Pryor S., editor, *Climate change in the Midwest: Impacts, risks, vulnerability, and adaptation.* Indiana Univ. Press,Bloomington. p. 271–288.

Philander S. G. H. 1990. *El Niño, La Niña and the Southern Oscillation.*Elsevier Academic Press, San Diego, CA.

Pielke R. A. Sr.., Adegoke J., Hossain F., Kallos G., Niyogi D., Seastedt T., Suding K., Wright C. 2013. *Climate vulnerability: Understanding, and addressing threats to essential resources.* 1st ed. Elsevier Academic press, China.

Stewart K. 2012. *Heat and drought lead to ear rot potential in corn grain, silage.* Purdue University News Service. www.purdue.edu/newsroom/outreach/2012/120802WiseAflatoxin.html. (Accessed 4 November 2013.)

Trenberth K. 2011. Changes in precipitation with climate change. Clim. Res. **47**:123–138.

USDA. 2009. Aflatoxin handbook. Chapter 1. Grain inspection, packers and stockyards administration. Federal Grain Inspection Service. www.gipsa.usda.gov/publications/fgis/handbooks/aflatoxin/aflatoxin-ch01.pdf. (Accessed 24 November 2013.)

Wallace J. M., Hobbs P. V. 2006. *Atmospheric science: An introductory survey.* 2nd ed. Elsevier Academic Press, Canada. p. 419–446.

Walthall C. L., Hatfield J., Backlund P., Lengnick L., Marshall E., Walsh M., Adkins S., Aillery M., Ainsworth E. A., Ammann C., Anderson C. J., Bartomeus I., Baumgard L. H., Booker F., Bradley B., Blumenthal D. M., Bunce J., Burkey K., Dabney S. M., Delgado J. A., Dukes J., Funk A., Garrett K., Glenn M., Grantz D. A., Goodrich D., Hu S., Izaurralde R. C., Jones R. A. C., Kim S.-H., Leaky A. D. B., Lewers K., Mader T. L., McClung A., Morgan J., Muth D. J., Nearing M., Oosterhuis D. M., Ort D., Parmesan C., Pettigrew W. T., Polley W., Rader R., Rice C., Rivington M., Rosskopf E., Salas W. A., Sollenberger L. E., Srygley R., Stöckle C., Takle E. S., Timlin D., White J. W., Winfree R.,Wright-Morton L., Ziska L. H. 2012. Climate change and agriculture in the United States: Effects and adaptation. *USDA Technical Bulletin No. 1935.*USDA, Washington, DC. p. 1–8. www.usda.gov/oce/climate_change/effects_2012/CC%20and%20Agriculture%20Report%20%2802-04-2013%29b.pdf (Accessed 12 November 2013.)

Wilhite D. A., Glantz M. H. 1985. Understanding the drought phenomenon: The role of definitions. Water Int. **10**:111–120.

4.7 Figures

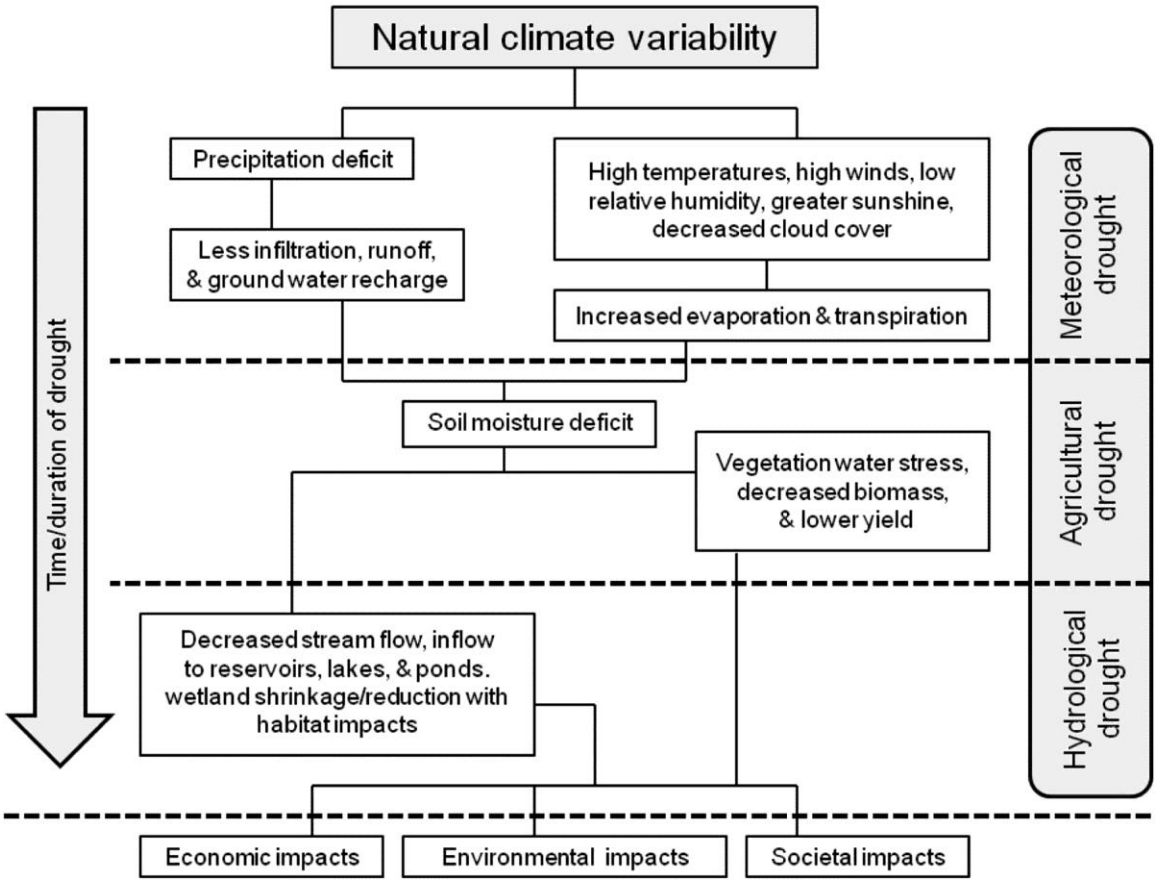

Figure 4.1: Temporal and categorical characteristics and impacts of drought. Adapted from the National Drought Mitigation Center (NDMC). 2014. Types of drought. http://drought.unl.edu/DroughtBasics/TypesofDrought.aspx. (Accessed 20 May 2014).

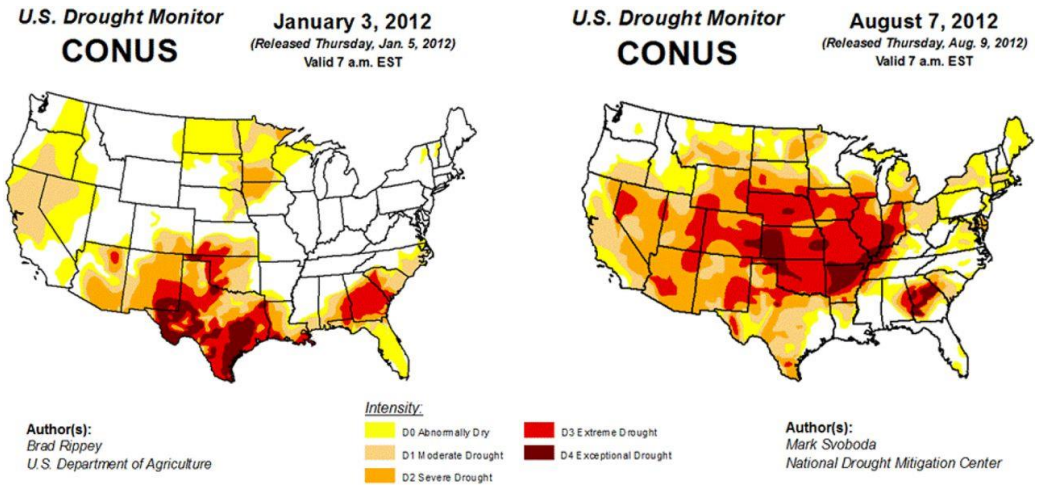

Figure 4.2: Evolution and extent of the 2012 drought from January to August 2012. CONUS is the acronym for "continental United States." The U.S. Drought Monitor is jointly produced by the National Drought Mitigation Center at the University of Nebraska – Lincoln, the USDA, and the National Oceanic and Atmospheric Administration. Map courtesy of National Drought Mitigation Center - University of Nebraska-Lincoln.

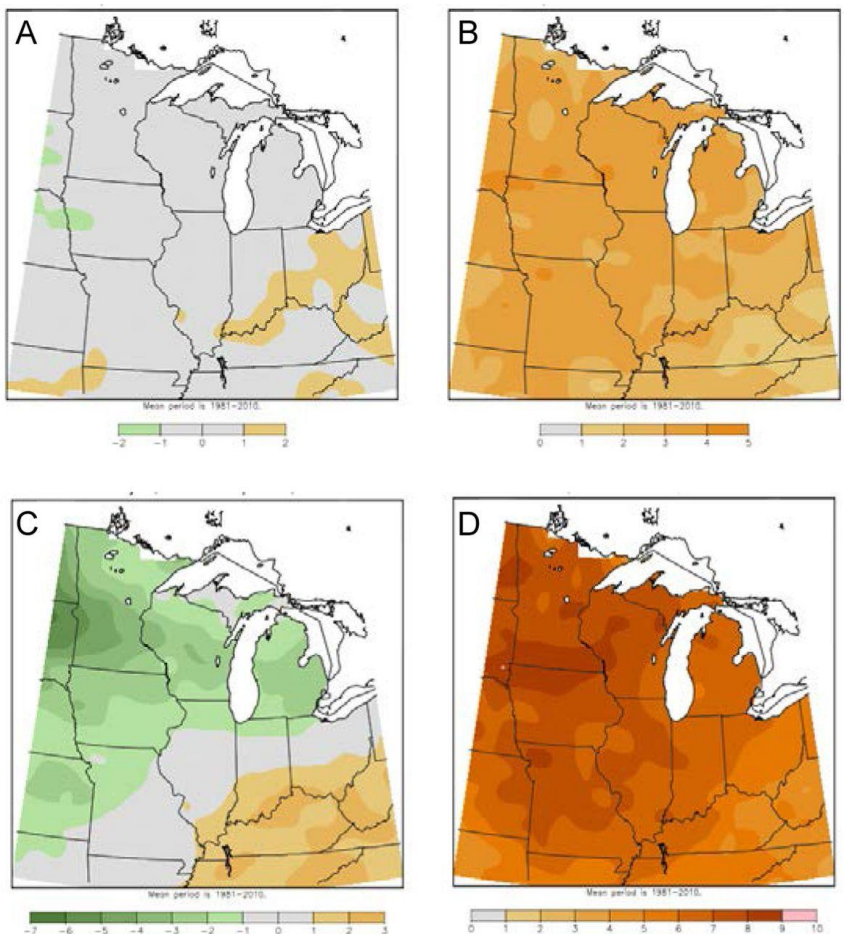

Figure 4.3: A and B: Departure from normal annual observed temperature comparing 2011 (left) to 2012 (right). C and D: Departure from normal seasonal (planting season: February 1 to April 30 of calendar year) observed temperature comparing 2011 (left) to 2012 (right). Data are from the Midwest Regional Climate Center (http://mrcc.isws.illinois.edu) and are given in degrees Fahrenheit. Climate normal period for anomaly calculation is 1981 through 2010.

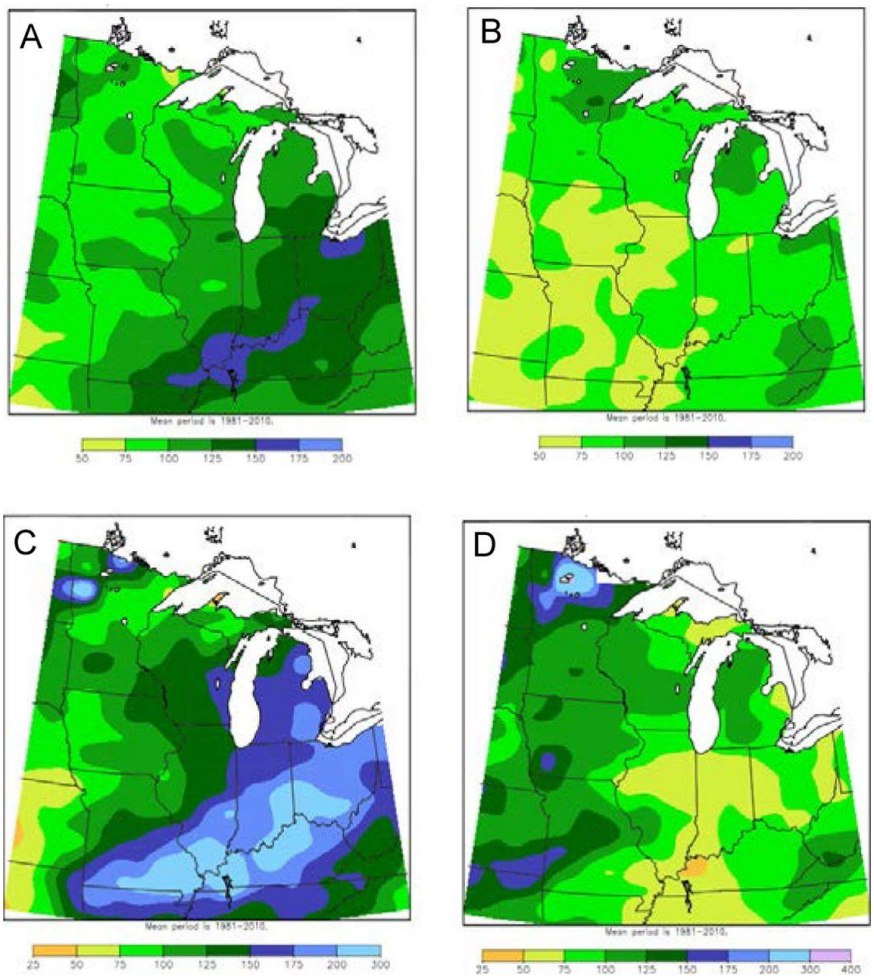

Figure 4.4: A and B: Percent of normal observed annual precipitation comparing 2011 (left) to 2012 (right). C and D: Percent of normal observed seasonal (planting season: February 1 to April 30 of calendar year) precipitation comparing 2011 (left) to 2012 (right). Data are from the Midwest Regional Climate Center (http://mrcc.isws.illinois.edu) and are given in percent of normal rainfall measured in inches. Climate normal period is 1981 through 2010.

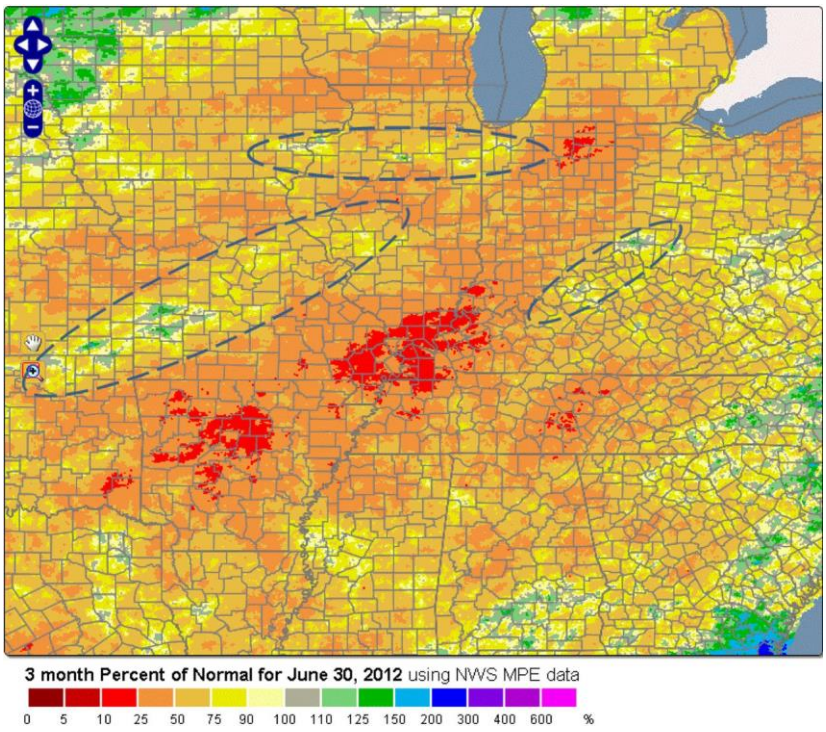

Figure 4.5: High-resolution drought trigger tool map of the Midwest portion of the U.S. Corn Belt April 1, 2012, to June 30, 2012. The detailed input of multisensor precipitation estimation data along with Standardized Precipitation Index data provides for a more fine-scale analysis of brief convective rainfall events that resulted in short-lived drought withdrawal (encircled with a dashed ellipse) across drought-stricken regions. Map generated from www.nc-climate.ncsu.edu/drought. NWS = National Weather Service; MPE = Multisensor Precipitation Estimation.

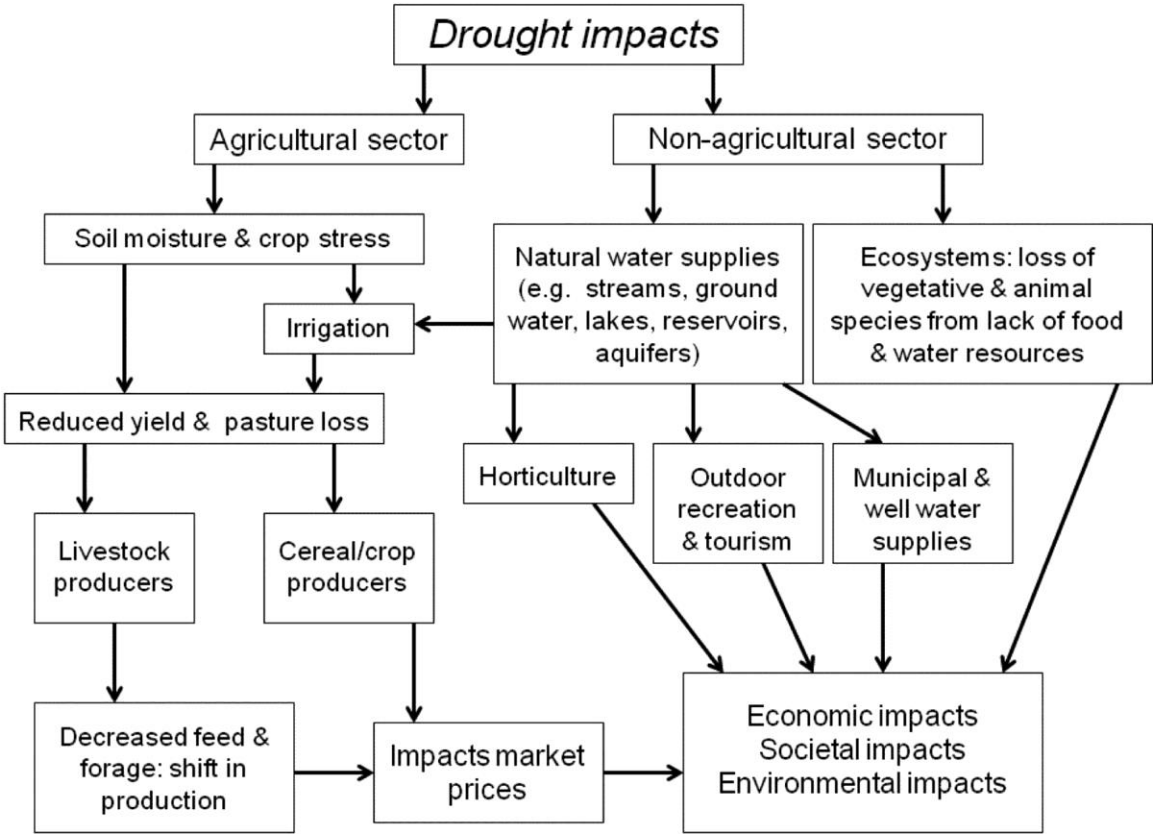

Figure 4.6: Drought impacts on the economy, societies, and the environment moving through time from the top of the chart to the bottom of the chart. Adapted with modification from Ding et al. (2010).

CHAPTER 5. LAND-FALLING TROPICAL SYSTEM RAINFALL CONTRIBUTION TO THE HYDROCLIMATE OF THE EASTERN U.S. CORN BELT 1981-2012

5.1 Introduction

Tropical cyclones (i.e. tropical systems) are an important element of global and regional hydroclimates in that they are synoptic scale weather phenomena that redistribute heat, moisture, and momentum from the tropical regions to the Subtropics and Midlatitudes in order to restore thermal and inertial balance in the Earth-atmosphere system. The transport of moisture-laden air from these storms to the Subtropics and Midlatitudes links the hydroclimate of the tropics to the hydroclimate of these other regions as water is taken from tropical oceans and released as rainfall over the Subtropics and Midlatitudes.

Precipitation that falls from tropical systems becomes linked to the hydroclimate of the Continental United States (CONUS) and its regions once the storm makes landfall. With an average of 11.7 named tropical and subtropical storms for the Atlantic Basin during the period 1900-2013 and with an average of 1.7 of these storms making landfall (Landsea 2014), the annual precipitation defining the hydroclimate within the U.S. Corn Belt east of the Rocky Mountains (Atlantic Basin Hurricanes do not go west of this divide) is comprised in part by tropical system (TS) rainfall. The most active time for tropical cyclones in the Atlantic Basin is during hurricane season which is defined by the months of May to November. Hurricane season also coincides with the primary agricultural production season in the United States. Recalling the importance of rainfall to yield as discussed in chapters two, three, and four, understanding what quantity of crop growing season rainfall comes from specific meteorological sources can help producers

better prepare for wet and dry periods, irrigation, fertilizer application, field work days, and harvest.

This chapter discusses a land-falling TS climatology developed for the years 1981-2012 for the Midwest United States. The climatology, coupled with historic crop data and historic rainfall data, attempts to determine the role of land-falling TS rainfall in crop production at state climate division and crop reporting district levels for the states of Wisconsin, Michigan, Illinois, Indiana, Ohio, and Kentucky. Findings discussed in detail in the next section support the need to include hurricane season forecasts, and more specifically land-falling TS forecasts, into seasonal rainfall outlooks for producers due to the relationships found between historic yields and TS rainfall in some climate divisions/crop reporting districts.

5.2 Land-falling Tropical System Rainfall Contribution to the Hydroclimate of the Eastern U.S. Corn Belt 1981-2012

As Submitted to the Journal of *Weather and Climate Extremes,* February 26th, 2015.

Full citation: Kellner, O., D. Niyogi, and F.D. Marks, 2015: Land-falling Tropical System Rainfall Contribution to the Hydroclimate of the Eastern U.S. Corn Belt 1981-2012. *Wea. and Cli. Extremes,* Submitted.

Abstract

This study provides a climatology (1980-2012) of land-falling tropical systems in the eastern Corn Belt and investigates the total contribution of land-falling tropical system-based rainfall on the monthly climatological total rainfall for states in Midwest United States. The primary focus is on rainfall impacts from land-falling tropical systems on historic corn yields at the climate division and crop reporting district level with inclusion of El Niño-South Oscillation analysis. Drought conditions for historic monthly observed rainfall are identified using the Palmer Drought Severity Index (PDSI) and the Standardized Precipitation Index (SPI). Analysis using these historic drought indices reveals that without land-falling tropical system rainfall drought conditions across the domain increased from 16% up to over 200%.

It is found that land-falling tropical storm system rainfall accounts for about 30% of the observed monthly rainfall during June, 12% during July, 21% during August, 26% during September, 15% during October, and 13% during November across the eastern Corn Belt. For the hurricane season, land-falling tropical system rainfall across the domain comprises 20% of the observed seasonal rainfall 1980-2012. Correlation between the annual number of land-falling tropical systems and annual yield by state within the domain yields no relationship, but correlation of monthly observed rainfall by climate division during August to crop reporting district annual yields has a weak to moderate correlation in Ohio districts 30-60 and Indiana CRD 90. September rainfall has correlation in Ohio district 80 and Kentucky district 30. Statistical analysis suggests that land-falling tropical storm rainfall may actually reduce yields in some states climate divisions/crop reporting districts while increasing yield in others.

Although land-falling tropical systems alleviate drought conditions across the domain, the results presented here suggest that there is a balance between storms providing sufficient rainfall and too much rainfall to be of benefit to crops. Kentucky's western hydroclimate and annual production appears related to the frequency of land-falling tropical systems. Findings aim to provide information to producers, crop advisers, risk managers and commodity groups so that a seasonal hurricane forecasts can potentially be utilized in planning for above or below normal precipitation during phenologically important portions of the growing season.

5.3 Introduction

Tropical storm systems impacting the tropical and subtropical latitudes of the United States primarily originate in the descending branch of the Hadley cell circulation known as the northeasterly trade winds over the Atlantic Ocean. Systems of sufficient organization track west, northwest across the tropics, and eventually become embedded in westerly flow whereupon the storm takes a right turn (easterly turn) and heads towards the subtropical latitudes of North America. Climatological assessment of rainfall resulting from tropical systems has been completed for coastal regions along the Gulf of Mexico and the East Coast of the United States (e.g. Cry 1967; Knight and Davis 2009;

Nogueira and Keim 2011; LaRow 2013; Maxwell et al. 2013); however, lesser attention has been paid to the contribution of land-falling tropical systems to the eastern U.S. Corn Belt hydroclimate, especially in regards to agricultural production.

The Midwest region of the United States includes of a vast expanse of agricultural land primarily devoted to the growth of soybeans and corn. Seasonal rainfall from midlatitude weather systems and convective thunderstorms is typically sufficient for the growth of corn across much of the region without need for irrigation except in regions of sandy soils such as northern Indiana and southern Michigan, and portions of Illinois. Corn reaches its critical grain-fill period during the months of August and September (depending on planting date) when heat and moisture stress within a two week window can vastly affect the yield potential of the crop (Nielsen 2011; Takle et al. 2014). As discussed in this study, it is during August and September that the Midwest also sees its greatest amount of rainfall from tropical-based systems that made landfall over the United States.

Hydroclimatological analyses are valuable tools allowing for a better understanding of hydroclimatic processes in light of potential climate variability and change identified in the last several years (e.g. IPCC 2014, Charusombat and Niyogi 2011). As the world's largest producer of corn, the United States' Corn Belt is located in a region known to experience climate variability and change. Climate change projections indicate longer dry spells, heavier rain events, and longer growing seasons resulting from warmer days and warmer nights (Melillo et al. 2014). Being prepared to face climate change begins with understanding climate variability. A hydroclimatology helps provide a better understanding of climate variability in the climate system.

Climate variability is responsible for the different temperatures and precipitation patterns that are above or below what is considered climatologically normal for a given area. Climate variability is most commonly driven by teleconnection patterns such as the El Niño Southern-Oscillation (ENSO) which has been found to impact rainfall amount and distribution across the United States depending on ENSO phase. Climatologically normal rainfall for a given region is determined over a 30-year period (e.g. Trewin 2007; Wright 2012) and is inclusive of all types of observed precipitation events. Thus,

climatologically normal precipitation values are inclusive of (but not limited to) events such as rainfall from tropical systems, blizzards, flood events, and convective thunderstorms. The percentage contribution of each type of precipitation event to the monthly climatological normal, however, is not readily available. In an effort to understand the role of land-falling tropical storm system rainfall in the Midwest's hydroclimate, this climatology investigates land-falling tropical system rainfall impact on the Midwest. The period reviewed is 1980-2012 to coincide with the release of newest set of climate division normals used to compute if observed rainfall is in drought conditions according to the Palmer Drought Severity Index.

The Midwest is selected as the study area because of its contribution to crop production in the United States and because it experiences warm-season weather phenomena including tropical and extratropical cyclones, convective storms and tornadoes, floods, and droughts which are governed by various teleconnection patterns. Research efforts to determine the contribution of tropical cyclone rainfall to seasonal rainfall in the United States have been completed over the last several years (e.g. Corbosiero et al. 2009; Knight and Davis 2009; La Row 2013; Maxwell et al. 2013; Nogueira and Keim 2001; Rodgers et al., 2001; Cry 1967) for coastal regions; however, these studies have a strict adherence to "tropical" categorization which removes the influence of tropical depressions, extra-tropical transitioning systems, and remnant lows from these studies. Many tropical storm systems traverse far inland impacting the Midwest during the growing season such as Tropical Storm Arlene, hurricane Katrina, and hurricane Rita in 2005. Rippey (2010) shows a possible link between corn yield and Atlantic tropical cyclone activity/inactivity in his assessment of the PDO and ENSO, showing that the number of land-falling tropical systems may influence crop yields. This study further investigates the hypothesis that land-falling tropical systems (TSs) play an important part of the Midwest hydroclimate as related to agriculture.

In addition to the aforementioned studies investigating tropical cyclone rainfall budgets, a number of hydroclimatologies were completed for select regions of the United States (e.g. the tropics, the southeastern United States, the western United states). However, none of these hydroclimatologies investigate the coupled relationships of

teleconnection patterns to annual or sub-annual regional rainfall, and none identify the portion of climatological warm-season rainfall attributable to land-falling tropical systems as influenced by teleconnections such as ENSO. Haberlie et al. (2013) recently completed an analysis of tropical system rainfall in the Eastern Corn Belt, which is similar in intent to the work herein, but differs in tools, methodology, and classification of storm. The primary difference between Haberlie et al., (2013) and this paper is that Haberlie et al., (2013) identify the role of land-falling TSs as "drought-busting events" based on the storm producing a specific precipitation threshold value with the drought of 2012 serving as the primary driver for the investigation. While this study investigates drought conditions with and without land-falling TS rainfall, the primary goal of this study is to determine the total climatological contribution of seasonal rainfall (hurricane season defined as May – November) from land-falling TSs and what impact this rainfall has on crop production. This information is expected to help agricultural producers, risk managers and commodity groups be better informed when making decisions related to crop production when a hurricane season outlook is available.

5.4 Data & Methods

5.4.1 Tropical Systems 1980-2012

HURDAT2 data is collected from 1980-2012 for the Atlantic Basin. Storms that made landfall in the Continental United States (CONUS) are identified through maps of best track data, and further selected based on the criteria that the storm traveled inland far enough before dissipating for the center pressure to come within 150 miles of a state boundary of the domain (Wisconsin, Illinois, Indiana, Ohio, Michigan, and Kentucky) and producing precipitation. 150 miles is selected because the average tropical storm system diameter is 300 miles with outer rain bands a few miles to tens of miles wide and 50-300 miles long (NOAA 1999). Once a storm is within 150 miles of the domain based on 6 hour latitude and longitude coordinates, climate records are queried for daily precipitation amounts. States queried for daily precipitation from identified land-falling tropical systems are identified through archived Weather Prediction Center (WPC) (National Centers for Environmental Prediction (NCEP)) maps of tropical rainfall

distribution (available at: http://www.wpc.ncep.noaa.gov/tropical). If a state is not impacted by a given storm, daily rainfall and monthly observed rainfall values are not collected.

5.4.2 Rainfall 1980-2012

Daily rainfall totals are collected at the state climate division (SCD) level from the Midwest Regional Climate Center's (MRCC) Application Tools Environment (cli-MATE) for those dates the storm is present in the domain. The domain has a total of 51 state climate divisions. The rainfall data is from the National Climatic Data Center (NCDC) nClimDiv dataset which became operational and available to the public on March 17, 2014 (Vose et al. 2014). The nClimDiv dataset is a 5-km gridded dataset based on the Global Historical Climatology Network-Daily (GHCN-D) and differs from the previous dataset (DRD964x) through use of a grid-based calculation for daily values, incorporating more stations with pre-1903's data, and implementing updated quality-control techniques (NCDC 2014).

A tropical system is considered within proximity of affecting the domain through analysis of 6 hourly best track data when it is 150 miles or less from domain state boundary, or when available radar data shows precipitation from rain bands over the domain area (radar data from: http://locust.mmm.ucar.edu/). Because radar data used for 1996-2012 storms are time-stamped in Coordinated Universal Time (UTC) (radar images prior to 1996 are unavailable), any time stamp of 0600 UTC on a radar image showing tropical system induced rainfall within the domain indicates that rainfall fell on the previous day in the United States. This is accounted for where necessary in this analysis. Table 5.1 provides a list of all storms meeting the aforementioned criteria.

Daily precipitation data for a SCD is collected from the day a storm enters the domain till the date the storm exits the domain to determine the total storm rainfall. If more than one storm enters the domain in a given month, the storm totals are added together to determine the total amount of monthly observed precipitation attributable to the land-falling TS (from now on "tropical system rain" or TSR). Monthly observed rainfall (from now on MOR) and the monthly climate normals (1981-2010) (from now on

NORM) for precipitation are also collected at SCD level. The NORMs are reduced by 15% (i.e. NORM – (NORM*0.15) to find the threshold value of observed precipitation below which would be considered drought conditions for a given month (from now on DRO) as discussed in Palmer (1965). Following the findings of Palmer (1965), reducing NORMs by 15% is representative of Palmer Drought Index (PDI or PDSI – Palmer Drought Severity Index) drought classification without a land-falling tropical system's rainfall. The PDSI index incorporates temperature, precipitation, and soil data to determine water supply and demand helping to make it suitable for un-irrigated cropland (Palmer 1965). The PDSI is selected because it is the primary agricultural drought indicator and this paper investigates TSR influences (if present) on crop production. A second index, the Standardized Precipitation Index (SPI) is assessed as well due to its rapid response to precipitation surplus or deficit. The SPI responds quickly because it considers only observed precipitation and is based on the standardized probability of observing a specific amount of precipitation across temporal scales (short-term and long-term) with focus on application to water availability and use (Guttman 1998). Under the SPI, an SCD is marked as DRO when the SPI index value reaches -0.51 or greater (i.e. "abnormally dry").

The MOR is then compared to DRO values to determine which climate divisions in the domain are in drought conditions despite all observed rainfall. Another dataset, MOR minus TSR is determined (from now on MOR_TSR) to compute the monthly observed rainfall in a given SCD had a land-falling TS not entered the domain. Those MOR_TSR values above DRO indicate that the land-falling TSR was assumed enough to provide drought relief in the climate division.

5.4.3 Crop Production 1980-2012

Yield data is collected down to county level across the United States with regional summaries provided at CRD levels. Most CRD boundaries coincide with the climate division boundaries in a given state, making annual crop yields at crop reporting district spatial scales suitable for rainfall analysis at state climate division spatial scales. However, while using a gridded rainfall dataset, some smaller-scale rainfall variability

impacts to crop yields a localized field scale that may not be captured. However, the spatial resolution used in this study is deemed sufficient for analysis. For the period in review, the state with the average highest annual detrended yield time series is Illinois (141.4 bushels/acre), followed by Wisconsin (134.7 bushels/acre), Ohio (134.0 bushels/acre), Indiana (133.1 bushels/acre), Michigan (125.3 bushels/acre), and Kentucky (110.1 bushels/acre), respectively. All yield data at the CRD level is detrended through a one-year lag linear regression and tested with the Durbin-Watson statistic to ensure no autocorrelation exists in the detrended yield time series (Montgomery et al., 2006). The The predicted 2012 yield is used as the detrending benchmark.

5.5 Findings

5.5.1 Tropical System Climatology 1980-2012

Annual past track seasonal maps for the Atlantic Basin are collected from the National Hurricane Center's data archive (http://www.nhc.noaa.gov/data/#annual). Four hundred tropical systems are identified during the hurricane seasons of 1980-2012. Of the 400 storms, 116 of these storms made landfall in the Continental United States (CONUS) with only 28 storms entering the Midwest domain. Figure 5.1 provides annual seasonal total, annual season total making landfall, and the annual seasonal total of land-falling hurricanes entering the Midwest. Annually, 2005 is the year with the highest number of named storms (28) and the highest number of land-falling systems to enter the Midwest (5). For all land-falling storms (those entering and not entering the domain), the years 1985, 2002, and 2004 tied for the years with the highest number of land-falling tropical systems at eight each year. The year 1983 is the year with the lowest number of named tropical systems with only 4 identified in the Atlantic Basin. The years 1990, 1993, and 1997 only had one storm make landfall in the CONUS. For the Midwest, the years 1982-1984, 1986, 1987, 1990, 1991, 1993, 1997-2000, 2007, 2009, 2010, and 2013 experienced no land-falling tropical systems. On average, for the time period 1981-2012, the Atlantic Basin saw 12 storms a year (median value: 12). Land-falling tropical systems for the CONUS average 3 per year (median value of 3), and land-falling storms entering the Midwest averages less than 1 per year (0.85 with a median value of 1). By

month, the most active month in the Atlantic Basin hurricane season is September with land-falling hurricanes in the CONUS occurring most often in August and September (tied at 24). For land-falling storms entering the Midwest, the most active month is September with 13 storms (Figure 5.2). When a storm spanned two months, the storm was assigned to the month during which it spent the most time in, and if the storm equally spanned two months, it was assigned the month during which the storm made land-fall. If the storm did not make landfall, it was assigned to the month in which it was identified. Out of the six state domain, Ohio and Kentucky are the states that were most affected by land-falling tropical systems 1981-2012. Through the time period, 23 storms contributed to observed rainfall in these states, followed by the state of Indiana at 17 storms, Illinois with 16 storms, and Wisconsin at 4 storms. The average time a tropical system spent in the domain is 45.8 hours (median value of 44.5 hours). This time frame is computed from 6 hourly best track data with a storm considered within the domain when it is 150 miles or less from domain state boundary, or when available radar data shows precipitation from rain bands over the domain area (radar data from: http://locust.mmm.ucar.edu/).

Similar to findings of Bove et al. (1998) and Klotzbach (2011) who investigate all land-falling hurricanes, the number of land-falling hurricanes to enter the Midwest during a La Niña or Neutral-phased ENSO event (18 and 6 storms for the Midwest 1981-2012, respectively) is much greater than during an El Niño event (4 storms). When land-falling storms are separated by ENSO phase at the time of landfall, storms making landfall during an El Niño or La Niña phase favored landfall across the Gulf Coast states of Louisiana, Florida (Panhandle), Mississippi, and Alabama with Hurricane Gilbert (1989) making landfall over Mexico before being caught in Westerly flow and entering the United States and tracking over the eastern U.S. Corn Belt. Land-falling TCs impacting the domain that made landfall during a neutral ENSO event made landfall on both the Eastern Seaboard (Virginia, North Carolina, South Carolina, and Florida) and in the Gulf Coast States. Klotzbach (2011) also investigates the relationship between ENSO phase and where storms make landfall for the years 1900-2009. During neutral and La Niña phases, there is an increased hurricane probability impact of land-falling storms for

the Gulf Coast while the hurricane probability impact of land-falling storms during an El Niño is higher for the East Coast. Although Klotzbach's findings differ slightly compared to those in this study, this is likely attributable to the limited sample size of storms and ENSO events. Additionally, all events made landfall at storm strength as designated in the storm's name (i.e. Hurricane Fran made landfall as a hurricane) except for Tropical Storm Bret 1981 (made landfall as a tropical depression), Hurricane Cindy 2005 (made landfall as a tropical storm), and Hurricane Ernesto 2006 (made landfall as tropical storm). These three events all occurred during ENSO neutral events. Additionally, there is no relationship found between storm intensity at time of landfall and recorded TSR, agreeing with Cline (2002).

5.5.2 Rainfall and Historic Drought Conditions 1980-2012

During the study period 1981-2012, drought conditions developed across much of the domain with more significant impacts to agricultural production during some years compared to others. Five years experiencing major drought across much of the U.S. Corn Belt (1983, 1988, 1991, and 2012) were identified and excluded from yield analysis due to the increased amount of yield loss. In order to investigate the role of land-falling hurricanes in the hydroclimate of the Midwest and their impacts on drought conditions and yield at SCD level, rainfall records had to be collected for each month and year a storm impacted one or more states. This resulted in a total of 811 separate records of SCD rainfall. Note that records are only collected in those states/climate divisions impacted by a tropical storm, so not all years and records are collected and investigated for each SCD.

5.5.2.1 Palmer Drought Severity Index Analysis

Monthly observed rainfall is compared to DRO values to determine which climate divisions in the domain are in drought conditions despite all observed monthly rainfall (TSR + other rainfall). Illinois had 65 climate division records of observed rainfall 1981-2012 in drought conditions despite tropical storms moving through the region. Without any land-falling tropical systems, 17 more climate divisions would have been in drought conditions for a total of 82 climate division records in drought status benefitting

by the rainfall from land-falling tropical systems. The number of Illinois SCDs not experiencing drought conditions is 71. This means that 53.6% of SCDs impacted by a land-falling TS would have been categorized as experiencing drought without rainfall from land-falling tropical systems. Illinois shows the highest percentage of SCDs that would have been categorized as experiencing drought conditions without rainfall from land-falling tropical systems, followed by Ohio (50.4%), Indiana (48.8%), Wisconsin (47.2%), and Kentucky (42.0%). It is found in this study that the upper peninsula of Michigan experiences more climatologically dry conditions than wet conditions, giving Michigan a bias to drought conditions without TSR. Thus, it should not be considered the second highest state.

5.5.2.2 Standardized Precipitation Index Analysis

To determine the role of TSR in alleviating drought conditions as determined by the SPI, the 1-month SPI is computed using MOR and then computed once again with MOR_TSR. The number of SCDs entering DRO status once TSR has been subtracted from MOR are counted and compared to those SCDs in drought status with MOR. Using SPI, Illinois had 68 climate division records of observed rainfall 1981-2012 in drought conditions despite tropical storms moving through the region. Without any land-falling tropical systems, 11 more climate divisions would have been in drought conditions for a total of 79 climate division records in drought status benefitting by the rainfall from land-falling tropical systems. The number of Illinois SCDs not experiencing drought conditions is 74. This means that 51.6% of SCDs would have been categorized as experiencing drought conditions without rainfall from land-falling tropical systems. Unlike PDSI, Indiana (not Illinois) shows the highest percentage of SCDs that would be categorized as experiencing drought conditions without rainfall from land-falling tropical systems, followed by Illinois (51.6%), Ohio (37.9%), Kentucky (38%) and Wisconsin (33.3%). Once again, Michigan experiences more climatologically dry conditions than wet conditions, giving Michigan a bias to drought conditions without TSR. Thus, it should not be considered the second highest state. Table 5.2 summarizes this information for PDSI and SPI for all states in the domain.

5.5.2.3 Percentage of Monthly Rainfall Climatology that is Tropical System Rainfall

The amount of TSR from each storm is determined as a percentage of the total monthly observed rainfall for a state and climate division. This provides an idea of how much TSR constitutes the total climatological rainfall in a state and climate division. Storms are documented to impact the domain in the months of June through November during the time frame 1980-2012 so climatological rainfall budgets are only computed for these months by averaging the percentages of TSR to MOR for each month. Climate divisions with greater than 20% of MOR attributable to TSR are highlighted to determine the month(s) most impacted by TSR, denoting the months of August and September having the greatest amount of SCDs with 20% or greater MOR attributable to TSR. August and September are also crucial months for corn maturity and are investigated further in the next section.

5.5.2.4 ANOVA of Hurricane Season

Monthly observed rainfall for the months of May-November are summed for each year for each state and then separated into two groups for ANOVA analysis. Group one includes only those years in which a land-falling TS impacted the domain during hurricane season and group two includes only those years in which no land-falling TS impacted the domain during the hurricane season. The states of Ohio, Kentucky, and Wisconsin have statistically significant differences in the seasonal rainfall observed in storm years and non-storm years. During storm years, Ohio averages 26.7 inches of rainfall during hurricane season whereas without a storm, it only averages 23.8 inches of rainfall which is a 12.2% increase with land-falling TSR during hurricane season. Kentucky averages 29.5 inches of rainfall when land-falling TSs enter the domain but only 26.6 inches during hurricane season with no storms (a 10.0% increase). Wisconsin averages 25.8 inches during hurricane season when land-falling storms are present in the domain and only 22.9 inches if no storm is present (a 12.6% increase).

5.5.3 Land-falling Midwest Tropical Systems and Historic Yields 1980-2012

States with some to all climate divisions in the Midwest experiencing drought conditions despite experiencing rainfall from a land-falling TSs during the major droughts previously mentioned include Illinois (1988 and 2012), Michigan (1988 and 2012) Indiana (1988 and 2012), Ohio (1988 and 2012), Kentucky (2012), and Wisconsin (2012) (Figure 5.3). The yield data for these years is removed from analysis. While the 1983 and 1991 droughts did not impact the entire domain, the drought impacted some states within the domain enough that all yield data was removed for these years as well to be keep datasets as far removed from bias as possible (yields greater than one standard deviation below the mean).

Correlation and ANOVA are completed to investigate relationships that may exist between TSR and crop production. ANOVA is used to investigate the role of TSR on crop production through yield residuals (amount depicting how far above or below the observed yield is from the mean yield of a developed linear regression equation for all yields) in the following three analysis: 1) Years during which a TS passed through a state and/or climate division versus years during which a storm did not pass through a state and/or climate division; 2) years during which a TS passed through a state and/or climate division during August only versus all other years; and 3) years during which a TS passed through a state and/or climate division during September only versus all other years. Correlation of the number of land-falling TSs impacting a state within the domain per year to the reported average annual yield of that state is completed, along with correlation of state climate division August MOR to reported annual yields for each state climate division and September MOR to reported annual yields for each state climate division.

5.5.3.1 ANOVA

ANOVA (80% and 90% CIs) for crop residuals (percentage of yield above or below trend as determined through linear regression from detrended yield time series) during storm years and no storm years results in statistically significant relationships that are itemized in Table 5.3(a) and mapped in Figure 5.4. ANOVA for crop residuals during August storm years and years with no storm in August results in statistically

significant relationships as shown in Figure 5.5 **w**ith residuals provided in Table 5.3(b). ANOVA for crop residuals during September storm years and no storm in September years results in statistically significant relationships which are provided in Table 5.3(c) and mapped in Figure 5.6. There are not crop reporting districts that are statistically significant at the 80% CI.

5.5.3.2 Correlation

Correlation of the number of land-falling tropical systems impacting a state within the domain per year to the reported annual yield of that state results in no statistically significant relationships despite similar high and low points in moving averages (Figure 5.7). Correlation of August and September monthly rainfall at climate division/crop reporting district level to reported annuals yields, however, does return some statistically significant relationships. Indiana CRD 90 has a moderate to strong significance at 90% CI. Ohio CRDs 30 - 60 (which is Ohio SCDs 6 and 7) have moderate to strong significance at 90% CI as well during the month of August. For correlation of observed September rainfall and historic yield, only Ohio CRD 80 and Kentucky CRD 30 have a statistically significant (90% CI) moderate relationship. The correlation that does exist between historic detrended yield time series and observed rainfall inclusive of land-falling TSs establishes a generalized direct working relationship (land-falling TSR results in increased yield and less to no land-falling TSR rainfall results in decreased yield) between receiving land-falling TS rainfall and yields in the respective CRDs that these relationships are present. In terms of agricultural application, it provides an agricultural producer the understanding of a possible greater (lesser) than expected yield with an active (quiet) hurricane season forecast.

5.6 Discussion

The intent of this climatology is to determine the contribution of land-falling TSR to the climatological normal amount of rainfall across the Midwest at the crop reporting district/climate division level. This is completed as an effort to help producers in the region make more informed farm-related decisions when presented with seasonal rainfall forecasts. Understanding that there is a greater (or lesser) likelihood for TSR in a given

season can help farmers plan irrigation schedules and field work days more effectively (Takle et al. 2014). Additional questions addressed in this climatology include:

1) *Is there a relationship between annual yields and the number of land-falling TSs entering the Midwest?* Findings: While no correlation exists between the number of land-falling TSs and annual yield, there are statistical relationships present (both positive and negative) between annual yields and TSR for the entire season, and TSR during the months of August and September in select states and climate divisions/crop reporting districts.

2) *Is there a relationship between ENSO phase and the number of TSs that affect landfall in the Midwest?* Findings: The number of land-falling TSs by ENSO phase shows a greater likelihood of land-falling TSs to enter the Midwest during an ENSO neutral (with entry from the Gulf of Mexico or the Atlantic Seaboard/East Coast) or La Niña event (with entry from the Gulf of Mexico). They are least likely to occur during an El Niño event (with entry from the Gulf of Mexico – except for Hurricane Frances 2004, however rainfall from this storm impacted only the far northeastern portions of the domain). This would suggest that El Niño events reduce the chance of experiencing TSR within the domain. These findings align with the identified relationships between ENSO and drought conditions over the United States as discussed in Cole and Cook (1998). Cole and Cook (1998) find through PDSI analysis that Midwest drought conditions are correlated with El Niño events and that central and western United States drought conditions are correlated to La Niña events.

3) *Is there a relation between ENSO phases and where TSs make landfall (e.g. Eastern Seaboard versus Gulf Coast as they affect the Midwest)?* Findings: Past literature exploring the relationship between ENSO phase and yield point to increased yields during cooler and wetter El Niño years and reduced yields during hotter and drier La Niña events. This climatology shows that land-falling TSR is most common during ENSO neutral events, indicating that rainfall across the domain during El Niño years

primarily originates from extratropical disturbances. La Niña events had the second highest number of land-falling tropical systems to enter the domain, but the number is small compared to ENSO neutral events. Once again, these findings point to the importance of extratropical disturbances in rainfall occurrence across the Midwest hydroclimate during La Niña and El Niño events. With ENSO neutral events providing the greatest opportunity for land-falling TSR to occur in the Midwest, it is apparent that a shift in synoptic scale dynamics due to orientation and placement of the Polar Jet Stream occurs. This shift drives the rainfall budget across the Midwest from one experiencing more extratropical system rainfall towards a rainfall budget in which TSs contribute to a larger portion of total observed rainfall. This appears to impact crop production in some regions depending on antecedent conditions.

4) *Is there a relationship between which month(s) of the growing season TSR occurs and affect yield*? Findings: For those states with relationships established to be statistically significant with for storm years versus no storm years, August storm years versus all other years, and September storm years versus all other years are reviewed. Because a majority of storms occurred during ENSO neutral events, and TSR rainfall is found to reduce yields in Illinois, Indiana, and Ohio (higher yield residuals on average in years where TSR rainfall did not fall during August, September, or during the season), a link with ENSO yield relationships and ENSO TSR frequency and yield cannot be established with confidence. It is found that yields in Kentucky improve when TSR occurs in August, and during the season (i.e. storm years versus no storm years). Again, ENSO phase during these times is predominantly neutral. This suggests that Kentucky's corn production is the western portion of the state may be dependent on TSR rainfall due to the orientation of the mean storm track across the Midwest during an ENSO neutral event.

5.7 Conclusions

A majority of extreme weather events in the Midwest can be categorized as drought events, flooding, severe thunderstorms, tornado outbreaks, and snow storms (Changnon and Kunkel 2006). This study shows that land-falling TSs are an important

part of the Midwest hydroclimate in that rainfall from these systems serve to alleviate drought conditions in roughly 33-56% of SCDs during the hurricane season, with greatest contributions during the months of August and September across the domain - months during which crop yields are highly sensitive to heat and moisture stress.

The Midwest (defined in this analysis by the states of Wisconsin, Illinois, Indiana, Ohio, Michigan, and Kentucky) on average experiences slightly less than one land-falling TS event a year (0.85) for the years 1980-2012, account for 24% of the 116 land-falling TSs that impacted the U.S. While the year 2005 is the most active year on record for land-falling TSs to enter the Midwest (5), there are 15 years within the 1981-2012 timeframe that experienced no land-falling TSs. September is the month during which land-falling TSs occurred most often, followed by August. Ohio and Kentucky are the states most frequently impacted by land-falling TSs with Wisconsin being the least impacted. Land-falling TSs spend on average 44.5 hours (~2 days) in the Midwest from time of entry to exit of the domain. Land-falling TSs are also most likely during ENSO neutral events and least common during El Niño events.

Monthly observed rainfall during all months is reviewed and the percentage of TSR to total MOR is computed. August and September are investigated more deeply to determine if land-falling TSs are important contributors to the monthly rainfall budgets and crop production in the Midwest portion of the U.S. Corn Belt. These two months are selected because it is found that the average TSR is 21-26% of MOR across the domain during these two months. It is apparent from this climatology that without TSR, drought conditions would be more prevalent across the Midwest. Of all states in the Midwest, the percentage increase in the number of SCDs not in drought status with TRS rainfall (PDSI and SPI) to drought status conditions without TSR is greatest for the state of Ohio. Kentucky is impacted the least in this regard. However, Kentucky's SCDs encompass much larger land area than SCDs in other states which serves to make drought impact greater than it appears. The one-month SPI analysis reaches the same conclusions. ANOVA of hurricane season rainfall of storm years to years with no storm shows significance for Ohio, Kentucky, and Wisconsin.

ANOVA analysis of historic, detrended yield time series residual data further shows that TSR during some months appears to be beneficial for corn production (higher yields) in some states while being detrimental (reduced yields) in other states despite partial contribution of TSR to drought alleviation. It may be that the prolonged and often greater amounts of rainfall associated with land-falling TSs may be detrimental to increased production due to saturated soils. A moderate to strong correlation of August rainfall to annual yield is found in this study showing the importance of August rainfall to overall yield in certain regions.

The findings of this study show that land-falling TSs play an important role in the hydroclimate and crop production in the Midwest when land-falling TSs enter the domain in terms of drought alleviation and total contribution to climatologically normal rainfall, especially in Ohio and Kentucky. The findings of this study are aimed to help serve as guidance to producers and commodity trades when complimented with a tropical cyclone forecast in situations such as planning for irrigation during times of heat and moisture stress in August and September, and progress in crop dry-down during September. Findings will be incorporated into the decision support tool suite of products developed by the Useful to Usable (AgClimate4U.org) agricultural and food research initiative.

Acknowledgements: Useful to Usable (U2U) Transforming Climate Variability and Change Information for Crop Producers and Development of a High-Resolution Drought Trigger Tool (HIRDTT) for the United States; Agriculture and Food Research Initiative Competitive Grants 2011-68002-30220 and 2011-67019-20042 from the USDA National Institute of Food and Agriculture (NIFA). NASA Earth and Space Science Fellowship NNX10AN70H awarded to Olivia Kellner; NSF CAREER – Dev Niyogi.

5.8 References

Andresen, J., S. Hilberg, K. Kunkel, 2012: Historical Climate and Climate Trends in the Midwestern USA. In: U.S. National Climate Assessment Midwest Technical Input Report. Great Lakes Integrated Sciences and Assessments (GLISA) Center. http://glisa.msu.edu/docs/NCA/MTIT_Historical.pdf. (Accessed 3 July 2014.)

Bove, M.C., J.B. Elsner, C.W. Landsea, and X. Niu, 1998: Effect of El Niño on U.S. landfalling hurricanes, revisited. *Bull. Amer. Meteor. Soc.*, 79, 2477-2482.

Changnon, S.A. and K.E. Kunkel, 2006: Severe storms in the Midwest. *Illinois State Water Survey Report I/EM 2006-06.* http://www.isws.illinois.edu/pubdoc/IEM/ISWSIEM2006-06.pdf. (Accessed 2 December 2014.)

Charusombat, U., and D. Niyogi, 2011: A hydroclimatological assessment of regional drought vulnerability: A case study of Indiana droughts. *Earth Interactions*, 15, 1-65.

Cline, J., 2002: Surface-based rain, wind, and pressure fields in tropical cyclones over North Carolina since 1989. *NOAA Technical Memorandum NWS ER-94*, Bohemia, New York. http://www.erh.noaa.gov/er/hq/ssd/erps/tm/tm94.pdf. (Accessed 2 October 2014.)

Cole, J.E. and E.R. Cook, 1998: The changing relationship between ENSO variability and moisture balance in the continental United States. *Geophys. Res. Lett,* Vol. 25, No. 24, 4529-4532.

Corbosiero, K.L., M.J. Dickinson, L.F. Bosart, 2009: The contribution of Eastern North Pacific tropical cyclones to the rainfall climatology of the southwest United States, *Mon. Wea. Rev*. 137, 2415-2435, doi: 10.1175/2009MWR2768.1.

Cry, G.W., 1967: Effects of tropical cyclone rainfall on the distribution of precipitation over the eastern and southern United States. ESSA Professional Paper 1. US Department of Commerce, Environmental Science Services Administration: Washington, DC.

Guttman, N.Bl, 1998: Comparing the Palmer Drought Index and the Standardized Precipitation Index. *Jour. Amer. Water Res. Assoc.*, 34 (1), 113-121.

Haberlie, A., K. Gale, D. Changnon, and M. Tannura, 2014: Climatology of tropical system rainfall in the eastern Corn Belt. *J. Appl. Meteor. Climatol.*, 53 (2), 395-405.

IPCC, 2014: Climate change 2014: Impacts, adaptation, and vulnerability. Part B: Regional aspects. Contribution of working group II to the Fifth Assessment Report of the Intergovernmental Panel on climate change [Barros, V.R., C.B. Field, D.J. Dokken, M.D. Mastrandrea, K.J. Mach, T.E. Bilir, M.Chatterjee, K.L. Ebi, Y.O. Estrada. R.C. Genova, B. Girma, E.S. Kissle, A.N. Levy, S. MacCracken, P.R. Mastrandrea, and L.L. White (eds)]. Cambridge University Presss, Cambridge, United Kingdom and New York, NY, USA, Chapter 26.

Klotzbach, P.J., 2011: El Niño-Southern Oscillation's impact on Atlantic Basin hurricanes and U.S. landfalls. *J. Climate*, 24, 1252-1263.

Knight, D.B. and R.E. Davis, 2009: Contribution of tropical cyclones to extreme rainfall events in the southeastern United States. *J. Geophys. Res.*, 114: D23102, doi: 10.1029/2009JD012511.

LaRow, T., 2013: An analysis of tropical cyclones impacting the southeast United States from a regional reanalysis. *Reg. Environ. Change*, 13 (Suppl 1), 35-43, doi: 10.1007/s10113-012-0374-6.

Maxwell, J.T., J.T. Ortegren, P.A. Knapp, P.T. Soule, 2013: Tropical cyclones and drought amelioration in the Gulf and southeastern coastal United States. *J. of Clim.*, **26**, 8440-8452.

Melillo, Jerry M., Terese (T.C.) Richmond, and Gary W. Yohe, Eds., 2014: *Climate Change Impacts in the United States: The Third National Climate Assessment*. U.S. Global Change Research Program, 841 pp. doi:10.7930/J0Z31WJ2.

Montgomery, D.C., E.A. Peck, and G.G. Vining, 2006: Introduction to linear regression analysis, 4th edition. Hoboken: John Wiley and Sons. 504pp.

National Climatic Data Center (NCDC), 2014: Transitioning to a gridded climate divisional dataset. National Oceanic and Atmospheric Administration. http://www.ncdc.noaa.gov/news/transitioning-gridded-climate-divisional-dataset. (Accessed 30 June 2014.)

Nielsen, R.L., 2011: Predicting corn grain maturity dates for delayed plantings. Corny news Network. Purdue University, West Lafayette, IN. http://www.agry.purdue.edu/ext/corn/news/timeless/RStagePrediction.html. (Acccessed 26 November 2014.)

National Oceanic Atmospheric Administration, 1999: NOAA Hurricane basics. Naval Postgraduate School Homeland Security Digital Library publication nps41-090209-01. https://www.hsdl.org/?view&did=34038/ (Accessed 28 November 2014.)

Nogueira, R. C., and B. D. Keim, 2011: Contributions of Atlantic tropical cyclones to monthly and seasonal rainfall in the eastern United States1960–2007. *Theor. Appl. Climatol*., 103, 213–227.

Palmer, W. C., 1965: Meteorological drought. Research Paper 45, U.S. Dept. of Commerce, 58 pp.

Rippey, B., 2010: The Pacific Ocean's influence on drought and wetness in the continental United States and the nation's breadbasket. Proc. from the 22nd Conf. on Climate Variability and Change, and 18th Conference on Applied Climatology, J10.6, Atlanta, GA.

Rodgers, E.B., R.F. Adler, H. F. Pierce, 2001: Contribution of tropical cyclones to the North Atlantic climatological rainfall as observed from satellites. *J. Appl. Meteor.*, 40, 1785–1800. doi: http://dx.doi.org/10.1175/1520-0450(2001)040<1785:COTCTT>2.0.CO;2.

Takle, E.S., C.J. Anderson, J. Andresen, J. Angel, R.W. Elmore, B.M. Gramig, P. Guinan, S. Hilberg, D. Kluck, R. Massey, D. Niyogi, J.M. Schneider, M.D. Shulski, D. Todey, and M. Widhalm, 2014: Climate Forecasts for Corn Producer Decision Making. *Earth Interact.*, 18, 1–8. doi: http://dx.doi.org/10.1175/2013EI000541.1.

Trewin, B., 2007: The role of climatological normals in a changing climate. World Climate Data and Monitoring Program No 61, WMO-TD No 1377. http://www.wmo.int/pages/prog/wcp/wcdmp/documents/WCDMPNo61.pdf. (Accessed 14 October 2014) 46pp.

Vose, R.S., Applequist, S., Durre, I., Menne, M.J., Williams, C.N., Fenimore, C., Gleason, K., Arndt, D. 2014: Improved Historical Temperature and Precipitation Time Series for U.S. Climate Divisions. *J. of Appl. Meteor. and Climatol.* DOI: http://dx.doi.org/10.1175/JAMC-D-13-0248.1

Wright, W., 2012: Discussion paper on the calculation of the standard climate normals: a proposal for a dual system. World Climate Data and Monitoring Program. http://www.wmo.int/pages/prog/wcp/wcdmp/documents/Rev_discussion_paper_May2012.pdf . (Accessed 14 October 2014) 5pp.

5.9 Tables

Table 5.1: Midwest land-falling tropical systems and the states impacted by rainfall. H = hurricane strength at landfall. TS = a tropical systems at landfall.

Year	Name	Date	States	Year	Name	Date	States
1981	TS Bret	June 29 - July 1	IL, IN, KY, OH	2003	H Isabel	Sep. 6 - 19	OH, MI
1985	H Danny	Aug. 12 - 18	KY	2004	H Frances	Aug. 25 - Sep. 8	KY, OH
1985	H Elena	Aug. 28 - Sep. 4	IL, IN, KY	2004	H Ivan	Sep. 2 - 24	KY , OH
1985	H Juan	Oct. 26 - Nov. 1	IL, IN, KY, MI, OH, WI	2005	TS Arlene	June 8 - 13	IL, IN, KY, MI, OH
1988	H Gilbert	Sep. 8 - 19	IL, IN, MI, OH, WI	2005	H Cindy	July 3 - 7	KY
1989	H Hugo	Sep. 10 - 22	KY, OH	2005	H Dennis	July 4 - 13	IL, IN, KY, OH
1992	H Andrew	Aug. 16 - 28	IL, IN, KY, OH	2005	H Katrina	Aug. 23 - 30	IL, IN, KY, OH
1994	TS Beryl	Aug. 14 - 19	KY, OH	2005	H Rita	Sep. 18 - 26	IL, IN, KY, MI, OH
1995	H Erin	July 21 - Aug. 6	IL, IN, KY, OH	2006	H Ernesto	Aug. 24 - Sep. 1	KY, OH
1995	H Opal	Sep. 27 - Oct. 5	IN, KY, MI, OH	2008	TS Fay	Aug. 15 - 26	KY, OH
1996	H Fran	Aug. 23 - Sep. 8	OH, MI	2008	H Gustav	Aug. 25 - Sep. 4	IL, IN, KY, MI, WI
2001	TS Barry	Aug. 2-7	IL, IN, KY	2008	H Ike	Sep. 1 - 14	IL, IN, MI, OH, WI
2002	H Isidore	Sep. 14 - 27	IL, IN, KY, MI, OH	2011	TS Lee	Sep. 2 - 5	IL, IN, KY, MI, OH
2002	H Lili	Sep. 21 - Oct 4	KY	2012	H Isaac	Aug. 21 - Sep. 1	IL, IN, KY, OH

Table 5.2: Summary of state climate division (SCD) records during those months and years that a land-falling tropical system impacts the domain. The role of tropical storm system rainfall (TSR) in alleviating drought conditions expressed as a percentage of total records. PDSI is the top table and SPI is the bottom table.

Palmer Drought Severity Index						
State	**Illinois**	**Indiana**	**Ohio**	**Michigan**	**Wisconsin**	**Kentucky**
Total SCDs impacted by TSs in which MOR is in Drought Status	65	42	54	30	7	23
Total SCDs impacted by TSs in State added to drought if TSR removed (in drought without TSR)	17	37	67	31	10	19
Total SCDs in drought when TSR removed	82	79	121	61	17	42
Percentage of total SCDs in drought when TSR removed	53.6%	48.8%	50.4 %	50.8%	47.2%	42.0%
Percentage increase of SCDs in drought when TSR removed	26.2%	88.1%	124.1 %	103.3%	142.9%	82.6%
Total SCDs impacted by TCs by state 1980-2012	153	162	240	120	36	100

Standardized Precipitation Index						
State	**Illinois**	**Indiana**	**Ohio**	**Michigan**	**Wisconsin**	**Kentucky**
Total SCDs impacted by TSs in which MOR is in Drought Status	68	57	45	26	4	22
Total SCDs impacted by TSs in State added to drought if TSR removed (in drought without TSR)	11	33	46	14	8	16
Total SCDs in drought when TSR removed	79	90	91	40	12	38
Percentage of total SCDs in drought when TSR removed	51.6%	55.6%	37.9 %	33.3%	33.3%	38.0%
Percentage increase of SCDs in drought when TSR removed	16.2%	57.9%	102.2 %	53.8%	200.0%	72.7%
Total SCDs impacted by TCs by state 1980-2012	153	162	240	120	36	100

Table 5.3: States and those crop reporting districts (CDRs) with statistically significant relationships between the crop residuals during years in which a) a land-falling tropical system entered the domain and did not enter the domain; b) a land-falling tropical system entered the domain in August and did not enter the domain in August; and c) a land-falling tropical system entered the domain during the month of September and not during the month of September at 80% and 90% confidence intervals (CI). Those states that are significant at 80% are also significant at 90%. If a state is not listed, no relationship was found.

a. Storm Year versus No Storm Year – ANOVA 80% CI		
	Average Crop Residual with Storm	Average Crop Residual with No Storm
Indiana: CRD 30	-1.2	6.2
Kentucky: CRD 20	9.5	1.3
Storm Year versus No Storm Year – ANOVA 90% CI		
Kentucky: CRD 10	12.8	0.1

b. August Storm Year versus No Storm in August Year – ANOVA 80% CI		
	Average Crop Residual with Storm	Average Crop Residual with No Storm
Ohio: CRD 30	11.8	1.1
Illinois: CRD 30	-5.8	5.6
Kentucky: CRD 20	11.2	2.7
August Storm Year versus No Storm in August Year – ANOVA 90% CI		
Illinois: CRD 10	-5.2	5.7
Illinois: CRD 20	-6.1	6.3
Illinois: CRD 40	-4.9	6.4
Kentucky: CRD 10	13.7	3.6

c. September Storm Year versus No Storm in September Year – ANOVA 90% CI		
	Average Crop Residual with Storm	Average Crop Residual with No Storm
Indiana: CRD 30	-3.6	5.4
Michigan: CRD 60	9.9	-0.5

5.10 Figures

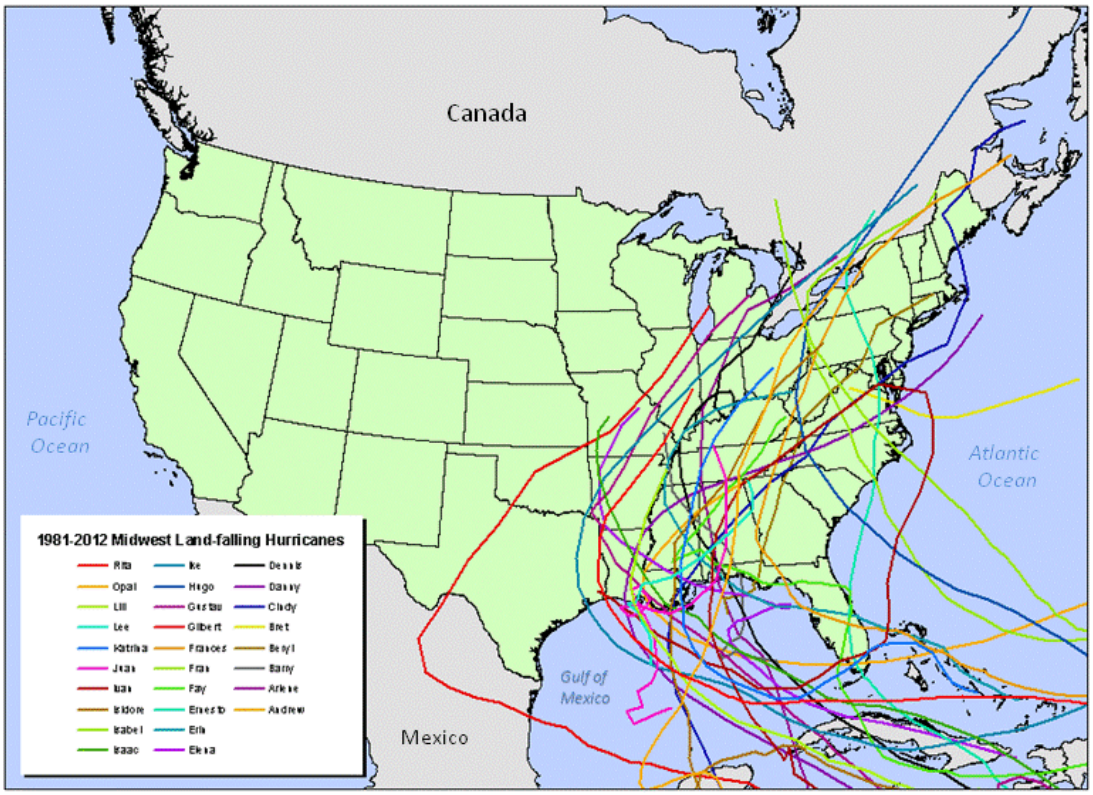

Figure 5.1: Land-falling tropical systems to impact the Midwest 1981-2012. Tracks are from 6-hourly HURDAT2 best track data available from the National Hurricane Center.

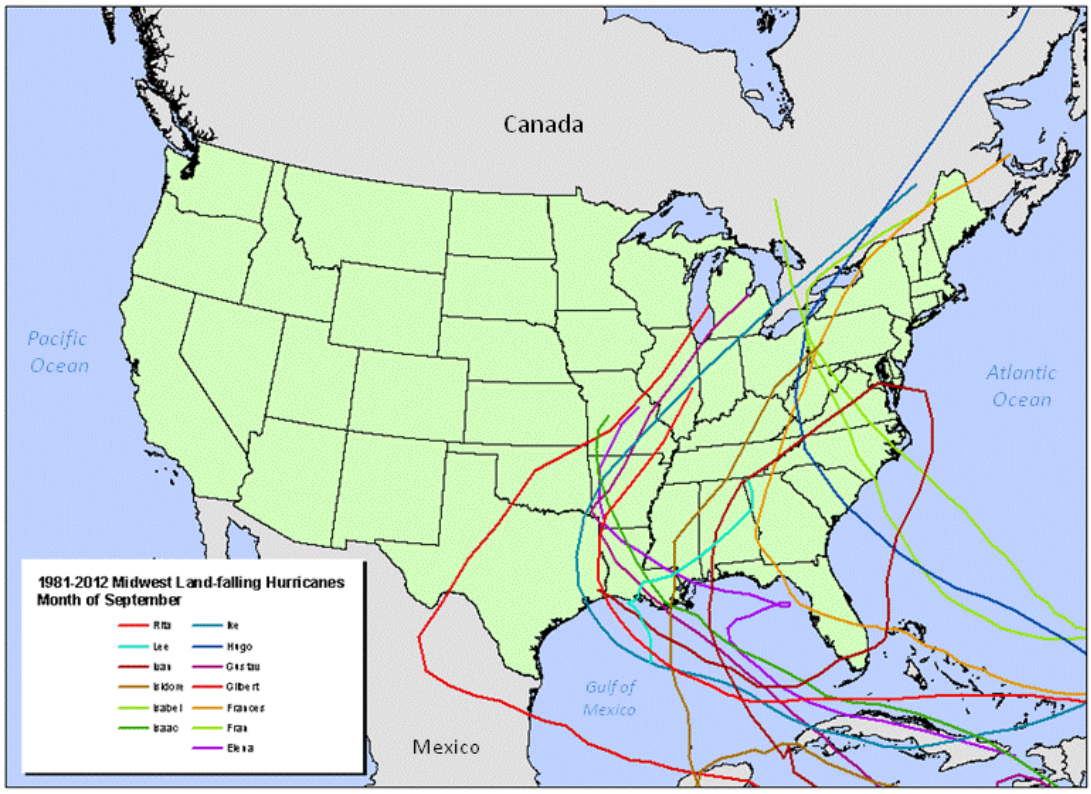

Figure 5.2: Land-falling hurricanes to impact the Midwest 1981-2012 during the month of September. Tracks are from 6-hourly HURDAT2 best track data available from the National Hurricane Center.

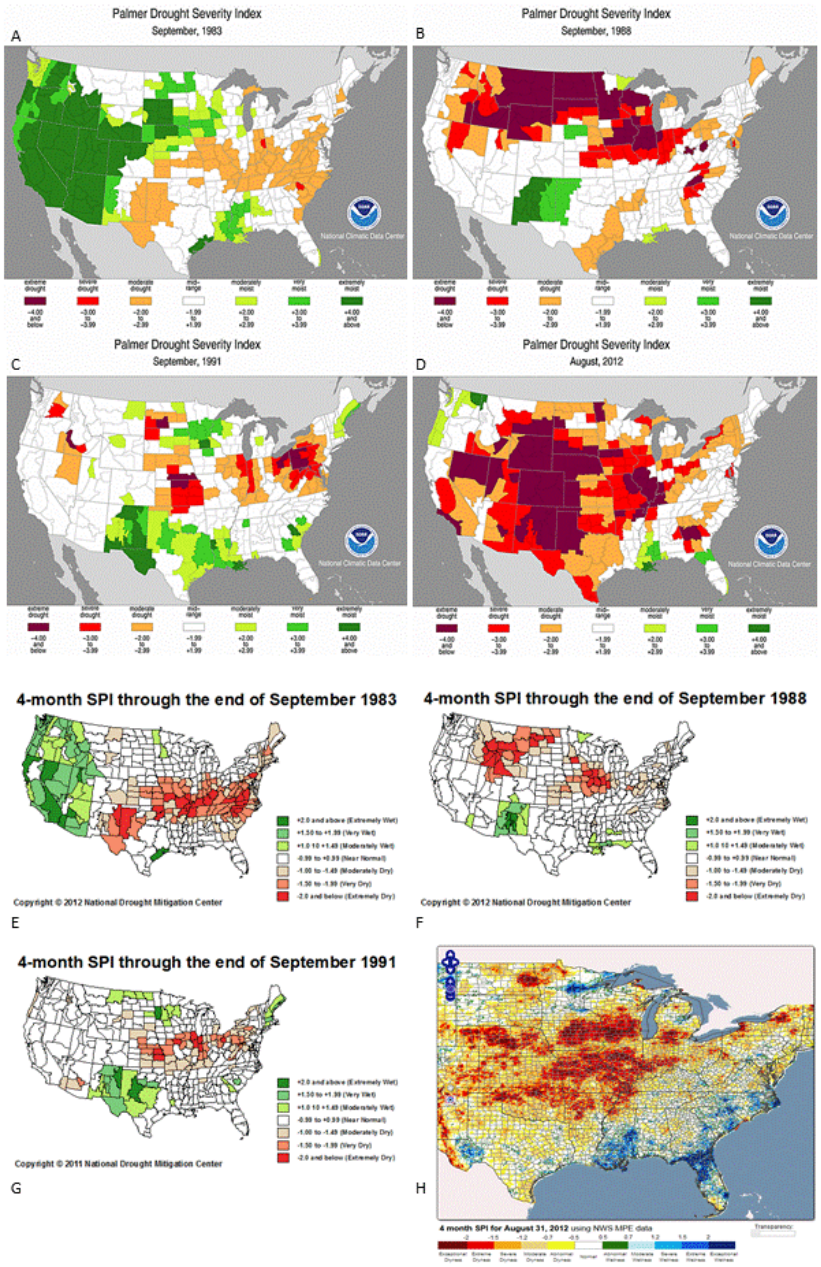

Figure 5.3: (A-D) PDSI maps showing drought conditions during August or September of the 1983, 1988, 1991, and 2012 growing seasons. These years are removed from analysis due to much below normal yields. (E-H) Four-month SPI maps showing drought conditions during August or September of the 1983, 1988, 1991, and 2012 growing seasons. PDSI maps from the National Climatic Data Center; 4-month SPI maps from the National Drought Mitigation Center and the University of North Carolina High Resolution Drought Trigger Tool user interface.

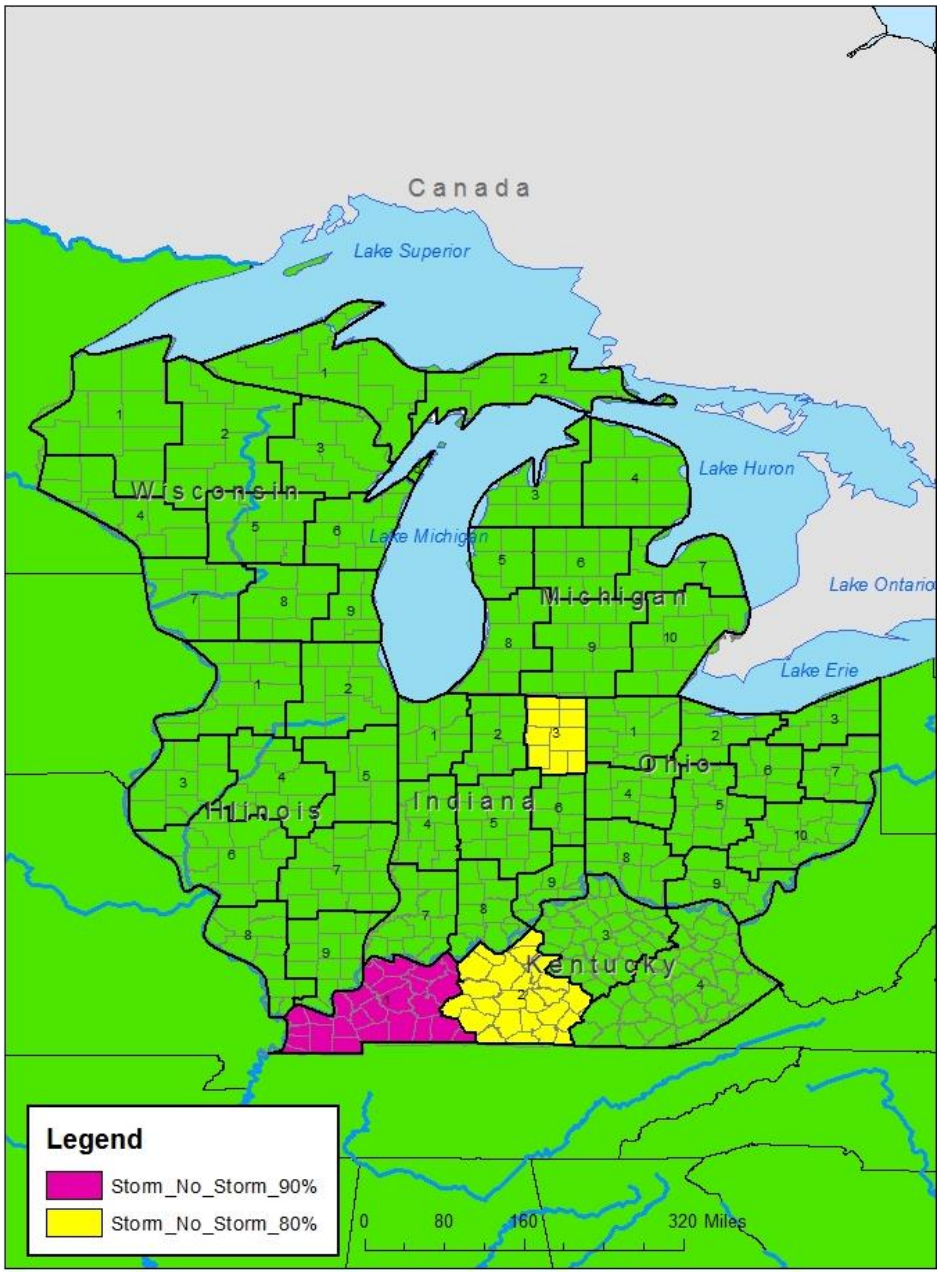

Figure 5.4: Crop reporting districts that have statistically significant differences between the mean residual of crop production during years with tropical storm passage and years without tropical storm passage during the hurricane season.

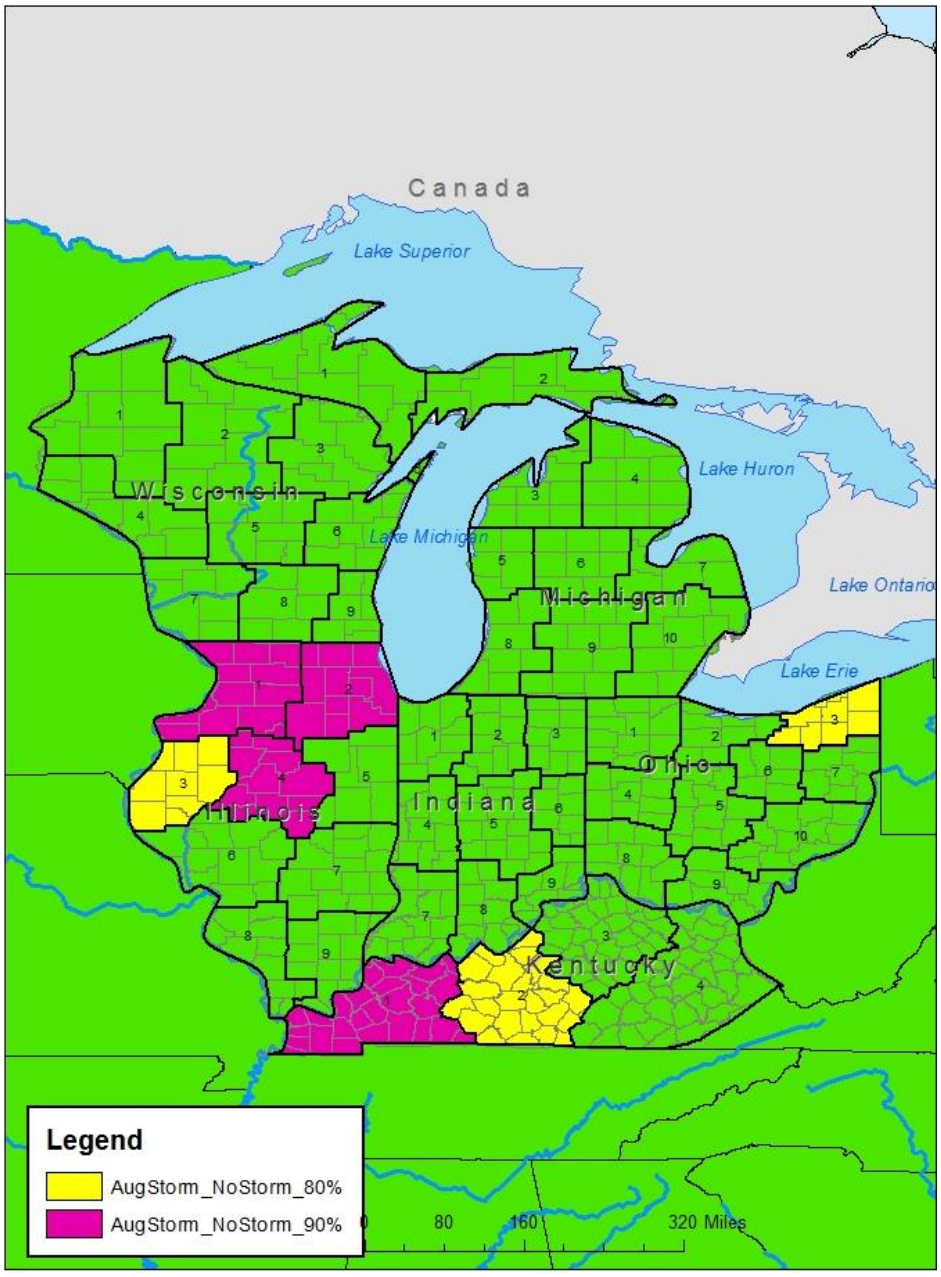

Figure 5.5: Crop reporting districts that have statistically significant (90% CI and 80% CI) differences between the mean residual of crop production during years with tropical storm passage during August vs. all other years. Note that those crop reporting districts that are significant at 80% CI are also significant at 90% CI.

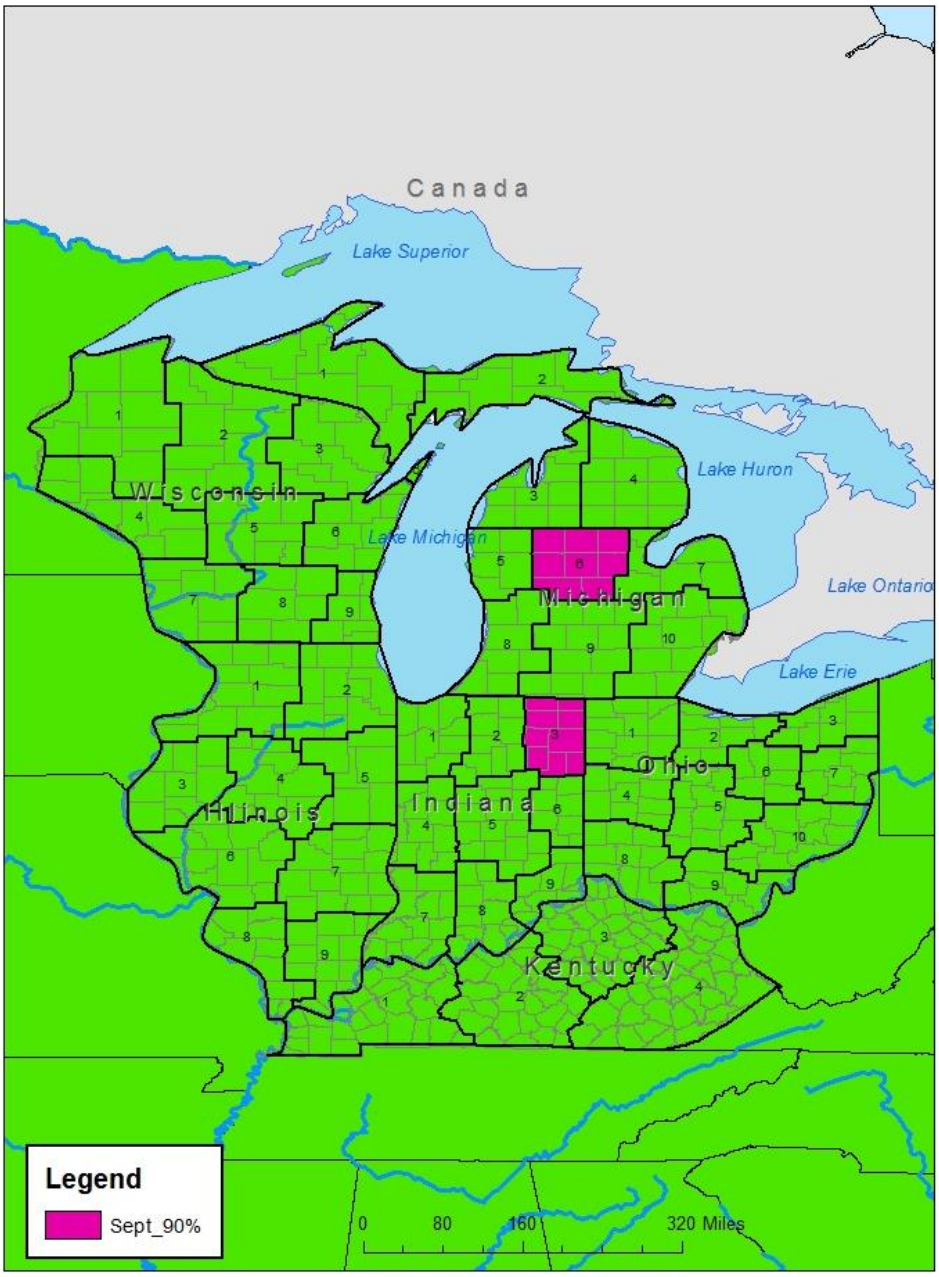

Figure 5.6: Same as Figure 5 except for September. No other crop reporting districts had significance, even at 80% CI.

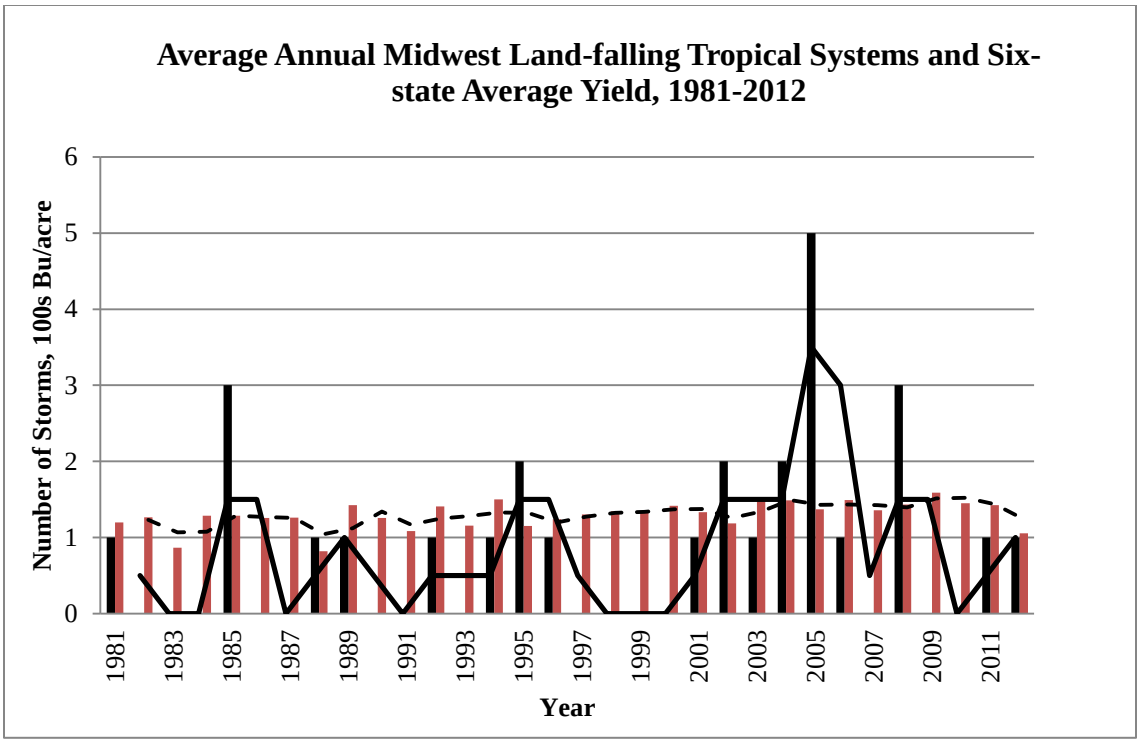

Figure 5.7: Bar graph showing the average number of land-falling storms per year in the domain (blue bars) alongside the six-state average yield in bushels an acre (green bars, in hundreds of bushels an acre). The solid black line is the two-year moving average of total Midwest land-falling tropical systems. The dashed black line is the two-year moving average of the six-state average annual yield. No relationship is found between the average number of storms per year within the domain and the average total yield of the domain.

CHAPTER 6. THE ROLE OF ANTECEDENT SOIL MOISTURE ON THE INLAND REINTENSIFICATION OF TROPICAL SYSTEMS EXAMINED USING REMOTELY SENSED DATA AND MODEL VERIFICATION

6.1 Introduction

Thermodynamic interactions between tropical storm systems and the ocean or land surface are fundamental to the growth, evolution, and decay of tropical systems over ocean waters and land. The development of hurricane-specific mesoscale forecast models such as the Hurricane Weather Research and Forecast (HWRF) Model and hurricane research completed using HWRF over the last several years has shed light on and improved hurricane forecasts. However, despite research to improve hurricane forecasts (e.g. Hurricane Forecast Improvement Project: Gall et al., 2013), hurricane track forecasts possess levels of uncertainty that need to be improved upon to better prepare and mitigate the hazards associated with land-falling hurricanes such as localized flooding, flash flooding, tropical cyclone induced tornadoes, wind damage, and storm surge damage. With knowledge of the large role that ocean temperatures, latent heat flux, and sensible heat flux play in tropical storm development, organization, migration, and sustainment, this research project investigates the possibility of such relationships also existing over land, in essence acting as a "Brown Ocean" to land-falling tropical cyclones (e.g., Andersen and Shepherd 2013).

While a large quantity of research exists investigating the role of antecedent synoptic environment interactions with land-falling tropical systems (i.e. jet streaks and vorticity maximums embedded in westerly flow) and antecedent oceanic environments (shallow continental shelves and warm water upwelling - see Wu and Shi, et al. 1997; Cheng, 1999; Hanley, et al. 2001; Emanuel et al. 2004), research on land surface interactions serving as energy sources for land-falling tropical systems is a new area of

research that is quickly expanding as an untapped source of information regarding tropical system lifecycle processes. The possible role of dust in the air (e.g. Wu, 2007; Sun et al. 2008; Braun, 2010) and the antecedent state of the land surface serving to restrengthen/reintensify or weaken storms post-landfall (e.g. Shen et al., 2002; Emanuel et al., 2008; Kellner et al., 2011; Kishtawal et al., 2011; Andersen and Shepherd 2013) has pointed to new understandings in tropical system lifecycle processes upon making landfall.

Land surface heterogeneity, most simply defined as changes in land cover such as urban to rural areas, vegetated to non-vegetated surfaces, or soil moisture discontinuities, has been a focused area of research for decades. Numerous studies have demonstrated that land surface heterogeneities on the spatial scales of ~10-20 km can result in mesoscale baroclinic circulations, a result of localized moisture and heat flux discontinuities stemming from the land surface heterogeneity. These mesoscale circulations have been demonstrated through numerical modeling to be strong enough to perturb weaker synoptic conditions and lead to the development of mesoscale rainfall and thunderstorms (Clark and Arritt, 1995; Baidya Roy and Avissar, 2000; Pielke 2001).

With rainfall memory studies completed by Findell and Eltahir (1997) and Pal and Eltahir (2003) demonstrating a positive feedback between the antecedent condition of the underlying soil, coupled with the aforementioned land surface heterogeneity feedbacks, this study investigates the role (or lack thereof) of the antecedent synoptic environment and the role of antecedent land surface conditions and surface fluxes resulting from soil moisture and land surface heterogeneity on inland tropical storm system sustainment, reintensification, and decay.

Here we use historic meteorological, climatological, and land surface data complimented with remotely sensed data and numerical weather prediction model verification to explore the working hypothesis that wetter antecedent soil conditions can aid in the reintensification of some land-falling tropical storm systems by acting as a latent heat source with the corollary hypothesis being that dry soils act to increase the rate at which land-falling tropical cyclones decay over land due to a lack of latent heat (i.e. moisture). This working hypothesis is built from work investigating the role of

antecedent surface conditions on tropical systems in the Indian Monsoon Region (Chang et al., 2009; Kishtawal et al., 2010) and Typhoon Abigail over Western Australia (Emanuel et al., 2008). The results of these studies and the findings of this study have the potential to be generalized and applied in the operational community in regions around the world where the state of the land surface is readily monitored and included in the tropical system forecast and monitoring process.

6.2 Hypothesis

Land-falling tropical systems are recognized as potential sources of severe weather and extreme climate hazards such as inland flooding, wind damage, and tropical cyclone induced tornadoes. With heightened recognition of the cost associated with such storm damages, increased effort to better predict, prepare for, and mitigate the effects of these systems has been seen over the last decade. Analysis of extreme events such as Tropical Storm (TS) Erin (2007) is one example of a poorly predicted storm that impacted unprepared communities. TS Erin (2007) demonstrated the need for improved understanding of inland tropical storm systems, especially inland storm system interaction with the land surface and how forecast tools can be improved to better capture such synergistic feedbacks.

TS Erin (2007) is an ideal example of a land-falling tropical system that appears to experience a feedback between antecedent land surface conditions and the storm's intensity and evolution post-landfall, far from a warm water energy source. TS Erin (2007) made landfall on the 16 of August 2007 near Corpus Christy, Texas, traveling northwest into central Texas before turning north and then turning northeast and traveling into an anomalously wet Oklahoma (second wettest spring and early summer on record – Arndt et al., 2009) where the storm reorganized and formed an eye-like structure over central Oklahoma. Observational/operational weather data from the Oklahoma Mesonet, upper air data and surface data from the University Corporation for Atmospheric Research (UCAR), mesoanalysis data from the National Oceanic Atmospheric Administration (NOAA) Storm Prediction Center (SPC), and tropical cyclone reports from the National Hurricane Center (NHC) are supportive of land surface interactions

between the anomalously wet land surface in Oklahoma and the storm in August 2007. These findings lend support to the completion of a series of soil moisture sensitivity analyses using the WRF model to test the working hypothesis that wetter soils sustained and reintensified TS Erin (2007) inland away from a warm water energy source (Kellner 2011).

To examine the antecedent soil moisture hypothesis and tropical storm feedback hypothesis in more detail, the WRF model is initialized with North American Regional Reanalysis (NARR) forecast data and North American Mesoscale (NAM) forecast data. For each experiment, soil moisture availability values in the model are increased or reduced within the domain to represent anomalously dry, standard, and anomalously wet antecedent soil moisture conditions (0.5 soil moisture, standard soil moisture, and 1.5 x soil moisture.), and a forecast is generated to investigate how the model simulates/forecasts TS Erin with different soil moisture conditions (Table 6.1). Kellner (2011) and Kellner et al. (2011) discuss the findings of these studies in detail. Results of the analysis suggest that the anomalous soil moisture conditions in Oklahoma at the time of TS Erin's passage contributed in part to TS Erin's reintensification via priming of the mesoscale environment and priming of the boundary layer which initiated a positive feedback between the land surface, the atmosphere, and the tropical storm.

The initial findings from Kellner et al. (2011) investigating TS Erin lend support to further study antecedent storm environments and land-falling tropical storms. Three additional case studies of land-falling tropical systems in anomalous environments are identified and investigated through observational-based case studies (e.g. archived upper air maps, surface data, rainfall and temperatures, soil moisture conditions, and mesoanalysis) and WRF soil moisture sensitivity experiments. The storms are TS Arlene (2005), TS Don (2011), and Hurricane Isaac (2012). TS Arlene made land fall in a climatologically drier than normal climate (May 1.47 inches below normal and 0.59 inches below normal for month of June across the Midwest – OH, IN, IL, KY, WI, MN, IA, and MO). However, TS Arlene remained classified as a tropical system far inland, similar to TS Erin invoking a comparable investigation. TS Don 2011 made landfall in an extremely drier than normal climate (1.68 inches below normal, third driest July on

record in Texas) (MRCC 2014) igniting hopes of drought relief in southern Texas as the storm approached. TS Don is selected to serve as the corollary hypothesis case study. Finally, Hurricane Isaac 2012 made landfall during the widespread and catastrophic drought of 2012 that crippled much of the Great Plains and Midwest that year. It serves as an additional corollary hypothesis event for this study on soil moisture anomaly feedbacks to land-falling tropical systems.

6.3 Data and Methods

6.3.1 Methods

An important component to numerical weather prediction, especially at smaller spatial scales, is the selection of a land surface parameterization scheme. Land surface parameterization schemes are responsible for partitioning and determining the heat and moisture fluxes between the land surface, the storm environment, and the storm as forecast by the model (Stensrud 2009). Land surface schemes can be simple or complex in nature, varying by how each scheme views the land surface and subsurface (e.g. one or two layers versus five layers), if soil temperature or soil moisture (or both) is (or is not) forecast prognostically, and if the parameterization scheme can account for features such as cooling of soil temperatures from rain water infiltration, cooling of the boundary layer from evaporation, runoff and further feedback into the storm environment, or accounting well for snow and ice (Stensrud 2009). In this analysis (and WRF in general), the two primary land surface models/parameterization schemes considered for soil moisture sensitivity analysis are Slab (5-layer thermal diffusion) and Noah. The two schemes differ from each other in several regards.

The Slab LSM (also known as the 5-Layer Thermal Diffusion LSM, see Dudhia 1996**)** is a land surface scheme that only determines soil temperature (and not soil moisture) prognostically. Soil moisture is a function of land use category only and does not change in time as the model progresses forward in the forecast. The Slab LSM also does not include explicit representation of vegetation. Using Slab highlights the model's forecast sensitivity to the initial soil moisture value. The Noah LSM prognostically forecasts soil moisture and soil temperature, and includes explicit vegetation

representation providing for the most realistic evolutionary forecasts possible of the event. The Noah LSM includes heat and moisture fluxes as driven by atmospheric forcings of precipitation, temperature, humidity, surface pressure, winds, and radiation. The Noah LSM is inclusive of soil variables such temperature, water, ice, and texture with land surface variables such as vegetation type, slope, albedo, and roughness. It can be run as coupled or uncoupled and applies finite-differencing to compute the governing equations of physical processes of the land surface between soils, vegetation, and the snowpack (Mitchell 2005; Stensrud 2009). It is the more realistic land surface model compared to the Slab LSM.

The WRF soil moisture sensitivity analysis experiments in this series of soil moisture sensitivity case study analysis are completed using the Slab and Noah LSMs. Slab is primarily used to assess the sensitivity of the model to the initial soil moisture value. Model runs are initialized using NAM and NARR data. NAM differs from NARR in that NAM is a forecast model generated dataset while NARR is a reanalysis product. Using reanalysis products and land data assimilation systems have been shown to better forecast past weather events because the model is constantly calibrated through the forecast process with observed surface, upper air, and satellite data (among others). However, the improvement of forecasts through the use of reanalysis products does not discredit datasets such as NAM, as reanalysis datasets also contain biases inherent from the numerous remotely sensed datasets of different time intervals that may introduce error into the reanalysis forecast. Thorough analysis of the NAM and NARR forecasts for TS Erin can be found in Kellner 2011. Forecasts for TS Don, TS Arlene, and Hurricane Isaac show similar sensitivity to initial soil moisture values as noted with TS Erin in Kellner (2011) and Kellner et al. (2011) in that drier conditions result in forecasts of weaker convection while higher soil moisture contributes to stronger convection forecast by the model.

From analysis of Slab forecasts in Kellner (2011), it is identified that WRF forecasts convection that is sensitive to initial soil moisture conditions. From these findings it is noted that investigation of the more dynamic interactions of antecedent soil moisture conditions with a LSM that is better representative of the real environment (i.e.

the Noah-LSM) is needed. Thus, the focus of this paper is on how the Noah-LSM forecasts land surface feedbacks and interactions with land-falling tropical systems that interact with an antecedent environment suffering from moisture deficit or surplus.

The Noah-LSM forecasts of TS Erin, TS Arlene, TS Don, and Hurricane Isaac in this analysis are generated using the Goddard Earth Sciences Data and Information Services Center (GES DISC) Interactive Online Visualization and Analysis Infrastructure (Giovanni) user interface and visual display query system developed and supported by the Goddard Earth Sciences Data and Information Services Center (GES DISC) rather than WRF. Local-scale climate parameters of surface specific humidity, surface evaporation/evapotranspiration or total evapotranspiration, surface latent heat flux, surface sensible heat flux, surface ground heat flux, and total column soil moisture (specific soil moisture layers when total column soil moisture is not available as a parameter) are analyzed due to their diagnostic relationship in understanding land surface partitioning of soil moisture and heat fluxes in the soil-vegetation-atmospheric (SVAT) system.

Noah-LSM forecasts and land-falling tropical storm interactions are investigated through the parameters of surface specific humidity, surface evaporation/evapotranspiration or total evapotranspiration, surface latent heat flux, surface sensible heat flux, surface ground heat flux, and soil moisture parameters. These parameters are plotted at six-hourly UTC intervals using Giovanni with forecasts initialized in one of the following manners: 24 hours prior to storm landfall, 24 hours prior to storm reintensification, or initialization times are adjusted to capture certain flux parameters prior to rainfall from the tropical system impacting the land surface. All parameters are mapped via a time-averaged, latitude-longitude map except for specific humidity data which is a time series plot for the same time frame of 24 hours prior to model run initialization to end of model initialization. Domain areas are inclusive of the entire landmass area from where the storm made landfall till where the storm experiences extratropical transition or dissipation.

6.3.2 Data Sets

The Noah-LSM analysis that is completed on the four land-falling tropical cyclones representing possible interaction with soil moisture anomalies utilizes three remotely-sensed datasets. These include the Modern-era Retrospective Analysis for Research and Applications (MERRA), the North American Land Dada Assimilation System-2 (NLDAS), and the Global Land Data Assimilation System-1 (GLDAS). MERRA differs from NLDAS and GLDAS in that it is a reanalysis product. Reanalysis datasets are developed through the assimilation of six, 12-hourly observational datasets (satellite, buoy, aircraft, ship, radiosonde, and surface observations) into a forecast model(s) for the period being analyzed. Land data assimilation systems include the ingestion of weather observations as well to generate a forecast, but run independently of a forecast/atmospheric model. By doing this, land data assimilation systems remove the bias of NWP models that drive reanalysis products.

6.3.2.1 Modern-era Retrospective Analysis for Research and Applications (MERRA)

MERRA is a reanalysis product developed from the Goddard Earth Observing System Data Assimilation System Version 5 (GOES-5). It has two-dimensional diagnostics such as surface flux parameters which are produced at hourly intervals of one-half degree latitude by two-thirds degree longitude (55.5 km x 74 km) grid resolution. Three-dimensional (MERRA 3D) is available as well. MERRA is developed from GOES-5 atmosphere data using an atmospheric data assimilation system that merges various observations from the satellite era (1979-present). Because the assimilation system is time-fixed (i.e. data is assimilated into the model at equal time steps regardless of the weather event), the data produced from MERRA is viewed as steady and reliable making it ideal for climatological applications. A weather-focused/NWP forecast analysis differs through time in that systematic changes resulting from the weather or weather/storm events in the model contribute to forecast evolution. MERRA is more suitable for climatological applications because all weather and climatological data is included – forecasts are not generated for just specific weather events (MERRA 2012). Incorporating specific weather event data only results in an exclusive storm dataset that

drives the model. This can actually serve to drive the forecasts towards anomalous representation of the climate system. Focusing only on anomaly events may drive the model more towards one direction or another (MERRA 2012). Assimilated satellite products in the MERRA dataset include data from the NOAA Polar Orbiter High Resolution Infrared Radiation Sounder, GOES platforms, TIROS, Nimbus-7, and the AQUA Advanced Microwave Sounding Unit (MERRA 2012).

6.3.2.2 North American Land Dada Assimilation System-2 (NLDAS)

NLDAS provides hourly products of land surface parameters at a spatial resolution of $1/8^{th}$ a degree (13.875 km x 13.875 km). NLDAS is produced from non-precipitation land surface forcing fields developed from the NCEP North American Regional Reanalysis (NARR) which is a high resolution reanalysis (32km/45 layer) of the North America region (Canada, the United States, and Mexico) (Rodell 2014 (a)). Once NLDAS is initialized, it produces forecasts using the NCEP Eta Model which further uses the Regional Data Assimilation System (RDAS) to assimilate precipitation and radiances into the model. Surface, downward shortwave radiation is bias-corrected by using five years of hourly $1/8^{th}$ degree GOES-based surface downward shortwave radiation fields. Precipitation is not of NARR precipitation forcing, but from a gauge-only Climate Prediction Center analysis of 24-hour precipitation that has been separated into hourly time intervals and that accounts for orography based on PRISM climatology (Mesinger et al., 2005; Shafran et al., 2006). Assimilated satellite products in NLDAS include MODIS evapotranspiration, AMSR-E near surface soil moisture, and AVHRR land cover data built upon NAI and NDVI indexes (Rodell et al. 2004).

6.3.2.3 Global Land Data Assimilation System-1 (GLDAS)

GLDAS provides three-hourly products that are in produced at a 1^{o} x 1^{o} (111 km x 111 km) spatial resolution. GLDAS is initialized by data from NCEP's Global Data Assimilation System (GDAS), Climate Prediction Center (CPC) Merged Analysis of Precipitation (CMAP), and Air Force Weather Agency (AFWA) radiation. GLDAS is a project focused on combining satellite data and ground observational data into land surface models through data assimilation. GLDAS is viewed as a "sister" project to the

Land Information System (LIS) project, and its results can be produced in near real-time. Time-separated CMAP precipitation (6 hourly mean rain rate) drives precipitation forcing in GLDAS, with additional input data to GLDAS similar to that of NLDAS (Rodell 2014 (b)). GLDAS and NLDAS are similar projects with the primary difference between the two being spatial resolution.

6.4 Discussion of Findings

Interactions between Earth's atmosphere and the land surface occur daily in response to solar radiation. During the daytime, radiative energy from the sun propagates as shortwave radiation downward towards Earth's surface heating the atmosphere and surface components that are struck by it. Uneven heating across Earth's surface due to differences in vegetation, soil moisture content, albedo, terrain, and latitude (different inclination angle of the sun) results in atmospheric convection, conduction of heat through different mediums (e.g. air, water, and soil), and evapotranspiration of water. The atmosphere works to redistribute heat (shortwave and longwave radiative energy), mass (water), and momentum (winds) to restore equilibrium to the atmospheric system that results from uneven heating at Earth's surface. The daily surface radiation balance equation ($R_n = L + H + G$) results in a sign convention of positive fluxes of sensible and latent heat from the land surface during the day and negative at night. The ground heat flux works to move heat from the top layers of the land surface into deeper soils resulting in a negative sign convention. At night, the signs of these heat flux terms reverse (Oke 1987; Stull 1988; Shelton 2009).

The importance of understanding the surface radiation balance equation in relation to land-falling tropical systems is that the strength/intensity and sign (positive or negative) of each type of heat flux during daytime and nighttime indicates how a tropical storm may be utilizing energy from the land surface in the forms of sensible and latent heat. Tropical storm systems are self-sustaining systems that draw energy from the warm water of tropical oceans with the common understanding that once a tropical storm system makes landfall, it will dissipate rather quickly since its energy source (the warm water) has been cut off (Emanuel 2003).

The analysis completed here focuses on sensible and latent heat fluxes during the daytime and nighttime hours, along with antecedent soil moisture and surface specific humidity values during the inland progression of the four land-falling tropical systems identified in previous sections as optimal case studies. Flux values (positive or negative), proximity to inland storm track, proximity to reintensification, and the presence of mesoscale boundaries in the form of heat fluxes, soil moisture, or surface specific humidity (if present) are identified to assess the following relationships as set forth by the proposed hypotheses:

1) Any positive sensible and latent heat fluxes over land during nighttime hours (ground heat flux will be negative to follow sign conventions) indicate heat lost to the atmosphere which suggests that the storm system is extracting energy from the land surface to sustain itself;
2) Any gradients of sensible heat, latent heat, or moisture that may serve as mesoscale sources of "invisible" (i.e. not identifiable on a surface weather map such as a frontal boundary) baroclinicity/vorticity boundaries suggests further possible positive feedback to storm sustainment, reintensification, and storm steering.

6.4.1 WRF Soil Moisture Sensitivity Analysis, NARR and NAM Data

The WRF-Slab soil moisture sensitivity analyses using NARR and NAM data as completed and discussed in Kellner 2011 and Kellner et al. (2011) shows that the amount of soil moisture available from the land surface to the storm environment contributes to the evolution of the storm and its convection over land. Those model runs (for all events) show that when more soil moisture is available in the model for evaporation/evapotranspiration, convection is heightened. When soil moisture is limited (i.e. less), convection is forecast as less intense. While these results are partially driven by the simplistic nature of the model parameterization schemes, in theory the relationship between soil moisture and availability of soil moisture for evaporation and latent heat release that drives convection is sound. These findings agree with past modeling studies

on land surface heterogeneity and the soil moisture memory effect as described in the introduction section of this chapter.

6.4.2 Giovanni MERRA, NLDAS, and GLDAS Analysis

MERRA, NLDAS, and GLDAS analyses with the Noah-LSM all result in different values of surface flux data for case study forecasts. However, all generally forecast similar locations and spatial extent where fluxes are positive or negative during the time of the storm event. When reviewing all three datasets, it is apparent in the results that the spatial resolution at which surface sensible and latent heat flux, ground heat flux, soil moisture, specific humidity, and evapotranspiration are forecast influence the degree and certainty of feedback occurring between the land surface and the tropical storm. While GLDAS provides surface parameter maps of similar spatial distribution, it has the coarsest spatial resolution and does not perform well in capturing potential land surface feedbacks. This serves to dilute or smooth out distinct regions of flux data (e.g. sensible, latent, ground heat flux), but not parameters of soil moisture or humidity. MERRA and NLDAS are of finer spatial resolution (55.5 km x 74 km and 13.875 km x 13.875 km, respectively) and show distinct regions of positive surface flux data into the tropical systems during the nighttime hours (00Z-06Z and 06Z-12Z – 8pm-2am and 2am-8am LST).

All case study events as shown/produced by MERRA, NLDAS, and GLDAS appear to have interaction with surface flux parameters directly relatable to antecedent soil moisture conditions. Soil moisture is shown to be a critical component of the hydroclimate, as it determines surface albedo, the partitioning of sensible and latent heat fluxes, likelihood of surface ponding of water and runoff, and the rate of transfer of heat between the atmosphere and ground. As such, this is why soil moisture is investigated as a possible diagnostic tool for inland tropical storm intensification or decay. In the following sections, each case study event is briefly described with findings related to soil moisture and surface flux data reviewed for each MERRA, NLDAS, and GLDAS.

6.4.2.1 Tropical Storm Erin (2007)

Tropical Storm (TS) Erin is the original tropical storm event that led to the development of the antecedent soil moisture hypothesis investigated in this study, and is the storm that sparked the investigation of soil moisture and antecedent environmental relationships in additional studies such as those completed by Arndt et al., (2009), Monteverdi and Edwards (2010), and Evans et al., (2011). TS Erin is unique because after making landfall on August 16th near Corpus Christy, TX, the storm tracked inland, weakening along the way, and then experienced a period of reintensification over west-central Oklahoma during the early morning hours of August 19, 2007 (Knabb 2008). Reintensification is defined in this study as a period of time during which the low pressure center deepened (lowered) and convection became enhanced (e.g. Kellner et al. 2011). Furthermore, the generation of a hurricane-like eye feature over west-central Oklahoma (roughly 600 miles inland) occurred during this time with TS Erin which had not been seen before during the storm's lifetime. Additionally, the evolution of TS Erin overland is unique because during the months prior to landfall and reintensification over Oklahoma, observed rainfall amounts resulted in the second wettest spring on record across much of the state (Arndt et al., 2009; Kellner et al., 2011). These antecedent soil moisture conditions and the reintensification of TS Erin over this region formulate the hypothesis that anomalous soil moisture (wetter than normal or drier than normal) may contribute to the reinvigoration, sustainment, or more rapid demise of land-falling and inland-tracking tropical systems. Figures 6.1-6.6 highlight land surface feedbacks witnessed with the reintensification of TS Erin with a complete analysis of the TS Erin soil moisture hypothesis available in Kellner (2011) and Kellner et al., (2011).

6.4.2.2 Tropical Storm Arlene (2005)

Tropical Storm Arlene made landfall in the Florida Panhandle on June 12th, 2005 after organizing in the Atlantic Ocean east of Honduras close to where the Gulf of Mexico and Caribbean Sea meet. Upon making landfall, TS Arlene moved northward just east of the Mississippi River as a tropical depression till the afternoon of June 13th, 2005 when the storm transitioned to an extratropical low pressure system over south-

central Michigan. TS Arlene moved north, northeast over the Midwest where rainfall had been below normal leading up to the storm's passage. During the time that TS Arlene moved northward, the system generated two tornadoes in east-central Indiana and produced 1.0-3.0 inches of rainfall across the region (Lixion and Brown 2005; Schultz and Cecil 2009). TS Arlene is chosen as an ideal case study for this research proposal in that extratropical transition did not occur till 950 miles inland, farm from a warm ocean energy source similar to TS Erin.

While antecedent soil moisture conditions were not anomalous in nature across much of the land surface over which TS Arlene passed in June 2005, interesting land surface feedbacks are identified between the antecedent soil moisture conditions in Indiana and where TS Arlene generated two tornadoes. NLDAS and MERRA show surface evaporation occurring during the overnight hours of June 12, 2005 with weak, positive values of surface evaporation/evapotranspiration present suggesting a flux from the surface into the overlying atmosphere. Enhanced values are seen in NDLAS over Indiana on 13 June 2005 when two tornadoes are reported (Figure 6.7**).** Latent heat flux is related to surface evapotranspiration, thus similar relationships (positive flux – into the overlying atmosphere at night) with latent heat flux are seen with NLDAS and MERRA productions. NLDAS shows greater detail of latent heat flux, with highest amounts in vicinity of where the two tornadoes are reported (Figure 6.8). As with TS Erin, a soil moisture gradient prior to migration of the storm through the region is present, with higher soil moisture values in proximity to where the increased rates of surface evaporation, latent heat, and tornadoes occur (Figure 6.9).

6.4.2.3 Tropical Storm Don (2011)

Experiencing severe drought since the beginning of the year in 2011 (USDM 2011), Texas welcomed TS Don as a hopeful form of drought relief for portions of the state. However, TS Don rapidly dissipated after making landfall on July 30, 2011 near Padre Island National Seashore, quickly diminishing any hope of drought relief anywhere in the state. Within six hours of landfall, the circulation center of the storm completely dissipated over southwest Texas (Brennan 2011). Investigating TS Don's rapid demise in relation to exceptionally dry antecedent soil moisture conditions serves as an excellent

corollary hypothesis case study event to TS Erin. Exceptionally dry soil moisture anomalies present as severe drought in the vicinity of the storm's landfall and surrounding regional landscape are opposite of those antecedent soil moisture conditions present with TS Erin. No studies investigating the role of hydroclimatological extreme events such as drought resulting in a faster dissipation rate for land-falling tropical systems has been completed.

Land surface feedbacks occurring in the vicinity of TS Don as the storm made landfall and dissipated are interesting in that plots show similar feedbacks as those seen with TS Erin and TS Arlene. Upon landfall, TS Don moved over a land surface with weak evapotranspiration (Figure 6.10). Latent heat flux plots, however, show a positive heat flux to the atmosphere (i.e. positive feedback/interaction with the storm) such as those seen with TS Erin and TS Arlene. These observations suggest that land-falling tropical storms continue to extract heat from the land surface for energy. Additionally, there are pockets of enhanced latent heat flux in west-central Texas where TS Don tracked (Figure 6.11 and Figure 6.12). Sensible heat flux plots during the overnight hours (8pm to 2am local time) are weak, but positive as well below the storm. A larger pocket of sensible heat flux is noted on the plots and is located in a location towards which the storm center tracked (Figure 6.13). Albeit in drought, soil moisture is scrutinized to see if any soil moisture anomalies or gradients are present in Texas in the vicinity of TS Don's track. It is noted in Figure 6.14 that the circulation center of TS Don appears to track towards a region of higher soil moisture in Texas.

Although TS Don rapidly dissipated over the exceptionally dry surface present in Texas, analysis of surface flux parameters shows that the circulation center associated with TS Don tracked towards regions of higher surface evaporation/evapotranspiration and sensible heat. Possible explanations of TS Don's circulation center following this storm track include ideal gas law relationships - the boundary layer over areas of warmer, more moist air should produce lighter, more unstable air the system may have sought out as an energy source. Knowing that more unstable air also rises, the diagnostic environmental parameter of surface pressure falls along TS Don's track is reviewed for any indication of weak low pressure forming over areas of heightened surface

evaporation/evapotranspiration and sensible heat. However, any pressure falls (if present) appear not significant enough to be detected by mesoanalysis products provided by the SPC mesoanalysis archive database (http://www.spc.noaa.gov/exper/ma_archive/).

6.4.2.4 Hurricane Isaac (2012)

The year 2012 is a historic drought year (i.e. a hydroclimatological anomaly, e.g. Shelton 2009) in the United States during which drought reached levels comparable to the Dust Bowl (Fuchs et al., 2014). The United States agriculture industry was heavily impacted by the lack of rainfall during the growing season and news of Isaac's projected path into the Midwest brought hope for drought relief (Healy 2012). Isaac made its final landfall on August 29, 2012 in Louisiana as a tropical storm and tracked northwest into western Arkansas before curving northeastward and tracking across central Missouri toward St. Louis. The circulation center of Isaac then entered south-central Illinois and dissipated over southern Illinois, Indiana, and western Kentucky (Berg 2013). While drought relief was provided, the rainfall was not enough to break drought status in the storm's wake. During Isaac's lifetime, it is documented to have produced 34 tornadoes from August 27th – September 4th. Tornado events within the domain post-landfall include those tornadoes reported on August 30th, 31st, and September 1st, 2012 (Berg 2013).

Similar to TS Don, the antecedent soil moisture conditions of extreme drought serve as an excellent corollary hypothesis case study to TS Erin. Hurricane Isaac is unique compared to TS Don, however, in that the storm did not rapidly dissipate upon making landfall despite the prolific and wide-spread drought conditions across much of the country. It is worth noting, however, that Louisiana was not in drought status during Isaac's landfall and that Texas was in a drought during TS Don's landfall. Based on findings from TS Erin, TS Arlene, and TS Don, this may have allowed Isaac to remain organized after making landfall rather than undergoing rapid dissipation like TS Don.

GLDAS, NLDAS, and MERRA plots all show land surface feedbacks occurring post-landfall between Hurricane Isaac and the land surface overnight. Figure 6.15 and Figure 6.16 both document what appears to be Hurricane Isaac trying to continue the self-sustaining process of obtaining sensible and latent heat flux from the land surface for

energy. Although fluxes are weak, they are positive (during the nighttime hours) beneath and slightly ahead of where the storm center advances. The highest rates of evaporation/evapotranspiration after landfall also happen to coincide with times of more active convection and the numerous tornado reports across Illinois, Indiana, Missouri, Kentucky and Arkansas. This is similar to the behavior documented with TS Arlene. MERRA and NLDAS provided more detailed analysis of this noted storm behavior due to their more finite spatial resolution.

6.5 Conclusions

Antecedent soil moisture conditions have been identified in this land-falling tropical storm event analysis as an important and underappreciated ingredient in land-falling tropical storm system forecasts of track, intensity, and inland duration. Observational analysis, analysis with NLDAS, GLDAS, and MERRA remotely sensed satellite products, and soil moisture sensitivity analysis using the WRF model on TS Erin (2007), TS Don (2011), TS Arlene (2005), and Hurricane Isaac (2012) supports the hypothesis that land-falling tropical systems interact with the land surface in the same manner that tropical systems interact with the ocean surface. Tropical storm systems are warm core, self-sustaining low pressure systems that obtain their energy from the warm ocean surface through high surface fluxes of sensible and latent heat. The analysis completed here demonstrates that land-falling tropical systems entering anomalous soil moisture conditions are attracted to regions of higher sensible and latent heat flux when synoptic scale environments do not dictate inland migration and track, and increased wind shear present in the Midlatitudes does not aid in the more rapid dissipation of the tropical storm system over land. The storms reviewed in this climatology likely exhibit strong, interactive behavior with the land surface because the systems made landfall when synoptic scale weather features were not present to influence storm dynamics. This allowed the storms to continue the self-sustaining process of warm-core systems by pulling energy from the land surface after making landfall.

Soil moisture and its antecedent conditions is the key variable investigated in this study because of the crucial role soil moisture plays in the partitioning of heat and

moisture fluxes between the sub-surface and surface, and land surface and the atmosphere (e.g. Shelton 2009; Grundstein and Bentley 2001). Anomalous soil moisture is investigated for a possible relationship to land-falling tropical systems due to unexplained and observed reintensification of tropical systems far inland from a warm ocean energy source (e.g. Kellner et al., 2011). Observational weather data and numerical model sensitivity analysis with WRF supports the hypothesis that wetter antecedent soils can act to enhance or sustain inland tropical systems and that drier soils act to enhance the rate at which a land-falling system will decay over land. Even though Hurricane Isaac made landfall while a large portion of the country was in drought conditions, the system likely remained organized longer farther inland because it was much larger than TS Don at landfall, and the immediate land surface upon making landfall was not under drought conditions as seen with TS Don. All systems investigated in this climatology show that tropical systems continue to pull energy and moisture from the land surface even when the radiative forcing mechanisms of surface fluxes (i.e. the sun) has set for the day. Typically sensible and latent heat fluxes, along with evapotranspiration, are negative at night. However, in this study the fluxes are found to be positive during overnight hours indicating that energy is being pulled from the land surface by forcing mechanisms other than radiation forcing directly from the sun. The fluxes are also found to be highest nearest to the tropical storm system center of low pressure.

These findings (see also Kellner 2011; Kellner et al., 2011) stress the increased need for more detailed, timely assimilation of remotely-sensed data describing land surface characteristics such as soil moisture, evapotranspiration, vegetation, and surface fluxes into hurricane prediction/forecast systems, especially when it has been forecast that synoptic scale dynamics will be weak or non-existent when a storm makes landfall. The findings also demonstrate the need of high-resolution land surface datasets to capture all interactions of land-falling tropical systems with the land surface and how these interactions may influence the intensity of land-falling tropical storm forecasts. This last point is important for future projections of land-falling tropical systems that are forecast in general circulation models (much larger spatial resolution, generalized land surface

features) for global climatological analysis under warming scenarios. This suggestion is made due to the findings in this study that NLDAS and MERRA analyses, both of finer spatial resolution, did a better job at capturing land surface feedbacks between the storm and the land surface. WRF soil moisture sensitivity analysis at spatial resolutions of 1 km to 4.25 km further supports the need for fine-scale forecast model prediction to best capture land-falling tropical system feedbacks and evolution over land.

6.6 References

Andersen, T.K, and J. M. Shepherd, 2013: A global spatiotemporal analysis of inland tropical cyclone maintenance or intensification. *Int. J. Climatol.*, 34: 391-402.

Arndt, D.A., J.B. Basara, R.A. McPherson, B.G. Illston, G.D. McManus, and D.B. Demko, 2009: The overland reintensification of Tropical Storm Erin (2007). *Bull. Amer. Meteor. Soc.*, 90, 1079–1093.

Baidya Roy, S., and R. Avissar, 2000: Scales of response of the convective boundary layer to land-surface heterogeneity. *Geophys. Res. Letters*, 27(4), 533–536.

Berg, R., 2013: Tropical cyclone report: Hurricane Isaac. *National Hurricane Center.* http://www.nhc.noaa.gov/data/tcr/AL092012_Isaac.pdf. 28 January 2013 (Accessed 4 December 2014.)

Brennan, M.J., 2011: Tropical cyclone report: Tropical Storm Don. *National Hurricane Center.* http://www.nhc.noaa.gov/data/tcr/AL042011_Don.pdf. 28 October 2011 (Accessed 4 December 2014.)

Clark, C. and Arritt, P., 1995: Numerical Simulations of the Effect of Soil Moisture and Vegetation Cover on the Development of Deep Convection. *J. of Appl. Meteor.,* 34**,** 2029-2045.

Dudhia, J. (1996): A multilayer soil temperature model for MM5, paper presented at Sixth PSU/NCAR Mesoscale Model Users‟ Workshop, National Center for Atmospheric Research. Boulder, Colorado.

Emanuel, K., 2003: Tropical cyclones. *Annu. Rev. Earth Planet. Sci.,* 31, 75-104. doi: 10.1146/annurev.earth.31.100901.141259.

Emanuel, K., Desautels, C. Holloway, C, and Korty, R, 2004: Environmental control of tropical cyclone intensity. *J. of the Atmos. Sci.*, 61.

Emanuel, K., J. Callaghan, and P. Otto, 2008: A hypothesis for the re-development of warm-core cyclones over northern Australia. *Mon. Wea. Rev.*, 136, 3863 – 3872.

Evans, C., R.S. Schumacher, and T.J. Galarneau Jr, 2011: Sensitivity in the overland reintensification of Tropical Cyclone Erin (2007) to near-surface soil moisture characteristics. *Mon. Wea. Rev*., 139 (12), 3848-3870.

Findell, K. and Eltahir, E., 1997: An analysis of soil moisture-rainfall feedback, based on direct observations from Illinois. *Water Resources Res*.**,** 33(4), 725-735.

Fuchs, B.A., D.A. Wood, and D. Ebbeka, Eds. 2014: From Too Much to Too Little: How the Midwest drought of 2012 evolved out of one of the most devastating floods on record in 2011. NOAA Central Region Drought Assessment. 2014.

Gall, R., J. Franklin, F. Marks, E.N. Rappaport, and F. Toepfer, 2013: The Hurricane Forecast Improvement Project. *Bull. Amer. Meteor. Soc.*, 94, 329–343. doi: http://dx.doi.org/10.1175/BAMS-D-12-00071.1.

Grundstein, A.J. and M.L. Bentley, 2001" A growing-season hydroclimatology, focusing on soil moisture deficits for the Ohio Valley Region. *J. Hydrometeor*., 2, 345-355.

Hanley, D, Malinari, J, and Keyser, D., 2001: A composite study of interactions between tropical cyclones and upper-tropospheric troughs. *Mon. Wea. Rev.*, 129, 2570-2584.

Healy, J., 2012: Isaac brings touch of relief, hope for next season, to Corn Belt. *The New York Times*. 2 September 2012. http://www.nytimes.com/2012/09/03/us/hurricane-isaac-brings-some-relief-to-corn-belt.html?_r=0. (Accessed 4 December 2014.)

Kellner, O., 2011: The role of anomalous soil moisture on the inland reintensification of Tropical Storm Erin (2007). Master's Thesis, Purdue University.

Kellner, O., D. Niyogi, M. Lei, and A. Kumar, 2011: Operational and model analysis on the reintensification of Tropical Storm Erin 2007: The Role of Anomalous Soil Moisture. *Nat. Haz.* – Tropical Cyclones of 21st Century Special Issue. DOI: 10.1007/s11069-011-9966-6.

Kishtawal C. M., D. Niyogi, A. Kumar, M. Laureano, O. Kellner, 2011: Observed sensitivity of inland decay of tropical cyclones to soil surface characteristics, *Nat. Haz.* - Tropical Cyclones of 21st Century Special Issue, DOI: 10.1007/s11069-011-0015-2.

Knabb, R.D., 2008: Tropical cyclone report: Tropical Storm Erin. *National Hurricane Center*. http://www.nhc.noaa.gov/data/tcr/AL052007_Erin.pdf. 7 April 2008 (Accessed 4 December 2014.)

Lixion, A.A. and D.P. Brown, 2005: Tropical Cyclone report: Tropical Storm Arlene. *National Hurricane Center.* http://www.nhc.noaa.gov/data/tcr/AL012005_Arlene.pdf. 20 July 2005 (Accessed 4 December 2014.)

MERRA: Modern era-retrospective analysis for research and applications. NASA Goddard Space Flight Center, Earth Sciences Division. Silver Springs, Maryland. 11 April 2012. http://gmao.gsfc.nasa.gov/research/merra/intro.php (Accessed 8 September 2014.)

Mesinger, F., G. DiMego, E. Kalnay, P. Shafran, W. Ebisuzaki, D. Jovic, J. Woollen, K. Mitchell, E. Rogers, M. Ek, Y. Fan, R. Grumbie, W. Higgins, H. Li, Y. Lin, G. Manikin, D. Parrish, and W. Shi, 2005: NCEP Regional Reanalysis. NARR Users Workshop, San Diego, CA. 11 January 2005. http://www.emc.ncep.noaa.gov/mmb/rreanl/ (Accessed 9 September 2014.)

Mitchell, Kenneth, 2005: The community Noah land –surface model (LSM): User's guide public release version 2.7.1. National Center for Environmental Prediction. Environmental Modeling Center. 9 February 2005. ftp://ftp.emc.ncep.noaa.gov/mmb/gcp/ldas/noahlsm/ver_2.7.1 (Accessed 10 November 2014.)

Midwest Regional Climate Center (MRCC), 2014. NCDC state monthly precipitation obtained from the Midwest Regional Climate Center, cli-MATE (MRCC Application Tools Environment), http://mrcc.isws.illinois.edu/CLIMATE/. (Accessed 11 September 2014.)

Monteverdi, J.P. and R. Edwards, 2010: The redevelopment of a warm-core structure in Erin: A case of inland tropical storm formation. *Electronic J. Severe Storms Meteor.*, 5(6). 1-18.

Oke, T.R., 1987: Boundary layer climates. Second Edition. New York: Routledge Press. Pp 435.

Pal, J and Eltahir, E., 2003: A feedback mechanism between soil moisture distribution and storm tracks. *Qtrly J. Royale Meteor. Soc.*, 129, 2279-2297.

Pielke, R. A., Sr., 2001: Influence of the Spatial Distribution of Vegetation and Soils on the Prediction of Cumulus Convective Rainfall, *Rev. Geophys.*, 39(2), 151–177.

Rodell, M., 2014 (a): NLDAS-2 forcing dataset information. NASA LDAS Land Data Assimilation Systems. Silver Springs, Maryland. 7 August 2014. http://ldas.gsfc.nasa.gov/nldas/NLDAS2forcing.php (Accessed 8 September 2014.)

Rodell, M., 2014 (b): GLDAS forcing datasets. NASA LDAS Land Data Assimilation Systems. Silver Springs, Maryland. 7 August 2014. http://ldas.gsfc.nasa.gov/gldas/GLDASforcing.php (Accessed 8 September 2014.)

Rodell, M., P.R. Houser, U. Jambor, J. Gottschalck, K. Mitchell, C.-J. Meng, K. Arsenault, B. Cosgrove, J. Padakkovich, M. Bosilovich, J.K. Entin, J.P. Walker, D. Lohmann, and D. Toll, 2004: The Global land data assimilation system. *Bull. Amer. Meteor. Soc.*, 85(3), 381-394. DOI: 10.1175/BAMS-85-3-381.

Schultz, L. and D. Cecil (2009): Tropical cyclone tornadoes, 1950-2007. *Mon. Wea. Rev.*, 137, 3471-3484.

Shafran, P.C., J. Woollen, W. Ebisuzaki, W. Shi, Y. Fan, R.W. Grumbine, and M. Fennessy, 2006: Observational data used for assimilation in the NCEP North American Regional Reanalysis. AMS annual meeting Seattle, WA. January 2004. Updated 12 June 2006. http://www.emc.ncep.noaa.gov/mmb/rreanl/ (Accessed 8 September 2014.)

Shelton, M.L., 2009: Hydroclimatology: Perspectives and applications. New York: Cambridge University Press. Pp 426.

Shen, W., Ginis, I., and Tuleya, R., 2002: A numerical investigation of land surface water on landfalling hurricanes. *J. of the Atmos. Sci.*, 59(4), 789-802.

Shi, JJ, SW Chang, and S. Raman, 1997: Interaction between Hurricane Florence (1988) and an upper- tropospheric westerly trough. *J. of Atmos. Sci.*, 54, 1231-1247.

Stensrud, D.J., 2009: Parameterization schemes: Keys to understanding numerical weather prediction models. New York: Cambridge University Press, 480 pp.

Stull, R., 1988: An introduction to boundary layer meteorology. Kluwer Academic, Pp 666.

United States Drought Monitor (USDM), 2011: U.S. Drought Monitor Map Archive of Texas, July 26, 2011. *The National Drought Mitigation Center*. Lincoln, NE. http://droughtmonitor.unl.edu/MapsAndData/MapArchive.aspx. (Accessed 4 December 2014.)

Wu, C-C and Cheng, H-J, 1999: An observational study of environmental influences on the intensity changes of Typhoons Flo (1990) and Gene (1990). *Mon. Wea. Rev.*, 173, 3003-3031.

6.7 Tables

Table 6.1: WRF model set up for the four select case studies exploring the soil moisture feedback hypothesis.

	Land Surface Parameterization, Initialization Dataset, Soil Moisture (SM) Values					
Storms	*Slab NAM*	*Slab NAM*	*Slab NAM*	*Slab NARR*	*Slab NARR*	*Slab NARR*
TS Erin (2007)	0.5 x SM	Default	1.5 x SM	0.5 x SM	Default	1.5 x SM
TS Don (2011)	0.5 x SM	Default	1.5 x SM	0.5 x SM	Default	1.5 x SM
H Isaac (2012)	0.5 x SM	Default	1.5 x SM	0.5 x SM	Default	1.5 x SM
TS Arlene (2005)	0.5 x SM	Default	1.5 x SM	0.5 x SM	Default	1.5 x SM

6.8 Figures

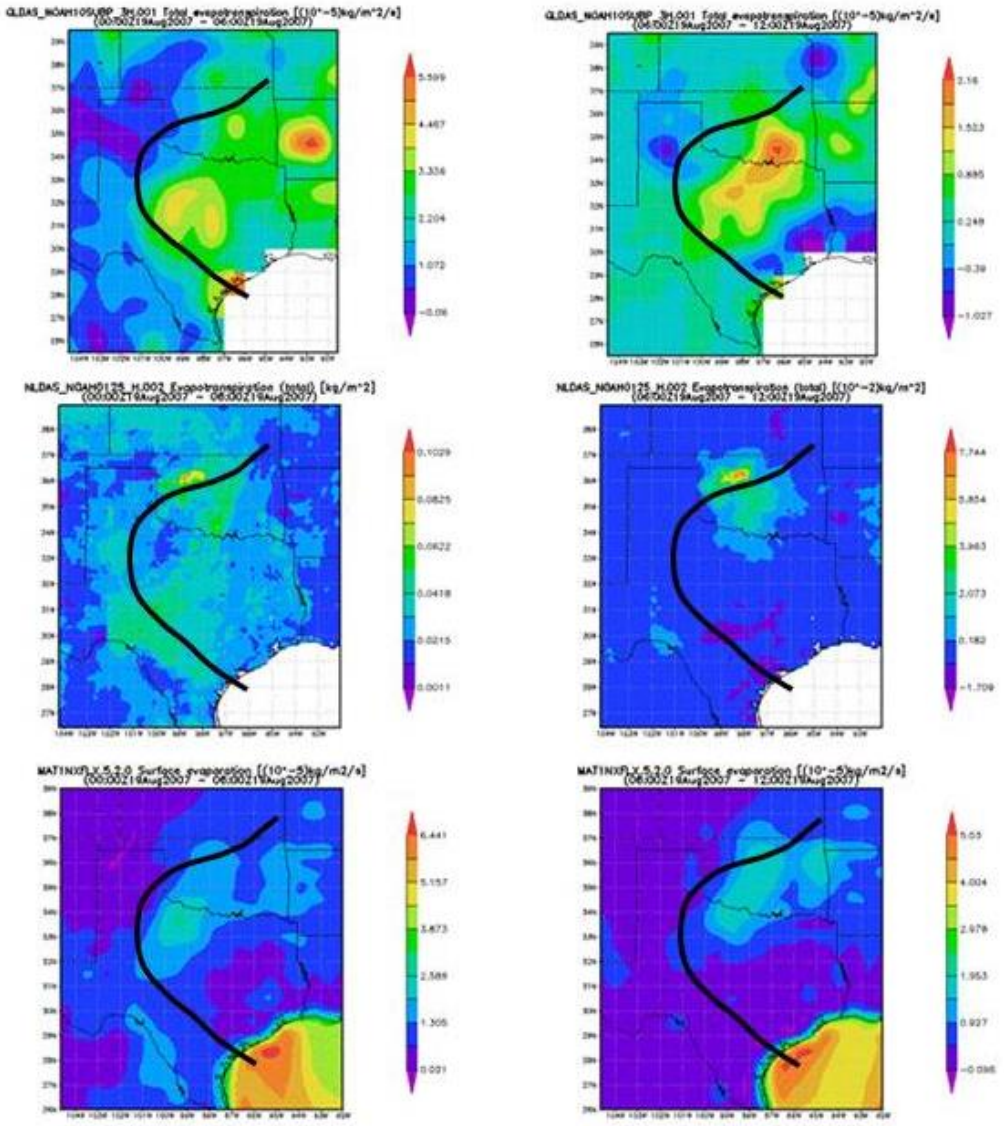

Figure 6.1: Plots of total evapotranspiration (GLDAS [top] and NLDAS [middle]) and surface evaporation (MERRA - bottom) prior to (00Z-06Z 19 August 2007) and during storm reintensification (06Z-12Z 19 August 2007). TS Erin's track is denoted by the thick black line. Values are highest during reintensification (4-10Z 19 August 2007) and are positive despite it being nighttime.

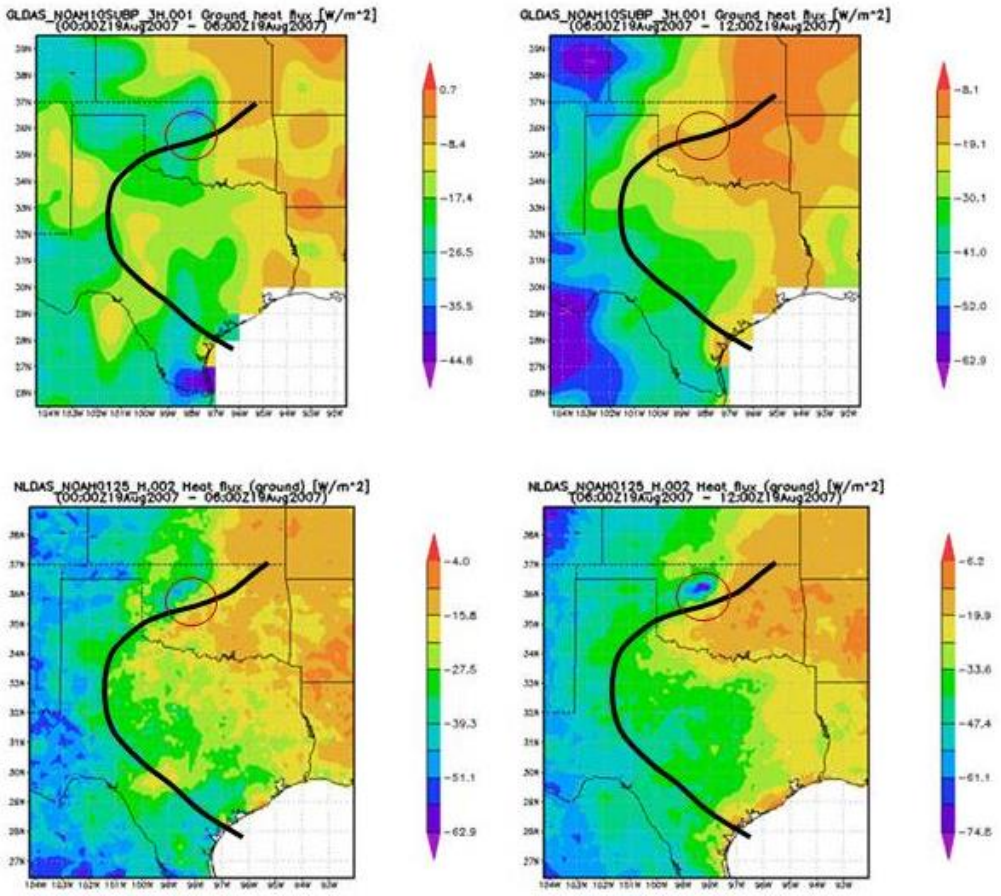

Figure 6.2: GLDAS (top) and NLDAS (bottom) ground heat flux prior to and during reintensification. Negative values note flux towards atmosphere while positive values indicate flux into the ground. Along TS Erin's path (thick black line) there is a ground heat flux gradient with increased/heightened levels of heat flux into the atmosphere at the time of reintensification noticeable in NLDAS image of 06-12Z 19 August 2007 (circled in red).

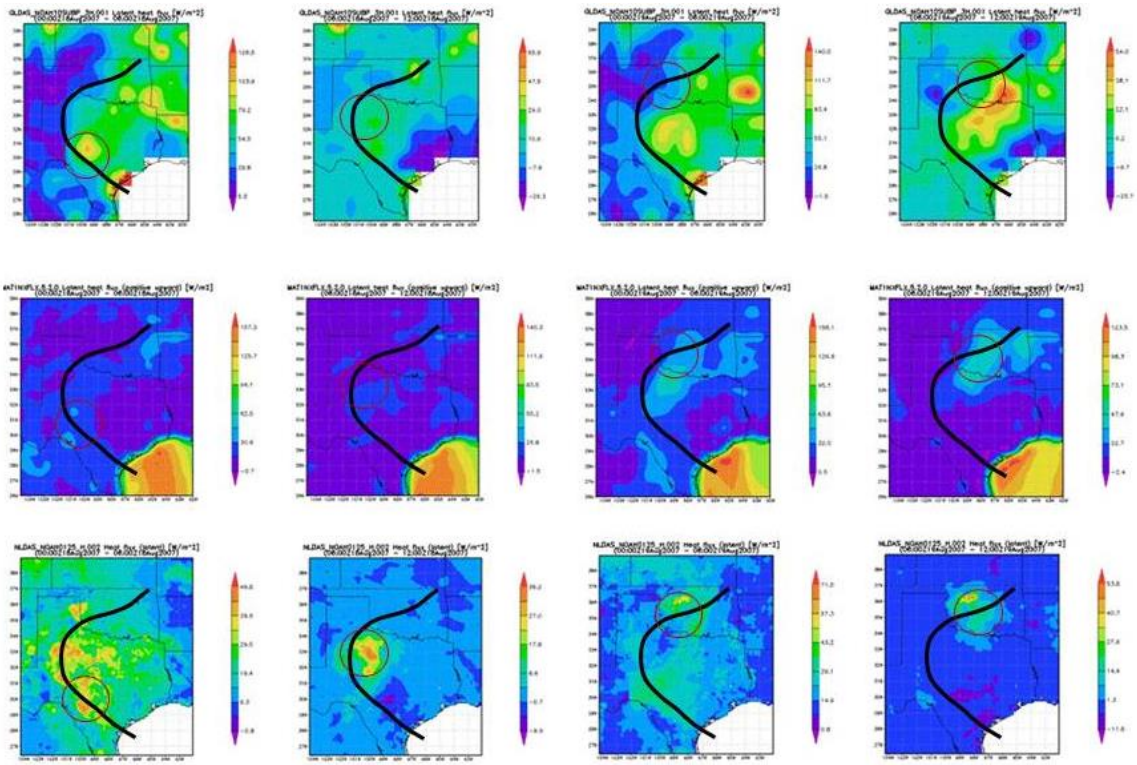

Figure 6.3: GLDAS (top row), MERRA (middle), and NLDAS (bottom row) latent heat flux plots for six hour intervals during the nighttime hours the day before (18 August 2007) and day of reintensification (19 August 2007). Positive values indicate latent heat flux from the surface into the atmosphere. All products show enhanced/heightened latent heat flux during the night hours into the storm (circled in red), especially leading up to reintensification. NLDAS captures the most detail and verifies with observations of where and when the storm restrengthened. MERRA and GLDAS show increased latent heat flux during reintensification, however is not as spatially precise as NLDAS. GLDAS appears to displace latent heat flux bull's-eye south east of where reintensification occurs.

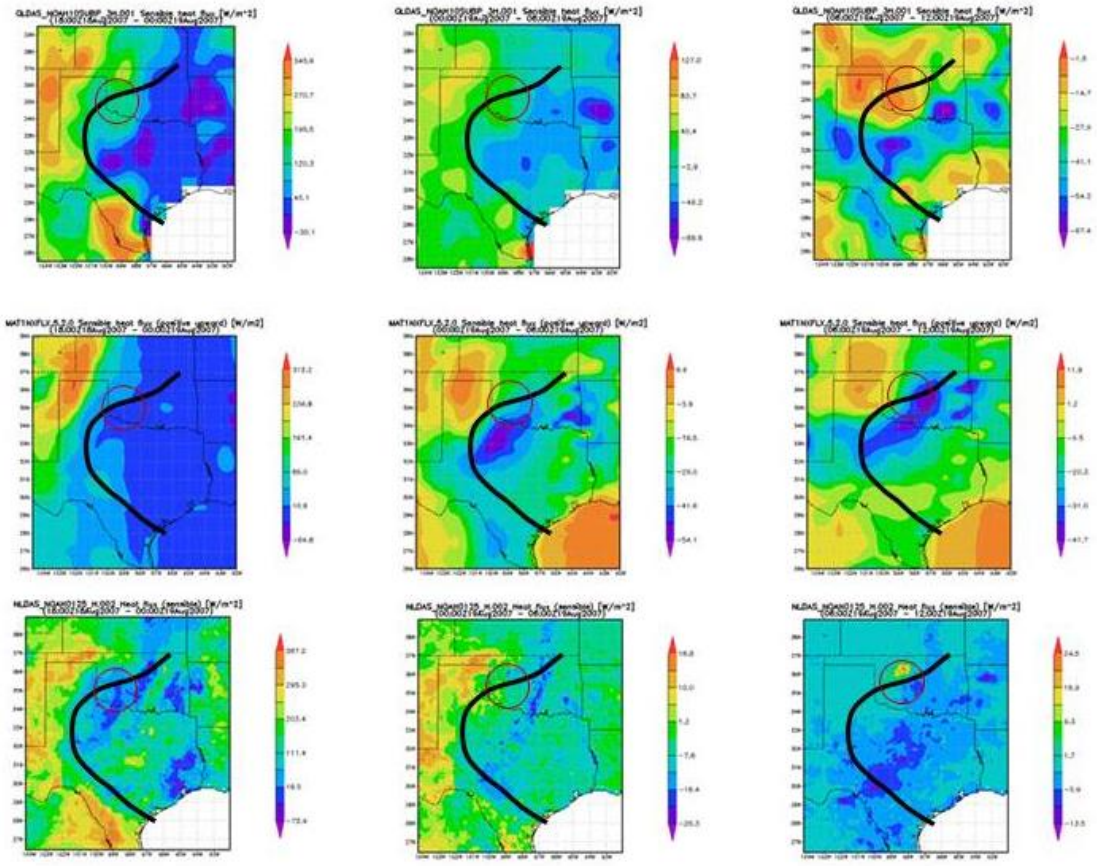

Figure 6.4: Same as Figure 3 except sensible heat flux plots. Sign conventions are the same. Time frame is by 6 hourly intervals for 1800Z 18 August 2007 to 1200Z 19 August 2007. As with latent heat flux, there is a positive sensible heat flux into the storm from the land surface. However, it is much weaker than the latent heat flux due to the portioning of fluxes by the daily surface radiation budget equation. Once again a distinct gradient of heat flux in vicinity of TS Erin's track and region of reintensification is visible.

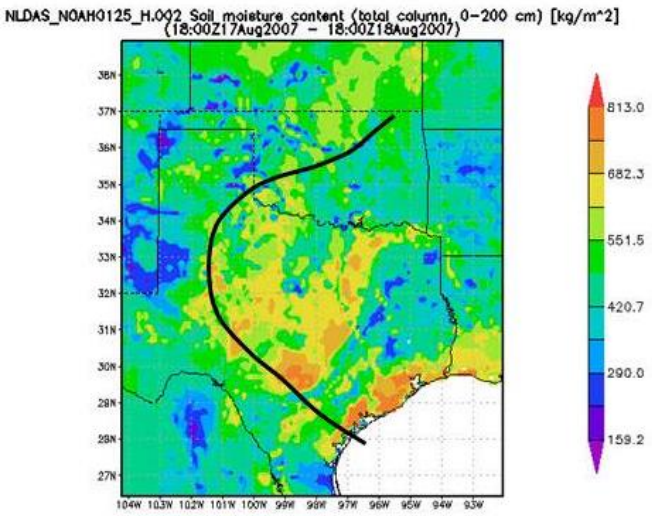

Figure 6.5: Total column soil moisture for the region over which TS Erin tracked. The track readily follows the western edge of the soil moisture gradient through southwest and western Texas then northeast into Oklahoma.

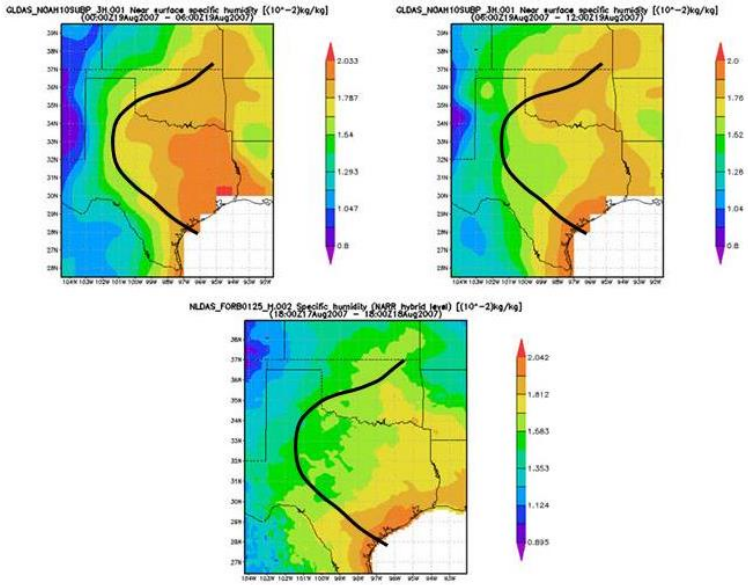

Figure 6.6: GLDAS (top row) and NLDAS (bottom) plots of surface specific humidity. TS Erin appears to have traverse along the western boundary of increased specific humidity which is influenced by surface characteristics such as soil moisture and vegetation cover.

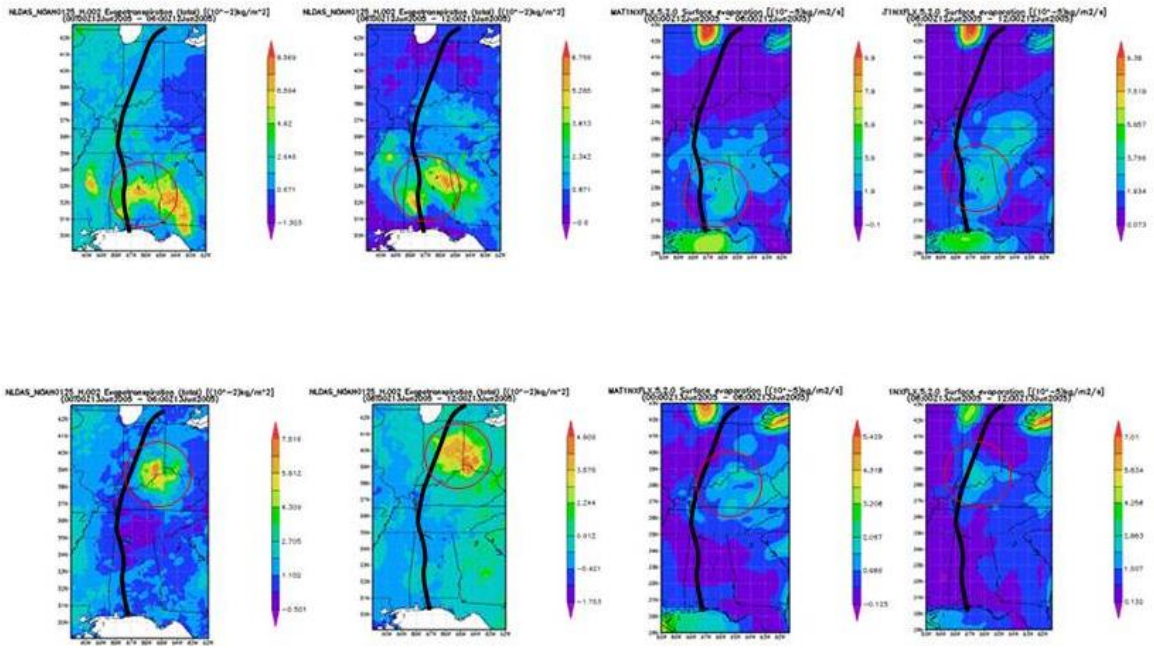

Figure 6.7: NLDAS evapotranspiration (2 left columns) and MERRA (2 right columns) surface evaporation during the overnight hours June 12 (top row) and 13(bottom row), 2005. Weak, but positive values (circled in red) of surface evaporation/evapotranspiration suggest a flux from the land surface to the atmosphere with enhanced values over Indiana on the 13 June 2005 when tornadoes were reported. NLDAS places the enhanced evapotranspiration in close proximity to where tornadoes touched down whereas MERRA fails to capture the same location and detail. TS Arlene's track is noted by the thick black line.

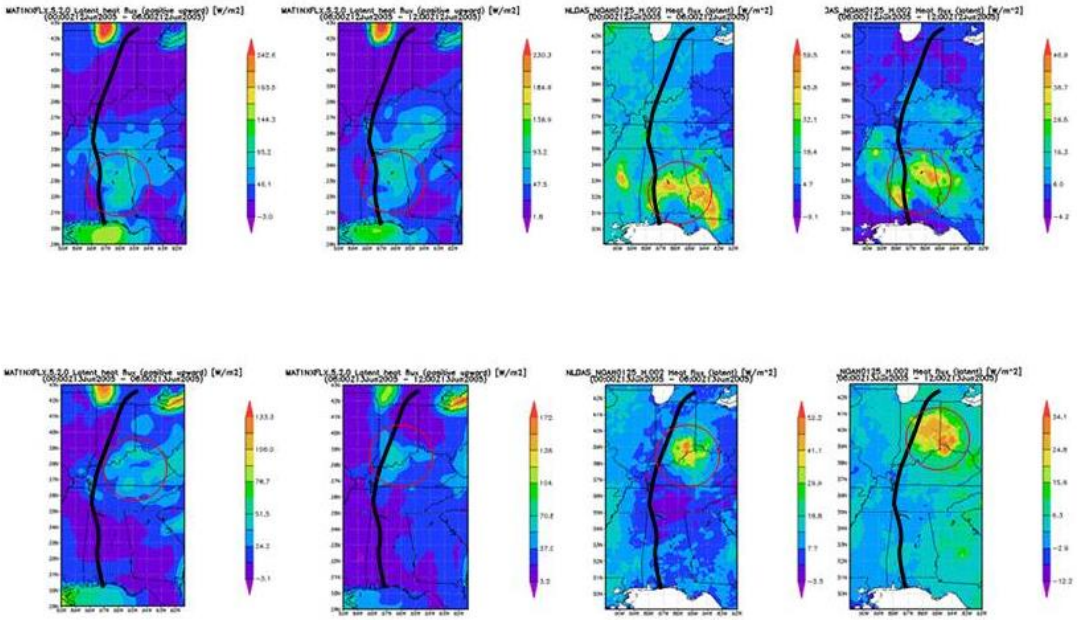

Figure 6.8: NLDAS latent heat flux (2 right columns) and MERRA latent heat flux (2 left columns) during the overnight hours June 12 (top row) and 13(bottom row) 2005. Like Figure 7, positive values suggest a flux from the land surface to the atmosphere with enhanced values over Indiana on the 13 June 2005 when tornadoes were reported. NLDAS places the enhanced latent heat flux amounts in close proximity to where tornadoes touched down whereas MERRA once again fails to capture the same location and detail.

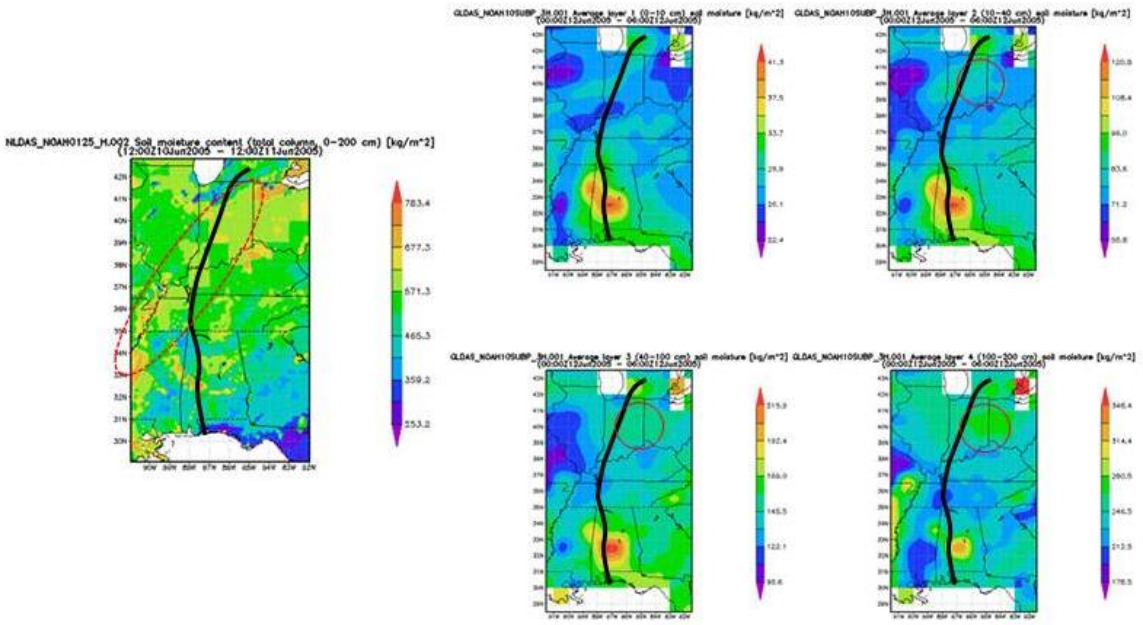

Figure 6.9: Soil moisture data from NLDAS (total column, left figure) 24 hours prior to landfall and GLDAS (0-10cm, 10-40cm, 40-100cm, and 100-200cm layers, right 4 figures) soil moisture at landfall. Like TS Erin, there is a soil moisture gradient (NLDAS image, encircled with dashed red) in the vicinity of the storm's track. Worth noting in the GLDAS imagery is the increased soil moisture at 10-40cm, 40-100cm, and 100-200cm layers in the vicinity of increased surface evaporation, latent heat flux, and reported tornadoes (solid red circles).

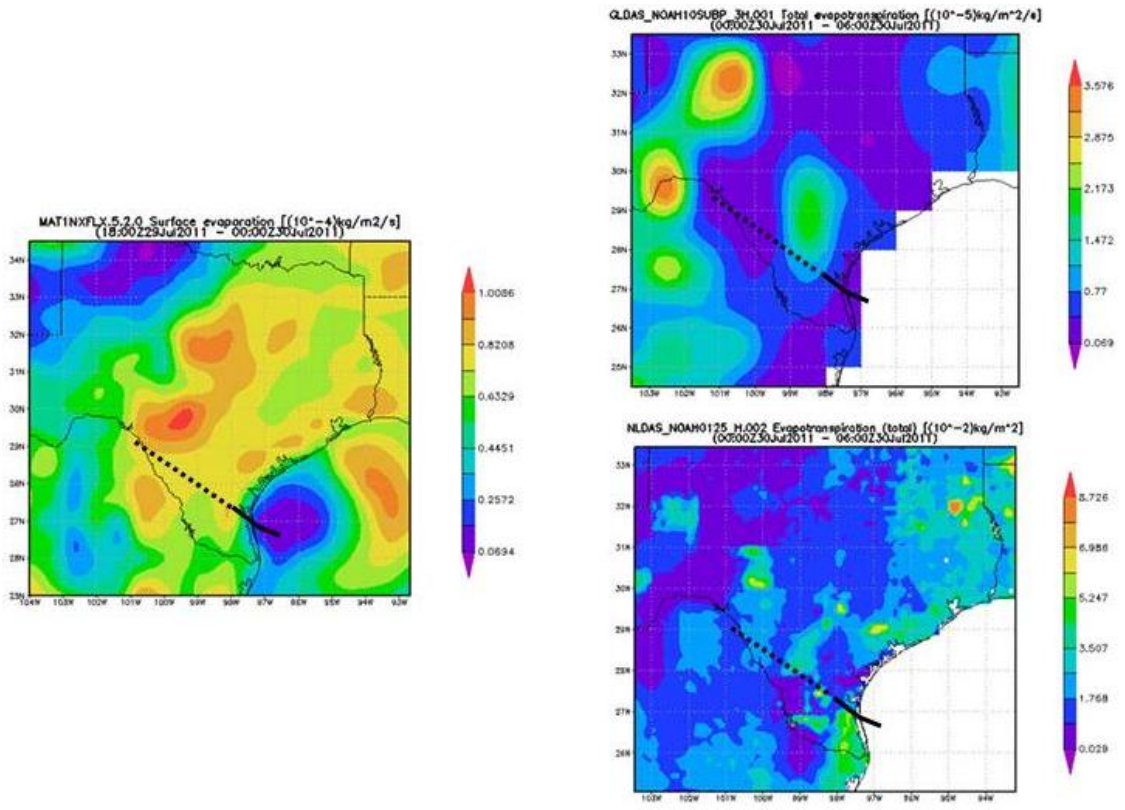

Figure 6.10: MERRA surface evaporation (left), GLDAS total evapotranspiration (top right), and NLDAS total evapotranspiration (bottom right) during TS Don's landfall. Images show weak evapotranspiration near to where the storm made landfall. However, no strong surface boundary is present with TS Don.

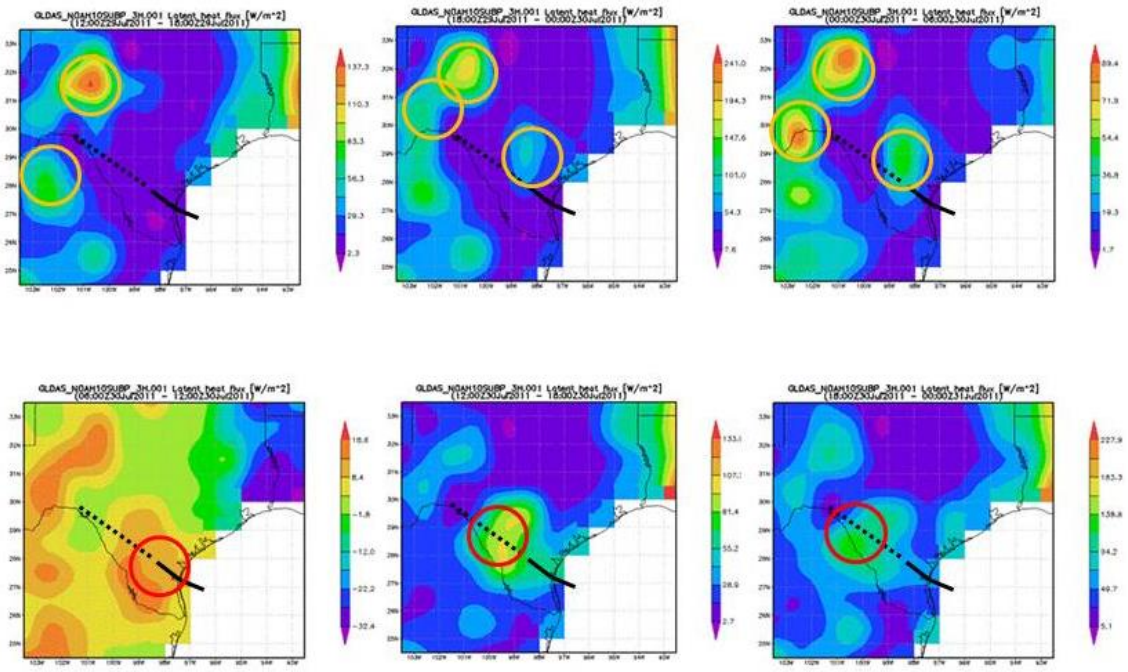

Figure 6.11: GLDAS latent heat flux plots 12 hours prior to landfall by 6 hour intervals (first two images, top row) till dissipation (by 6 hour intervals). Even during overnight hours, TS Don managed to extract latent heat from the surface after making landfall (circled in red) and before dissipating. Orange circles (top row) denote regions of enhanced latent heat flux from the land surface prior to landfall and in the direction that TS Don tracked.

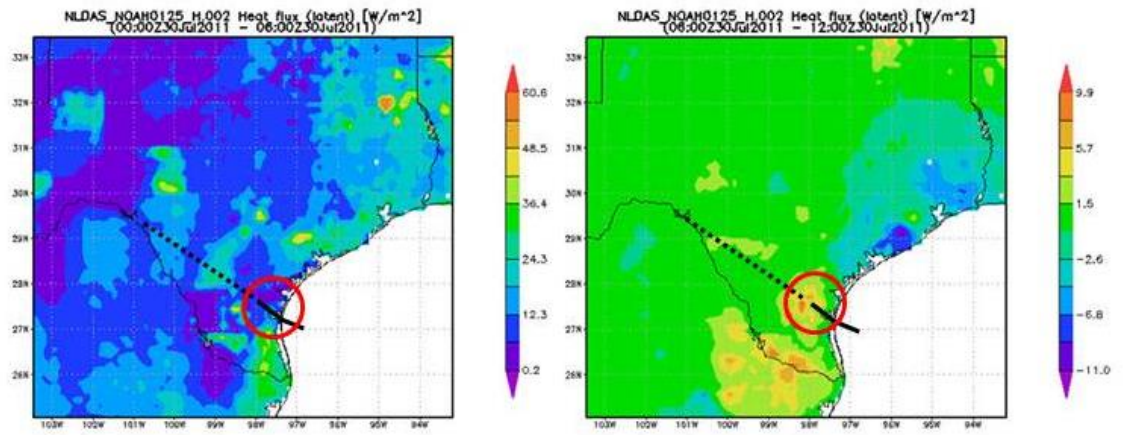

Figure 6.12: Like GLDAS in Figure 11, a positive latent heat flux is shown in proximity to the storm's center in southern Texas after moving inland (right figure). Location of the storm is circled for convenience.

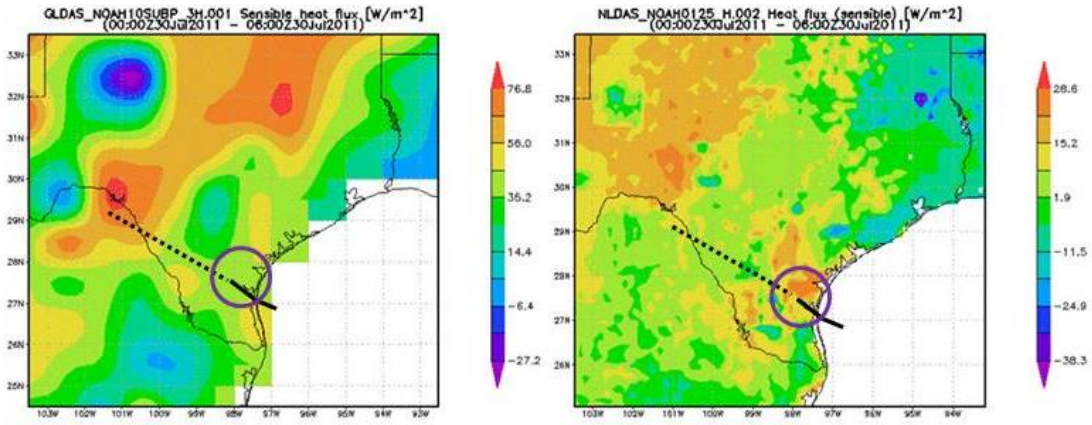

Figure 6.13: Sensible heat flux from 8pm (29 July 2011) - 2am (30 July 2011) local time. TS Don made landfall at 1030pm 29 July 2011. Weak but positive sensible heat flux is shown beneath the storm center (circled) at this time with the highest sensible heat flux northwest of where TS Don made landfall and the circulation center eventually tracked (dashed line).

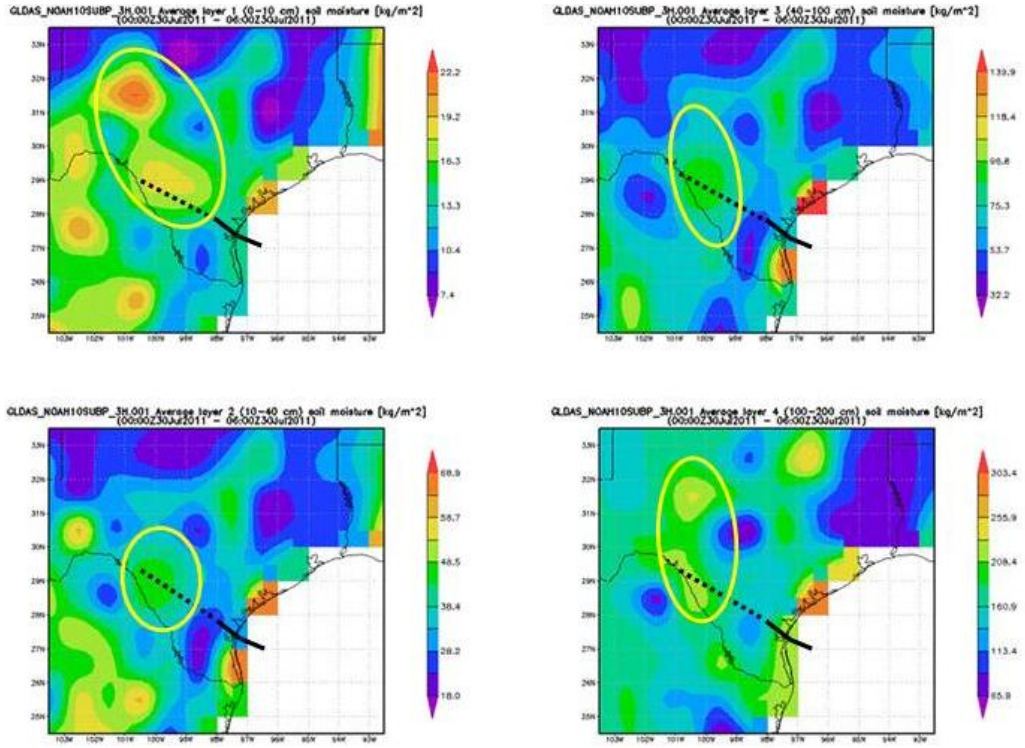

Figure 6.14: GLDAS soil moisture plots (0-10cm, 10-40cm, 40-100cm, and 100-200cm layers) leading up to and during the time TS Don makes landfall. The circulation center appears to track towards regions of higher soil moisture (circled in yellow).

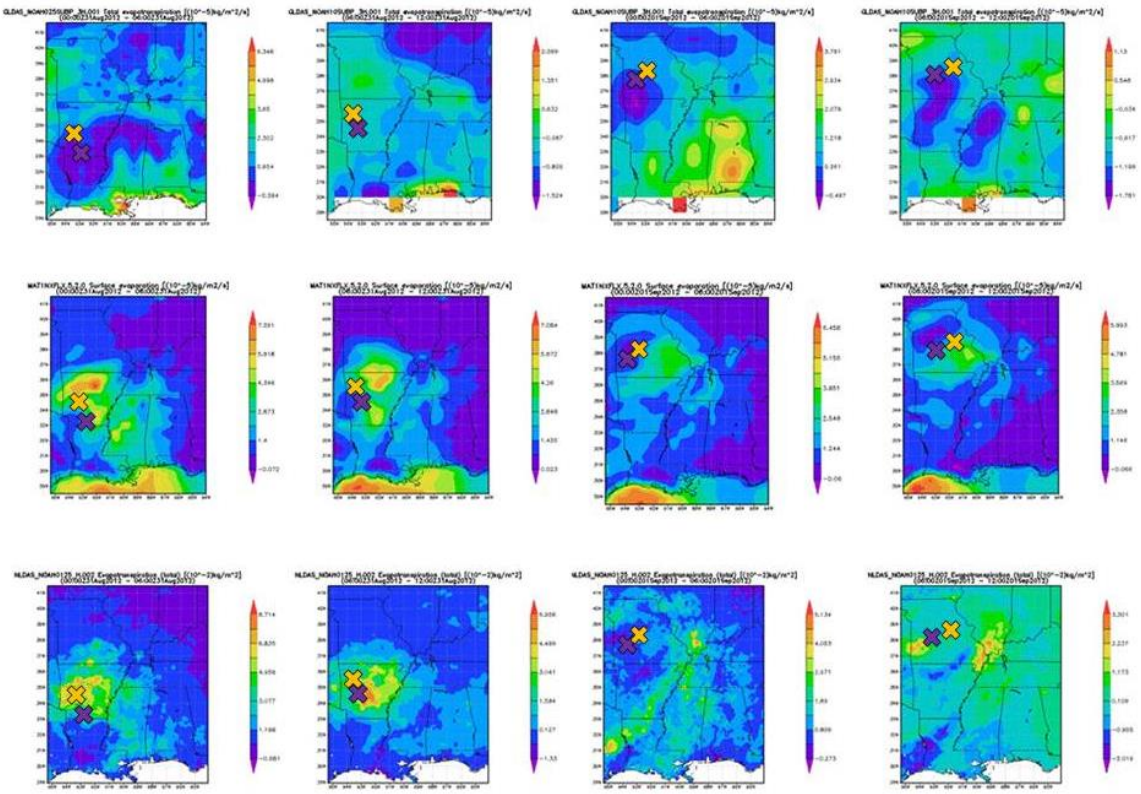

Figure 6.15: Total evapotranspiration (GLDAS – top row and NLDAS – bottom row) and surface evaporation MERRA (middle row) during the overnight hours after Isaac's landfall (final landfall at 2am LST 29 August 2012) as Isaac tracked inland. Center of Isaac marked on the map for the beginning time (purple X) and end time (orange X) of the image. It can be seen that the self-sustaining process of tropical systems readily encouraged evaporation/evapotranspiration (albeit weak) as a moisture source from the land surface near and ahead of the center despite the absence of daytime solar radiation. Highest rates of evaporation/evapotranspiration also coincide with times of active convection during which tornadoes occurred in IL, IN, MO, KY, and AR (see http://www.spc.noaa.gov/climo/reports/120831_rpts.html and http://www.spc.noaa.gov/climo/reports/120901_rpts.html for tornado report information) as found with TS Arlene 2005 over east-central Indiana. MERRA and NLDAS (high spatial resolution show more detailed and slightly higher rates of evaporation/evapotranspiration than GLDAS).

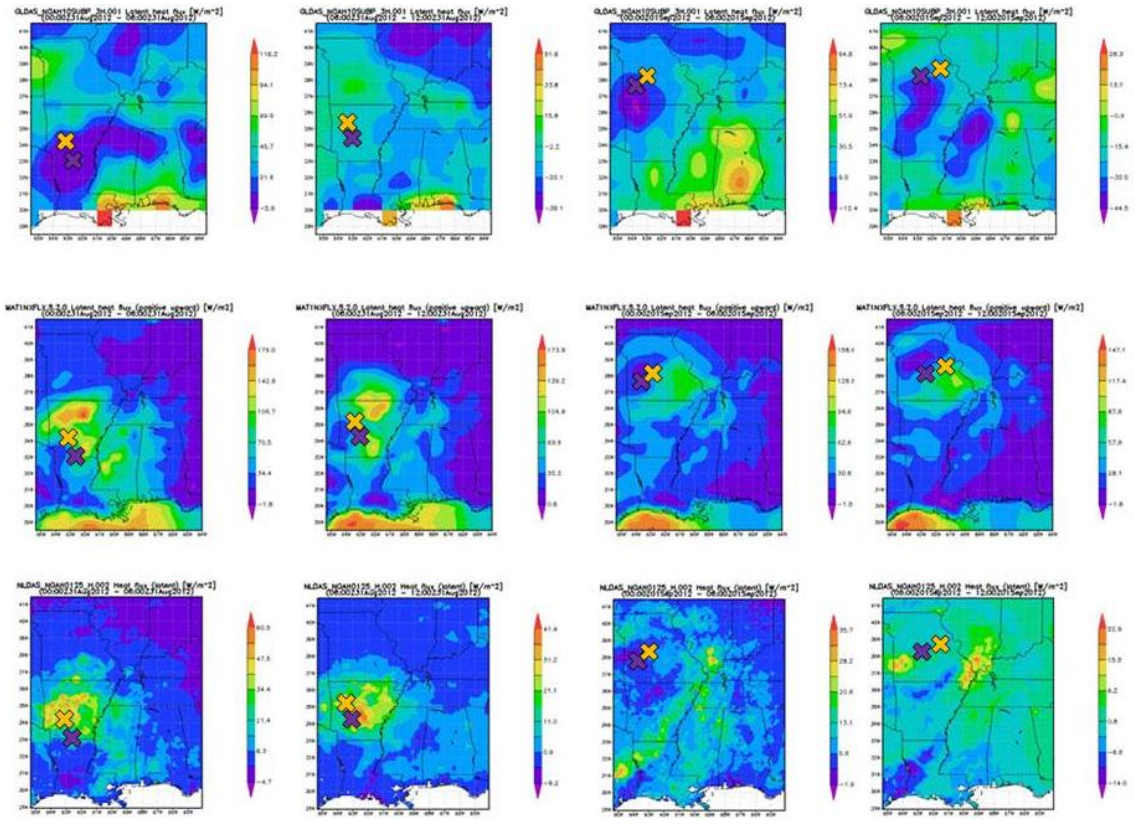

Figure 6.16: Same as figure 15 except latent heat flux.

CHAPTER 7. CONCLUSION

7.1 Hydroclimate Systems

The Earth-atmosphere system is a highly complex, dynamical series of interconnected spheres (i.e. subsystems): the atmosphere, the biosphere, the lithosphere, the hydrosphere, and the cryosphere. Climate, and more specifically the hydroclimate, is influenced by characteristics and properties inherent to each of these spheres. The hydroclimate of a given area is established by climates of the first and second kind with each type of climate resulting from the thermodynamic and hydrodynamic properties inherent to the transfer and flux of heat, mass (water), and momentum across different spatial and temporal scales. Hydroclimatology is the coupled science of hydrology, meteorology, and climatology. The hydrologic cycle is intricately linked to the atmosphere in that the atmosphere serves as the primary input to the hydrological cycle in the form of precipitation. Additionally, evaporation, a component of the hydrosphere, serves as input to the atmosphere. Additional evaporative input to the atmosphere comes from the land surface (biosphere and lithosphere).

7.1.1 Types of Climate

Climate as a science is subdivided into two parts: 1) climate as determined by general atmospheric circulation and 2) climate as determined by the flux of heat and moisture between the overlying atmosphere, the land surface and the subsurface. These two separate climates have been identified as large-scale and local-scale climate, respectively (e.g. Shelton 2009). Large-scale and local-scale climates are linked in that the established temperature and precipitation regimes as determined by large-scale

climates work synergistically with local-scale climates. Large-scale climate determines the rates of input and output for local-scale climate with the output (e.g. flux of heat and moisture from the land surface to the atmosphere) from local-scale climate further being able to contribute to the evolution of large-scale climate.

7.1.2 Climate Variability and Change

Humans, a component of the biosphere, modify climate systems that have been established for thousands of years on Earth. The geologic time frame that encompasses when humans began to influence the physical processes of the Earth-atmosphere system through hunting and gathering, agriculture, land use change, and the burning of fossil fuels has been identified as the Anthropocene (Steffen et al., 2007). Climate systems are documented to have experienced episodes of natural climate variability for thousands of years primarily through proxy data analysis. However, with the onset of the industrial revolution, human impact to the Earth-atmosphere system shifted to a much higher and impactful level because of the abundant release of carbon dioxide due to burning of fossil fuels for energy (Steffen et al., 2007). Humans elicit changes in climate through modification of the land surface through processes such as urbanization and deforestation and modification of the atmosphere through the burning of fossil fuels which release greenhouse gases such as carbon dioxide, nitrous oxide, and methane into the atmosphere adding to the natural greenhouse gasses already present. While climate variability and change can occur naturally from volcanic eruptions, changes in Earth's orbit, and solar cycles, human modification of the natural climate systems has been identified and is noted as human-induced climate change. Climate change resulting from humans is receiving more attention than in the past due to the rate of warming documented in the last approximately 100 years and the ability of scientist to show that the warming is not completely a function of natural causes (e.g. Steffen et al., 2007).

7.1.3 Weather and Climate Data History

The collection of weather and climate data began approximately during the late 1700s, spreading in countries around the world as industrialization of societies began.

Commerce and economies needed to track weather systems due to weather's impacts on the transportation of goods (Monmonier 1999). With the establishment of weather observers and the invention of the telegraph, weather prediction began to unfold in the early 1900s. The collection of daily weather data has led to the establishment of a weather record dataset spanning almost 130 years in some areas of the world. The efforts to observe, understand, and predict the weather has provided a solid base of observations to which meteorologists and climatologists have been able to monitor changes in weather and climate through time. Advancements in remotely sensed technologies such as satellites provide additional weather and climate data from locations where humans are unable to monitor weather and climate changes first-hand.

Through scientific collection of weather and climate data, an increased comprehension of anthropogenic feedbacks to hydroclimates has been identified. It is recognized that humans are contributing to global climate change (e.g. Melillio 2014; IPCC 2014) through land surface change and increased levels of greenhouse gases. Accounting for these changes in climate models, model projections forecast shifts in precipitation patterns and temperatures. With temperature (radiation) and precipitation being the two primary drivers of hydrological processes, it is expected with global climate change that local hydroclimate change will occur as well. Although a consensus has been reached in the scientific community through applied research and numerical prediction that Earth will warm and shifts in temperature and precipitation will occur, there is uncertainty in how future generations will understand, prepare for, predict, and mitigate the effects of projected changes in climate and weather.

7.1.4 Importance of Analysis for the Future

Hydroclimatology is far-reaching and highly applicable to many components of peoples' lives. Understanding how hydroclimatology will change in a warming climate is best completed through a comprehensive, thorough analysis of hydroclimates across temporal and spatial scales. Understanding past behaviors of a climate system is highly critical to determining possible future behaviors of a climate system. This hydroclimatological analysis serves to obtain a deeper understanding of current

hydroclimates and components of hydroclimates from past and current climate data to apply findings from each study to strengthen climate change mitigation and resiliency. Enhancing climate resiliency is becoming more important as hydroclimatological extremes begin to occur more frequently under projected warming climate scenarios (Melillio et al., 2014; IPCC 2014).

7.1.5 Spatial and Temporal Scales

The hydroclimates of the world vary across spatial and temporal scales and they are open systems that regularly interact with each other. Hydroclimates vary in scale from microclimates such as those established around a plant (with fluxes of heat, mass, and momentum occurring across time frames of seconds to minutes), up to planetary scale hydroclimates such as those established by general circulation cells that dictate Midlatitude climate regimes on time frames of months, seasons, and decades. Hydroclimates can experience natural climate variability from sources such as teleconnections (weeks) or volcanic eruptions (e.g. Krakatoa in 1883 – "year without a summer"). Hydroclimates can also experience climate change through time as a result of natural and human causes (decades). Impacts from climate variability and change are not reserved to specific hydroclimates, but can impact hydroclimates across all spatial and temporal scales.

7.1.6 Classification of Primary Hydroclimate Variables: Normal, Anomaly, and Change

As discussed in Chapter 1, hydroclimates are driven by movement of heat and moisture through a climate system. Heat is most commonly quantified in the form of temperature (daily, monthly, annual and maximum, minimum, and average temperatures) which contributes to relationships such as evapotranspiration and saturation vapor pressure. Temperatures are further influenced by climate variability which can result in heat waves and cold spells, and are further influenced by climate change which can lead to an increase or decrease in average temperature in a given area over time. Additionally, ambient temperatures are strongly influenced by the radiation balance at the surface. The partitioning of surface radiation into different surface fluxes of heat, mass, and

momentum on different types of surfaces (vegetation, soil, or impervious) and moisture content influences temperature as well. Precipitation (rainfall, snowfall, tropical cyclones, blizzards, etc.) which serves as the input component of the hydrologic cycle, is the largest input of moisture to the hydroclimate system. Established precipitation patterns within a hydroclimate can experience extreme or anomalous events such as floods or droughts which can commonly be attributed to climate variability and but hydroclimates can also undergo climate change. Climate change will shift a hydroclimate system into a new state of hydroclimatological balance. The variable 'climate normal' allows scientists to determine if weather is normal, anomalous (within the mean distribution of a normal climate, just within the tails of the distribution), or a manifestation of climate change.

7.2 Hydroclimatic Assessments across Spatial and Temporal Scales

7.2.1 Agroclimatology

The development of human societies results from the domestication and production of vegetation and animals by humans. Thousands of years of trial and error for plant and animal domestication occurred before humans were able to identify those plants and animals that could be domesticated and survive in varying climates around the world. It is the variation in climates as established by general circulation of the atmosphere that provide Earth with various regions of primary agronomic production such as the U.S. Corn Belt which is favorable for corn, soybean, cattle, and sheep production. The Fertile Crescent is another production region, which is suitable for wheat, barley, flax, chickpeas, and lentil. Mediterranean climates are ideal for fruits such as olives, figs, pomegranate, and citrus, and subtropical climates favorable for cotton, tobacco, rice, poultry, and swine. With agriculture and agronomic production intricately linked to weather and climate, understanding the evolution of agriculture in relation to past weather and climate regimes is key to exploration of agricultural evolution into the future as weather and climate experiences variability and change. Chapter 2, "Agroclimatology" provides a comprehensive discussion on the history, the growth, and the efforts underway to improve future agronomic practices as related to past, present, and future weather and climate. In this chapter, the hydroclimate system is investigated

primarily with a focus on the relationships between large-scale climate and agricultural production. Local-scale climate is also discussed due to the intricate connection of crop phenology and parameters such as soil moisture, soil temperatures, and evapotranspiration.

7.2.2 Climate Variability and the U.S. Corn Belt: ENSO and AO Episode-dependent Hydroclimatic Feedbacks to Corn Production at Regional and Local Scales

Hydroclimatic variability most commonly manifests itself in the form of record high and low temperatures or precipitation events which lie in the "tails" of what is the normal probability distribution of the climatological variable in question. While rare, these events are part of the normal climate system. However, the rate at which climate variability occurs is expected to increase under a warming climate scenario. Thus, understanding the response of past crop production, specifically corn, to climate variability in the form of temperature and precipitation changes resulting from ENSO and AO teleconnections is important. Chapter 3 discusses the development of usable tools for agricultural producers through the application of past climate data. This allows producers to better prepare for increased climate variability and change in the future. Efforts such as the ENSO and AO climatology developed in Chapter 3 demonstrate the efforts of climate scientists working with the agricultural community to develop adequate tools and adaptable behaviors to ensure continued, successful food production in future decades as the world begins to face greater rates of food and water scarcity. It will be the proper management of water resources in drier Midlatitude climates that will ensure producers reach their highest production potential. The climatology and tool development described in Chapter 3 provides producers with climatological scenarios showing which atmospheric indexes (large-scale climate) will result in drier or wetter conditions in their fields (local-scale climate) months ahead of time. Analogue historic production compliments the climatological scenarios present in the climatology with the primary goal of the climatology and tool to help farmers better plan for optimal planting, fertilizing, water, and harvesting as the climate becomes more variable with time.

7.2.3 Assessing Drought Vulnerability of Agricultural Production Systems in Context of the 2012 Drought

Drought is an example of the hydroclimatological extreme event of a profound rainfall deficit (the opposite extreme event to a drought is a flood). Because drought varies in type (e.g. meteorological, hydrological, agricultural, or socioeconomic), it has far-reaching impacts across societies and manifests itself in the hydro-thermodynamics of both large-scale and local-scale climate. With agriculture being such a large component of the United States economy and the United States being such a large contributor to the world food market, the 2012 drought that impacted the United States is the most recent example of an extreme climate event worthy of detailed analysis to gain a comprehensive understanding of drought triggers, atmospheric circulation associated with historic drought events, and the scale of impacts to production and world food markets in order to be better prepared for future drought events of such magnitude. The drought of 2012 was widespread, with up to 63% of the land area in the Continental United States classified as being in Moderate to Exceptional Drought (USDM 2012) and comparable in magnitude to the droughts in the 1980s and the Dust Bowl. The heat and moisture deficit not only drastically impacted corn and soybean productions, it impacted forage and feed with a chain reaction into cattle production and prices. Drought and high temperatures commonly occur together increasing rates of heat stress on cattle which further impacts reproduction and lactation rates of cows. Assessing drought vulnerability in agricultural production systems under the most recent drought events brings forth the reality that adapting agricultural practices more resilient to drought and practicing mitigative drought measures will ensure less drastic impacts to agricultural production systems under future drought scenarios.

7.2.4 Land-falling Tropical System Rainfall Contribution to the Hydroclimate of the Midwest 1981-2012

The unifying theme in four of the six hydroclimatological assessments is the impact of hydroclimatic variability and change to agricultural production across the U.S.

Corn Belt. Chapter 2 encapsulates the highly coupled relationships between climate, agriculture, and agronomy. Chapter 3 discusses hydroclimate variability stemming from ENSO and AO teleconnections with impacts to agricultural production across the North Central Region of the United States, and Chapter 4 demonstrates the drastic impacts of extreme climate events on the agroclimate during the 2012 drought. While the primary agricultural production region of North America receives precipitation from rainfall generated by Midlatitude weather systems and summertime convective thunderstorms fed by moisture from the Gulf of Mexico, land-falling tropical cyclones are also a generator of hydroclimatological rainfall across the Central and Eastern United States. Depending on antecedent seasonal rainfall, these land-falling storms may result in flood events (e.g. Villarini et al., 2014), or may serve as drought busting events (e.g. Haberlie et al., 2014). Regardless, land-falling tropical systems are a part of the Midwest hydroclimate that are not readily quantified as a total percentage of rainfall. Furthermore, land-falling tropical systems are not experienced every year. Thus a storm's presence may or not may impact the overall production in a growing season. Chapter 5 investigates the average observed total seasonal rainfall contribution from land-falling tropical systems to the Midwest hydroclimate in the Eastern U.S. Corn Belt. Findings show that land-falling tropical systems do play an important role in production, especially over regions in Illinois and Kentucky where shifts in the jet stream greatly impact where Midlatitude weather systems traverse and produce rainfall. With these results, an accurate hurricane forecast may help agricultural producers in the region better plan for a drier or wetter than expected season.

7.2.5 Role of Antecedent Soil Moisture Conditions on the Inland Reintensification of Tropical Systems Examined Using Remotely Sensed Data and Model Verification

Local-scale climate is the climate established at the atmosphere and land surface interface where heat, moisture, and momentum fluxes occur based on the daily radiation budget. While tropical systems are regarded as self-sustaining, warm core systems that mainly derive energy from the warm ocean waters, recent research points to land-falling tropical systems interacting with the land surface in a way such that inland longevity of a

tropical storm system is prolonged rather than the storm dissipating quickly after making landfall. These observations have led to the proposed hypotheses that land-falling tropical systems, a phenomena of large-scale climate, interact with local-scale climate to sustain, reintensify, or more readily dissipate land-falling/inland tropical storm systems depending on antecedent hydroclimate conditions. Chapter 6 thoroughly investigates the proposed hypothesis that inland anomalously wet antecedent hydroclimatic conditions serve as an energy source to land-falling tropical systems with the corollary hypothesis that inland anomalously dry (i.e. drought) antecedent hydroclimatic conditions serve as an accelerant to land-falling tropical system dissipation. Operational hydroclimatic analysis coupled with remotely sensed datasets prior to and during inland storm tracking show land surface interactions supportive of the proposed hypothesis. Model verification using WRF further supports anomalous antecedent hydroclimatic interactions between land-falling tropical systems and the land surface.

7.3 Summary and Future Research Directions

The Earth-atmosphere system is comprised of hydroclimates across spatial and temporal scales that embody different dynamic and thermodynamic properties. Hydroclimates across Earth determine how humans and other life forms live and prosper. A hydroclimate is determined by its proximity to large-scale climate influences resulting from general atmospheric circulation. However, large-scale hydroclimates are further influenced by local-scale land surface characteristics such as land cover, land use, vegetation, topography, soil type, and albedo. While large-scale climates influence large, regional land areas and result in regional climate characteristics such as arable land for agriculture, local-scale land surface characteristics further influence hydroclimatic responses. Humans and societies are intricately entwined with hydroclimates because of human dependency on agriculture and commerce. This dependency makes understanding the physical relationships that drive hydroclimates across temporal and spatial scales vital for human resiliency to climate variability and change in the future.

The primary purpose of this U.S. Corn Belt hydroclimatological assessment across spatial and temporal scales is to identify hydroclimatic relationships important to

agricultural production as discussed in Chapter 2. Chapter 4 highlights the driving hydroclimatic relationships that led to the 2012 drought and how these hydroclimatic relationships impacted agronomic decision making and agronomic markets. The main goal of Chapter 2 is to provide readers with drought information to improve resiliency to future drought. As noted in Chapter 3, prior assessments of the hydroclimates across the U.S. Corn Belt analyze large-scale hydroclimatic influences such as ENSO with different indexes, across different spatial scales, and across different time frames. Additionally, hydroclimatic analysis of the AO on agricultural production is more limited in literature than ENSO. Thus, the AO analysis in Chapter 3 provides a new glimpse to AO hydroclimate influences on agricultural production across the U.S. Corn Belt. Together, the findings in Chapter 3 that discuss ENSO and AO episode-dependent feedbacks to agricultural production show the scale-dependency of temperature and precipitation hydroclimate relationships across the U.S. Corn Belt. Presented in a manner useful to producers, the findings in Chapter 3 allow for more tailored and accurate decision making by producers when faced with climate variability in the future. Future episode-dependent hydroclimatic assessments should investigate the relationship between teleconnections such as the Pacific North American Pattern (PNA), the North Atlantic Oscillation (NAO), and the Pacific Decadal Oscillation (PDO) and agricultural production.

Tropical Storm systems regularly make landfall along the Gulf and East Coasts of the United States. Upon making landfall, storms commonly begin to weaken for several reasons: lack of a latent heat source, interaction with higher wind speeds found in Westerly flow, and friction from the land surface that disrupts balanced airflow into the core of the storm (Rhome and Raman 2006). However, some storms remain organized and can track far inland before transitioning to extratropical systems. These land-falling tropical systems serve as a new hydroclimate "input" in the form of tropical system rainfall (rather than the more common extratropical system rainfall observed across the Subtropics and Midlatitudes of the United States). Understanding the role of tropical system rainfall to the Eastern U.S. Corn Belt hydroclimate is important for agriculture production because the region experiences episodes of climate variability in the form of wetter than normal or drier than normal conditions. Chapter 5 shows that during these

abnormally dry or wet conditions, tropical system rainfall can either be of benefit to crop production in some states, or detrimental to production in some states. The findings suggest that with timely and accurate tropical storm season outlooks, producers can make more informed decisions ahead of time to reduce yield loss and increase yield during the growing season. Future research to support these findings should focus on improving hurricane season forecasts so that the results in Chapter 5 may be applied in agronomic decision making.

The hydroclimatic analysis completed in Chapter 6 examines the open-system relationships between local-scale and large-scale hydroclimate phenomena. The analysis specifically investigates the role of antecedent, anomalous soil moisture conditions at several different spatial resolutions using remotely-sensed datasets and numerical modeling. The results show that soil moisture anomalies may contribute to tropical storm system evolution over land, and it is suggested from these findings that land-surface interactions are given more weight in land-falling tropical system forecasts as part of the Hurricane Forecast Improvement Project. Like other chapters, Chapter 6 also demonstrates the spatial scale dependency of hydroclimatic analysis with results from GLDAS, NLDAS, and MERRA showing differences in flux values and location despite all being input datasets being driven by the Noah-LSM. GLDAS has the coarsest spatial resolution (111 x 111 km) and fails to capture the heat and moisture flux detail that NLDAS (13.875 x 13.87 5km) and MERRA (55.5 x 74 km) provide. This suggests an increased need of higher spatial resolution hydroclimatic analyses and modeling in land-falling tropical system forecasts for convection.

Comprehensively, this hydroclimatic assessment shows that the spatial and temporal scale at which hydroclimatic assessments are completed reveal different relationships and feedbacks, all of which are important to consider and all of which are applicable to agronomic decision making and forecasting. Because agriculture is fundamental to human societies, understanding hydroclimate responses across regions at spatial and temporal scales relevant to producers is critical to helping producers make more informed decisions as the world shifts into a more hydroclimatologically volatile state.

7.4 References

Haberlie, A., K. Gale, D. Changnon, and M. Tannura, 2014: Climatology of tropical system rainfall in the Eastern Corn Belt. *J. Applied Meteorol. And Climatol.*, 53.2, 395-405.

Rhome, J. R. and S. Raman, 2006: Environmental influences on tropical cyclone structure and intensity: A review of past and present literature. *Indian Journal of Marine Sciences*, 35(2), 61-74.

Steffen, W., P.J. Crutzen, and J.R. McNeill, 2007: The Anthropocene: Are humans now overwhelming the great forces of nature. *AMBIO: J. of the Human Environ.*, 36 (8), 614-621.

Trapp, R.J., E.D. Mitchell, G.A. Tipton, D.A. Effertz, A.I. Watson, D.L. Andra, and M.A. Magsig, 1999: Descending and non-descending tornadic vortex signatures detected by WSR-88D's. Weather and Forecasting, 14, 625-639.

Villarini, G., G. Radoslaw, J.A. Smith, and G.A. Vecchi, 2014: North Atlantic tropical cyclones and U.S. flooding. *Bulletin of the American Meteorological Society*, 95(9), 1381-1388. DOI: 10.1175/BAMS-D-13-00060.1.

APPENDICES

Appendix A Chapter Three Supplemental Material

Seasonal Teleconnection Phase Climatology

Bold values are highest average observed values of all three phases within the state climate division. *Italicized* values are the lowest average observed values of all three phases within the state climate division.

Indiana Average Observed Seasonal Precipitation (inches) per AO Phase 1980-2010					
Phase	**Cli. Div.**	**Spring (MAM)**	**Summer (JJA)**	**Fall (SON)**	**Winter (DJF)**
Positive	**1**	3.19	*4.13*	**3.82**	**2.67**
Negative	**1**	*2.93*	**4.62**	3.23	*1.87*
Neutral	**1**	**3.86**	4.16	*3.17*	2.10
Positive	**2**	3.37	**4.37**	**3.54**	**2.70**
Negative	**2**	*2.97*	4.26	*3.03*	*2.12*
Neutral	**2**	**3.73**	*4.14*	3.10	2.19
Positive	**3**	3.46	4.05	**3.40**	**2.64**
Negative	**3**	*3.03*	**4.16**	*2.96*	*2.00*
Neutral	**3**	**3.73**	*4.02*	2.98	2.22
Positive	**4**	3.88	4.46	**3.82**	**2.80**
Negative	**4**	*3.45*	**4.63**	3.26	*2.27*
Neutral	**4**	**4.29**	*4.15*	*3.12*	2.44
Positive	**5**	4.18	4.22	**3.80**	**2.89**
Negative	**5**	*3.67*	**4.25**	3.30	*2.39*
Neutral	**5**	**4.22**	*4.11*	*2.97*	2.72
Positive	**6**	3.87	*4.02*	**3.55**	**2.67**
Negative	**6**	*3.50*	**4.19**	3.07	*2.14*
Neutral	**6**	**3.92**	4.17	*2.79*	2.54
Positive	**7**	**4.78**	4.06	**4.62**	**3.78**
Negative	**7**	4.88	**4.19**	3.57	*2.95*
Neutral	**7**	*4.71*	*3.79*	*3.39*	3.13
Positive	**8**	4.79	4.21	**4.54**	**3.72**
Negative	**8**	**4.86**	**4.65**	3.56	*3.05*
Neutral	**8**	*4.66*	*3.86*	*3.10*	3.19
Positive	**9**	4.68	4.22	**4.25**	**3.58**
Negative	**9**	**4.70**	**4.53**	3.34	*2.99*
Neutral	**9**	*4.47*	*4.08*	*2.93*	3.11

Indiana Average Observed Seasonal Mean Temperature (degrees F) per AO Phase 1980-2010					
Phase	**Cli. Div.**	**Spring (MAM)**	**Summer (JJA)**	**Fall (SON)**	**Winter (DJF)**
Positive	**1**	47.0	70.8	51.5	**28.8**
Negative	**1**	*45.9*	*69.4*	*49.8*	*24.9*
Neutral	**1**	**52.7**	**71.7**	**54.8**	27.0
Positive	**2**	47.1	70.9	51.5	**29.2**
Negative	**2**	*45.9*	*69.4*	*49.9*	*25.3*
Neutral	**2**	**52.8**	**71.7**	**54.8**	27.4
Positive	**3**	46.5	70.6	51.1	**29.2**
Negative	**3**	*45.5*	*69.2*	*49.5*	*25.1*
Neutral	**3**	**52.3**	**71.5**	**54.4**	27.1
Positive	**4**	49.7	72.5	53.2	**31.3**
Negative	**4**	*48.2*	*70.9*	*51.5*	*27.2*
Neutral	**4**	**54.9**	**73.1**	**56.3**	29.5
Positive	**5**	49.4	72.2	53.1	**31.6**
Negative	**5**	*47.9*	*70.6*	*51.2*	*27.5*
Neutral	**5**	**54.5**	**72.9**	**56.1**	29.6
Positive	**6**	48.1	71.1	52.2	**30.7**
Negative	**6**	*46.7*	*69.5*	*50.4*	*26.7*
Neutral	**6**	**53.3**	**71.7**	**55.1**	28.7
Positive	**7**	53.3	75.2	56.2	**35.7**
Negative	**7**	*51.8*	*73.9*	*54.6*	*32.1*
Neutral	**7**	**58.1**	**75.9**	**59.4**	33.6
Positive	**8**	52.1	73.7	54.9	**35.1**
Negative	**8**	*50.5*	*72.3*	*53.3*	*31.4*
Neutral	**8**	**56.7**	**74.3**	**57.9**	33.1
Positive	**9**	51.7	73.8	55.0	**35.0**
Negative	**9**	*50.3*	*72.2*	*53.3*	*31.2*
Neutral	**9**	**56.4**	**74.2**	**57.9**	32.9

Illinois Average Observed Seasonal Precipitation (inches) per AO Phase 1980-2010					
Phase	**Cli. Div.**	**Spring (MAM)**	**Summer (JJA)**	**Fall (SON)**	**Winter (DJF)**
Positive	**1**	*2.98*	4.33	*2.93*	**1.82**
Negative	**1**	3.06	**5.22**	*2.93*	*1.53*
Neutral	**1**	**3.75**	*4.16*	**3.02**	1.67
Positive	**2**	3.14	4.52	**3.31**	**2.14**
Negative	**2**	*2.91*	**4.77**	*3.06*	*1.67*
Neutral	**2**	**3.65**	*3.83*	3.08	1.86
Positive	**3**	*3.25*	*4.08*	**3.18**	**2.06**
Negative	**3**	3.42	**4.47**	*3.07*	*1.61*
Neutral	**3**	**4.18**	4.12	3.12	1.94
Positive	**4**	3.26	**4.01**	**3.40**	**2.45**
Negative	**4**	*3.18*	*3.91*	*3.01*	*1.77*
Neutral	**4**	**3.98**	3.80	3.04	2.05
Positive	**5**	3.28	4.17	**3.63**	**2.51**
Negative	**5**	*3.12*	**4.42**	3.08	*1.78*
Neutral	**5**	**4.04**	*3.97*	*2.92*	2.16
Positive	**6**	3.45	3.82	**3.54**	**2.48**
Negative	**6**	*3.37*	**3.96**	3.34	*2.01*
Neutral	**6**	**4.11**	*3.66*	*3.23*	2.21
Positive	**7**	4.05	*3.74*	**4.04**	**2.81**
Negative	**7**	*3.58*	**4.22**	3.45	*2.44*
Neutral	**7**	**4.29**	3.80	*3.28*	2.79
Positive	**8**	**4.41**	*3.53*	**4.29**	**3.44**
Negative	**8**	4.39	**4.61**	3.84	*2.75*
Neutral	**8**	*4.37*	3.61	*3.41*	3.06
Positive	**9**	**4.67**	3.77	**4.46**	**3.97**
Negative	**9**	4.65	**4.29**	3.63	*2.96*
Neutral	**9**	*4.62*	*3.54*	*3.34*	3.34

Illinois Average Observed Seasonal Mean Temperature (degrees F) per AO Phase 1980-2010					
Phase	**Cli. Div.**	**Spring (MAM)**	**Summer (JJA)**	**Fall (SON)**	**Winter (DJF)**
Positive	**1**	46.4	71.0	50.2	**25.9**
Negative	**1**	*45.5*	*69.3*	*47.9*	*22.4*
Neutral	**1**	**52.5**	**72.1**	**53.8**	24.8
Positive	**2**	46.1	70.9	51.1	**27.4**
Negative	**2**	*45.2*	*69.1*	*48.8*	*23.9*
Neutral	**2**	**52.0**	**72.1**	**54.5**	26.1
Positive	**3**	49.2	73.4	52.5	**29.3**
Negative	**3**	*48.3*	*71.6*	*50.4*	*25.5*
Neutral	**3**	**55.0**	**74.0**	**56.2**	27.8
Positive	**4**	48.4	72.2	52.1	**29.1**
Negative	**4**	*47.2*	*70.7*	*50.0*	*25.2*
Neutral	**4**	**54.1**	**73.0**	**55.6**	27.7
Positive	**5**	48.4	72.2	52.1	**29.1**
Negative	**5**	*47.2*	*70.7*	*50.0*	*25.2*
Neutral	**5**	**54.1**	**73.0**	**55.6**	27.7
Positive	**6**	51.1	74.3	54.2	**32.1**
Negative	**6**	*49.8*	*72.6*	*52.0*	*28.3*
Neutral	**6**	**56.4**	**74.9**	**57.6**	30.5
Positive	**7**	51.6	74.5	54.7	**33.0**
Negative	**7**	*50.1*	*72.9*	*52.5*	*29.1*
Neutral	**7**	**56.7**	**75.1**	**58.0**	31.2
Positive	**8**	54.1	76.0	56.4	**35.9**
Negative	**8**	*52.5*	*74.9*	*54.5*	*32.7*
Neutral	**8**	**58.8**	**76.7**	**59.8**	34.6
Positive	**9**	54.0	75.8	56.3	**36.2**
Negative	**9**	*52.3*	*74.5*	*54.5*	*32.9*
Neutral	**9**	**58.7**	**76.4**	**59.8**	34.7

Ohio Average Observed Seasonal Precipitation (inches) per AO Phase 1980-2010					
Phase	**Cli. Div.**	**Spring (MAM)**	**Summer (JJA)**	**Fall (SON)**	**Winter (DJF)**
Positive	**1**	3.34	3.72	**3.19**	**2.54**
Negative	**1**	*2.84*	**3.86**	2.95	*1.86*
Neutral	**1**	**3.40**	*3.62*	*2.56*	2.26
Positive	**2**	3.33	3.92	**3.40**	**2.66**
Negative	**2**	*2.88*	**4.18**	3.13	*1.93*
Neutral	**2**	**3.39**	*3.69*	*2.70*	2.42
Positive	**3**	**3.63**	*3.87*	**3.77**	**2.99**
Negative	**3**	*3.13*	**4.50**	3.65	*2.38*
Neutral	**3**	3.54	3.86	*3.42*	2.73
Positive	**4**	**3.71**	**4.19**	**3.34**	**2.69**
Negative	**4**	*3.18*	*3.74*	3.06	*2.16*
Neutral	**4**	3.67	4.13	*2.54*	2.53
Positive	**5**	**3.81**	*3.78*	**3.48**	**2.85**
Negative	**5**	*3.36*	**4.11**	2.96	*2.18*
Neutral	**5**	3.65	4.02	*2.59*	2.70
Positive	**6**	**3.97**	*3.79*	**3.51**	**2.87**
Negative	**6**	*3.37*	**4.64**	3.13	*2.23*
Neutral	**6**	3.76	4.18	*2.81*	2.76
Positive	**7**	**3.80**	*3.77*	**3.49**	2.83
Negative	**7**	*3.31*	**4.64**	3.38	*2.42*
Neutral	**7**	3.59	3.98	*2.77*	**3.01**
Positive	**8**	**4.38**	4.03	**3.63**	**3.26**
Negative	**8**	*4.07*	**4.38**	3.23	*2.55*
Neutral	**8**	4.27	*3.71*	*2.67*	2.90
Positive	**9**	**4.33**	*3.61*	**3.84**	**3.23**
Negative	**9**	*3.75*	**4.85**	*2.95*	*2.60*
Neutral	**9**	3.96	3.82	2.36	**3.23**
Positive	**10**	**4.03**	*3.87*	**3.80**	3.01
Negative	**10**	*3.67*	**4.63**	3.25	*2.42*
Neutral	**10**	3.76	4.01	*2.56*	**3.03**

Ohio Average Observed Seasonal Mean Temperature (degrees F) per AO Phase 1980-2010					
Phase	**Cli. Div.**	**Spring (MAM)**	**Summer (JJA)**	**Fall (SON)**	**Winter (DJF)**
Positive	**1**	46.6	71.0	51.6	**29.9**
Negative	**1**	*45.7*	*69.5*	*49.4*	*25.9*
Neutral	**1**	**52.5**	**71.9**	**54.8**	27.6
Positive	**2**	46.5	70.7	52.0	**30.5**
Negative	**2**	*45.3*	*69.1*	*49.8*	*26.7*
Neutral	**2**	**52.0**	**71.5**	**55.0**	28.2
Positive	**3**	45.6	69.3	51.5	**30.6**
Negative	**3**	*44.4*	*67.4*	*49.2*	*26.7*
Neutral	**3**	**51.0**	**69.9**	**54.2**	28.2
Positive	**4**	47.9	71.1	52.2	**30.8**
Negative	**4**	*46.4*	*69.7*	*49.8*	*26.8*
Neutral	**4**	**53.2**	**71.7**	**55.1**	28.8
Positive	**5**	49.1	71.7	53.1	**32.4**
Negative	**5**	*47.4*	*70.4*	*50.8*	*28.4*
Neutral	**5**	**54.0**	**72.4**	**55.9**	30.1
Positive	**6**	46.8	69.6	51.2	**30.7**
Negative	**6**	*45.4*	*67.9*	*49.0*	*26.7*
Neutral	**6**	**51.9**	**70.3**	**53.9**	28.2
Positive	**7**	47.3	69.8	51.9	**31.8**
Negative	**7**	*45.6*	*68.1*	*49.4*	*27.6*
Neutral	**7**	**52.3**	**70.6**	**54.3**	29.6
Positive	**8**	50.6	72.8	54.2	**34.0**
Negative	**8**	*48.9*	*71.3*	*52.0*	*29.9*
Neutral	**8**	**55.3**	**73.5**	**57.2**	31.7
Positive	**9**	51.5	72.4	54.6	**35.6**
Negative	**9**	*49.7*	*71.3*	*52.3*	*31.7*
Neutral	**9**	**56.0**	**73.2**	**57.0**	33.4
Positive	**10**	49.2	70.7	53.0	**33.5**
Negative	**10**	*47.4*	*69.4*	*50.6*	*29.5*
Neutral	**10**	**53.9**	**71.5**	**55.6**	31.1

Michigan Average Observed Seasonal Precipitation (inches) per AO Phase 1980-2010					
Phase	**Cli. Div.**	**Spring (MAM)**	**Summer (JJA)**	**Fall (SON)**	**Winter (DJF)**
Positive	**1**	2.48	*2.92*	*2.62*	*1.70*
Negative	**1**	*2.19*	3.07	3.10	1.92
Neutral	**1**	**2.53**	**3.36**	**3.57**	**1.96**
Positive	**2**	2.27	2.99	*2.91*	1.92
Negative	**2**	*1.95*	*2.86*	3.50	*1.87*
Neutral	**2**	**2.29**	**3.09**	**3.55**	**1.99**
Positive	**3**	2.37	**3.19**	*3.06*	**2.04**
Negative	**3**	*2.05*	*2.88*	3.35	*1.89*
Neutral	**3**	**2.74**	3.09	**3.51**	1.94
Positive	**4**	2.40	**3.34**	*2.81*	**1.87**
Negative	**4**	*2.02*	*2.95*	2.83	*1.61*
Neutral	**4**	**2.68**	3.17	**2.95**	1.70
Positive	**5**	3.04	3.21	3.42	**2.15**
Negative	**5**	*2.18*	**3.24**	*3.34*	*1.83*
Neutral	**5**	**3.16**	*3.14*	**3.81**	2.01
Positive	**6**	2.98	**3.41**	3.18	**2.00**
Negative	**6**	*2.31*	*3.16*	*2.99*	*1.65*
Neutral	**6**	**3.14**	3.23	**3.42**	1.86
Positive	**7**	**2.86**	**3.39**	*3.05*	**1.99**
Negative	**7**	*2.35*	3.21	3.16	*1.71*
Neutral	**7**	2.81	*3.14*	**3.28**	1.79
Positive	**8**	3.16	3.61	3.65	**2.54**
Negative	**8**	*2.60*	**3.95**	*3.26*	*2.18*
Neutral	**8**	**3.34**	*3.59*	**3.68**	2.35
Positive	**9**	3.07	*3.76*	**3.39**	**2.06**
Negative	**9**	*2.49*	3.79	*2.95*	*1.70*
Neutral	**9**	**3.15**	**3.41**	3.18	1.86
El Nino	**10**	2.94	3.63	**3.05**	**2.30**
Neutral	**10**	*2.60*	**3.70**	2.98	*1.85*
La Nina	**10**	**2.96**	*3.26*	*2.93*	2.08

Michigan Average Observed Seasonal Mean Temperature (degrees F) per AO Phase 1980-2010					
Phase	**Cli. Div.**	**Spring (MAM)**	**Summer (JJA)**	**Fall (SON)**	**Winter (DJF)**
Positive	**1**	*35.6*	62.9	42.7	**17.4**
Negative	**1**	35.8	*60.8*	*40.1*	*15.9*
Neutral	**1**	**42.5**	**63.5**	**46.4**	16.5
Positive	**2**	35.2	62.7	44.2	**20.3**
Negative	**2**	*36.0*	*61.0*	*41.8*	*18.3*
Neutral	**2**	**42.3**	**63.4**	**47.7**	18.7
Positive	**3**	*38.8*	65.0	46.7	**24.1**
Negative	**3**	*38.8*	*63.5*	*44.3*	*21.9*
Neutral	**3**	**45.5**	**66.1**	**50.0**	22.6
Positive	**4**	*38.4*	65.1	45.8	**22.8**
Negative	**4**	38.6	*63.2*	*43.5*	*20.6*
Neutral	**4**	**45.3**	**65.9**	**49.2**	21.4
Positive	**5**	41.6	66.4	47.9	**26.6**
Negative	**5**	*41.3*	*64.9*	*45.7*	*24.4*
Neutral	**5**	**47.9**	**67.6**	**51.3**	25.1
Positive	**6**	42.0	67.7	47.7	**25.4**
Negative	**6**	*41.7*	*66.1*	*45.4*	*22.9*
Neutral	**6**	**48.6**	**68.7**	**51.2**	23.7
Positive	**7**	*41.5*	67.3	48.3	26.1
Negative	**7**	*41.5*	*65.7*	*46.2*	**23.5**
Neutral	**7**	**48.0**	**68.2**	**51.8**	*24.5*
Positive	**8**	44.4	69.0	50.4	28.4
Negative	**8**	*43.8*	*67.7*	*48.2*	**25.6**
Neutral	**8**	**50.4**	**70.2**	**53.6**	*26.7*
Positive	**9**	43.8	68.4	49.1	**27.2**
Negative	**9**	*43.1*	*67.0*	*46.9*	*24.1*
Neutral	**9**	**50.0**	**69.5**	**52.4**	25.4
Positive	**10**	44.4	69.6	50.2	**28.1**
Negative	**10**	*43.8*	*67.9*	*48.0*	*24.9*
Neutral	**10**	**50.4**	**70.5**	**53.6**	26.2

Wisconsin Average Observed Seasonal Precipitation (inches) per AO Phase 1980-2010					
Phase	**Cli. Div.**	**Spring (MAM)**	**Summer (JJA)**	**Fall (SON)**	**Winter (DJF)**
Positive	**1**	2.50	4.19	*2.37*	*0.93*
Negative	**1**	*2.03*	*3.56*	2.43	**1.07**
Neutral	**1**	**2.77**	**4.21**	**3.72**	1.02
Positive	**2**	2.69	3.99	*2.52*	*1.15*
Negative	**2**	*2.05*	*3.60*	2.81	**1.20**
Neutral	**2**	**2.70**	**4.07**	**3.66**	1.19
Positive	**3**	2.63	3.66	*2.42*	*1.19*
Negative	**3**	*2.09*	*3.31*	2.80	**1.25**
Neutral	**3**	**2.77**	**3.78**	**3.32**	1.21
Positive	**4**	2.87	**4.69**	*2.50*	*0.97*
Negative	**4**	*2.33*	*3.91*	2.62	**1.10**
Neutral	**4**	**3.24**	4.58	**3.19**	1.04
Positive	**5**	2.93	**4.36**	*2.43*	**1.22**
Negative	**5**	*2.19*	*3.68*	2.79	1.18
Neutral	**5**	**3.10**	4.35	**2.98**	*1.15*
Positive	**6**	2.63	**3.70**	*2.53*	**1.42**
Negative	**6**	*1.95*	*3.45*	2.75	1.40
Neutral	**6**	**2.96**	3.63	**2.89**	*1.32*
Positive	**7**	2.90	4.65	*2.59*	1.20
Negative	**7**	*2.48*	*4.45*	2.67	**1.29**
Neutral	**7**	**3.72**	**4.73**	**2.93**	*1.15*
Positive	**8**	2.93	**4.68**	*2.75*	**1.52**
Negative	**8**	*2.36*	*4.18*	*2.75*	*1.43*
Neutral	**8**	**3.58**	4.32	**3.09**	1.49
Positive	**9**	2.94	**4.57**	2.87	1.69
Negative	**9**	*2.31*	4.15	*2.72*	*1.59*
Neutral	**9**	**3.45**	*3.76*	**3.01**	**1.70**

Wisconsin Average Observed Seasonal Mean Temperature (degrees F) per AO Phase 1980-2010					
Phase	**Cli. Div.**	**Spring (MAM)**	**Summer (JJA)**	**Fall (SON)**	**Winter (DJF)**
Positive	**1**	38.5	65.8	43.4	**16.2**
Negative	**1**	*38.4*	*63.7*	*40.9*	*13.9*
Neutral	**1**	**45.7**	**66.4**	**47.2**	15.5
Positive	**2**	*37.2*	64.3	42.6	**16.3**
Negative	**2**	*37.2*	*62.2*	*40.0*	*14.4*
Neutral	**2**	**44.6**	**65.1**	**46.3**	15.6
Positive	**3**	*38.1*	64.8	43.6	**18.2**
Negative	**3**	38.3	*63.0*	*41.2*	*16.4*
Neutral	**3**	**45.2**	**65.5**	**47.2**	17.3
Positive	**4**	42.0	68.6	45.9	**19.6**
Negative	**4**	*41.5*	*66.5*	*43.5*	*16.7*
Neutral	**4**	**49.0**	**69.3**	**49.7**	18.7
Positive	**5**	41.6	67.9	46.0	**20.8**
Negative	**5**	*41.4*	*65.9*	*43.7*	*18.2*
Neutral	**5**	**48.5**	**68.7**	**49.8**	19.8
Positive	**6**	*40.5*	67.2	47.3	**22.8**
Negative	**6**	40.6	*65.3*	*44.9*	*20.3*
Neutral	**6**	**46.8**	**68.0**	**50.8**	21.6
Positive	**7**	43.3	68.9	47.3	**22.2**
Negative	**7**	*42.9*	*67.1*	*44.9*	*19.1*
Neutral	**7**	**49.9**	**69.9**	**51.0**	21.2
Positive	**8**	43.3	68.9	47.7	**23.1**
Negative	**8**	*42.9*	*67.2*	*45.4*	*20.0*
Neutral	**8**	**49.8**	**69.9**	**51.3**	22.1
Positive	**9**	43.0	68.6	49.0	**25.0**
Negative	**9**	*42.5*	*66.7*	*46.5*	*22.0*
Neutral	**9**	**48.8**	**69.6**	**52.3**	23.8

Missouri Average Observed Seasonal Precipitation (inches) per AO Phase 1980-2010					
Phase	**Cli. Div.**	**Spring (MAM)**	**Summer (JJA)**	**Fall (SON)**	**Winter (DJF)**
Positive	**1**	*3.23*	*4.07*	*2.96*	**1.69**
Negative	**1**	3.59	**4.88**	**3.44**	*1.32*
Neutral	**1**	**4.33**	4.79	3.31	1.50
Positive	**2**	*3.64*	*4.04*	*3.40*	**2.37**
Negative	**2**	3.69	**4.55**	**3.67**	*2.01*
Neutral	**2**	**4.29**	4.11	3.46	2.27
Positive	**3**	*3.86*	*3.91*	3.90	**2.24**
Negative	**3**	4.17	**4.89**	**3.96**	*1.91*
Neutral	**3**	**4.59**	4.45	*3.57*	2.03
Positive	**4**	4.50	*3.52*	4.30	**2.97**
Negative	**4**	*4.22*	**4.43**	**4.34**	2.42
Neutral	**4**	**4.47**	3.93	*3.90*	*2.36*
Positive	**5**	4.55	*3.40*	**4.37**	**3.56**
Negative	**5**	*4.24*	**4.13**	4.24	*2.71*
Neutral	**5**	**4.58**	3.80	*3.66*	2.78
Positive	**6**	**4.87**	3.46	**4.68**	**4.66**
Negative	**6**	*4.02*	**3.57**	3.99	*3.30*
Neutral	**6**	4.79	*3.38*	*3.48*	3.57

Missouri Average Observed Seasonal Mean Temperature (degrees F) per AO Phase 1980-2010					
Phase	**Cli. Div.**	**Spring (MAM)**	**Summer (JJA)**	**Fall (SON)**	**Winter (DJF)**
Positive	**1**	50.9	74.7	53.0	**30.8**
Negative	**1**	*49.6*	*72.9*	*51.3*	*27.7*
Neutral	**1**	**55.8**	**75.2**	**56.9**	30.0
Positive	**2**	51.9	75.0	54.5	**33.0**
Negative	**2**	*50.5*	*73.5*	*52.4*	*29.3*
Neutral	**2**	**56.8**	**75.7**	**58.1**	31.3
Positive	**3**	53.3	76.0	55.6	**34.7**
Negative	**3**	*51.8*	*74.6*	*53.8*	*31.6*
Neutral	**3**	**57.7**	**76.6**	**59.2**	33.5
Positive	**4**	54.2	75.3	55.9	**36.5**
Negative	**4**	*52.7*	*74.4*	*54.5*	*34.0*
Neutral	**4**	**58.1**	**76.1**	**59.5**	35.6
Positive	**5**	53.8	75.1	55.5	**36.0**
Negative	**5**	*52.3*	*74.0*	*53.7*	*33.1*
Neutral	**5**	**58.0**	**75.8**	**59.0**	34.7
Positive	**6**	56.8	77.9	58.3	**38.8**
Negative	**6**	*55.4*	*77.5*	*56.7*	*36.3*
Neutral	**6**	**61.1**	**78.7**	**61.9**	37.8

Iowa Average Observed Seasonal Precipitation (inches) per AO Phase 1980-2010					
Phase	**Cli. Div.**	**Spring (MAM)**	**Summer (JJA)**	**Fall (SON)**	**Winter (DJF)**
Positive	**1**	*2.60*	3.72	**2.51**	**0.73**
Negative	**1**	2.83	*3.51*	*1.91*	0.77
Neutral	**1**	**3.15**	**4.37**	2.39	*0.70*
Positive	**2**	2.93	*4.01*	**2.56**	0.99
Negative	**2**	*2.83*	4.23	*2.13*	**1.05**
Neutral	**2**	**3.81**	**4.98**	2.53	*0.86*
Positive	**3**	2.90	*4.46*	**2.77**	1.18
Negative	**3**	*2.72*	4.85	*2.57*	**1.31**
Neutral	**3**	**3.90**	**4.90**	2.76	*1.07*
Positive	**4**	*2.85*	*3.91*	**2.59**	*0.92*
Negative	**4**	2.87	4.41	*2.18*	**0.93**
Neutral	**4**	**3.78**	**4.44**	2.29	0.77
Positive	**5**	3.24	*4.15*	**2.80**	**1.13**
Negative	**5**	*2.98*	**5.07**	*2.52*	**1.13**
Neutral	**5**	**3.87**	4.88	2.56	*0.92*
Positive	**6**	*2.76*	*4.18*	*2.68*	**1.48**
Negative	**6**	3.05	**5.41**	2.91	1.39
Neutral	**6**	**3.75**	4.50	**2.93**	*1.34*
Positive	**7**	*2.92*	*3.61*	**2.72**	1.06
Negative	**7**	3.24	**5.08**	2.67	**1.07**
Neutral	**7**	**4.20**	4.70	*2.48*	*0.96*
Positive	**8**	*3.08*	*4.04*	2.86	**1.35**
Negative	**8**	3.25	4.80	**3.15**	1.16
Neutral	**8**	**4.17**	**5.00**	*2.85*	*1.07*
Positive	**9**	*3.05*	*4.23*	*2.87*	**1.63**
Negative	**9**	3.36	**5.21**	**3.30**	*1.43*
Neutral	**9**	**4.14**	4.56	3.13	1.56

Iowa Average Observed Seasonal Mean Temperature (degrees F) per AO Phase 1980-2010					
Phase	**Cli. Div.**	**Spring (MAM)**	**Summer (JJA)**	**Fall (SON)**	**Winter (DJF)**
Positive	**1**	43.7	70.4	46.6	**20.7**
Negative	**1**	*42.8*	*68.3*	*44.5*	*17.8*
Neutral	**1**	**50.3**	**70.8**	**50.8**	19.7
Positive	**2**	43.3	70.0	46.7	**20.4**
Negative	**2**	*42.9*	*67.9*	*44.5*	*17.3*
Neutral	**2**	**50.3**	**70.5**	**50.9**	19.3
Positive	**3**	43.8	70.0	47.6	**21.8**
Negative	**3**	*43.6*	*68.0*	*45.3*	*18.5*
Neutral	**3**	**50.7**	**70.7**	**51.6**	21.0
Positive	**4**	46.4	72.1	48.7	**24.0**
Negative	**4**	*45.4*	*69.8*	*46.7*	*21.0*
Neutral	**4**	**52.2**	**72.3**	**53.0**	23.0
Positive	**5**	45.8	71.6	48.7	**23.7**
Negative	**5**	*45.1*	*69.3*	*46.6*	*20.6*
Neutral	**5**	**52.0**	**72.0**	**52.8**	22.7
Positive	**6**	46.4	71.7	49.7	**24.9**
Negative	**6**	*45.8*	*69.8*	*47.6*	*21.6*
Neutral	**6**	**52.8**	**72.4**	**53.7**	24.0
Positive	**7**	48.5	73.2	50.6	**26.7**
Negative	**7**	*47.2*	*71.0*	*48.5*	*23.6*
Neutral	**7**	**53.6**	**73.7**	**54.8**	25.8
Positive	**8**	47.8	72.6	50.5	**26.8**
Negative	**8**	*46.7*	*70.4*	*48.5*	*23.5*
Neutral	**8**	**53.3**	**73.0**	**54.4**	25.8
Positive	**9**	48.8	73.5	51.8	**28.0**
Negative	**9**	*47.9*	*71.5*	*49.7*	*24.4*
Neutral	**9**	**54.6**	**74.1**	**55.8**	26.5

Minnesota Average Observed Seasonal Precipitation (inches) per AO Phase 1980-2010					
Phase	**Cli. Div.**	**Spring (MAM)**	**Summer (JJA)**	**Fall (SON)**	**Winter (DJF)**
Positive	**1**	1.57	**3.74**	*1.61*	*0.59*
Negative	**1**	*1.26*	*3.42*	1.96	**0.70**
Neutral	**1**	**2.10**	3.63	**2.32**	0.63
Positive	**2**	1.74	**4.03**	*2.00*	*0.66*
Negative	**2**	*1.49*	*3.19*	2.04	**0.74**
Neutral	**2**	**2.33**	3.89	**2.69**	0.68
Positive	**3**	1.93	**3.90**	*2.21*	*0.87*
Negative	**3**	*1.58*	*3.31*	2.33	**0.90**
Neutral	**3**	**2.35**	3.87	**3.37**	**0.90**
Positive	**4**	2.10	*3.28*	2.05	*0.51*
Negative	**4**	*1.68*	3.33	*1.91*	**0.84**
Neutral	**4**	**2.43**	**3.77**	**2.30**	0.70
Positive	**5**	2.48	3.97	2.26	*0.65*
Negative	**5**	*1.93*	*3.64*	*1.99*	**0.94**
Neutral	**5**	**2.77**	**4.24**	**2.79**	0.74
Positive	**6**	2.43	4.10	2.26	0.80
Negative	**6**	*1.91*	*3.62*	*2.13*	**0.99**
Neutral	**6**	**2.87**	**4.30**	**3.27**	*0.83*
Positive	**7**	2.52	3.64	2.25	*0.55*
Negative	**7**	*2.49*	*3.42*	*2.06*	**0.81**
Neutral	**7**	**2.85**	**3.90**	**2.33**	0.63
Positive	**8**	2.74	4.32	2.44	*0.76*
Negative	**8**	*2.68*	*3.76*	*2.24*	**1.04**
Neutral	**8**	**3.24**	**4.56**	**2.66**	0.84
Positive	**9**	2.84	4.65	2.57	*0.90*
Negative	**9**	*2.52*	*4.10*	*2.44*	**1.11**
Neutral	**9**	**3.40**	**4.68**	**2.97**	1.00

Minnesota Average Observed Seasonal Mean Temperature (degrees F) per AO Phase 1980-2010					
Phase	**Cli. Div.**	**Spring (MAM)**	**Summer (JJA)**	**Fall (SON)**	**Winter (DJF)**
Positive	**1**	*36.6*	**66.5**	40.7	**11.0**
Negative	**1**	37.1	*63.9*	*38.6*	*8.4*
Neutral	**1**	**45.2**	**66.5**	**45.2**	10.3
Positive	**2**	*36.2*	65.1	40.8	**11.3**
Negative	**2**	36.7	*62.7*	*38.1*	*9.4*
Neutral	**2**	**44.2**	**65.4**	**44.8**	10.9
Positive	**3**	*34.4*	62.3	40.2	**12.3**
Negative	**3**	34.9	*60.3*	*37.6*	*10.7*
Neutral	**3**	**41.7**	**62.6**	**44.0**	12.0
Positive	**4**	*39.9*	69.1	43.8	**16.3**
Negative	**4**	40.3	*66.6*	*41.9*	*12.8*
Neutral	**4**	**48.1**	**69.2**	**48.2**	14.9
Positive	**5**	*40.5*	68.8	44.3	**16.7**
Negative	**5**	40.8	*66.7*	*42.3*	*13.9*
Neutral	**5**	**48.5**	**69.3**	**48.6**	15.8
Positive	**6**	*39.6*	67.3	43.8	**16.1**
Negative	**6**	39.7	*65.6*	*41.5*	*13.7*
Neutral	**6**	**47.2**	**68.0**	**47.8**	15.4
Positive	**7**	42.1	69.7	45.4	**19.5**
Negative	**7**	*41.7*	*67.5*	*43.2*	*15.9*
Neutral	**7**	**49.3**	**70.1**	**49.6**	18.2
Positive	**8**	42.4	69.8	46.0	**19.6**
Negative	**8**	*42.0*	*67.7*	*43.7*	*16.2*
Neutral	**8**	**49.8**	**70.3**	**50.2**	18.2
Positive	**9**	42.2	69.2	46.2	**19.7**
Negative	**9**	*41.8*	*66.9*	*43.8*	*16.6*
Neutral	**9**	**49.4**	**69.7**	**50.1**	18.8

North Dakota Average Observed Seasonal Precipitation (inches) per AO Phase 1980-2010					
Phase	**Cli. Div.**	**Spring (MAM)**	**Summer (JJA)**	**Fall (SON)**	**Winter (DJF)**
Positive	**1**	1.26	*2.20*	*0.85*	*0.48*
Negative	**1**	*1.17*	2.41	0.94	**0.53**
Neutral	**1**	**1.39**	**2.62**	**1.25**	**0.53**
Positive	**2**	1.30	*2.48*	*0.95*	*0.46*
Negative	**2**	*1.08*	2.92	1.19	**0.55**
Neutral	**2**	**1.68**	**3.06**	**1.56**	0.51
Positive	**3**	1.37	*2.88*	*1.18*	*0.48*
Negative	**3**	*1.17*	3.24	1.41	**0.58**
Neutral	**3**	**1.71**	**3.29**	**1.74**	0.52
Positive	**4**	1.43	*2.36*	*0.81*	*0.38*
Negative	**4**	*1.22*	**2.68**	1.08	0.48
Neutral	**4**	**1.58**	2.61	**1.36**	**0.49**
Positive	**5**	1.32	*2.78*	*1.12*	*0.41*
Negative	**5**	*1.17*	**3.18**	1.27	**0.53**
Neutral	**5**	**1.74**	3.00	**1.60**	0.52
Positive	**6**	1.59	3.13	*1.32*	*0.54*
Negative	**6**	*1.32*	*3.08*	1.78	**0.67**
Neutral	**6**	**1.96**	**3.28**	**1.97**	0.57
Positive	**7**	1.35	*2.05*	*0.79*	*0.28*
Negative	**7**	*1.26*	**2.61**	1.01	**0.42**
Neutral	**7**	**1.62**	2.25	**1.27**	**0.42**
Positive	**8**	1.40	*2.38*	*0.80*	0.38
Negative	**8**	*1.22*	**3.02**	1.15	**0.49**
Neutral	**8**	**1.81**	2.69	**1.36**	*0.37*
Positive	**9**	1.73	*2.68*	*1.47*	*0.43*
Negative	**9**	*1.47*	**3.24**	1.54	**0.64**
Neutral	**9**	**2.19**	3.11	**1.88**	0.53

North Dakota Average Observed Seasonal Mean Temperature (degrees F) per AO Phase 1980-2010					
Phase	**Cli. Div.**	**Spring (MAM)**	**Summer (JJA)**	**Fall (SON)**	**Winter (DJF)**
Positive	**1**	*37.6*	**66.3**	39.7	**14.2**
Negative	**1**	38.0	*63.7*	*38.4*	*11.0*
Neutral	**1**	**44.4**	66.0	**44.4**	13.1
Positive	**2**	*36.2*	**65.9**	39.1	**11.4**
Negative	**2**	36.5	*63.3*	*37.9*	*8.5*
Neutral	**2**	**43.8**	65.6	**43.7**	10.4
Positive	**3**	*35.9*	**66.4**	39.8	**10.5**
Negative	**3**	36.2	*63.5*	*37.9*	*7.7*
Neutral	**3**	**44.2**	66.0	**44.3**	9.7
Positive	**4**	*38.9*	**67.4**	41.3	**16.9**
Negative	**4**	39.2	*64.4*	*39.9*	*13.4*
Neutral	**4**	**45.2**	67.1	**45.8**	15.5
Positive	**5**	*37.9*	**67.4**	40.9	**14.2**
Negative	**5**	38.4	*64.5*	*39.5*	*10.9*
Neutral	**5**	**45.2**	67.1	**45.5**	12.7
Positive	**6**	*37.9*	**67.7**	41.4	**13.0**
Negative	**6**	38.3	*64.9*	*39.5*	*9.7*
Neutral	**6**	**45.9**	67.4	**46.0**	11.8
Positive	**7**	*39.7*	**67.7**	41.8	**19.9**
Negative	**7**	40.1	*64.5*	*40.8*	*16.4*
Neutral	**7**	**45.3**	67.3	**46.1**	19.1
Positive	**8**	*39.6*	**68.2**	41.8	**17.5**
Negative	**8**	39.8	*64.9*	*40.7*	*14.0*
Neutral	**8**	**45.8**	68.0	**46.3**	16.2
Positive	**9**	*39.2*	**68.4**	42.3	**15.6**
Negative	**9**	39.6	*65.5*	*40.7*	*12.2*
Neutral	**9**	**46.6**	68.3	**46.7**	14.3

South Dakota Average Observed Seasonal Precipitation (inches) per AO Phase 1980-2010					
Phase	**Cli. Div.**	**Spring (MAM)**	**Summer (JJA)**	**Fall (SON)**	**Winter (DJF)**
Positive	**1**	*1.44*	*1.99*	*0.96*	*0.29*
Negative	**1**	1.84	**2.63**	1.02	**0.51**
Neutral	**1**	**2.19**	2.29	**1.23**	0.43
Positive	**2**	1.52	*2.36*	*1.10*	*0.34*
Negative	**2**	*1.51*	**2.91**	1.24	**0.54**
Neutral	**2**	**2.08**	2.80	**1.42**	0.39
Positive	**3**	1.83	*2.90*	1.74	*0.42*
Negative	**3**	*1.65*	3.06	*1.61*	**0.67**
Neutral	**3**	**2.43**	**3.45**	**1.92**	0.54
Positive	**4**	*2.01*	*2.54*	1.41	*0.58*
Negative	**4**	2.71	**3.04**	*1.31*	**0.75**
Neutral	**4**	**2.85**	2.65	**1.60**	0.70
Positive	**5**	*1.56*	*2.08*	1.14	*0.35*
Negative	**5**	2.11	**2.57**	*1.12*	**0.50**
Neutral	**5**	**2.40**	2.28	**1.28**	0.44
Positive	**6**	*1.62*	*2.29*	*1.22*	*0.35*
Negative	**6**	1.98	**3.11**	1.33	**0.59**
Neutral	**6**	**2.33**	2.74	**1.47**	0.41
Positive	**7**	2.14	3.19	1.89	*0.43*
Negative	**7**	*2.06*	*3.18*	*1.78*	**0.69**
Neutral	**7**	**2.48**	**3.48**	**1.99**	0.50
Positive	**8**	*2.01*	*2.70*	*1.39*	*0.40*
Negative	**8**	2.37	**3.16**	1.49	**0.64**
Neutral	**8**	**2.80**	2.88	**1.65**	0.50
Positive	**9**	*2.22*	*2.85*	1.98	0.56
Negative	**9**	2.65	3.08	*1.88*	**0.64**
Neutral	**9**	**2.91**	**3.49**	**2.03**	*0.50*

South Dakota Average Observed Seasonal Mean Temperature (degrees F) per AO Phase 1980-2010					
Phase	**Cli. Div.**	**Spring (MAM)**	**Summer (JJA)**	**Fall (SON)**	**Winter (DJF)**
Positive	**1**	41.5	**69.8**	43.8	**22.7**
Negative	**1**	*41.4*	*66.1*	*43.0*	*19.3*
Neutral	**1**	**46.7**	69.4	**48.4**	21.9
Positive	**2**	40.7	**69.5**	43.4	**18.7**
Negative	**2**	*40.5*	*66.4*	*42.0*	*15.0*
Neutral	**2**	**47.1**	**69.5**	**47.9**	17.5
Positive	**3**	*39.9*	69.0	43.4	**16.8**
Negative	**3**	40.1	*66.2*	*41.7*	*13.2*
Neutral	**3**	**47.2**	**69.1**	**47.9**	15.4
Positive	**4**	40.0	**65.2**	43.1	25.6
Negative	**4**	*39.5*	*62.3*	*42.0*	*24.4*
Neutral	**4**	**44.0**	**65.2**	**46.8**	**26.0**
Positive	**5**	44.1	**71.2**	46.1	**26.3**
Negative	**5**	*43.3*	*67.7*	*45.2*	*24.0*
Neutral	**5**	**48.6**	70.9	**50.6**	25.9
Positive	**6**	43.4	**71.8**	45.9	**22.8**
Negative	**6**	*42.5*	*68.6*	*44.7*	*18.8*
Neutral	**6**	**49.1**	71.7	**50.6**	21.7
Positive	**7**	41.6	69.7	44.7	**19.4**
Negative	**7**	*41.2*	*67.0*	*42.9*	*15.8*
Neutral	**7**	**48.5**	**69.9**	**49.0**	17.9
Positive	**8**	44.7	71.6	47.1	**26.2**
Negative	**8**	*43.3*	*68.7*	*45.6*	*22.5*
Neutral	**8**	**49.4**	**71.7**	**51.5**	24.9
Positive	**9**	44.8	72.0	47.4	**23.2**
Negative	**9**	*43.8*	*69.4*	*45.5*	*19.7*
Neutral	**9**	**51.0**	**72.3**	**51.8**	21.9

Nebraska Average Observed Seasonal Precipitation (inches) per AO Phase 1980-2010					
Phase	**Cli. Div.**	**Spring (MAM)**	**Summer (JJA)**	**Fall (SON)**	**Winter (DJF)**
Positive	**1**	*1.55*	*1.96*	1.05	**0.41**
Negative	**1**	1.96	**2.67**	*0.98*	0.40
Neutral	**1**	**2.08**	2.38	**1.17**	*0.39*
Positive	**2**	*2.11*	*3.00*	*1.55*	0.50
Negative	**2**	2.61	3.04	**1.68**	**0.57**
Neutral	**2**	**2.67**	**3.18**	1.61	*0.46*
Positive	**3**	*2.41*	**3.79**	**2.22**	**0.77**
Negative	**3**	2.94	*3.13*	*1.92*	0.67
Neutral	**3**	**3.25**	3.69	2.19	*0.60*
Positive	**5**	*2.35*	*3.01*	**1.83**	**0.64**
Negative	**5**	2.83	**3.58**	*1.57*	0.52
Neutral	**5**	**2.93**	3.49	1.73	*0.48*
Positive	**6**	*2.41*	*3.33*	**2.42**	**0.87**
Negative	**6**	3.04	**4.29**	*1.97*	0.75
Neutral	**6**	**3.61**	4.01	2.12	*0.72*
Positive	**7**	*1.79*	*2.78*	1.28	**0.54**
Negative	**7**	2.28	**3.42**	**1.34**	*0.42*
Neutral	**7**	**2.34**	2.94	*1.22*	0.45
Positive	**8**	*2.08*	*3.32*	**1.73**	**0.67**
Negative	**8**	2.80	3.33	1.72	*0.48*
Neutral	**8**	**3.11**	**3.52**	*1.58*	0.50
Positive	**9**	*2.39*	*3.35*	*2.19*	**0.89**
Negative	**9**	3.16	**4.42**	**2.31**	*0.82*
Neutral	**9**	**3.87**	4.10	2.28	0.85

Nebraska Average Observed Seasonal Mean Temperature (degrees F) per AO Phase 1980-2010					
Phase	**Cli. Div.**	**Spring (MAM)**	**Summer (JJA)**	**Fall (SON)**	**Winter (DJF)**
Positive	**1**	44.8	**70.5**	45.7	27.4
Negative	**1**	*43.5*	*67.2*	*45.3*	*26.8*
Neutral	**1**	**48.3**	70.0	**50.5**	**27.8**
Positive	**2**	45.5	71.3	47.0	**26.7**
Negative	**2**	*44.0*	*68.7*	*45.9*	*24.0*
Neutral	**2**	**50.0**	**71.5**	**51.5**	25.7
Positive	**3**	46.4	72.4	48.3	**25.2**
Negative	**3**	*45.1*	*69.9*	*46.7*	*22.2*
Neutral	**3**	**51.8**	**72.6**	**52.7**	24.2
Positive	**5**	46.9	**72.3**	47.9	**27.1**
Negative	**5**	*45.3*	*69.7*	*47.0*	*24.9*
Neutral	**5**	**51.4**	**72.3**	**52.7**	26.6
Positive	**6**	48.5	74.0	50.3	**27.3**
Negative	**6**	*47.3*	*71.4*	*48.7*	*24.5*
Neutral	**6**	**53.6**	**74.1**	**54.7**	26.5
Positive	**7**	47.9	**73.2**	48.9	29.1
Negative	**7**	*46.3*	*70.4*	*48.2*	*28.2*
Neutral	**7**	**51.7**	73.1	**53.6**	**29.4**
Positive	**8**	48.9	74.0	49.9	28.8
Negative	**8**	*47.4*	*71.5*	*48.9*	*27.1*
Neutral	**8**	**53.1**	**74.1**	**54.7**	**29.0**
Positive	**9**	49.6	74.6	51.4	**28.8**
Negative	**9**	*48.4*	*72.3*	*50.0*	*26.2*
Neutral	**9**	**54.4**	**74.8**	**55.8**	28.4

Kansas Average Observed Seasonal Precipitation (inches) per AO Phase 1980-2010

Phase	Cli. Div.	Spring (MAM)	Summer (JJA)	Fall (SON)	Winter (DJF)
Positive	**1**	*2.56*	*3.28*	*2.12*	**1.06**
Negative	**1**	**3.15**	**3.90**	**2.13**	*0.81*
Neutral	**1**	3.14	3.81	*2.12*	0.94
Positive	**2**	*2.28*	*3.34*	*1.88*	**0.83**
Negative	**2**	2.92	3.59	**1.93**	*0.67*
Neutral	**2**	**3.18**	**3.80**	1.92	0.81
Positive	**3**	*2.90*	*3.82*	*2.73*	**1.28**
Negative	**3**	3.56	4.68	**3.02**	*0.98*
Neutral	**3**	**3.98**	**4.85**	2.83	1.11
Positive	**4**	*1.81*	*2.64*	**1.36**	**0.74**
Negative	**4**	**2.37**	3.01	1.31	*0.45*
Neutral	**4**	2.13	**3.03**	*1.17*	0.56
Positive	**5**	*2.79*	*3.07*	*1.84*	**0.98**
Negative	**5**	**3.26**	3.90	**2.05**	*0.76*
Neutral	**5**	3.07	**4.00**	2.03	0.97
Positive	**6**	*3.22*	*3.87*	3.06	**1.51**
Negative	**6**	3.98	4.72	**3.25**	*1.17*
Neutral	**6**	**4.05**	**4.75**	*3.04*	1.28
Positive	**7**	*1.63*	*2.71*	**1.37**	**0.68**
Negative	**7**	**2.09**	**3.05**	*1.12*	*0.47*
Neutral	**7**	1.98	2.85	1.27	0.62
Positive	**8**	*2.76*	*3.61*	*1.87*	**1.07**
Negative	**8**	**3.39**	**4.18**	2.06	*0.82*
Neutral	**8**	3.09	3.71	**2.17**	1.02
Positive	**9**	*3.89*	*3.76*	**3.69**	**1.84**
Negative	**9**	4.28	**5.15**	*3.29*	1.54
Neutral	**9**	**4.51**	4.54	3.48	*1.49*

Kansas Average Observed Seasonal Mean Temperature (degrees F) per AO Phase 1980-2010					
Phase	**Cli. Div.**	**Spring (MAM)**	**Summer (JJA)**	**Fall (SON)**	**Winter (DJF)**
Positive	**1**	49.3	74.2	50.2	30.5
Negative	**1**	*47.4*	*71.9*	*49.6*	*30.1*
Neutral	**1**	**52.6**	**74.3**	**55.1**	**31.0**
Positive	**2**	51.1	76.3	52.7	**31.0**
Negative	**2**	*49.6*	*74.2*	*51.5*	*28.9*
Neutral	**2**	**55.1**	**76.6**	**57.3**	30.7
Positive	**3**	51.9	76.0	53.7	**31.4**
Negative	**3**	*50.6*	*74.1*	*52.0*	*28.6*
Neutral	**3**	**56.3**	**76.3**	**57.9**	31.0
Positive	**4**	50.8	75.2	51.7	31.8
Negative	**4**	*48.9*	*73.2*	*51.1*	*31.6*
Neutral	**4**	**53.9**	**75.5**	**56.5**	**32.5**
Positive	**5**	52.7	77.5	54.3	**32.9**
Negative	**5**	*51.2*	*75.5*	*53.3*	*31.0*
Neutral	**5**	**56.5**	**77.8**	**59.0**	**32.9**
Positive	**6**	53.1	76.4	54.8	**33.4**
Negative	**6**	*51.8*	*74.9*	*53.4*	*30.6*
Neutral	**6**	**57.1**	**76.9**	**59.0**	32.7
Positive	**7**	52.9	76.6	53.6	33.9
Negative	**7**	*51.1*	*74.9*	*53.3*	*33.7*
Neutral	**7**	**56.1**	**76.9**	**58.6**	**34.8**
Positive	**8**	54.1	78.2	55.5	**34.8**
Negative	**8**	*52.5*	*76.6*	*54.7*	*33.3*
Neutral	**8**	**57.7**	**78.7**	**60.3**	**34.8**
Positive	**9**	54.6	77.4	56.4	**35.8**
Negative	**9**	*53.4*	*76.1*	*55.2*	*33.3*
Neutral	**9**	**58.5**	**77.9**	**60.5**	35.3

El Niño-Southern Oscillation

Indiana Average Observed Seasonal Precipitation (inches) per ENSO Phase 1980-2010					
Phase	**Cli. Div.**	**Spring (MAM)**	**Summer (JJA)**	**Fall (SON)**	**Winter (DJF)**
El Niño	**1**	3.49	4.15	3.22	2.14
Neutral	**1**	**3.56**	**4.44**	**3.99**	*2.06*
La Niña	**1**	*3.00*	*3.64*	*2.71*	**2.45**
El Niño	**2**	3.40	4.23	3.05	*2.22*
Neutral	**2**	**3.57**	**4.36**	**3.65**	2.31
La Niña	**2**	*3.09*	*3.61*	*2.81*	**2.51**
El Niño	**3**	3.37	3.93	3.00	*2.15*
Neutral	**3**	**3.59**	**4.25**	**3.46**	2.29
La Niña	**3**	*3.29*	*3.63*	*2.69*	**2.41**
El Niño	**4**	3.86	4.22	3.23	*2.38*
Neutral	**4**	**4.18**	**4.56**	**3.83**	2.48
La Niña	**4**	*3.50*	*3.46*	*2.84*	**2.64**
El Niño	**5**	*3.86*	3.96	3.10	*2.53*
Neutral	**5**	**4.29**	**4.49**	**3.82**	2.65
La Niña	**5**	3.77	*3.43*	*2.80*	**2.77**
El Niño	**6**	3.65	4.02	2.85	*2.27*
Neutral	**6**	**4.00**	**4.43**	**3.49**	2.45
La Niña	**6**	*3.47*	*3.41*	*2.77*	**2.57**
El Niño	**7**	*4.57*	*3.53*	3.99	*3.12*
Neutral	**7**	**4.96**	**4.15**	**4.06**	3.13
La Niña	**7**	*4.57*	3.89	*3.12*	**3.61**
El Niño	**8**	*4.53*	3.93	3.78	*3.11*
Neutral	**8**	**4.88**	**4.20**	**3.92**	3.24
La Niña	**8**	4.72	*3.78*	*3.03*	**3.63**
El Niño	**9**	*4.25*	4.31	3.49	*3.03*
Neutral	**9**	**4.80**	**4.35**	**3.53**	3.10
La Niña	**9**	4.47	*3.29*	*3.10*	**3.56**

Indiana Average Observed Seasonal Mean Temperature (degrees F) per ENSO Phase 1980-2010					
Phase	**Cli. Div.**	**Spring (MAM)**	**Summer (JJA)**	**Fall (SON)**	**Winter (DJF)**
El Niño	**1**	**50.5**	*70.3*	*52.2*	**28.7**
Neutral	**1**	*48.8*	71.5	52.3	*25.7*
La Niña	**1**	*48.8*	**72.2**	**52.9**	26.1
El Niño	**2**	**50.6**	*70.3*	*52.3*	**29.0**
Neutral	**2**	*48.8*	71.5	*52.3*	*26.1*
La Niña	**2**	48.9	**72.0**	**52.8**	26.6
El Niño	**3**	**50.2**	*70.1*	*51.8*	**28.7**
Neutral	**3**	48.3	71.3	*51.8*	25.9
La Niña	**3**	*48.2*	**71.9**	**52.5**	*26.6*
El Niño	**4**	**52.8**	*71.7*	*53.8*	**30.9**
Neutral	**4**	51.3	73.0	53.9	*28.3*
La Niña	**4**	*51.0*	**73.5**	**54.4**	28.7
El Niño	**5**	**52.5**	*71.6*	53.8	**31.1**
Neutral	**5**	50.9	72.7	*53.7*	*28.6*
La Niña	**5**	*50.6*	**73.2**	**54.2**	29.0
El Niño	**6**	**51.3**	*70.5*	*52.8*	**30.2**
Neutral	**6**	49.7	71.5	*52.8*	*27.8*
La Niña	**6**	*49.4*	**72.1**	**53.1**	28.0
El Niño	**7**	**55.8**	*74.8*	*57.0*	**35.0**
Neutral	**7**	55.1	**75.8**	*57.0*	*33.0*
La Niña	**7**	*54.1*	**75.8**	**57.3**	33.4
El Niño	**8**	**54.6**	*73.3*	55.7	**34.3**
Neutral	**8**	53.7	74.1	*55.6*	*32.5*
La Niña	**8**	*52.8*	**74.7**	**55.9**	32.7
El Niño	**9**	**54.4**	*73.1*	*55.6*	**34.2**
Neutral	**9**	53.3	74.1	55.7	*32.3*
La Niña	**9**	*52.6*	**74.6**	**55.8**	32.5

Illinois Average Observed Seasonal Precipitation (inches) per ENSO Phase 1980-2010					
Phase	**Cli. Div.**	**Spring (MAM)**	**Summer (JJA)**	**Fall (SON)**	**Winter (DJF)**
El Niño	**1**	3.23	**4.48**	*2.90*	1.59
Neutral	**1**	**3.52**	4.43	**3.18**	*1.52*
La Niña	**1**	*3.05*	*3.81*	2.79	**1.90**
El Niño	**2**	3.25	4.05	3.11	1.89
Neutral	**2**	**3.48**	**4.28**	**3.43**	*1.74*
La Niña	**2**	*2.95*	*3.64*	*2.77*	**2.04**
El Niño	**3**	3.72	4.11	3.16	1.86
Neutral	**3**	**3.89**	**4.38**	**3.27**	*1.79*
La Niña	**3**	*3.22*	*3.54*	*2.88*	**1.91**
El Niño	**4**	3.46	3.83	3.26	2.12
Neutral	**4**	**3.74**	**4.05**	**3.41**	*2.01*
La Niña	**4**	*3.23*	*3.22*	*2.61*	**2.13**
El Niño	**5**	3.63	4.08	3.11	*2.05*
Neutral	**5**	**3.71**	**4.33**	**3.57**	2.08
La Niña	**5**	*3.17*	*3.21*	*2.66*	**2.28**
El Niño	**6**	**3.85**	*3.47*	**3.58**	**2.37**
Neutral	**6**	3.83	**3.87**	3.57	2.18
La Niña	**6**	*3.29*	3.83	*2.75*	*2.14*
El Niño	**7**	*3.79*	*3.55*	3.48	2.67
Neutral	**7**	**4.24**	3.99	**3.98**	*2.58*
La Niña	**7**	3.81	**4.03**	*3.00*	**2.74**
El Niño	**8**	*4.12*	3.68	3.86	**3.14**
Neutral	**8**	**4.56**	*3.65*	**4.06**	*3.03*
La Niña	**8**	4.29	**4.23**	*3.27*	3.06
El Niño	**9**	*4.44*	*3.58*	3.84	3.47
Neutral	**9**	**4.80**	3.68	**3.94**	*3.25*
La Niña	**9**	4.51	**4.02**	*3.30*	**3.54**

Illinois Average Observed Seasonal Mean Temperature (degrees F) per ENSO Phase 1980-2010					
Phase	**Cli. Div.**	**Spring (MAM)**	**Summer (JJA)**	**Fall (SON)**	**Winter (DJF)**
El Niño	**1**	**50.2**	*70.5*	*51.0*	**26.6**
Neutral	**1**	48.5	71.8	51.1	23.2
La Niña	**1**	*48.2*	**72.2**	**51.5**	*23.0*
El Niño	**2**	**49.8**	*70.4*	*51.8*	**27.8**
Neutral	**2**	*48.0*	71.7	*51.8*	*24.7*
La Niña	**2**	*48.0*	**72.6**	**52.4**	*24.7*
El Niño	**3**	**52.7**	*72.6*	*53.3*	**29.3**
Neutral	**3**	51.2	**74.0**	53.5	*26.6*
La Niña	**3**	*50.9*	**74.0**	**53.9**	*26.6*
El Niño	**4**	**52.5**	*72.2*	*53.2*	**29.3**
Neutral	**4**	50.9	73.5	53.3	*26.4*
La Niña	**4**	*50.5*	**73.6**	**53.8**	26.6
El Niño	**5**	**51.9**	*71.6*	*52.9*	**29.2**
Neutral	**5**	50.2	72.9	53.0	*26.2*
La Niña	**5**	*50.1*	**73.3**	**53.5**	26.5
El Niño	**6**	**54.3**	*73.6*	*54.9*	**31.7**
Neutral	**6**	52.9	**74.9**	55.1	*29.3*
La Niña	**6**	*52.1*	74.7	**55.5**	29.7
El Niño	**7**	**54.5**	*73.8*	*55.3*	**32.4**
Neutral	**7**	53.3	**75.1**	55.5	*30.1*
La Niña	**7**	*52.5*	**75.1**	**55.9**	30.6
El Niño	**8**	**56.6**	*75.5*	*57.2*	**35.4**
Neutral	**8**	55.7	**76.7**	57.3	*33.6*
La Niña	**8**	*54.8*	**76.7**	**57.8**	34.1
El Niño	**9**	**56.3**	*75.2*	*57.2*	**35.5**
Neutral	**9**	55.7	76.3	57.3	*34.0*
La Niña	**9**	*54.7*	**76.6**	**57.7**	34.2

Ohio Average Observed Seasonal Precipitation (inches) per ENSO Phase 1980-2010					
Phase	**Cli. Div.**	**Spring (MAM)**	**Summer (JJA)**	**Fall (SON)**	**Winter (DJF)**
El Niño	**1**	3.20	*3.53*	2.69	*2.11*
Neutral	**1**	**3.28**	**3.79**	**3.22**	2.20
La Niña	**1**	*3.18*	3.61	*2.52*	**2.30**
El Niño	**2**	*3.13*	*3.65*	*2.81*	**2.35**
Neutral	**2**	**3.31**	**3.95**	**3.48**	2.34
La Niña	**2**	3.22	3.68	2.62	*2.26*
El Niño	**3**	*3.17*	3.78	*3.28*	*2.72*
Neutral	**3**	3.51	**4.20**	**4.03**	2.58
La Niña	**3**	**3.69**	*3.52*	3.36	**2.77**
El Niño	**4**	*3.27*	3.82	2.70	*2.39*
Neutral	**4**	**3.78**	**4.45**	**3.26**	2.46
La Niña	**4**	3.35	*3.41*	*2.68*	**2.48**
El Niño	**5**	*3.31*	3.93	2.87	2.57
Neutral	**5**	**3.82**	**4.27**	**3.11**	*2.48*
La Niña	**5**	3.51	*3.16*	*2.78*	**2.60**
El Niño	**6**	*3.43*	4.07	*2.92*	2.59
Neutral	**6**	**3.83**	**4.48**	**3.35**	*2.58*
La Niña	**6**	3.79	*3.39*	2.95	**2.62**
El Niño	**7**	*3.47*	3.79	3.19	*2.61*
Neutral	**7**	**3.65**	**4.47**	**3.39**	2.63
La Niña	**7**	3.56	*3.08*	*2.73*	**2.90**
El Niño	**8**	4.08	3.86	*2.92*	*2.82*
Neutral	**8**	**4.42**	**4.13**	**3.37**	2.84
La Niña	**8**	*4.05*	*3.02*	*2.92*	**3.02**
El Niño	**9**	*3.49*	3.85	**3.24**	2.89
Neutral	**9**	**4.38**	**4.19**	2.80	*2.81*
La Niña	**9**	3.79	*3.25*	*2.68*	**3.26**
El Niño	**10**	*3.35*	3.87	3.26	2.80
Neutral	**10**	**4.05**	**4.47**	**3.13**	*2.53*
La Niña	**10**	3.82	*3.22*	*2.81*	**3.02**

Ohio Average Observed Seasonal Mean Temperature (degrees F) per ENSO Phase 1980-2010					
Phase	**Cli. Div.**	**Spring (MAM)**	**Summer (JJA)**	**Fall (SON)**	**Winter (DJF)**
El Niño	**1**	**50.4**	*70.5*	52.4	**29.3**
Neutral	**1**	*48.5*	71.6	*52.3*	*26.7*
La Niña	**1**	*48.5*	**72.2**	**52.8**	27.3
El Niño	**2**	**49.8**	*70.3*	52.8	**29.8**
Neutral	**2**	48.3	71.2	*52.6*	*27.6*
La Niña	**2**	*48.0*	**71.7**	**52.9**	28.0
El Niño	**3**	**49.1**	*68.9*	**52.2**	**29.6**
Neutral	**3**	47.3	69.6	*51.9*	*27.7*
La Niña	**3**	*46.9*	**70.2**	**52.2**	28.1
El Niño	**4**	**51.2**	*70.7*	52.9	**30.2**
Neutral	**4**	49.5	71.5	*52.7*	*27.9*
La Niña	**4**	*49.3*	**72.1**	**53.0**	28.2
El Niño	**5**	**52.0**	*71.4*	**53.8**	**31.4**
Neutral	**5**	50.5	72.1	*53.6*	*29.6*
La Niña	**5**	*50.1*	**72.8**	53.7	29.8
El Niño	**6**	**50.0**	*69.3*	*51.8*	**29.6**
Neutral	**6**	48.4	69.9	*51.8*	*27.9*
La Niña	**6**	*48.0*	**70.3**	**51.9**	28.1
El Niño	**7**	**50.1**	*69.6*	52.3	**30.6**
Neutral	**7**	48.9	70.1	*52.2*	*29.2*
La Niña	**7**	*48.2*	**70.9**	**52.4**	*29.2*
El Niño	**8**	**53.4**	*72.4*	*54.9*	**32.9**
Neutral	**8**	52.0	73.2	*54.9*	*31.2*
La Niña	**8**	*51.4*	**73.8**	**55.1**	31.4
El Niño	**9**	**53.6**	*72.1*	55.1	**34.5**
Neutral	**9**	53.0	72.9	*54.9*	*32.9*
La Niña	**9**	*52.3*	**73.8**	**55.2**	33.3
El Niño	**10**	**51.9**	*70.7*	**53.6**	**32.3**
Neutral	**10**	50.6	71.0	*53.4*	*30.7*
La Niña	**10**	*50.0*	**71.9**	53.5	31.1

Michigan Average Observed Seasonal Precipitation (inches) per ENSO Phase 1980-2010					
Phase	**Cli. Div.**	**Spring (MAM)**	**Summer (JJA)**	**Fall (SON)**	**Winter (DJF)**
El Niño	**1**	2.35	3.31	*3.02*	*1.65*
Neutral	**1**	**2.50**	*3.09*	3.09	1.79
La Niña	**1**	*2.30*	**3.61**	**3.51**	**2.11**
El Niño	**2**	2.19	3.10	*3.22*	1.71
Neutral	**2**	**2.24**	*2.93*	3.30	*1.69*
La Niña	**2**	*2.02*	**3.28**	**3.63**	**2.36**
El Niño	**3**	2.41	*3.06*	3.34	*1.74*
Neutral	**3**	**2.57**	3.09	*3.32*	1.88
La Niña	**3**	*2.17*	**3.11**	**3.39**	**2.24**
El Niño	**4**	2.51	**3.22**	**2.92**	*1.51*
Neutral	**4**	**2.55**	3.15	*2.85*	1.65
La Niña	**4**	*1.98*	*3.13*	2.88	**2.02**
El Niño	**5**	*2.52*	**3.26**	3.56	1.83
Neutral	**5**	**3.06**	3.18	**3.79**	*1.78*
La Niña	**5**	2.78	*2.93*	*3.30*	**2.37**
El Niño	**6**	2.71	**3.36**	3.18	1.67
Neutral	**6**	**3.05**	3.22	**3.48**	*1.65*
La Niña	**6**	*2.68*	*3.10*	*2.98*	**2.17**
El Niño	**7**	2.65	3.28	3.01	*1.63*
Neutral	**7**	**2.88**	*3.26*	**3.54**	1.68
La Niña	**7**	*2.48*	**2.79**	*2.94*	**2.18**
El Niño	**8**	*2.87*	**4.03**	3.56	2.24
Neutral	**8**	**3.26**	3.56	**4.04**	*2.21*
La Niña	**8**	3.02	*3.08*	*2.91*	**2.61**
El Niño	**9**	*2.72*	3.77	3.00	1.77
Neutral	**9**	**3.11**	**3.49**	**3.64**	*1.74*
La Niña	**9**	2.90	*3.12*	*2.79*	**2.10**
El Niño	**10**	2.74	**3.51**	2.77	1.99
Neutral	**10**	**3.00**	*3.31*	**3.52**	*1.93*
La Niña	**10**	*2.68*	3.37	*2.52*	**2.30**

Michigan Average Observed Seasonal Mean Temperature (degrees F) per ENSO Phase 1980-2010					
Phase	**Cli. Div.**	**Spring (MAM)**	**Summer (JJA)**	**Fall (SON)**	**Winter (DJF)**
El Niño	**1**	**40.5**	*61.8*	43.7	**18.9**
Neutral	**1**	38.2	63.5	*43.4*	*15.4*
La Niña	**1**	*38.0*	**64.0**	**44.0**	15.5
El Niño	**2**	**40.2**	*61.8*	45.3	**21.2**
Neutral	**2**	38.1	63.3	*44.6*	*17.7*
La Niña	**2**	*37.9*	**64.1**	**45.7**	18.5
El Niño	**3**	**43.2**	*64.4*	47.7	**24.7**
Neutral	**3**	41.3	65.9	*47.0*	*21.4*
La Niña	**3**	*41.2*	**66.7**	**48.0**	22.6
El Niño	**4**	**42.9**	*64.4*	46.9	**23.4**
Neutral	**4**	*41.0*	65.8	*46.2*	*20.1*
La Niña	**4**	41.1	**66.5**	**47.1**	21.2
El Niño	**5**	**45.7**	*66.0*	48.9	**27.0**
Neutral	**5**	43.9	67.4	*48.4*	*24.3*
La Niña	**5**	*43.8*	**68.0**	**49.2**	25.0
El Niño	**6**	**46.2**	*67.1*	48.7	**25.7**
Neutral	**6**	*44.3*	68.4	*48.1*	*22.8*
La Niña	**6**	44.5	**69.4**	**49.2**	23.6
El Niño	**7**	**45.7**	*66.6*	49.4	**26.3**
Neutral	**7**	*43.9*	68.0	*48.8*	*23.4*
La Niña	**7**	44.1	**68.9**	**49.7**	24.3
El Niño	**8**	**48.3**	*68.8*	51.2	**28.5**
Neutral	**8**	46.5	69.9	*50.9*	*25.9*
La Niña	**8**	*46.4*	**70.7**	**51.7**	26.4
El Niño	**9**	**47.6**	*68.0*	49.9	**27.1**
Neutral	**9**	*45.9*	69.2	*49.7*	*24.4*
La Niña	**9**	*45.9*	**70.0**	**50.4**	25.1
El Niño	**10**	**48.3**	*69.1*	51.1	**27.8**
Neutral	**10**	46.5	70.3	*50.8*	*25.4*
La Niña	**10**	*46.4*	**71.0**	**51.5**	26.0

Wisconsin Average Observed Seasonal Precipitation (inches) per ENSO Phase 1980-2010					
Phase	**Cli. Div.**	**Spring (MAM)**	**Summer (JJA)**	**Fall (SON)**	**Winter (DJF)**
El Niño	**1**	*2.45*	*3.85*	3.01	*0.92*
Neutral	**1**	2.50	4.19	*2.80*	0.93
La Niña	**1**	**2.56**	**4.40**	**3.24**	**1.18**
El Niño	**2**	2.45	*3.80*	**3.17**	1.09
Neutral	**2**	**2.61**	4.03	*3.01*	*1.06*
La Niña	**2**	*2.42*	**4.23**	**3.17**	**1.38**
El Niño	**3**	**2.66**	*3.48*	**3.01**	*1.11*
Neutral	**3**	2.62	3.75	*2.80*	1.14
La Niña	**3**	*2.24*	**3.92**	2.99	**1.40**
El Niño	**4**	**2.97**	4.39	**3.00**	1.02
Neutral	**4**	2.96	**4.60**	*2.60*	*0.95*
La Niña	**4**	*2.65*	*4.38*	2.98	**1.14**
El Niño	**5**	2.85	*3.93*	2.80	1.15
Neutral	**5**	**2.87**	4.35	*2.73*	*1.06*
La Niña	**5**	*2.61*	**4.61**	**2.83**	**1.35**
El Niño	**6**	**2.70**	*3.32*	2.76	*1.28*
Neutral	**6**	2.67	**3.78**	**2.81**	1.29
La Niña	**6**	*2.31*	3.73	*2.68*	**1.60**
El Niño	**7**	**3.29**	*4.32*	2.75	1.19
Neutral	**7**	3.14	**4.91**	*2.72*	*1.09*
La Niña	**7**	*3.02*	4.65	**2.85**	**1.39**
El Niño	**8**	**3.18**	*4.02*	**2.99**	*1.33*
Neutral	**8**	3.06	**4.67**	2.96	*1.33*
La Niña	**8**	*2.97*	4.12	*2.73*	**1.78**
El Niño	**9**	2.96	3.81	2.84	1.56
Neutral	**9**	**3.08**	**4.19**	**3.09**	*1.51*
La Niña	**9**	*2.88*	*3.59*	*2.71*	**1.90**

Wisconsin Average Observed Seasonal Mean Temperature (degrees F) per ENSO Phase 1980-2010					
Phase	**Cli. Div.**	**Spring (MAM)**	**Summer (JJA)**	**Fall (SON)**	**Winter (DJF)**
El Niño	**1**	**43.5**	*64.7*	44.4	**17.9**
Neutral	**1**	*41.0*	66.4	*44.2*	13.9
La Niña	**1**	41.1	**66.8**	**44.7**	*13.8*
El Niño	**2**	**42.3**	*63.3*	**43.5**	**18.0**
Neutral	**2**	39.8	65.0	*43.3*	14.2
La Niña	**2**	*39.7*	**65.5**	43.9	*14.1*
El Niño	**3**	**42.9**	*63.8*	44.5	**19.8**
Neutral	**3**	40.8	65.5	*44.2*	16.2
La Niña	**3**	*40.6*	**66.0**	**45.0**	*16.0*
El Niño	**4**	**46.6**	*67.6*	46.9	**21.0**
Neutral	**4**	44.4	69.2	*46.8*	17.1
La Niña	**4**	*44.3*	**69.8**	**47.3**	*16.8*
El Niño	**5**	**46.0**	*66.9*	47.0	**22.1**
Neutral	**5**	44.1	68.6	*46.8*	18.5
La Niña	**5**	*44.0*	**69.2**	**47.4**	*18.2*
El Niño	**6**	**44.4**	*66.3*	48.2	**23.9**
Neutral	**6**	*42.9*	67.8	*47.9*	20.5
La Niña	**6**	*42.9*	**68.8**	**48.6**	*20.3*
El Niño	**7**	**47.3**	*68.2*	*48.1*	**23.3**
Neutral	**7**	*45.7*	69.7	48.2	19.7
La Niña	**7**	*45.7*	**70.3**	**48.6**	*19.4*
El Niño	**8**	**47.3**	*68.3*	48.7	**24.0**
Neutral	**8**	*45.6*	69.7	*48.4*	20.6
La Niña	**8**	45.7	**70.4**	**49.1**	*20.4*
El Niño	**9**	**46.4**	*67.9*	49.7	**25.8**
Neutral	**9**	*45.0*	69.2	*49.6*	22.5
La Niña	**9**	45.1	**70.5**	**50.1**	*22.4*

Missouri Average Observed Seasonal Precipitation (inches) per ENSO Phase 1980-2010					
Phase	**Cli. Div.**	**Spring (MAM)**	**Summer (JJA)**	**Fall (SON)**	**Winter (DJF)**
El Niño	**1**	**4.01**	4.63	*3.06*	1.56
Neutral	**1**	3.99	**4.85**	3.32	*1.47*
La Niña	**1**	*3.10*	*4.09*	**3.42**	**1.48**
El Niño	**2**	3.98	*3.93*	**3.70**	**2.36**
Neutral	**2**	**4.08**	4.27	3.64	*2.08*
La Niña	**2**	*3.54*	**4.28**	*3.08*	2.17
El Niño	**3**	4.17	*4.19*	**4.00**	**2.16**
Neutral	**3**	**4.50**	4.45	3.74	*1.99*
La Niña	**3**	*3.80*	**4.75**	*3.51*	2.04
El Niño	**4**	*4.19*	4.17	4.13	**2.76**
Neutral	**4**	**4.51**	*3.64*	**4.37**	2.55
La Niña	**4**	4.44	**4.40**	*3.82*	*2.50*
El Niño	**5**	*4.29*	3.95	4.07	**3.14**
Neutral	**5**	**4.60**	*3.54*	**4.26**	*2.92*
La Niña	**5**	4.43	**4.18**	*3.62*	3.04
El Niño	**6**	*4.38*	3.56	**4.12**	3.94
Neutral	**6**	**4.64**	*3.28*	*3.78*	**3.78**
La Niña	**6**	4.83	**3.62**	3.93	*3.83*

Missouri Average Observed Seasonal Mean Temperature (degrees F) per ENSO Phase 1980-2010					
Phase	**Cli. Div.**	**Spring (MAM)**	**Summer (JJA)**	**Fall (SON)**	**Winter (DJF)**
El Niño	**1**	**53.3**	*73.8*	53.9	**30.9**
Neutral	**1**	52.7	**75.3**	*54.3*	*28.6*
La Niña	**1**	*52.2*	75.0	**54.8**	28.8
El Niño	**2**	**54.5**	*74.2*	*55.2*	**32.4**
Neutral	**2**	53.6	75.4	**55.5**	*30.4*
La Niña	**2**	*53.0*	**75.6**	56.1	30.6
El Niño	**3**	**55.3**	*75.2*	*56.2*	**34.1**
Neutral	**3**	54.9	**76.7**	56.9	*32.6*
La Niña	**3**	*54.3*	76.4	**57.3**	32.8
El Niño	**4**	**55.8**	*74.7*	*56.7*	**36.2**
Neutral	**4**	55.7	**76.2**	57.3	*34.9*
La Niña	**4**	*54.8*	76.1	**57.5**	35.0
El Niño	**5**	**55.9**	*74.4*	*56.3*	**35.6**
Neutral	**5**	55.4	**75.9**	56.6	*33.9*
La Niña	**5**	*54.4*	75.7	**57.0**	34.2
El Niño	**6**	**58.8**	*77.5*	*59.4*	**38.5**
Neutral	**6**	58.5	**78.8**	*59.4*	*37.0*
La Niña	**6**	*57.4*	**78.8**	**59.8**	37.3

Iowa Average Observed Seasonal Precipitation (inches) per ENSO Phase 1980-2010					
Phase	**Cli. Div.**	**Spring (MAM)**	**Summer (JJA)**	**Fall (SON)**	**Winter (DJF)**
El Niño	**1**	**3.24**	**4.25**	**2.46**	**0.78**
Neutral	**1**	2.84	4.06	*1.93*	0.72
La Niña	**1**	*2.64*	*3.99*	2.53	*0.71*
El Niño	**2**	**3.48**	4.43	2.58	**1.08**
Neutral	**2**	3.40	**4.94**	*2.03*	*0.92*
La Niña	**2**	*2.81*	*4.35*	**2.74**	0.95
El Niño	**3**	**3.35**	*4.61*	**2.87**	1.19
Neutral	**3**	3.32	**4.97**	*2.52*	*1.08*
La Niña	**3**	*3.17*	4.72	2.75	**1.35**
El Niño	**4**	**3.45**	**4.36**	**2.50**	**0.99**
Neutral	**4**	3.44	4.33	*2.10*	*0.79*
La Niña	**4**	*2.63*	*4.27*	2.45	0.87
El Niño	**5**	3.58	4.54	**2.81**	**1.17**
Neutral	**5**	**3.62**	**4.99**	*2.34*	*1.03*
La Niña	**5**	*2.88*	*4.51*	2.72	*1.03*
El Niño	**6**	3.28	**4.71**	2.87	**1.37**
Neutral	**6**	**3.39**	4.68	**2.91**	*1.28*
La Niña	**6**	*2.98*	*3.93*	*2.79*	1.58
El Niño	**7**	**3.78**	**4.68**	2.60	**1.22**
Neutral	**7**	3.76	4.61	**2.62**	*0.93*
La Niña	**7**	*2.83*	*4.01*	*2.55*	0.97
El Niño	**8**	3.80	4.73	*2.85*	**1.23**
Neutral	**8**	**3.84**	**4.94**	2.98	*1.16*
La Niña	**8**	*2.79*	*4.37*	**2.99**	1.22
El Niño	**9**	3.59	4.45	*3.08*	**1.55**
Neutral	**9**	**3.85**	**4.81**	**3.13**	*1.45*
La Niña	**9**	*3.03*	*4.17*	3.12	1.61

Iowa Average Observed Seasonal Mean Temperature (degrees F) per ENSO Phase 1980-2010					
Phase	**Cli. Div.**	**Spring (MAM)**	**Summer (JJA)**	**Fall (SON)**	**Winter (DJF)**
El Niño	**1**	**47.3**	*69.2*	*47.7*	**21.8**
Neutral	**1**	*46.0*	**70.9**	**48.1**	*17.7*
La Niña	**1**	46.4	**70.9**	**48.1**	18.5
El Niño	**2**	**47.5**	*69.0*	*47.8*	**21.4**
Neutral	**2**	*45.8*	70.4	48.1	*17.5*
La Niña	**2**	46.2	**70.8**	**48.3**	18.0
El Niño	**3**	**48.1**	*69.1*	*48.5*	**22.8**
Neutral	**3**	*46.3*	70.5	48.7	19.2
La Niña	**3**	46.5	**71.2**	**49.0**	*19.1*
El Niño	**4**	**49.3**	*70.7*	*49.7*	**24.6**
Neutral	**4**	*48.4*	72.4	50.2	*21.2*
La Niña	**4**	48.6	**72.5**	**50.3**	22.0
El Niño	**5**	**49.2**	*70.4*	*49.7*	**24.5**
Neutral	**5**	*48.0*	71.9	50.0	*21.0*
La Niña	**5**	48.2	**72.5**	**50.3**	21.3
El Niño	**6**	**50.3**	70.9	*50.8*	**25.7**
Neutral	**6**	48.7	*72.2*	50.9	22.4
La Niña	**6**	*48.5*	**72.8**	**51.2**	*22.2*
El Niño	**7**	**51.0**	*72.0*	*51.5*	**27.2**
Neutral	**7**	*50.2*	**73.8**	51.9	*24.0*
La Niña	**7**	50.3	**73.8**	**52.3**	24.7
El Niño	**8**	**50.8**	*71.5*	*51.3*	**27.3**
Neutral	**8**	*49.6*	73.0	51.7	*24.3*
La Niña	**8**	49.7	**73.3**	**52.1**	*24.3*
El Niño	**9**	**52.1**	*72.7*	*52.7*	**28.2**
Neutral	**9**	50.8	74.0	53.0	*25.2*
La Niña	**9**	*50.7*	**74.5**	**53.4**	25.3

Minnesota Average Observed Seasonal Precipitation (inches) per ENSO Phase 1980-2010					
Phase	**Cli. Div.**	**Spring (MAM)**	**Summer (JJA)**	**Fall (SON)**	**Winter (DJF)**
El Niño	**1**	1.71	3.68	1.96	0.65
Neutral	**1**	*1.69*	*3.52*	*1.83*	*0.57*
La Niña	**1**	**1.84**	**3.80**	**2.37**	**0.72**
El Niño	**2**	1.86	*3.65*	2.19	*0.64*
Neutral	**2**	*1.80*	3.78	*2.18*	0.65
La Niña	**2**	**2.34**	**4.26**	**2.70**	**0.80**
El Niño	**3**	*1.85*	*3.46*	*2.53*	0.86
Neutral	**3**	2.04	3.81	2.55	*0.75*
La Niña	**3**	**2.20**	**4.45**	**3.34**	**1.06**
El Niño	**4**	*1.97*	3.60	2.07	*0.61*
Neutral	**4**	**2.20**	**3.63**	*1.95*	0.67
La Niña	**4**	2.18	*3.54*	**2.41**	**0.78**
El Niño	**5**	*2.36*	**4.36**	2.44	*0.68*
Neutral	**5**	2.49	3.98	*2.25*	0.75
La Niña	**5**	**2.52**	*3.91*	**2.63**	**0.92**
El Niño	**6**	*2.33*	4.18	2.68	0.83
Neutral	**6**	2.50	*4.13*	*2.50*	*0.80*
La Niña	**6**	**2.65**	**4.20**	**2.92**	**1.02**
El Niño	**7**	*2.61*	**4.00**	2.20	*0.66*
Neutral	**7**	**2.69**	3.79	*2.02*	**0.68**
La Niña	**7**	2.65	*3.24*	**2.54**	**0.68**
El Niño	**8**	**3.04**	**4.53**	2.57	0.86
Neutral	**8**	*2.91*	4.49	*2.12*	*0.81*
La Niña	**8**	*2.91*	*3.76*	**2.86**	**1.00**
El Niño	**9**	**3.10**	4.58	2.91	1.01
Neutral	**9**	3.06	**4.64**	*2.31*	*0.91*
La Niña	**9**	*2.74*	*4.40*	**2.99**	**1.11**

Minnesota Average Observed Seasonal Mean Temperature (degrees F) per ENSO Phase 1980-2010					
Phase	**Cli. Div.**	**Spring (MAM)**	**Summer (JJA)**	**Fall (SON)**	**Winter (DJF)**
El Niño	**1**	**42.7**	*64.8*	**42.2**	**13.1**
Neutral	**1**	39.8	66.7	*42.0*	*8.1*
La Niña	**1**	*39.7*	**66.9**	42.1	8.4
El Niño	**2**	**42.2**	*63.8*	**42.0**	**13.6**
Neutral	**2**	39.1	**65.6**	*41.6*	9.0
La Niña	**2**	*38.9*	65.4	41.9	*8.9*
El Niño	**3**	**39.7**	*61.1*	**41.3**	**14.4**
Neutral	**3**	37.1	62.8	*40.9*	10.4
La Niña	**3**	*36.9*	**62.9**	**41.3**	*10.2*
El Niño	**4**	**45.7**	*67.6*	*45.1*	**17.9**
Neutral	**4**	*42.8*	69.3	**45.3**	13.1
La Niña	**4**	43.2	**69.8**	**45.3**	*12.9*
El Niño	**5**	**46.1**	*67.7*	45.6	**18.3**
Neutral	**5**	*43.4*	69.3	*45.5*	14.2
La Niña	**5**	43.6	**69.8**	**45.9**	*13.8*
El Niño	**6**	**44.9**	*66.4*	*45.0*	**17.8**
Neutral	**6**	*42.3*	68.0	44.7	*13.7*
La Niña	**6**	*42.3*	**68.3**	**45.3**	*13.7*
El Niño	**7**	**46.5**	*68.4*	*46.5*	**20.6**
Neutral	**7**	*44.6*	70.2	46.8	*16.3*
La Niña	**7**	45.1	**70.5**	**46.9**	16.6
El Niño	**8**	**46.9**	*68.6*	*47.0*	**20.7**
Neutral	**8**	*44.9*	70.3	47.2	*16.5*
La Niña	**8**	45.5	**70.7**	**47.6**	16.7
El Niño	**9**	**46.8**	*68.0*	*47.0*	**20.9**
Neutral	**9**	*44.7*	69.6	47.4	17.2
La Niña	**9**	44.9	**70.3**	**47.6**	*16.8*

North Dakota Average Observed Seasonal Precipitation (inches) per ENSO Phase 1980-2010					
Phase	**Cli. Div.**	**Spring (MAM)**	**Summer (JJA)**	**Fall (SON)**	**Winter (DJF)**
El Niño	**1**	*1.21*	2.48	1.04	0.51
Neutral	**1**	**1.34**	**2.56**	*0.96*	*0.48*
La Niña	**1**	1.28	*2.40*	**1.20**	**0.55**
El Niño	**2**	*1.34*	2.92	1.29	0.55
Neutral	**2**	1.43	**2.99**	*1.18*	*0.41*
La Niña	**2**	**1.46**	*2.73*	**1.43**	**0.56**
El Niño	**3**	1.43	**3.29**	1.54	0.56
Neutral	**3**	**1.55**	3.24	*1.38*	*0.46*
La Niña	**3**	*1.32*	*2.89*	**1.59**	**0.57**
El Niño	**4**	*1.29*	2.59	**1.29**	*0.42*
Neutral	**4**	**1.50**	**2.67**	*0.98*	*0.42*
La Niña	**4**	1.47	*2.19*	1.13	**0.50**
El Niño	**5**	1.39	2.73	**1.52**	0.48
Neutral	**5**	**1.54**	**3.24**	*1.28*	*0.43*
La Niña	**5**	*1.36*	*2.67*	1.34	**0.54**
El Niño	**6**	*1.64*	**3.37**	1.81	0.62
Neutral	**6**	**1.72**	3.24	*1.51*	*0.49*
La Niña	**6**	1.66	*2.86*	**1.96**	**0.69**
El Niño	**7**	*1.38*	2.32	**1.26**	*0.33*
Neutral	**7**	**1.49**	**2.37**	*0.93*	**0.40**
La Niña	**7**	1.43	*1.79*	1.00	0.38
El Niño	**8**	*1.43*	*2.42*	**1.32**	*0.39*
Neutral	**8**	1.57	2.80	*1.02*	0.37
La Niña	**8**	**1.58**	**2.83**	1.10	**0.49**
El Niño	**9**	*1.78*	2.89	1.70	0.53
Neutral	**9**	**1.93**	**3.28**	*1.51*	*0.50*
La Niña	**9**	1.82	*2.58*	**1.85**	**0.58**

North Dakota Average Observed Seasonal Mean Temperature (degrees F) per ENSO Phase 1980-2010					
Phase	**Cli. Div.**	**Spring (MAM)**	**Summer (JJA)**	**Fall (SON)**	**Winter (DJF)**
El Niño	**1**	**42.0**	*64.7*	41.5	**15.8**
Neutral	**1**	40.3	66.2	**41.7**	*10.9*
La Niña	**1**	*40.2*	**66.3**	*41.2*	11.5
El Niño	**2**	**41.2**	*64.3*	**41.0**	**13.1**
Neutral	**2**	39.2	65.8	**41.0**	*8.5*
La Niña	**2**	*38.9*	**66.0**	*40.6*	8.7
El Niño	**3**	**41.6**	*64.7*	**41.5**	**12.3**
Neutral	**3**	39.0	**66.2**	41.4	*7.7*
La Niña	**3**	*38.9*	**66.2**	*40.9*	*7.7*
El Niño	**4**	**43.0**	*65.8*	43.0	**18.4**
Neutral	**4**	41.4	67.2	**43.2**	*13.5*
La Niña	**4**	*41.3*	**67.4**	*42.6*	13.8
El Niño	**5**	**42.9**	*65.7*	42.6	**15.7**
Neutral	**5**	40.7	67.1	**42.8**	*10.9*
La Niña	**5**	*40.6*	**67.8**	*42.3*	11.2
El Niño	**6**	**43.4**	*65.9*	**43.1**	**14.6**
Neutral	**6**	40.9	67.7	43.0	*9.8*
La Niña	**6**	*40.7*	**68.0**	*42.7*	10.0
El Niño	**7**	**43.2**	*65.9*	43.4	**21.5**
Neutral	**7**	*42.0*	67.5	**43.7**	*16.9*
La Niña	**7**	*42.0*	**67.9**	*43.3*	*16.9*
El Niño	**8**	**43.5**	*66.6*	43.5	**18.9**
Neutral	**8**	42.0	68.0	**43.8**	*14.1*
La Niña	**8**	*41.8*	**68.3**	*43.2*	14.5
El Niño	**9**	**44.2**	*66.8*	43.9	**17.2**
Neutral	**9**	*42.0*	68.4	**44.0**	*12.2*
La Niña	**9**	*42.0*	**68.9**	*43.6*	12.6

South Dakota Average Observed Seasonal Precipitation (inches) per ENSO Phase 1980-2010					
Phase	**Cli. Div.**	**Spring (MAM)**	**Summer (JJA)**	**Fall (SON)**	**Winter (DJF)**
El Niño	**1**	1.85	2.24	**1.19**	*0.34*
Neutral	**1**	*1.82*	**2.36**	*1.02*	**0.48**
La Niña	**1**	**2.03**	*2.14*	1.09	0.41
El Niño	**2**	*1.62*	2.56	*1.27*	*0.40*
Neutral	**2**	1.79	**2.93**	*1.27*	0.43
La Niña	**2**	**1.88**	*2.46*	**1.34**	**0.45**
El Niño	**3**	1.98	3.26	1.75	*0.51*
Neutral	**3**	**2.15**	**3.42**	*1.65*	0.54
La Niña	**3**	*1.88*	*2.88*	**2.02**	**0.59**
El Niño	**4**	**2.73**	2.61	**1.62**	*0.59*
Neutral	**4**	2.52	**2.78**	*1.33*	0.78
La Niña	**4**	*2.44*	*2.58*	1.46	**0.65**
El Niño	**5**	**2.32**	**2.38**	**1.29**	*0.40*
Neutral	**5**	1.99	*2.24*	*1.07*	**0.48**
La Niña	**5**	*1.98*	2.26	1.24	0.41
El Niño	**6**	**2.10**	3.02	*1.33*	*0.42*
Neutral	**6**	2.03	*2.55*	1.36	**0.49**
La Niña	**6**	*1.93*	**2.59**	**1.40**	0.46
El Niño	**7**	2.22	**3.63**	1.93	0.54
Neutral	**7**	**2.33**	3.29	*1.69*	*0.53*
La Niña	**7**	*2.20*	*3.13*	**2.16**	**0.57**
El Niño	**8**	**2.58**	**3.10**	1.57	*0.51*
Neutral	**8**	2.51	*2.78*	*1.39*	**0.52**
La Niña	**8**	*2.14*	*2.78*	**1.67**	**0.52**
El Niño	**9**	**2.87**	3.33	**2.08**	**0.64**
Neutral	**9**	2.61	*3.26*	*1.79*	*0.53*
La Niña	**9**	*2.42*	**3.39**	**2.08**	0.55

South Dakota Average Observed Seasonal Mean Temperature (degrees F) per ENSO Phase 1980-2010					
Phase	**Cli. Div.**	**Spring (MAM)**	**Summer (JJA)**	**Fall (SON)**	**Winter (DJF)**
El Niño	**1**	**44.7**	*67.8*	*45.4*	**24.1**
Neutral	**1**	43.6	69.5	**45.8**	*19.4*
La Niña	**1**	*43.0*	**70.0**	45.7	20.2
El Niño	**2**	**44.6**	*67.8*	44.9	**20.0**
Neutral	**2**	43.2	69.5	**45.4**	*15.1*
La Niña	**2**	*42.8*	**70.2**	*44.8*	15.9
El Niño	**3**	**44.8**	*67.5*	44.9	**18.4**
Neutral	**3**	*42.5*	69.1	**45.1**	*13.3*
La Niña	**3**	42.8	**69.8**	*44.8*	13.7
El Niño	**4**	**42.6**	*63.7*	*44.0*	**27.0**
Neutral	**4**	*41.3*	65.2	**44.8**	*24.3*
La Niña	**4**	*41.3*	**65.6**	44.5	24.5
El Niño	**5**	46.6	*69.3*	*47.4*	**27.5**
Neutral	**5**	**45.7**	71.0	**48.2**	*24.0*
La Niña	**5**	*45.5*	**71.4**	48.0	24.6
El Niño	**6**	**46.7**	*70.0*	*47.3*	**23.5**
Neutral	**6**	45.4	71.8	**48.1**	*19.5*
La Niña	**6**	*45.2*	**72.3**	47.7	20.1
El Niño	**7**	**45.9**	*68.2*	*45.8*	**20.4**
Neutral	**7**	*44.0*	69.9	**46.4**	*15.9*
La Niña	**7**	44.2	**70.4**	46.2	16.6
El Niño	**8**	**47.2**	*70.0*	*48.2*	**26.6**
Neutral	**8**	*46.1*	71.8	**49.1**	*22.9*
La Niña	**8**	46.3	**72.1**	48.8	23.9
El Niño	**9**	**48.3**	*70.7*	*48.6*	**23.8**
Neutral	**9**	*46.9*	72.3	**49.1**	*19.9*
La Niña	**9**	47.0	**72.4**	49.0	20.9

Nebraska Average Observed Seasonal Precipitation (inches) per ENSO Phase 1980-2010					
Phase	**Cli. Div.**	**Spring (MAM)**	**Summer (JJA)**	**Fall (SON)**	**Winter (DJF)**
El Niño	**1**	**2.06**	**2.56**	**1.16**	**0.46**
Neutral	**1**	*1.82*	2.27	1.06	0.38
La Niña	**1**	1.86	*2.12*	*1.03*	*0.36*
El Niño	**2**	**2.62**	3.11	**1.73**	**0.59**
Neutral	**2**	2.57	**3.14**	*1.42*	0.50
La Niña	**2**	*2.13*	*3.10*	1.72	*0.46*
El Niño	**3**	**3.29**	*3.52*	2.23	**0.77**
Neutral	**3**	2.83	3.65	*1.92*	0.66
La Niña	**3**	*2.68*	**3.79**	**2.26**	*0.63*
El Niño	**5**	**2.80**	*3.35*	**1.92**	**0.65**
Neutral	**5**	*2.74*	3.39	*1.52*	0.55
La Niña	**5**	2.60	**3.60**	1.70	*0.46*
El Niño	**6**	**3.43**	**4.21**	2.33	**0.94**
Neutral	**6**	3.09	*3.77*	*1.97*	*0.68*
La Niña	**6**	*2.73*	3.79	**2.19**	0.74
El Niño	**7**	2.19	2.99	**1.43**	**0.61**
Neutral	**7**	**2.21**	*2.95*	*1.18*	0.46
La Niña	**7**	*2.00*	**3.09**	*1.18*	*0.34*
El Niño	**8**	**2.94**	*3.17*	**1.87**	**0.70**
Neutral	**8**	2.71	3.56	*1.54*	0.51
La Niña	**8**	*2.48*	**3.70**	1.55	*0.45*
El Niño	**9**	**3.57**	**4.10**	**2.33**	**1.05**
Neutral	**9**	3.34	4.08	2.23	0.78
La Niña	**9**	*2.59*	*3.53*	*2.22*	*0.75*

Nebraska Average Observed Seasonal Mean Temperature (degrees F) per ENSO Phase 1980-2010					
Phase	**Cli. Div.**	**Spring (MAM)**	**Summer (JJA)**	**Fall (SON)**	**Winter (DJF)**
El Niño	**1**	**46.9**	*68.6*	*47.2*	**28.5**
Neutral	**1**	*45.6*	70.1	**48.1**	*26.6*
La Niña	**1**	46.0	**70.5**	48.0	26.8
El Niño	**2**	**47.9**	*70.0*	*48.3*	**27.1**
Neutral	**2**	*46.8*	**71.5**	48.9	*24.2*
La Niña	**2**	46.9	**71.5**	**49.0**	24.9
El Niño	**3**	**49.1**	*71.0*	*49.4*	**25.6**
Neutral	**3**	*48.2*	**72.7**	**50.1**	*22.4*
La Niña	**3**	48.3	**72.7**	**50.1**	23.4
El Niño	**5**	**49.1**	*70.9*	*49.4*	**27.7**
Neutral	**5**	48.3	**72.5**	**50.0**	*24.9*
La Niña	**5**	*48.2*	72.3	**50.0**	25.9
El Niño	**6**	**51.0**	*72.5*	*51.3*	**27.8**
Neutral	**6**	50.3	**74.4**	52.0	*24.7*
La Niña	**6**	*50.2*	74.0	**52.2**	25.7
El Niño	**7**	**49.7**	*71.7*	*50.4*	**30.0**
Neutral	**7**	*49.0*	**73.2**	**51.1**	*27.8*
La Niña	**7**	*49.0*	**73.2**	51.0	28.8
El Niño	**8**	**50.9**	*72.8*	*51.4*	**29.7**
Neutral	**8**	50.2	**74.3**	**52.0**	*27.0*
La Niña	**8**	*50.1*	74.0	**52.0**	28.0
El Niño	**9**	**51.8**	*73.3*	*52.4*	**29.3**
Neutral	**9**	51.3	**75.0**	53.2	*26.6*
La Niña	**9**	*51.2*	74.8	**53.3**	27.3

Kansa Average Observed Seasonal Precipitation (inches) per ENSO Phase 1980-2010					
Phase	**Cli. Div.**	**Spring (MAM)**	**Summer (JJA)**	**Fall (SON)**	**Winter (DJF)**
El Niño	**1**	2.32	3.09	**1.46**	**0.73**
Neutral	**1**	**2.42**	*2.96*	1.22	0.52
La Niña	**1**	*2.05*	**3.24**	*1.18*	*0.37*
El Niño	**2**	**3.13**	**3.81**	1.89	**0.97**
Neutral	**2**	2.89	3.69	**1.93**	0.68
La Niña	**2**	*2.47*	*3.37*	*1.86*	*0.64*
El Niño	**3**	**3.95**	4.54	*2.49*	**1.27**
Neutral	**3**	3.63	**4.80**	**3.07**	*1.04*
La Niña	**3**	*3.06*	*4.22*	3.01	1.06
El Niño	**4**	2.05	**3.27**	**1.36**	**0.81**
Neutral	**4**	**2.21**	*2.77*	1.19	0.54
La Niña	**4**	*1.98*	2.85	*1.18*	*0.39*
El Niño	**5**	3.24	**3.99**	*1.86*	**1.02**
Neutral	**5**	**3.11**	*3.69*	1.97	*0.80*
La Niña	**5**	*2.80*	3.78	**2.13**	0.85
El Niño	**6**	**4.17**	4.56	*2.82*	**1.38**
Neutral	**6**	3.85	**4.65**	3.05	*1.27*
La Niña	**6**	*3.29*	*4.35*	**3.49**	1.31
El Niño	**7**	*1.89*	**3.33**	**1.30**	**0.82**
Neutral	**7**	**1.94**	2.65	*1.14*	0.53
La Niña	**7**	*1.89*	*2.53*	**1.30**	*0.40*
El Niño	**8**	**3.30**	**4.16**	*2.00*	**1.14**
Neutral	**8**	3.03	*3.50*	**2.04**	*0.85*
La Niña	**8**	*2.90*	3.78	2.11	0.91
El Niño	**9**	**4.35**	4.61	3.52	**1.78**
Neutral	**9**	4.28	*4.32*	*3.34*	*1.51*
La Niña	**9**	*4.08*	**4.75**	**3.53**	1.60

Kansas Average Observed Seasonal Mean Temperature (degrees F) per ENSO Phase 1980-2010					
Phase	**Cli. Div.**	**Spring (MAM)**	**Summer (JJA)**	**Fall (SON)**	**Winter (DJF)**
El Niño	**1**	**50.8**	*73.0*	*51.7*	**31.4**
Neutral	**1**	50.2	74.4	52.4	*29.4*
La Niña	**1**	*50.1*	**74.5**	**52.5**	30.7
El Niño	**2**	**52.9**	*75.1*	*53.9*	**31.4**
Neutral	**2**	52.5	**76.8**	54.7	*29.1*
La Niña	**2**	*52.4*	76.5	**54.8**	29.9
El Niño	**3**	**53.9**	*74.9*	54.7	**31.6**
Neutral	**3**	53.6	**76.5**	*55.2*	*29.5*
La Niña	**3**	*53.1*	76.1	**55.5**	29.7
El Niño	**4**	**52.1**	*74.1*	*53.1*	**32.7**
Neutral	**4**	51.7	**75.6**	53.9	*30.9*
La Niña	**4**	*51.6*	75.5	**54.1**	32.3
El Niño	**5**	54.3	*76.2*	*55.4*	**33.3**
Neutral	**5**	*54.0*	**78.1**	56.3	*31.4*
La Niña	**5**	**53.9**	77.6	**56.6**	32.0
El Niño	**6**	**54.9**	*75.5*	*55.8*	**33.3**
Neutral	**6**	54.6	**77.1**	56.3	*31.6*
La Niña	**6**	*54.2*	76.7	**56.9**	*31.6*
El Niño	**7**	**54.2**	75.5	*55.0*	**34.5**
Neutral	**7**	*53.8*	*77.0*	56.0	*33.2*
La Niña	**7**	53.9	**77.1**	**56.2**	34.5
El Niño	**8**	55.4	*77.1*	*56.8*	**34.9**
Neutral	**8**	**55.5**	**78.9**	57.6	*33.5*
La Niña	**8**	*55.3*	78.6	**57.9**	34.3
El Niño	**9**	**56.2**	*76.4*	*57.4*	**35.5**
Neutral	**9**	**56.2**	**78.2**	58.0	*34.2*
La Niña	**9**	*55.7*	77.8	**58.4**	34.4

ENSO and AO classification breakdown:

Annual ENSO events: 8 El Niño, 6 La Niña, 17 Neutral
Growing season (A-O) events: 10 El Niño, 11 La Niña, 10 Neutral
JJA events: 7 El Niño, 6 La Niña, 18 Neutral
AMJ events: not determined for crop residual analysis. Average 3-month value of ENSO is only used in correlation analysis.

Annual AO events: 4 negative events, 2 positive events, 25 neutral events
Growing season (A-O) events: 2 positive events, 1 negative event, 28 neutral events
JJA events: 3 negative events, 3 positive events, 25 neutral events
AMJ events: not determined for crop residual analysis. Average 3-month value of the AO is only used in correlation analysis.

State Climate Divisions (SCDs) and Crop Reporting Districts (CRDs):

CRDs and SCDs share the same boundaries in all states except for the states of Ohio, Michigan, and Missouri. The number convention changes from 1, 2,…, 9 or 10 for SCDs to 10, 20, ..., 90 for CRDs.

In Ohio, SCDs 1 and 4 coincide with CRDs 10 and 40.
CRD 20 in OH is comprised of the following counties: Ottawa, Sandusky, Seneca, Wyandotte, Crawford, Richland, Ashland, Erie, Hurron, and Lorain.
CRD 30 is all of SCD 3, plus Mahoning, Columbiana, and Wayne counties.
CRD 50 is all counties of SCD 5 plus Knox and Ross counties.
CRD 60 is comprised of Holmes, Tuscarawas, Carroll, Jefferson, Belmont, Harrison, and Coshocton counties.
CRD 70 is comprised of the counties Preble, Montgomery, Greene, Clinton, Warren, Butler, Hamilton, and Clermont.
CRD 80 contains the counties of Brown, Highland, Pike, Scioto, Jackson, Gallia, and Lawrence. CRD 90 houses the counties of Guernsey, Muskingum, Perry, Morgan, Noble, Monroe, Hocking, Vinton, Athens, Washington, and Meigs.

Missouri's SCDs and CRDs differ in the following manner:
CRD 10 is comprised of counties Atchison, Nodaway, Worth, Harrison, Holt, Andrew, Gentry, De Kalb, Daviess, Caldwell, Clinton, Buchanan, Platte, Clay, and Ray;
CRD 20: Mercer, Grundy, Livingston, Carroll, Putnam, Schuyler, Adair, Macon, Linn, Sullivan, Chariton, and Randolph, 30: Scotland, Clark, Know, Lewis, Shelby, Marion, Monroe, Ralls, Audrain, and Pike;
CRD 40: Cass, Johnson, Jackson, Lafayette, Bates, Henry, Vernon, St. Clair, and Cedar;
CRD 50: Saline, Pettis, Benton, Hickory, Polk, Dallas, Camden, Morgan, Cooper, Howard, Boone, Moniteau, Cole, Miller, Laclede, Pulaski, Phelps, Maries, Osage, and Callaway.

CRD 60: Montgomery, Lincoln, Warren, St. Charles, Gasconade, Franklin, St. Louis, St. Louis City, Jefferson, Ste. Genevieve, Perry, St. Francoise, Washington, and Crawford;
CRD 70: Barton, Jasper, Newton, McDonald, Dade, Lawrence, Barry, Greene, Christian, and Stone;
CRD 80: Webster, Wright Texas, Dent, Iron, Madison, Bollinger, Wayne, Reynolds, Carter, Ripley, Shannon, Oregon, Howell, Ozark, and Taney;
CRD 90: Cape Girardeau, Scott, Stoddard, Butler, Dunklir, Pemiscot, New Madrid, and Mississippi.

Michigan: SCD 1 and 2 comprise CRD 10. SCD 3 is CRD 20, SCD 4 is CRD 30,…SCD 10 is CRD 90.

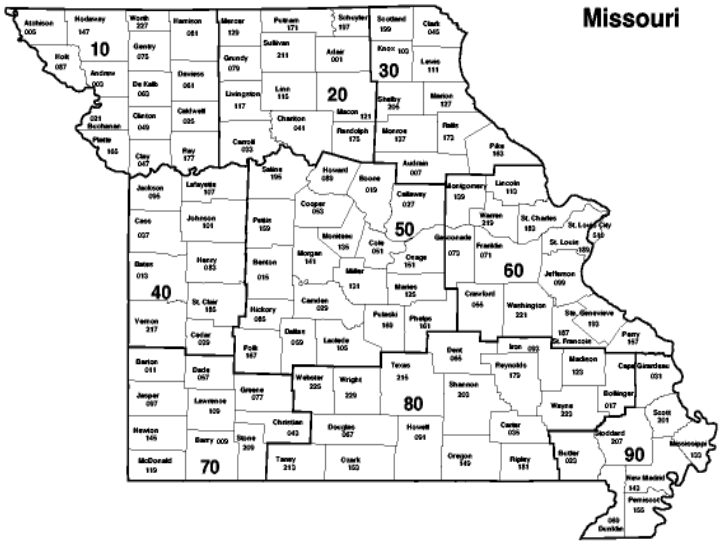
Missouri
10
30
20
50
60
40
80
90
70

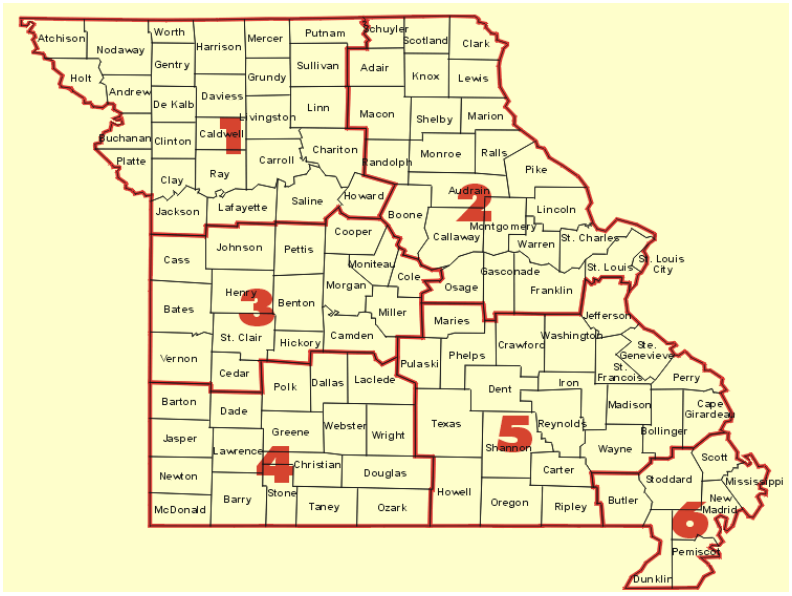
Atchison
Nodaway
Worth
Harrison
Mercer
Putnam
Schuyler
Scotland
Clark
Holt
Gentry
Sullivan
Adair
Knox
Lewis
Andrew
Daviess
Grundy
Linn
Macon
Shelby
Marion
De Kalb
Livingston
Caldwell
Buchanan
Clinton
Chariton
Randolph
Monroe
Ralls
Pike
Platte
Carroll
Clay
Ray
Howard
Audrain
Jackson
Lafayette
Saline
Boone
Lincoln
Cooper
Montgomery
Callaway
Warren
St. Charles
Johnson
Pettis
Moniteau
Gasconade
St. Louis
St. Louis City
Cass
Cole
Osage
Franklin
Henry
Morgan
Benton
Miller
Maries
Jefferson
Bates
St. Clair
Hickory
Camden
Washington
Crawford
Ste. Genevieve
Vernon
Phelps
Pulaski
St. Francois
Perry
Cedar
Polk
Dallas
Laclede
Iron
Dent
Barton
Dade
Madison
Cape Girardeau
Greene
Webster
Wright
Texas
Reynolds
Bollinger
Jasper
Lawrence
Christian
Shannon
Wayne
Scott
Newton
Douglas
Carter
Stoddard
Mississippi
Howell
Barry
Stone
Taney
Ozark
Oregon
Ripley
Butler
New Madrid
McDonald
Pemiscot
Dunklin
1
2
3
4
5
6

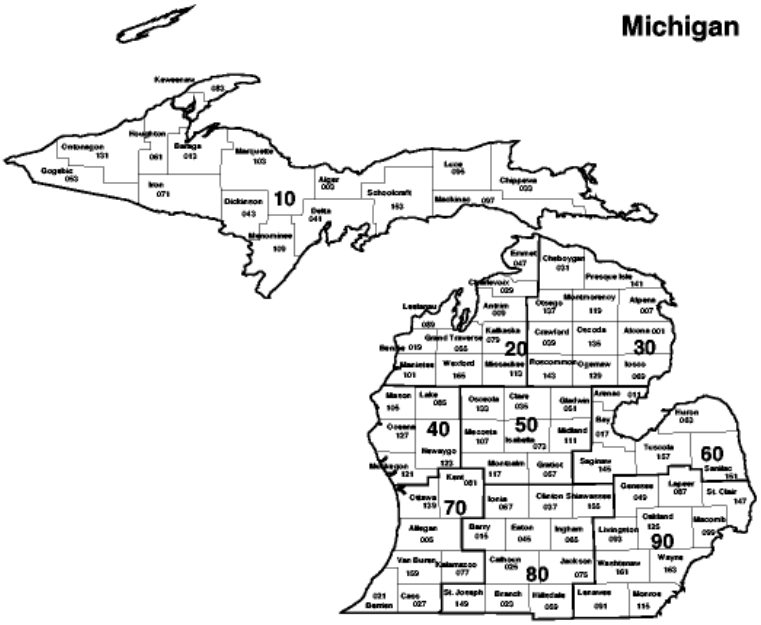

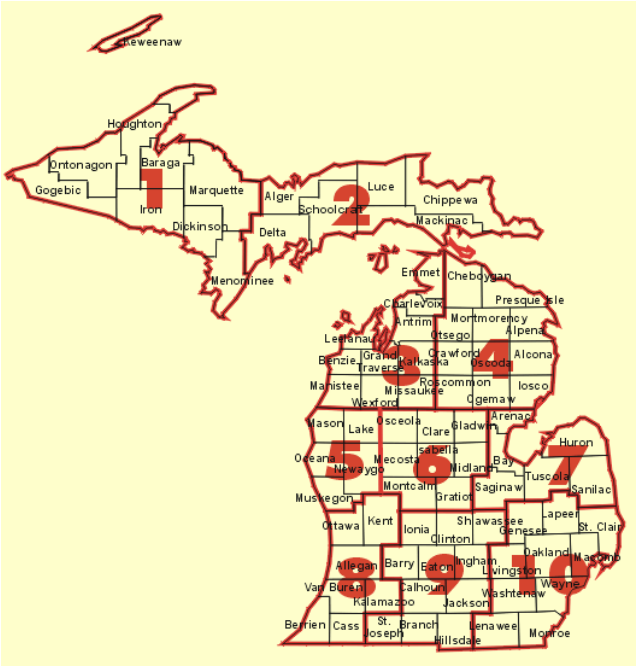

SCD maps can be found at:
http://www.cpc.ncep.noaa.gov/products/analysis_monitoring/regional_monitoring/CLIM_DIVS/states_counties_climate-divisions.shtml
CRD maps available by state at:
http://www.nass.usda.gov/Charts_and_Maps/Crops_County/boundary_maps/indexgif.asp

Appendix B Land Surface Heterogeneity Signature in Tornado Climatology? An Illustrative Analysis over Indiana, 1950-2012

As published in *Earth Interactions*.

Full Citation: Olivia Kellner and Dev Niyogi, 2014: Land Surface Heterogeneity Signature in Tornado Climatology? An Illustrative Analysis over Indiana, 1950–2012. *Earth Interact.*, 18, 1–32. doi: http://dx.doi.org/10.1175/2013EI000548.1.

Abstract

Land surface heterogeneity affects mesoscale interactions, including the evolution of severe convection. However, its contribution to tornadogenesis is not well known. Indiana is selected as an example to present an assessment of documented tornadoes and land surface heterogeneity to better understand the spatial distribution of tornadoes. This assessment is developed using a GIS framework taking data from 1950 to 2012 and investigates the following topics: temporal analysis, effect of ENSO, antecedent rainfall linkages, population density, land use/land cover, and topography, placing them in the context of land surface heterogeneity.

Spatial analysis of tornado touchdown locations reveals several spatial relationships with regard to cities, population density, land-use classification, and topography. A total of 61% of F0–F5 tornadoes and 43% of F0–F5 tornadoes in Indiana have touched down within 1 km of urban land use and land area classified as forest, respectively, suggesting the possible role of land-use surface roughness on tornado occurrences. The correlation of tornado touchdown points to population density suggests a moderate to strong relationship. A temporal analysis of tornado days shows favored time of day, months, seasons, and active tornado years. Tornado days for 1950–2012 are compared to antecedent rainfall and ENSO phases, which both show no discernible relationship with the average number of annual tornado days. Analysis of tornado touchdowns and topography does not indicate any strong relationship between tornado touchdowns and elevation. Results suggest a possible signature of land surface heterogeneity—particularly that around urban and forested land cover—in tornado climatology.

1. Introduction

Efforts to identify active regions of severe weather and tornado climatology spanning different spatial and temporal scales has been completed over the last several decades (e.g., Agee 1970; Pryor and Kurzhal 1997; Concannon et al. 2000; Brooks et al. 2003a; Brooks et al. 2003b; Schneider et al. 2004; Ashley 2007; Kis and Straka 2010; Dixon et al. 2011). Specific investigations of tornadoes as related to teleconnection patterns such as the El Niño–Southern Oscillation (Agee and Zurn-Birkhimer 1998; Rhome et al. 2000; Nunn and DeGaetano 2004; Mayes et al. 2007; Cook and Schaefer 2008) and synoptic features (Rose et al. 2004) have been completed as well. Research investigating tornadoes and population notes a possible feedback between higher tornado frequencies in areas of higher population and an increase in tornado reports with a surge in storm spotters in the late 1980s and early 1990s (Changnon 1982; Twisdale 1982; Tescon et al. 1983; McCarthy and Schaefer 2004). Of recent concern to operational meteorologists, the media, and county emergency managers is the desensitization of the public to tornado warnings. A recent 5-yr climatology of tornado false alarm rates shows how difficult it still remains to accurately detect and warn for a tornado (Brotzge et al. 2011), providing more persuasive evidence of the need to document, study, and consider local features for the possibility of anomalous trends in tornado frequencies and distributions.

There is growing body of literature (for a review, see Pielke et al. 2011) indicating land surface heterogeneity can impact the evolution of mesoscale convective systems. As discussed for instance in Holt et al. (Holt et al. 2006) and Niyogi et al. (Niyogi et al. 2006), landscape heterogeneity may alter the mesoscale convergence and energetics of the storm system from the microscale to the mesoscale. Studies such as Kellner et al. (Kellner et al. 2012) and Bozeman et al. (Bozeman et al. 2012) suggest possible larger-scale feedback of the land heterogeneity altering the storm track and sustenance of even tropical systems. Indeed, a number of factors need to work in concert with each other to lead to the evolution of a thunderstorm into a tornadic thunderstorm, and it is difficult to attribute surface processes as being a dominant factor. However, as discussed in Shepherd et al. (Shepherd et al. 2009), the intent of this climatology and spatial

assessment is to provide forecasters with additional local environmental factors they can consider in the forecast process as they seek to develop tornado watches or as they seek to issue a tornado warning on a storm. To that end, one additional goal of this assessment is to evaluate if there is any potential signature of landscape heterogeneity on tornado climatology, which until this time has been poorly studied.

Observations of tornadoes occurred long before national databases began keeping official records (1950) with the first photographed tornado documented in August 1884 approximately 20 miles southwest of Howard, South Dakota (Ross et al. 2011). The United States is well known for its "Tornado Alley," a region primarily covering Texas, Oklahoma, Kansas, Nebraska, southwestern Iowa, eastern South Dakota, and eastern Colorado (Edwards 2011) that has an increased risk for strong and violent tornadoes (as adapted by Concannon et al. 2000). However, the Midwest (defined here as Wisconsin, Michigan, Illinois, Indiana, Kentucky, and Ohio) sees a fair amount of tornadoes, such as the 1965 Palm Sunday outbreak and the 1974 super outbreak. In recent years, some national tornado climatologies have identified the Midwest as a branch or corridor extending from Tornado Alley, where an increase in tornado frequency is documented, more specifically through Illinois and into Indiana, especially when reviewed for strong (F2–F5) tornadoes (Agee and Zurn-Birkhimer 1998; Concannon et al. 2000; Rauber et al. 2005; Ashley 2007; Dixon et al. 2011).

Tornadoes form in many environments and form with different types of convection, which are all observed in Indiana: quasi-linear convective system (QLCS) tornadoes (50% of Indiana's reported tornadoes; e.g., Trapp et al. 2005), supercell tornadoes, low-top mini supercell tornadoes, landspout tornadoes, and gustnadoes, as well as tornado outbreaks (Agee and Jones 2009). The severe weather and tornadic environment on the Great Plains, by contrast, is more commonly impacted discrete cells/supercells (Smith et al. 2012). While national tornado climatologies show an increased frequency of tornadoes over Indiana, only two other climatologies for the state have been completed (Agee 1970; Pryor and Kurzhal 1997). This temporal and spatial climatology serves to complement these past studies, adding an additional decade of tornado data to the most current climatology for the state of Indiana (Pryor and Kurzhal

1997). The current sample size of annual tornado data and the amount of errors in the tornado databases the United States limits the scientific community's ability to decipher significant trends (e.g., Doswell 2007; Kunkel et al. 2013). Hence, the scientific community is encouraged to update severe weather and tornado reports to increase the sample size and make note of any evolving trends, especially as the United States continues to experience climate variability.

This climatology considers several variables instead of focusing on one: temporal analysis; ENSO; extreme climate events; population; and spatial distribution in relation to land surface characteristics such as land-use/land-cover (LULC) boundaries, topography, and surface roughness. The impact of LULC/land surface heterogeneity on mesoscale circulations and boundary layer destabilization has been studied for years (Clark and Arritt 1995; Pielke 2001; Mahmood et al. 2012) with tornadic environments analyzed as discussed in Cheresnick and Basara (Cheresnick and Basara 2005). It is studies such as these on land surface feedbacks to the storm environment that motivates this climatology to investigate the spatial distribution of tornado touchdown points in Indiana. Indiana is more specifically chosen for the following reasons: 1) uncertainties in tornado climatology datasets and the authors' familiarity with the state's weather and climate; 2) it is a land-locked state (except for those counties along Lake Michigan, which experience localized climate feedbacks), providing for local mesoscale feedbacks to develop across the state between land-cover and land-use transition zones instead of land and water boundaries; 3) a vast majority of tornadoes in Indiana are weak [i.e., enhanced Fujita scale 0 (EF0) to EF1] and are not driven by classic supercell dynamics: this suggests surface feedbacks can have a larger impact on surface heat and moisture fluxes that may interact with convective processes; and 4) the urban climate appears to influence or modify thunderstorms and rainfall patterns (e.g., Bornstein and Lin 2000; Niyogi et al. 2011), of which Indiana has sharply contrasting urban locales surrounded by agriculture land use.

2. Methodology

The geospatial dataset developed for this Indiana tornado climatology is obtained and developed from the Storm Prediction Center (SPC) Severe Geographic Information System (SVRGIS) database. "Tornado" and "states" shapefiles (the tornado shapefile is for tornado touchdown points in 1950–2011; 2012 is still considered preliminary at the time of this study) are downloaded and queried to extract and create shapefiles for the Midwest (Ohio, Indiana, Kentucky, Michigan, and Illinois). The tornado shapefile is a point shapefile that plots the starting latitude and longitude of a tornado (touchdown location). A 2010 U.S. Census population density raster file is also obtained from the SPC SVRGIS website (http://www.spc.noaa.gov/gis/svrgis/) for population analysis. Multiple queries are completed on the tornado shapefile from the SVRGIS webpage to create a Midwest F0–F5 tornadoes shapefile to use for analysis. The ArcGIS 10.1 spatial analyst tool for point density is applied to the point shapefile dataset to create a spatially interpolated shapefile that shows the highest and lowest locations of tornado touchdown point density in Indiana (Figure 1). The touchdown point density file is a spatial plot of the calculated magnitude per unit area (square kilometers) of point features (tornado touchdown points) that fall within a neighborhood (defined as 28 000 km^2, a default suggested value by the spatial interpolation algorithm within the GIS based on the size/area of the map data frame) around each cell. Simply put, it is the total number of points that fall within the specified neighborhood around a cell divided by the area of the neighborhood. "Natural breaks" is used to compute the density histogram with 18 classes. Natural breaks is a method of classification that seeks to find natural classes within the dataset histogram by optimally reducing the variance within classes while maximizing the variance between classes (de Smith et al. 2013). The tornado touchdown density raster file is smoothed with a bilinear interpolation filter for aesthetic appeal. The F scale is used instead of the EF scale because a majority of tornadoes in the NCDC database and all of the tornadoes in the SPC SVR GIS files are classified with F-scale rankings. A Midwest tornado shapefile is used instead of an Indiana shapefile in order to provide continuity to the density map across state borders. The spatial density distribution maps represent a general spatial distribution pattern, not an exact density distribution pattern.

This results from the use of several different map projections for the completion of this climatology that may result in plotting errors.

3. Discussion of Findings

3.1. Temporal Data

3.1.1. Tornado day and daily temporal distributions

A tornado day climatology for 1950–2012 is completed for Indiana for all tornadoes (F0–F5), weak tornadoes (F0–F1), and strong tornadoes (F2–F5). A tornado day in this study is developed from the definition proposed in Changnon and Schickedanz (Changnon and Schickedanz 1969) and equates a tornado day as a day with at least one tornado report (see also Shepherd et al. 2009). This provides an idea of how many days are favorable for tornadogenesis in a given year and month across Indiana. Storm reports are not used because of a noted bias of multiple reports for the same tornado. Tornado day information for Indiana is reviewed by month in efforts to determine seasonality and spatial shifts in seasonality if any are present and by 30-yr moving average to see if tornado days in Indiana have decreased, remained the same, or increased over time. A 30-yr moving average is used to follow the time frame of a climatic normal (Arguez and Vose 2011).

The temporal distribution of tornadoes in Indiana is analyzed via tornado days and is displayed in Tables 1 and 2. Bar graphs show the hourly distribution of tornado reports for 1950–2012, indicating the most likely time of day to see a tornado as shown in Figures 2–4. The hourly distribution of tornadoes is determined via storm report data, as time of report is required to see the hourly distribution. The most active time of day for weak tornadoes in local standard time (LST) is 1600–1900 LST; strong tornadoes have two active times, 1400–1600 LST and 1700–2000 LST; and all tornadoes are most active at 1600–2000 LST. Note that some days listed in the first column of Table 1 are also listed in the second column but not in the third column of Table 1. This demonstrates that 1) a majority of Indiana's tornado days are more conducive to weak tornadoes and 2) all years having an F2–F5 tornado day count greater than one standard deviation above the

average occurred before the implementation of the Fujita scale in 1974, except for 1980. This shows the bias nature of higher F-scale rankings preceding the development of the Fujita scale (McCarthy 2003; McCarthy et al. 2006; Edwards et al. 2013).

The 30-yr moving averages for annual tornado days are computed for all tornadoes, weak tornadoes, and strong tornadoes for the study region and are listed in Table 3. Regression analysis of the 30-yr moving averages for 1950–2012 show an insignificant very slight decrease in annual tornado days for all tornadoes, a slight increase in annual tornado days for weak tornadoes, and a slight decrease in annual tornado days for strong tornadoes.

The 30-yr moving averages for annual tornado days are also found by climate division. Indiana has nine climate divisions, allowing for tornado day analysis at a finer spatial scale. Annual tornado days for all tornadoes (F0–F5) for 1950–2012 are found and show a 30-yr moving average decrease in the number of annual tornado days in climate divisions 2 (north central), 3 (northeast), 4 (west central), 5 (central), and 6 (east central). Climate division 1 (northwest) has a steady 30-yr moving average with an average of 2 tornado days a year for 1950–75, 1 tornado day a year for 1976–92, and 2 tornado days a year for 1993–present. Climate divisions 7 (southwest), 8 (south central), and 9 (southeast) all show a 30-yr moving average increase in annual tornado days for 1950–2012. Climate divisions 7 and 8 see an increase in the 30-yr moving average number of annual tornado days from 1 tornado day a year to 3 days a year. Climate division 9 experiences the greatest increase in annual tornado days through time, increasing from 1 annual day on average to 4 annual days on average. Monthly analysis by climate divisions shows that the most tornado days for 1950–2012 are documented during the month of June in climate divisions 1, 2, 3, 4, 5, and 6, with the southernmost climate divisions peaking in monthly tornado days in May. These results highlight the scale dependency of the analysis.

3.1.2. ENSO and extreme precipitation relationships to tornado day distribution, 1950–2012

The 2012 drought is one example of an extreme climatic event potentially exacerbated by ENSO/La Niña. For this climatology, the oceanic Niño index (ONI) is used to determine El Niño, neutral, or La Niña years, with a minimum of 5 months of a 0.5 or greater anomaly for an El Niño or at or below the −0.5 anomaly for a La Niña. A comparison of tornado days and ENSO phase during the warm season months of April–September show no distinguishing trend in forecasting above or below active tornado seasons based on ENSO phase. Recently, Lee et al. (Lee et al. 2013) distinguish the trans-Niño index (TNI) and its relationship to the number of detrended intense tornadoes in the United States. Their findings cannot be readily compared to this study, as this climatology reviews all tornado days and Lee et al. (Lee et al. 2013) focus on tornado outbreak years. Lee et al. (Lee et al. 2013) identify 7 years from their list of top 10 extreme tornado outbreak years occurring with the transition of a La Niña to a different phase or occurring with a La Niña that persists beyond April and May while the TNI is in a positive phase: 1957, 1965, 1974, 1999, and 2008. Lee et al. (Lee et al. 2013) also identify the extreme years of 1983 and 1998 occurring with an El Niño transitioning to either a La Niña or neutral phase. Of these years, 1957, 1965, 1998, and 2008 are years listed in this tornado day climatology as years with annual tornado days one standard deviation or greater than the annual mean. Worth noting in this climatology are the years 1954, 1965, and 1973, which have some of the highest number of tornado days in the dataset. Each of these active years coincides with a 1.3, 1.6, and 1.8 swing of ENSO anomaly of El Niño to La Niña (1954), La Niña to El Niño (1965), and El Niño to La Niña (1973) when compared to the previous warm season (April–September) average anomaly. These findings, along with Lee et al. (Lee et al. 2013), suggest it is the rate and degree to which the ENSO phase transitions that may serve as in indicator of a more active or less active year for tornado outbreaks and tornado days. Maps of tornado touchdown point density are generated for La Niña, neutral, and El Niño years to see if any spatial shifts occur in tornado touchdown based on ENSO phase. Each phase shows

spatial variation in the density of tornado touchdown points (Figures 5–7). Density difference maps between ENSO neutral touchdown points and El Niño touchdown points and between ENSO neutral touchdown points and La Niña touchdown points is provided in Figures 8 and 9. A marked decrease of tornado touchdown points is seen during ENSO neutral events primarily across northwestern Indiana (climate division 1).

The 2011 tornado season is one the most active on record and is then followed by a relatively quiet season in 2012 with a majority of the country experiencing drought conditions through spring and summer. This study investigates the possibility of using drought years (85% of normal), normal years (those not 85% below normal or 15% above normal), and climatologically wet years (15% above normal) as indicators to expect more or less active tornado years. This process follows the wet/dry conditions and tornado occurrence as hypothesized in Shepherd et al. (Shepherd et al. 2009). Using an approach similar to Shepherd et al. (Shepherd et al. 2009), this study uses monthly state precipitation totals to determine cumulative antecedent rainfall amounts for 6 months prior (October, November, and December of previous year and January, February, and March of that year), 3 months prior (January, February, and March of that year), and 1 month prior to tornado season (March of that year) and compares total rainfall amounts to the number of tornado days for that year. Resulting data classes are as follows: 6-month drought and 6-month normal; 6-month wet and 6-month normal; 3-month drought and 3-month normal; 3-month wet and 3-month normal; 1-month drought and 1-month normal; and 1-month wet and 1-month normal.

A weak to moderate statistically significant (unpaired *t* test) correlation of −0.34 is found between 6-month normal rainfall and annual tornado days when classified into drought and normal 6-month cumulative rainfall classes (relationship: normal rainfall is equal to average or decreased tornado days). Alternatively, a weak, statistically significant correlation of 0.22 is found between 6-month drought conditions and annual tornado days when classified into drought and normal cumulative rainfall classes (relationship: drought is equal to increased tornado days). A weak, statistically significant correlation of −0.25 is found between 3-month total normal rainfall and annual tornado days when classified into drought and normal cumulative rainfall for the 3-month period

(relationship: normal rainfall is equal to average to decreased tornado days). When separating antecedent rainfall totals into wet and normal seasons, a weak to moderate statistically significant correlation of −0.30 is found between the 3-month cumulative wet conditions (relationship: wetter than normal is equal to decreased tornado days) and annual tornado days, and a weak, statistically significant correlation of 0.23 is found between normal rainfall and annual tornado days when separated into normal and wet classes (relationship: normal is equal to increased tornado days).

These findings look to be opposite of those found by Shepherd et al. (Shepherd et al. 2009) and Andersen and Shepherd (Andersen and Shepherd 2011) for the southeast United States but may be self-consistent. In that, for the southeast, Shepherd et al. (Shepherd et al. 2009) find a decrease in tornado days during spring when drought is present prior to tornado season, suggesting that the dynamic energetics of the region is such that the tornadic potential of storm systems shifts from the southeast and is more prevalent over the Midwest. Results in this study suggest that a 1-, 3-, and 6-month antecedent soil moisture/rainfall feedback hypothesis is sensitive to the length of cumulative rainfall/soil moisture and different hydroclimatic responses stemming from different land use/land cover, different synoptic-scale storm tracks and subsequent mesoscale storm environments, or a combination of both for each location. In general, this analysis shows weak statistically significant correlations that wetter than normal conditions at 3 and 6 months result in decreased average annual tornado days and that drought conditions at 3 and 6 months result in increased average annual tornado days.

3.2. Spatial analysis

ArcGIS 10.1 is used to develop the F0–F5 tornado touchdown point density map mentioned in the following discussion of spatial analyses. The tornado touchdown density map is compared to 1) a U.S. Census Bureau 2010 population density (people per square kilometer) raster file; 2) land surface features such as urban centers; 3) large changes in elevation (with respect to the overall change of elevation within the study domain); and 4) areas of land surface or land-use heterogeneity.

3.2.1 Population and tornado touchdown point distribution

Multiple studies in recent years highlight the population bias on the number of tornadoes reports, with the specific influence of tornado spotting and reporting through increased involvement of storm spotters (McCarthy 2003; McCarthy et al. 2006; Anderson et al. 2007). Past population and tornado report studies agree with a general understanding that the more (fewer) people in a given area, the more (fewer) people that are likely to see and report a tornado (Anderson et al. 2007). Our assessment takes a simple approach to assessing the impacts of Indiana's population distribution on tornado spotting and reporting: the 2010 U.S. Census population density (from SPC SVRGIS) is classified via natural breaks (previously described) into eight classes (class 1: 0–237; class 2: 238–847; class 3: 848–1779; class 4: 1780–3309; class 5: 3310–6497; class 6: 6498–13 879; class 7: 13 880–28 122; and class 8: 28 123–64 482) and converted into shapefiles for buffer analysis. Classes 7 and 8 are not found in Indiana (the SPC SVRGIS population raster file is a national dataset) and are omitted from analysis. Buffer analysis is completed with buffers applied at 1-, 2-, 3-, and 4-km distances from population class to count tornado touchdown points within each search radius. Class 1 of population density is not used, as it captures population density most likely not within/near a population center. Population classes 2–6 are present in Indiana and are used to determine if there is a population bias with documented tornadoes in Indiana. Results show that a large percentage of Indiana tornadoes have in fact touched down in regions of lower population density, with only a few tornadoes touching down within several kilometers of highly populated areas (Table 4). The correlation between the 2010 population density and number of reported tornadoes within 1–4 km is −0.80.

Although buffer analysis provides information on proximity of features to other features, an ideal method for this study, buffer analysis results in some biases that contribute to the strong anticorrelation found between population density and tornado touchdown points. Indiana is predominantly a rural state but has a majority of the state's population residing in urban centers. Because of this, Indiana's largest populations reside in a small fraction of the state's total land area. This results in a large decrease in the land

area encompassed by the applied buffers, thus decreasing the tornado count by default. The opposite is true for less populated land areas: larger amounts of land area occupied by smaller population density classes results in buffers covering a much larger amount of land area, capturing more tornado touchdown points. Therefore, it is likely that there is a population bias in tornado reporting present in Indiana. Weather professionals in the state of Indiana (and surrounding states) also agree that, in areas of low population density present in hilly and forested regions (e.g., southern Indiana), it is difficult to verify tornado touchdowns (D. McCarthy and J. Gordon, National Weather Service, 2013, personal communication). A similar point has been made with tornado detection in the Great Plains where land is largely agricultural and population is minimal. This scenario provides a decreased probability of visual observation/confirmation of a tornado and results in little to no damage indicators to verify tornado presence (Brooks et al. 2003a; Anderson et al. 2007).

3.2.2. Land surface heterogeneity

Studies have been completed for years showing that boundary layer feedbacks from LULC transition zones differing in latent and sensible heat fluxes can generate or enhance convection provided synoptic conditions are favorable for convection initiation (Clark and Arritt 1995; Pielke 2001; Niyogi et al. 2006; Niyogi et al. 2011; Boyles et al. 2007; Mahmood et al. 2010). Although roughly 50% of Indiana's tornadoes are QLCS tornadoes (Trapp et al. 2005) whose parent storms develop with strong synoptic forcing, there does appear to be more active regions of tornado touchdown points in Indiana that coincide with LULC. Indiana has two major LULC transition zones close to regions of enhanced tornadic activity: 1) forested hills of southern Indiana (topographic and vegetation variation) to flat farmland on the till plains and 2) larger, relatively urban areas such as Lafayette, Ft. Wayne, Indianapolis, and South Bend surrounded by rural farmland. A visual, spatial analysis of the possible land surface feedbacks between tornado touchdown locations and different land-use classifications, along with topography, is shown in Figures 10–13. The following two hypotheses are plausible for these regions: 1) Forested hills of southern Indiana to flat farmland on the till plains can generally present

atmospheric boundaries of moist static energy and surface roughness. If the synoptic environment is such that storm motion is southwest to the northeast, increased moist static energy (i.e., increased CAPE) from the forest may act to fuel the storm with surface roughness changes, resulting in local vorticity generation. 2) Urban environments result in temperature, moisture, and wind gradients/zones that can serve as sources of vorticity for storm ingestion and development into tornadoes. By default, urban areas result in a population bias to tornado reporting, but numerous accounts of tornadogenesis along local boundaries of moisture, temperature, or wind-shift lines (e.g. Markowski et al. 1998) support the possibility of urban environment contribution to localized increases in tornadogenesis near urban areas.

3.2.3. Land-use Classification Buffers

While currently not explicitly considered as part of the operational forecast process for the probability of tornado development, surface roughness has been analyzed for impacts on vortex dynamics for decades. Dessens (Dessens 1972) conducted a series of simple experiments exploring the effects of surface roughness on an air tornado model using two surface types: a smooth plate to simulate smooth flow and a wood plate with 6-mm pebbles to simulate a rough surface. Dessens's findings show that surface roughness acts to decrease the radius of maximum velocity while increasing the value of maximum vertical velocity (essentially increased stretching of the vortex column). This suggests that surface roughness resulting from features such as trees and houses results in a greater difference between the pressure gradient force and the centrifugal force at the ground boundary layer. This leads to larger convergence in this layer and a subsequent increase of vertical velocities in the vortex core. Dessens's (Dessens 1972) results lend support that land surface features may play a role in tornado touchdown location, as also found in our analysis. Diamond and Wilkins (Diamond and Wilkins 1984) show through laboratory experiments that the translation of tornadoes from different types of land cover (e.g., smooth to rough) can affect vortex size and structure resulting in the generation of a secondary vortex. These studies suggest important feedbacks occurring between the land surface and tornadoes. However, questions still remain regarding how storm-scale

dynamics control storm evolution and tornado development and when boundary layer land surface features may contribute to the storm evolution and/or tornado development (Elsom and Meaden 1982; Niyogi et al. 2011).

For the study domain, land-use/land-cover classification is completed using the 2005 enhanced historical land-use and land-cover datasets from the U.S. Geological Survey to assess the possible role of surface roughness associated with different types of LULC on tornadogenesis in Indiana. Polygon shapefiles of LULC data for Indiana are downloaded and separated into forest, urban, agriculture, barren, wetlands/water bodies, and rangeland shapefiles. Rangeland classification (land dominated by grasses and shrubs; Anderson et al. 1976) accounts for little land-cover classification in Indiana and contains no tornado touchdown points and thus is not part of the analysis. The majority of Indiana's land surface is agricultural; thus, it is not used in buffer analysis because of the bias it creates with tornado touchdown points being within a specified distance of agriculture land. Buffer analyses are completed on forest, urban, barren, and wetlands/water body shapefiles at 1 and 2 km for all tornadoes (F0–F5) and strong tornadoes (F2–F5).

The results from buffers on all tornadoes and strong tornadoes show little variation in the number of tornado touchdown points in relation to land-use category. For all tornadoes, buffer analysis shows 61% touching down within 1 km of urban land use, 43% touching down within 1 km of forest land use, 12% touching down within 1 km of wetland/water body land use, and 8% touching down within 1 km of barren land use. The 2-km buffer on all tornadoes results in 78% touching down within 2 km of urban land use, 65% touching down within 2 km of forest land use, 26% touching down within 2 km of wetland/water body land use, and 20% touching down within 2 km of barren land use. The decrease in percentage of tornado touchdown points as surface roughness decreases by land-use or land-cover type suggests the possible impact of surface roughness on boundary layer structure and tornado feedbacks.

Buffer analysis on strong tornado touchdown points shows similar spatial patterns in relation to land-use and land-cover classifications of urban, forest, wetland/water body, and barren land use. For strong tornadoes, buffer analysis shows 64% touching down

within 1 km of urban land use (Figure 14), 42% within 1 km of forest land use, 11% within 1 km of wetland/water body land use, and 7% within 1 km of barren land use. The 2-km buffer on strong tornadoes results in 80% touching down within 2 km of urban land use, 63% within 2 km of forest land use, 25% within 2 km of wetland/water body land use, and 21% within 2 km of barren land use. Again, the decrease in number of tornado touchdown points appears related to the decrease in surface roughness associated with land-use or land-cover type. While findings from this analysis lend support to increased tornado touchdowns in or near close proximity to land use or land cover associated with increased surface roughness, tornado touchdowns are documented to have impacted all land-use and land-cover types. Thus, although tornadoes in Indiana appear to favor touching down in or near regions of increased surface roughness, no causality can be identified from the analysis, and it is not to say that tornadogenesis should be disregarded over other land-use or land-cover types.

3.2.4. City centroid and urban area buffers

A city or town centroid is the geographic center of that city or town. This differs from the land-use categorization of urban area or land cover, as the land-use categorization is an area of land and the city centroid is a point. Incremental 1-km circular buffers at 1, 2, 3, …, and 20 km are applied around an "IN_Cities" point shapefile, which is inclusive of 70 cities, towns, census designated places, and consolidated cities in Indiana (Figure 15). A count of the number of tornado touchdown points within each search radius is determined and converted to a percentage of total tornadoes (1285 in all in the dataset for 1950–2011) within that distance. A regression analysis (Figure 16) is completed between the percentage of tornado touchdown points lying within the search radius and the distance of the search radius, revealing a linear trend in the number of observed tornado touchdown points with increasing distance from the city or town center. These findings are similar to those discussed in Elsom and Meaden (Elsom and Meaden 1982). The change in percentage of tornado touchdown points between 1-km buffer intervals experiences an increase of one standard deviation above the mean percentage change (2.8% km^{-1}) at the 2-, 14-, and 15-km range from the

centroid location. To identify any possible relationship between urban land areas in square kilometers, the same buffer analysis process is completed on an urban area shapefile for 1–10-km distances. When analyzing the number of tornado touchdown points in relation to a distance from urban land areas 20 km^2 in area and greater, a linear trend is also found. When looking at the change in percentage of tornado touchdown points between 1-km intervals there are again two buffers that show an increase of one standard deviation above the mean percentage change (1.9% km^{-1}) at the 3- and 8-km range from the edge of the urban area. These "rings" of slightly increased tornado touchdown points are similar to the suggested "tornado belt" coined by Fujita (Fujita 1973) after Fujita's review of 14 tornadoes around Tokyo from 1962 to 1971 (Elsom and Meaden 1982). The noted increase in percentage of tornado touchdown points at 2, 14, and 15 km for city centroids and 3 and 8 km for urban areas greater than 20 km^2 suggest the possibility of preferential occurrence of tornadoes with respect to urban boundaries that develop near these locations.

3.2.5. Elevation/topography

Coleman (Coleman 2010) and Bosart et al. (Bosart et al. 2004) discuss the possible role of topography on the generation of increased local vorticity, contributing favorable to tornadogenesis with an emphasis on river valleys and mountains/hills and associated valleys. To investigate the possibility of this occurring in Indiana, a digital elevation model (DEM) in raster format is downloaded and used to develop a digital elevation model shapefile. The slope tool in ArcGIS is used to compute changes in slope (in degrees) to assess if changes in elevation have any impact on tornado development within close proximity to sharp changes in elevation. Surface slope changes are categorized as 1) change in slope of 5° or more or 2) change in slope of less than 5° between each grid cell of the raster surface. The 5° change in slope over one DEM grid cell is selected because it represents an elevation change of roughly one-half of the total elevation change between Indiana's highest and lowest points (383 and 98 m, respectively). The raster surface is comprised of cells 94 m by 94 m; thus, the change in slope is computed over a distance of 94 m.

All tornadoes are once again reviewed in relation to elevation changes. Of all tornado touchdown points, 180 (14%) are located within 1 km of surface slope changing by 5° or more. Increasing the search distance to 2 km increases the amount of tornado touchdown points to 271 (21%). Strong tornadoes result in the same values: 53 of 380 (14%) strong tornadoes have touched down within 1 km of surface slope changing by 5° or more and 81 of 380 (21%) strong tornadoes have touched down within 2 km of surface slope changing by 5° or more. Changing the search radius to determine the number of tornadoes touching down within 1 km of surface slope changes of less than 5° results in 1281 of 1285 tornado touchdown points (F0–F5) being selected. For strong tornadoes, all 380 tornado touchdown points are selected. Changes in topography over short distances do not appear to have as strong as a relationship to the spatial location of tornado touchdowns in the relatively flat landscape across Indiana as compared to land-use type. However, the increased number tornado touchdown points east of the Knobstone Escarpment (a steep slope or cliff that results from erosion or faulting processes and separates two relatively level or more gently sloping areas of terrain) where the Scottsburg Lowlands rise into the Muscatatuck Plateau and Dearborn Uplands (Figure 17) suggest possible terrain feedbacks such as those mentioned by Coleman (Coleman 2010) and Bosart et al. (Bosart et al. 2004).

4. Conclusions

Tornado day analysis for all, weak, and strong tornadoes in 1950–2012 shows a distinct spring tornado season in Indiana with a majority of tornado days more conducive to weak tornadoes. In Indiana, tornado days occur most frequently during the months of June, May, and July (descending order). These three months are also the defining season for weak tornado days. A slight shift in tornado day occurrence for strong tornadoes is seen with the greatest number of strong tornado days occurring during the months of April (37 days), June (37 days), and May (30 days) for the 1950–2012 period. These findings are comparative to the average tornado frequency by month (1991–2010) as May, June, and April (in descending order) (National Climatic Data Center 2013). Total tornado days per year have not increased through time and, when reviewed at 30-yr

climatological intervals, show a slight insignificant decrease in the average number of tornado days per year for all, weak, and strong tornadoes in Indiana similar to findings at the national level as discussed by McCarthy and Schaefer (McCarthy and Schaefer 2004). Thus, no trend or conclusions regarding tornado days per year for 1950–2012 can be made from this analysis, agreeing with findings presented in Kunkel et al. (Kunkel et al. 2013). From 1950 to 2012, the years that are most active in Indiana (total tornado days per year that are one standard deviation or greater) span the entire time frame of this study (1950–2012). However, reviewing tornado day data in terms of just strong tornadoes, there has not been an active year in Indiana since 1980. All other active years are 1968 or earlier, the time frame of historic tornado records that some studies suggest show a bias toward over classification of tornado intensity because of the procedures used to assign F-scale ranking prior to the development of the F scale (McCarthy 2003; McCarthy et al. 2006;Edwards et al. 2013). The most active time of day for weak tornadoes in local standard time (LST) is 1600–1900 LST; strong tornadoes have two active times, 1400–1600 LST and 1700–2000 LST; and all tornadoes are most active at 1600–2000 LST.

The spatial analysis of this climatology (touchdown distribution across the state) agrees with the findings of Ashley (Ashley 2007), Concannon et al. (Concannon et al. 2000), and Dixon et al. (Dixon et al. 2011). There are pronounced areas throughout central Indiana that show locales of enhanced tornado occurrences. The spatial location of increased tornado touchdown points in the northern portion of the state can be largely attributed to outbreak events, whereas the central Indiana axis of enhanced tornado activity is influenced by a larger variety of tornado events.

ENSO phases are not found to be related to the number of tornado days but do appear to impact the spatial distribution of tornado events across the state. The map of El Niño tornado touchdowns show that tornado touchdown points are more widespread but concentrated across central Indiana. The neutral phase map shows a pronounced region of tornado touchdown points that coincides with the overall F0–F5 tornado touchdown point distribution. The La Niña maps show that tornado touchdown points appear to be centrally located around Indianapolis and in a cluster in southwest Indiana but are more

widespread across northern Indiana. A predominant ENSO phase does not appear to favor more or fewer tornado days in a given year across Indiana; however, the rate and intensity at which ENSO phase changes occur may impact the tornado season (Lee et al. 2013). Antecedent cumulative rainfall amounts 6 and 3 months prior to a given year's tornado season when separated into normal and drought conditions, along with 3 months prior when separated into normal and wet conditions appear to have a slight trend toward fewer annual tornado days for the following season/year.

Antecedent rainfall analysis of drought and normal conditions and then wetter than normal and normal conditions at 1, 3, and 6 months is completed for the study domain to identify possible soil moisture memory feedbacks to the convective storm environment. This analysis shows weak, statistically significant correlations that wetter than normal conditions at 3 and 6 months result in decreased average annual tornado days and that drought conditions at 3 and 6 months result in increased average annual tornado days.

Population distribution appears to play a role in the recorded number of tornadoes in Indiana, with the largest density of tornado touchdown points near the most densely populated county in the state. However, population bias may not be the sole contributing factor to the spatial distribution of tornado reports. Buffer analysis completed with city centroids and urban land areas shows a large percentage of total tornadoes touching down in low population density areas. This is likely a result of buffer analysis and population density clustering, as explained previously. Until tornado touchdown verification processes in some parts of the study domain are improved, the consensus of tornado touchdown locations having a population bias cannot be confidently made.

Land surface heterogeneity and associated surface roughness of land surface type appear to have a relationship with tornado touchdown locations in the study domain. Buffer analysis on land-use types show that for all tornadoes 61% have touched down within 1 km of urban land use and 43% have touched down within 1 km of forest land use. A total of 64% and 42% of strong tornadoes have touched down in urban and forest land-use types, respectively. The percentage of tornadoes touching down within 1 km of land use with decreased surface roughness (water bodies and barren land use) is found to

be much lower. Changes in topography over short distances do not appear to have as strong as a relationship to the spatial location of tornado touchdowns in the relatively flat landscape across Indiana as compared to land-use type.

Recent assessment of urban thunderstorms over the Indianapolis region (Niyogi et al. 2011) shows a possible relationship between urban landscapes and thunderstorm structure and life cycles. Pryor and Kurzhal (Pryor and Kurzhal 1997) suggest a trend of tornado touchdown points from 1950 to 1995 being located in counties with high surface roughness values and decreased population densities. The concentric rings/buffers at 1-km intervals of tornado touchdown points from cities and towns in Indiana show similar distributions as those discussed in Elsom and Meaden (Elsom and Meaden 1982) in greater London for weak tornadoes and in Fujita (Fujita 1973) for tornadoes around Tokyo. Topographic and elevation influences visually appear to play a possible role in Indiana tornado touchdown locations as well: most specifically, east of the Knobstone Escarpment, where terrain-induced surface vorticity as described by Coleman (Coleman 2010) and Bosart et al. (Bosart et al. 2004) could be generated provided surface wind conditions or other features of the storm environment act favorably in this area.

The comprehensive tornado climatology presented herein investigates and assesses the possible role that different climatological features such as ENSO, antecedent rainfall conditions, population density, land use/land cover, and topography have on tornado climatology in Indiana. It is apparent that there are local as well as climate variability feedbacks to the 1950–2010 tornado climatology. Changes in surface roughness and surface energy budgets associated with land surface heterogeneity appear to play a possible role in tornado touchdown locations because of the generation of local vorticity boundaries. Identification of land-use transition zones in convectively unstable environments while forecasters try to identify tornadogenesis may be worth considering as part of the forecast process in the future upon further analysis of land surface heterogeneity and tornado climatology. The GIS framework used in this study presents some limitations and uncertainties in the spatial climatology, especially with buffer analysis. Despite the visible population bias present in figures, tornado verification in

regions of the study domain remain a challenge, lending support to the premise that land surface heterogeneity may impact tornado climatology in Indiana.

Acknowledgements: We thank Evan Bentley, Northern Indiana National Weather Service, for help in assembling the tornado day climatology data and Dr. Ernest Agee, Purdue University, for review of portions of this manuscript. Research benefited in part by NASA Fellowship Grant 104798 awarded to O. Kellner, NSF STRONG Cities Project: NSF CBET 1250232, and Development of a High-resolution Drought Trigger Tool (HIRDTT) for the United States, Agriculture and Food Research Initiative Competitive Grant 2011-67019-20042.

References

Agee, E. M., 1970: The climatology of Indiana tornadoes. *Proc. Indiana Acad. Sci.*, 79, 299–308.

Agee, E. M., and S. Zurn-Birkhimer, 1998: Variations in USA tornado occurrences during El Niño and La Niña. *Proc. 19th Conf. on Severe Local Storms*, Minneapolis, MN, Amer. Meteor. Soc., 287–290.

Agee, E. M., and E. Jones, 2009: Proposed conceptual taxonomy for proper identification and classification of tornado events. *Wea. Forecasting*, 24, 609–617, doi:10.1175/2008WAF2222163.1.

Andersen, T. K., and J. M. Shepherd, 2011: Seasonal predictability of tornadic activity using antecedent soil moisture conditions. Earthzine. [Available online at http://www.earthzine.org/2011/06/10/seasonal-predictability-of-tornadic-activity-using-antecedent-soil-moisture-conditions/.]

Anderson, C. J., C. K. Wikle, Q. Zhou, and J. A. Royle, 2007: Population influence on tornado reports in the United States. *Wea. Forecasting*, 22,571–579, doi:10.1175/WAF997.1.

Anderson, J. R., E. E. Hardy, J. T. Roach, and R. E. Witmer, 1976: A land use and land cover classification system for use with remote sensor data. United States Geological Survey Rep., 41 pp.

Arguez, A. A., and R. S. Vose, 2011: The definition of the standard WMO climate normal. *Bull. Amer. Meteor. Soc.*, 92, 699–704, doi:10.1175/2010BAMS2955.1.

Ashley, W. S., 2007: Spatial and temporal analysis of tornado fatalities in the United States: 1880–2005. *Wea. Forecasting*, 22, 1214–1228, doi:10.1175/2007WAF2007004.1.

Bornstein, R., and Q. Lin, 2000: Urban heat islands and summertime convective thunderstoms in Atlanta: Three case studies. *Atmos. Environ.,* 34,507–516, doi:10.1016/S1352-2310(99)00374-X.

Bosart, L. F., K. LaPenta, A. Seimon, M. Dickinson, and T. J. Galarneau Jr., 2004, Terrain-influenced tornadogenesis in the northeastern United States. Preprints*, 11th Conf. on Mountain Meteorology and the Annual Mesoscale Alpine Program (MAP),* Bartlett, NH, Amer. Meteor. Soc., P17.3. [Available online at https://ams.confex.com/ams/pdfpapers/77126.pdf.]

Boyles, R., S. Raman, and A. Sims, 2007: Sensitivity of mesoscale precipitation dynamics to surface soil and vegetation contrasts over the Carolina Sandhills. *Pure Appl. Geophys.*, 164, 1547–1576, doi:10.1007/s00024-007-0227-2.

Bozeman, M. L., D. Niyogi, S. Gopalakrishnan, F. D. Marks Jr., X. Zhang, and V. Tallapragada, 2012: An HWRF-based ensemble assessment of the land surface feedback on the post-landfall intensification of Tropical Storm Fay (2008). *Nat. Hazards*, 63**,** 1543–1571, doi:10.1007/s11069-011-9841-5.

Brooks, H. E., C. A. Doswell III, and M. P. Kay, 2003a: Climatological estimates of local daily tornado probability for the United States. *Wea. Forecasting*, 18, 626–640, doi:10.1175/1520-0434(2003)018<0626:CEOLDT>2.0.CO;2.

Brooks, H. E., J. W. Lee, and J. P. Craven, 2003b: The spatial distribution of severe thunderstorm and tornado environments from global reanalysis data. *Atmos. Res.*, 67–68, 73–94, doi:10.1016/S0169-8095(03)00045-0.

Brotzge, J., S. Erickson, and H. Brooks, 2011: A 5-yr climatology of tornado false alarms. *Wea. Forecasting*, 26, 534–544, doi:10.1175/WAF-D-10-05004.1.

Changnon, S. A., 1982: Trends in tornado frequencies. *Proc. 12th Conf. on Severe Local Storms*, San Antonio, TX, Amer. Meteor. Soc., 42–44.

Changnon, S. A., and P. T. Schickedanz, 1969: Utilization of hail-day data in designing and evaluating hail suppression projects. *Mon. Wea. Rev.*, 97, 95–102, doi:10.1175/1520-0493(1969)097<0095:UOHDID>2.3.CO;2.

Cheresnick, D. R., and J. B. Basara, 2005: The impact of land–atmosphere interactions on the Benson, MN tornado of 11 June 201l. *Bull. Amer. Meteor. Soc.*, 86, 637–642, doi:10.1175/BAMS-86-5-637.

Clark, C., and R. Arritt, 1995: Numerical simulations of the effect of soil moisture and vegetation cover on the development of deep convection. *J. Appl. Meteor.*, 34, 2029–2045, doi:10.1175/1520-0450(1995)034<2029:NSOTEO>2.0.CO;2.

Coleman, T. A., 2010: The effects of topography and friction on mesocyclones and tornadoes. Preprints, *25th Conf. on Severe Local Storms,*Denver, CO, Amer. Meteor. Soc., P8.12.

Concannon, P. R., H. E. Brooks, and C. A. Doswell III, 2000: Climatological risk of strong and violent tornadoes in the United States. Preprints,*Second Symp. Environmental Applications,* Long Beach, CA, Amer. Meteor. Soc., 9.4.

Cook, A. R., and J. T. Schaefer 2008: The relation of El Niño–Southern Oscillation (ENSO) to winter tornado outbreaks. *Mon. Wea. Rev.,* 136**,** 3121–3137, doi:10.1175/2007MWR2171.1.

de Smith, M., P. Longley, and M. Goodchild, cited 2013: Geospatial analysis: A comprehensive guide. [Available online athttp://www.spatialanalysisonline.com/HTML/index.html.]

Dessens, J., Jr., 1972: Influence of ground roughness on tornadoes: A laboratory simulation. *J. Appl. Meteor.*, 11, 72–75, doi:10.1175/1520-0450(1972)011<0072:IOGROT>2.0.CO;2.

Diamond, C. J., and E. M. Wilkins, 1984: Translation effects on simulation tornadoes. *J. Atmos. Sci.*, 41, 2574–2580, doi:10.1175/1520-0469(1984)041<2574:TEOST>2.0.CO;2.

Dixon, P. G., A. E. Mercer, J. Choi, and J. S. Allen, 2011: Tornado risk analysis: Is Dixie Alley an extension of Tornado Alley? *Bull. Amer. Meteor. Soc.*, 92, 433–441, doi:10.1175/2010BAMS3102.1.

Doswell, C. A., III, 2007: Small sample size and data quality issues illustrated using tornado occurrence data. *Electron. J. Severe Storms Meteor.*, 2(5), 1–16.

Edwards, R., cited 2011: Frequently asked questions about tornadoes. Storm Prediction Center. [Available online athttp://www.spc.noaa.gov/faq/tornado/#About.]

Edwards, R., J. G. LaDue, J. T. Ferree, K. Scharfenberg, C. Maier, and W. L. Coulbourne, 2013: Tornado intensity estimation. *Bull. Amer. Meteor. Soc.,* 94, 641–653, doi:10.1175/BAMS-D-11-00006.1.

Elsom, D. M., and G. T. Meaden, 1982: Suppression and dissipation of weak tornadoes in metropolitan areas: A case study of greater London.*Mon. Wea. Rev.*, 110, 745–756, doi:10.1175/1520-0493(1982)110<0745:SADOWT>2.0.CO;2.

Fujita, T. T., 1973: Tornadoes around the world. *Weatherwise*, 26, 56–83, doi:10.1080/00431672.1973.9931633.

Holt, T., D. Niyogi, F. Chen, M. A. LeMone, K. Manning, and A.L.Qureshi, 2006: Effect of land–atmosphere interactions on the IHOP 24–25 May 2002 convection case. *Mon. Wea. Rev.*, 134, 113–133, doi:10.1175/MWR3057.1.

Kellner O., D. Niyogi, M. Lei, A. Kumar 2012: The role of anomalous soil moisture on the inland reintensification of Tropical Storm Erin (2007).*Nat. Hazards*, 63**,** 1575–1600, doi:10.1007/s11069-011-9966-6.

Kis, A. K., and J. M. Straka, 2010: Nocturnal tornado climatology. *Wea. Forecasting,* 25, 545–561, doi:10.1175/2009WAF2222294.1.

Kunkel, K., and Coauthors, 2013: Monitoring and understanding trends in extreme storms. *Bull. Amer. Meteor. Soc.*, 94, 499–514, doi:10.1175/BAMS-D-11-00262.1.

Lee, S. K., R. Atlas, D. Enfield, C. Wang, and L. Hailong, 2013: Is there an optimal ENSO pattern that enhances large-scale atmospheric processes conducive to tornado outbreaks in the United States? *J. Climate*, 26, 1626–1642, doi:10.1175/JCLI-D-12-00128.1.

Mahfouf, J.F., E. Richard, and P. Mascart, 1987: The influence of soil and vegetation on the development of mesoscale circulations, J. Climate Appl. Meteor., 26, 1483-1495.

Mahmood, R., and Coauthors, 2010: Impacts of land use/land cover change on climate and future research priorities. *Bull. Amer. Meteor. Soc.*, 91, 37–46, doi:10.1175/2009BAMS2769.1.

Mahmood, R., A. Littell, K. G. Hubbard, and J. You, 2012: Observed data-based assessment of relationships among soil moisture at various depths, precipitation, and temperature. *Appl. Geogr.*, 34, 255–264, doi:10.1016/j.apgeog.2011.11.009.

Markowski, P. M., E. N. Rasmussen, and J. M. Straka, 1998: The occurrence of tornadoes in supercells interacting with boundaries during VORTEX-95. *Wea. Forecasting*, 13, 852–859, doi:10.1175/1520-0434(1998)013<0852:TOOTIS>2.0.CO;2.

Mayes, B. E., C. Cogil, G. R. Lussky, J. S. Boyne, and R. Ryrholm, 2007: Tornado and severe weather climatology and predictability by ENSO phase in the north central U.S.: A compositing study. Preprints, *19th Conf. on Climate Variability and Change,* San Antonio, TX, Amer. Meteor. Soc., JP4.17. [Available online at https://ams.confex.com/ams/pdfpapers/117083.pdf.]

McCarthy, D. W., 2003: NWS tornado surveys and the impact on the National Tornado Database. Preprints, *First Symp. F-Scale and Severe-Weather Damage Assessment,* Long Beach, CA, Amer. Meteor. Soc., 3.2. [Available online at https://ams.confex.com/ams/pdfpapers/55718.pdf.]

McCarthy, D. W., and J. Schaefer, 2004: Tornado trends over the past thirty years. Preprints, *14th Conf. Applied Climatology*, Seattle, WA, Amer. Meteor. Soc., 3.4. [Available online at https://ams.confex.com/ams/pdfpapers/72089.pdf.]

McCarthy, D. W., J. Schaefer, and R. Edwards, 2006: What are we doing with (or to) the F-Scale? Preprints, *23rd Conf. Severe Local Storms,* St. Louis, MO, Amer. Meteor. Soc., 5.6. [Available online at https://ams.confex.com/ams/pdfpapers/115260.pdf.]

National Climatic Data Center, cited 2013: U.S. tornado climatology. [Available online athttp://www.ncdc.noaa.gov/oa/climate/severeweather/tornadoes.html.]

Niyogi, D., T. Holt, S. Zhong, P. C. Pyle, and J. Basara, 2006: Urban and land surface effects on the 30 July 2003 mesoscale convective system event observed in the southern Great Plains. *J. Geophys. Res.*, 111, D19107, doi:10.1029/2005JD006746.

Niyogi, D., P. Pyle, M. Lei, S. Pal Arya, C. M. Kishtawal, M. Shepherd, F. Chen, and B. Wolfe, 2011: Urban modification of thunderstorms: An observational storm climatology and model case study for the Indianapolis urban region. *J. Appl. Meteor. Climatol.*, 50, 1129–1144, doi:10.1175/2010JAMC1836.1.

Nunn, K. H., and A. T. DeGaetano, 2004: The El Niño-Southern Oscillation and its role in cold-season tornado outbreak climatology. Preprints, *14th Conf. on Applied Climatology*, Seattle, WA, Amer. Meteor. Soc., JP5.2. [Available online athttps://ams.confex.com/ams/pdfpapers/71587.pdf.]

Pielke, R. A., Sr., 2001: Influence of the spatial distribution of vegetation and soils on the prediction of cumulus convective rainfall. *Rev. Geophys.*, 39, 151–177, doi:10.1029/1999RG000072.

Pielke, R. A., Sr., and Coauthors, 2011: Land use/land cover changes and climate: Modeling analysis and observational evidence. *Wiley Interdiscip. Rev.: Climate Change,* 2**,** doi:10.1002/wcc.144.

Pryor, S. C., and T. Kurzhal, 1997: A tornado climatology for Indiana. *Phys. Geog.*, 18, 525–543.

Rauber, R. M., J. E. Walsh, and D. J. Charlevoix, 2005: *Severe and Hazardous Weather: An Introduction to High Impact Meteorology.* 2nd ed. Kendall Hunt, 558 pp.

Rhome, J. R., D. Niyogi, and S. Raman, 2000: Mesoclimatic analysis of severe weather and ENSO interactions in North Carolina. *Geophys. Res. Lett.*, 27, 2269–2272, doi:10.1029/1999GL011327

Rose, S. F., P. V. Hobbs, J. D. Locatelli, and M. T. Stoelinga, 2004: A 10-yr climatology relating the locations of reported tornadoes to the quadrants of upper-level jet streaks. *Wea. Forecasting*, 19, 301–309, doi:10.1175/1520-0434(2004)019<0301:AYCRTL>2.0.CO;2.

Ross, T., N. Lott, A. Graumann, and S. McCown, cited 2011: Climate-Watch, April 2001. National Oceanic and Atmospheric Administration/National Climatic Data Center. [Available online at http://www.ncdc.noaa.gov/oa/climate/extremes/2001/april/extremes0401.html.]

Schneider, R., J. D. Schaefer, and H. E. Brooks, 2004: Tornado outbreak days: An updated and expanded climatology (1875-2003). Preprints, *22nd Conf. on Severe Local Storms,* Hyannis, MA, Amer. Meteor. Soc., P5.1. [Available online at https://ams.confex.com/ams/pdfpapers/82031.pdf.]

Shepherd, M., D. Niyogi, and T. Mote, 2009: A seasonal-scale climatological analysis correlating spring tornadic activity with antecedent fall-winter drought in the southeastern United States. *Environ. Res. Lett.*, 4, 024012, doi:10.1088/1748-9326/4/2/024012.

Smith, B. T., R. L. Thompson, J. S. Grams, C. Broyles, and H. E. Brooks, 2012: Convective modes for significant severe thunderstorms in the contiguous United States. Part I: Storm classification and climatology. *Wea. Forecasting*, 27, 1114–1135, doi:10.1175/WAF-D-11-00115.1.

Tescon, J. J., T. T. Fujita, and R. F. Abbey Jr., 1983: Statistical analyses of U.S. tornadoes based on the geographic distribution of population, community, and other parameters. *Proc. 13th Conf. on Severe Local Storms,* Tulsa, OK, Amer. Meteor. Soc., 120–123.

Trapp, R. J., S. A. Tessendorf, E. S. Godfrey, and H. E. Brooks, 2005: Tornadoes from squall lines and bow echoes. Part I: Climatological distribution. *Wea. Forecasting*, 20, 23–34, doi:10.1175/WAF-835.1.

Twisdale, L. A., 1982: Regional tornado data base and error analysis. *Proc. 12th Conf. on Severe Local Storms,* San Antonio, TX, Amer. Meteor. Soc., 45–50.

Tables

Table 1 (A-C): (A) A list of the active tornado day years for all tornadoes defined by having the total number of tornado days one standard deviation (4 days) or more above the mean (9 days). (B) A list of the active tornado day years for weak tornadoes defined as defined by having the total number of tornado days one standard deviation (4 days) or more above the mean (7 days). (C) A list of the active tornado day years for strong tornadoes defined as having the total number of tornado days one standard deviation (3 days) or more above the mean (3 days).

A) Years 1 Standard Deviation above Average Annual Number of Tornado Days (F0-F5) 1950-2012		**B) Years 1 Standard Deviation above Average Annual Number of Tornado Days (F0-F1) 1950-2012**		**C) Years 1 Standard Deviation above Average Annual Number of Tornado Days (F2-F5) 1950-2012**	
1954: 20 days	1978: 14 days	1954: 12 days	1996: 11 days	1954: 11 days	1963: 7 days
1961: 15 days	1992: 14 days	1973: 18 days	1998: 13 days	1956-‘58: 7 days	1965: 11 days
1965: 19 days	1998: 14 days	1975: 13 days	2003: 17 days	1960: 6 days	1967: 9 days
1973: 21 days	2003: 17 days	1978: 14 days	2006: 11 days	1961: 13 days	1968: 6 days
1975: 13 days	2011: 15 days	1992: 13 days	2008: 11days	1962: 6 days	1980: 7 days
			2011: 14 days		

Table 2 (A-C): (A) A list of the total number of tornado days for all tornadoes (F0-F5) by month 1950-2012. The three most active months defining Indiana’s “tornado season” are the months of May, June, and July. (B): A list of the total number of tornado days for weak tornadoes by month 1950-2012. The three most active months defining Indiana’s “tornado season” for weak tornadoes only are the months of May, June, and July. (C): A list of the total number of tornado days for strong tornadoes by month 1950-2012. The three most active months defining Indiana’s “tornado season” for strong tornadoes only are the months of April, May, and June.

A) Number of F0-F5 Tornado Days by Month, 1950-2012				**B) Number of F0-F1 Tornado Days by Month, 1950-2012**				**C) Number of F2-F5 Tornado Days by Month, 1950-2012**			
January	10	July	89	January	8	July	73	January	4	July	24
February	12	August	49	February	10	August	36	February	4	August	14
March	35	September	29	March	26	September	21	March	22	September	11
April	78	October	20	April	64	October	16	April	37	October	8
May	104	November	17	May	84	November	11	May	30	November	10
June	128	December	6	June	98	December	3	June	37	December	4

Table 3 (A-C): (A) A list of the 30 year moving average number of tornado days per year for all tornadoes 1950-2012. (B): A list of the 30 year moving average number of tornado days per year for weak tornadoes. (C): A list of the 30 year moving average number of tornado days per year for strong tornadoes. Regression analysis shows a very slight decrease (-0.0036 slope) in F0-F5 annual average tornado days 1950-2012; a slight increase (0.0405 slope) in F0-F1 annual average tornado days 1950-2012; and a slight decrease (-0.032 slope) in F2-F5 annual average tornado days 1950-2012.

(A) 30 year Moving Average Annual Number of Tornado Days 1950-2012 (F0-F5)	**(B) 30 year Moving Average Annual Number of Tornado Days 1950-2012 (F0-F1)**	**(C) 30 year Moving Average Annual Number of Tornado Days 1950-2012 (F2-F5)**
11 days: 2011	**11 days**: 2011	**5 days**: 1950-1954
10 days: 1950-1957, 2000-2003, 2004-2009	**10 days**: 2003, 2010	**4 days**: 1955-1961
9 days: 1958-1977, 1984-1999	**9 days**: 1986-2002, 2004-2009	**3 days**: 1962-1967, 2004-2005, 2007-2008, 2011
8 days: 1978-1983	**8 days**: 1963, 1965, 1967-1985	**2 days**: 1968-2003, 2006, 2009-2010
7 days: 2012	**7 days**: 1951-1962, 1964, 1966, 2012	**1 day**: 2012
	6 days: 1950	

Table 4: Percentage of total tornado touchdown points 1950-2011 that fall within the designated distance in miles from the given population density (people per square km based on a national dataset) class. Only those population classes present in Indiana are included in this analysis.

Percentage of Total Tornadoes 1950-2012 (1285 total) within 1-4 km of Different 2010 Population Density Classes (People/km^2)

Class	**Class Range:**	**1 km**	**2 km**	**3 km**	**4 km**
Class 2	238-847	39	51	60	67
Class 3	848-1,779	24	30	35	41
Class 4	1,780-3,309	10	13	16	19
Class 5	3,310-6,497	1	2	3	4
Class 6	6,498-13,879	0	0	0	1

Figures

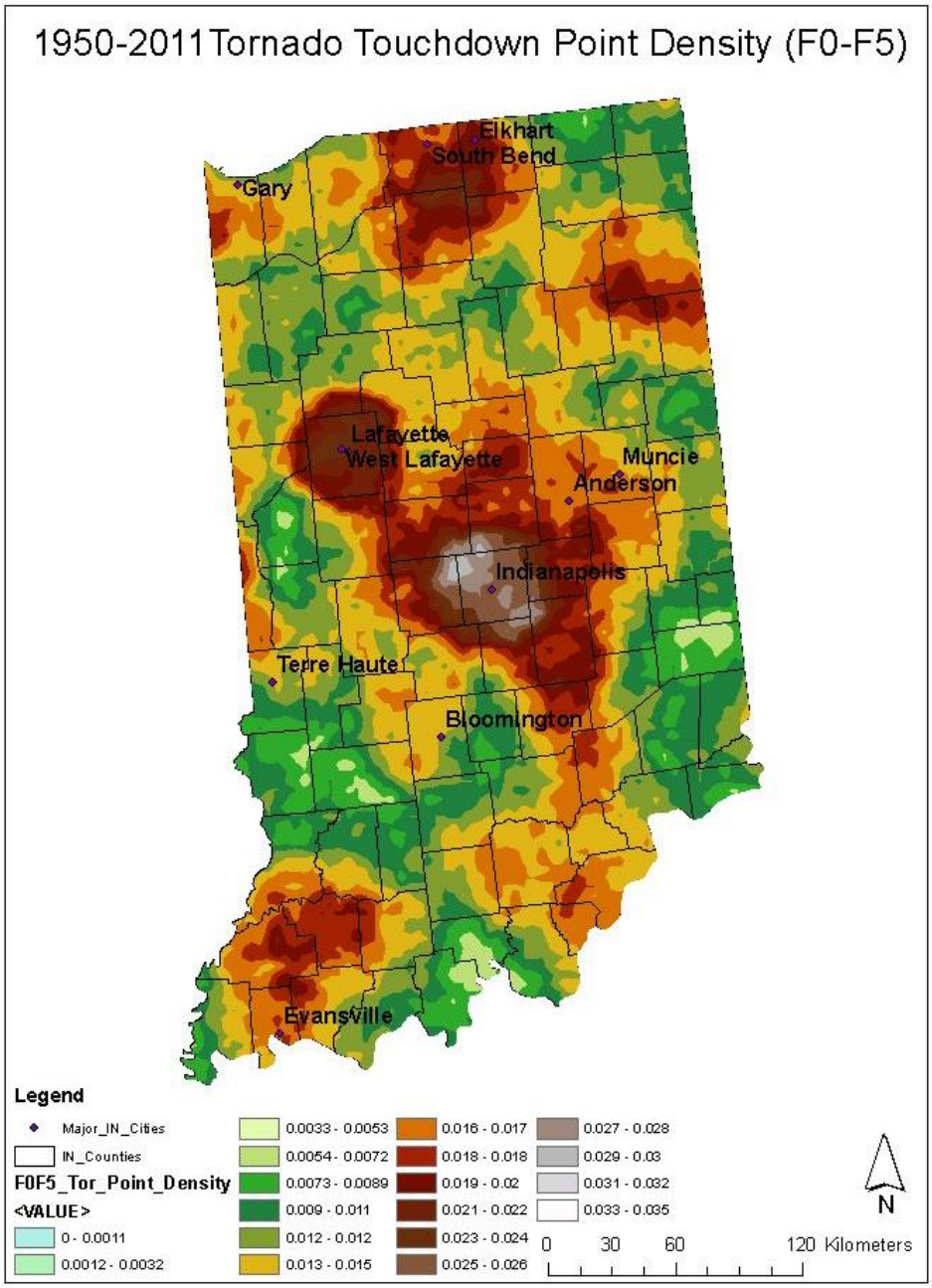

Figure 1: Tornado touchdown point density file for all tornadoes (F0-F5) from 1950-2011.

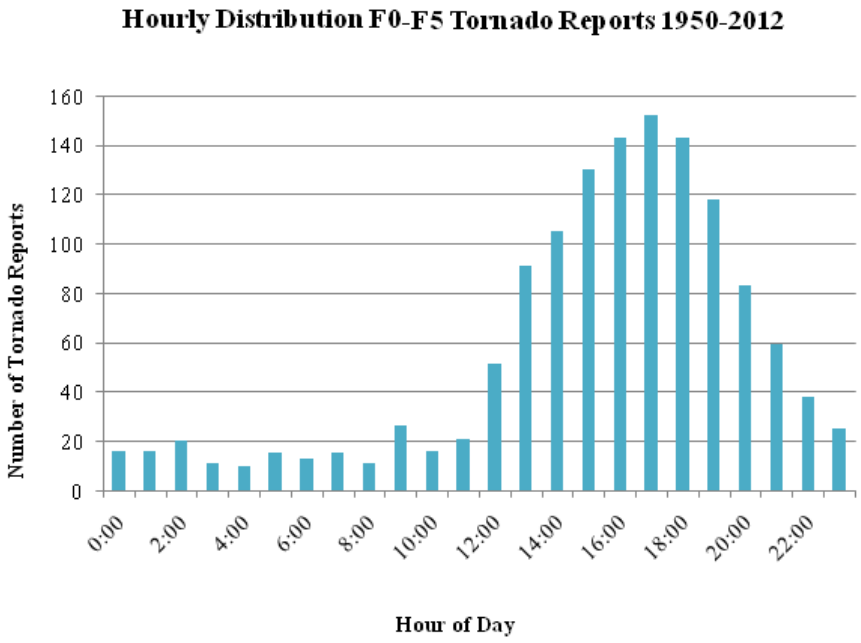

Figure 2: Hourly distribution of reported F0-F5 tornadoes in Indiana 1950-2012.

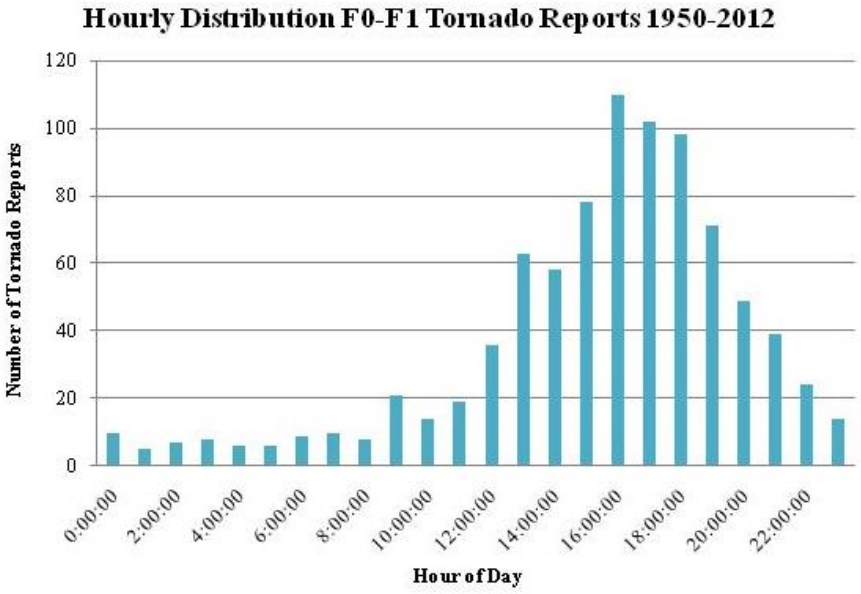

Figure 3: Hourly distribution of reported F0-F1 tornadoes in Indiana 1950-2012.

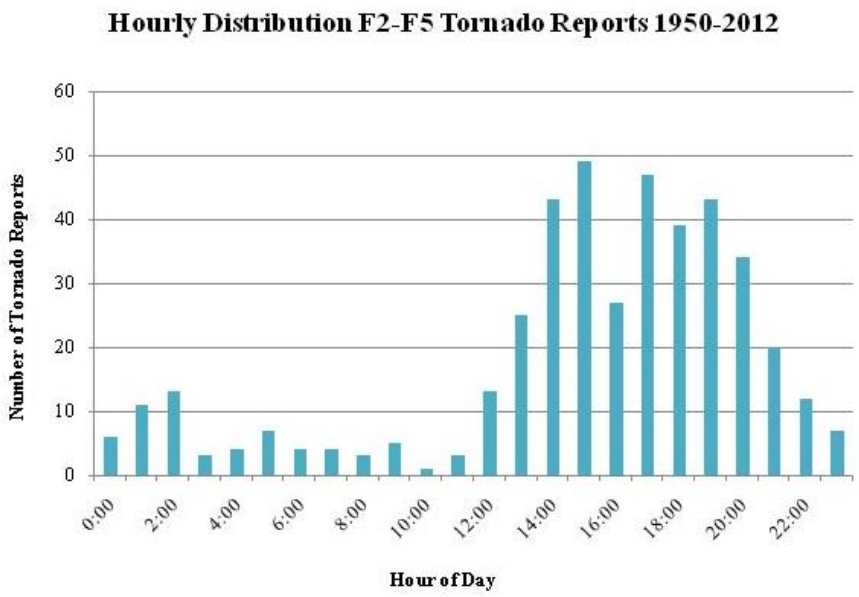

Figure 4: Hourly distribution of reported F2-F5 tornadoes in Indiana 1950-2012.

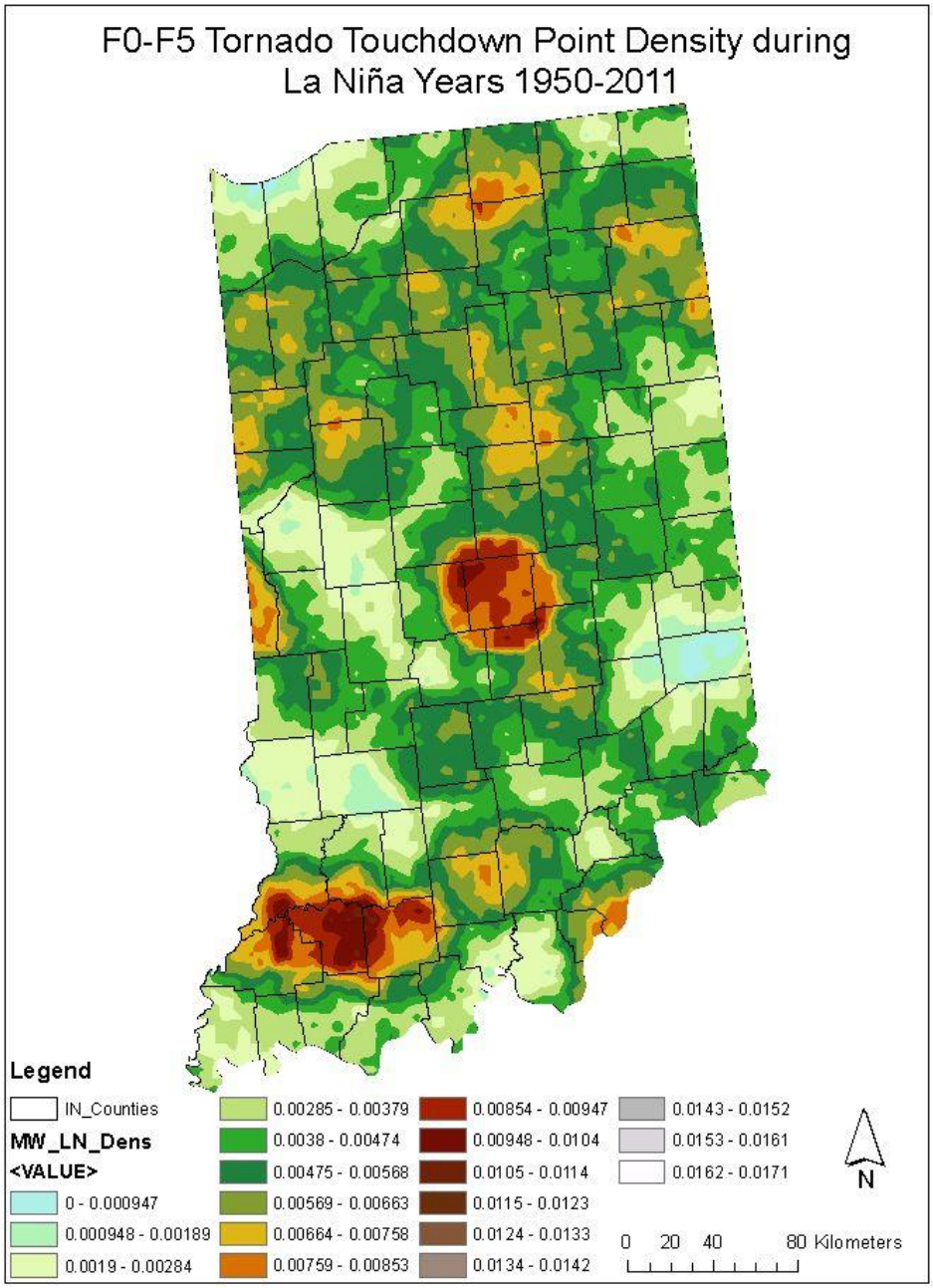

Figure 5: F0-F5 tornado touchdown point density map during La Niña years 1950-2011. A La Niña year is one in which a minimum of 5 months of the ONI index was at or below the -0.5 anomaly.

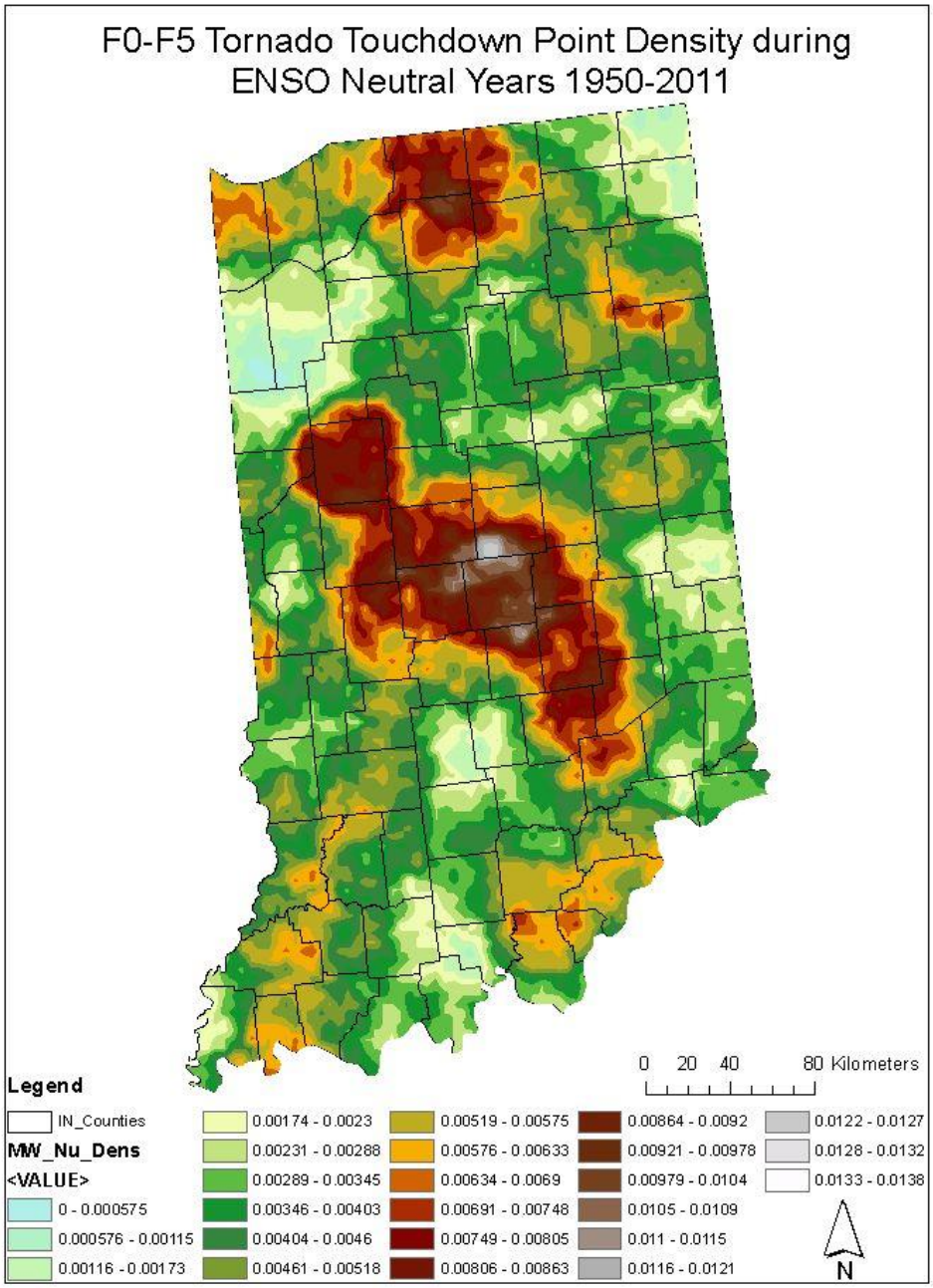

Figure 6: F0-F5 tornado touchdown point density map during ENSO Neutral years 1950-2011 (those years not classified as El Niño or La Niña).

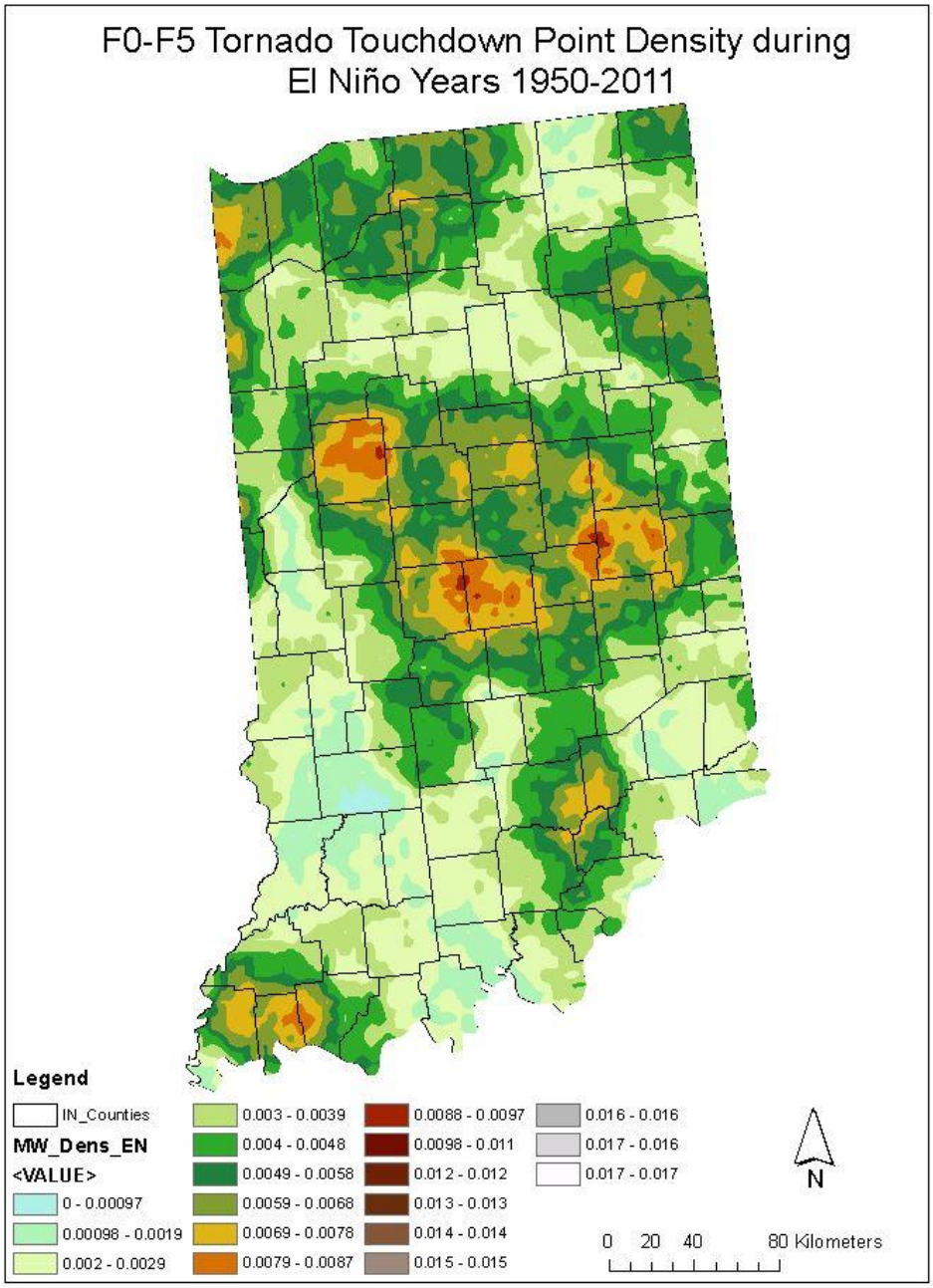

Figure 7: F0-F5 tornado touchdown point density map during El Niño years 1950-2011. An El Niño year is one in which 5 months or more of a 0.5 or greater anomaly was present.

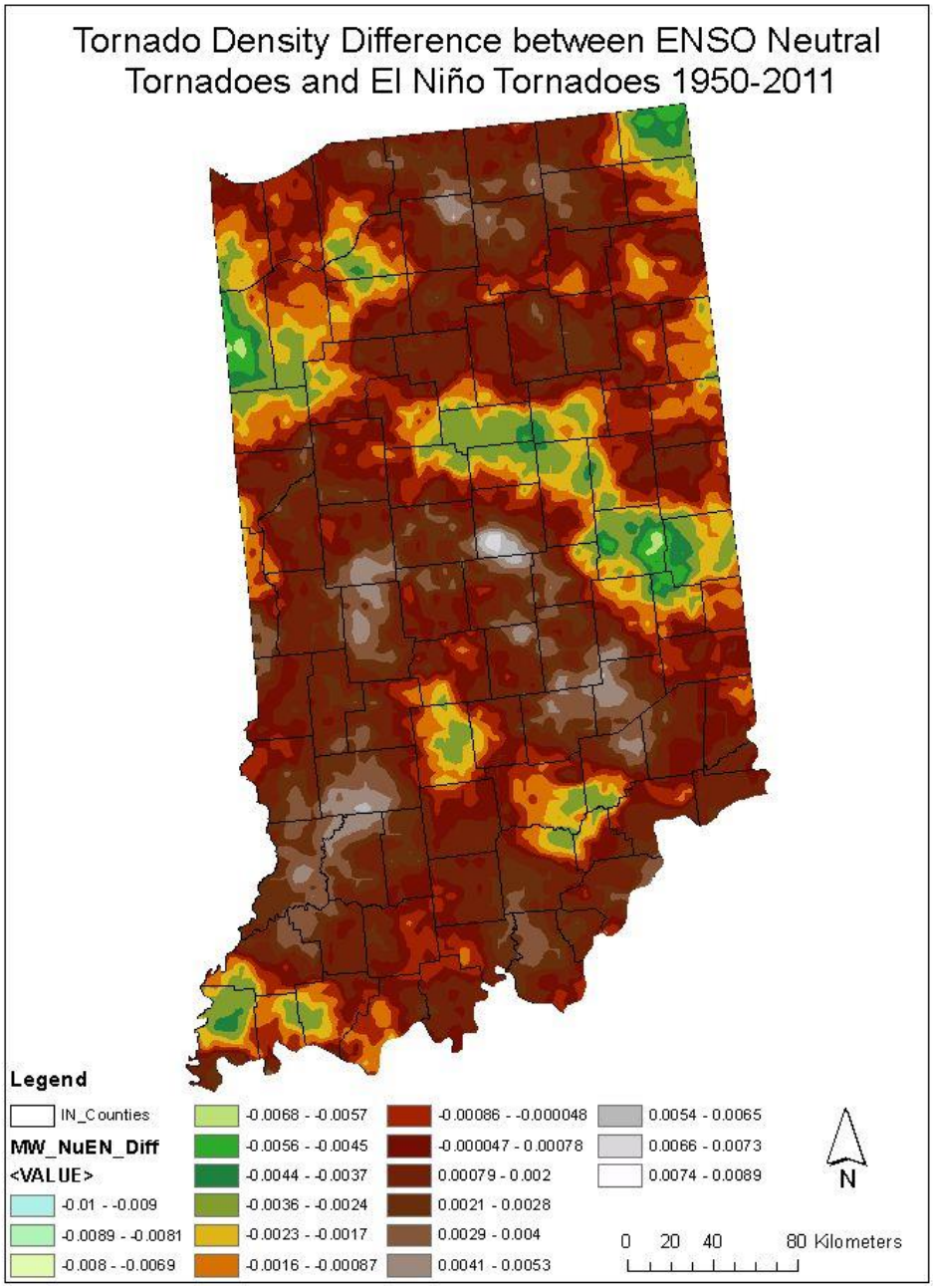

Figure 8: 1950-2011 F0-F5 tornado touchdown point density map showing the difference between ENSO Neutral years tornado touchdown point density and El Niño tornado touchdown point density. Where density values are positive, the ENSO Neutral point density value exceeds the El Niño point density value. Where density values are negative, the ENSO Neutral point density value is less than the El Niño point density value.

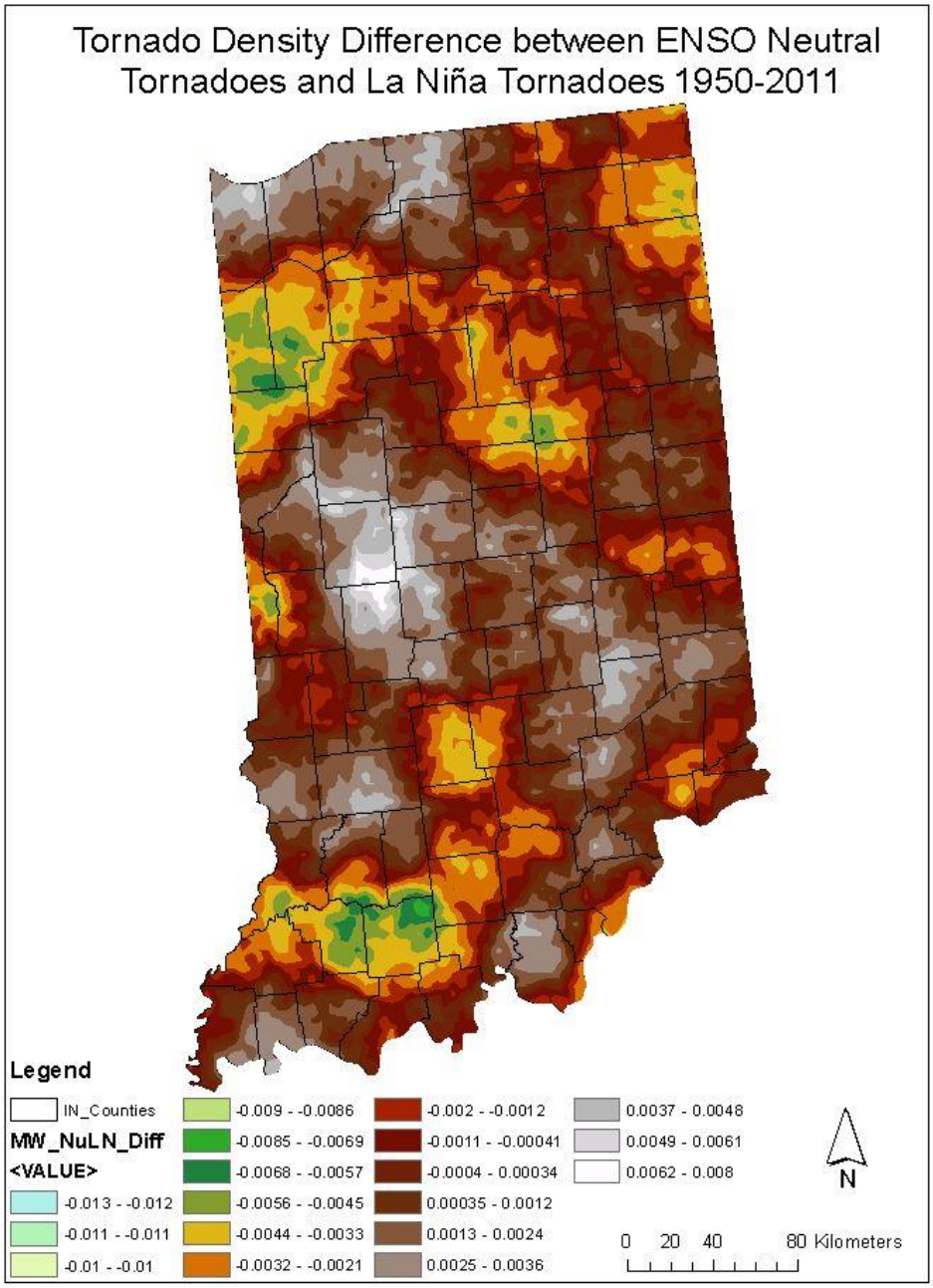

Figure 9: 1950-2011 F0-F5 tornado touchdown point density map showing the difference between ENSO Neutral years tornado touchdown point density and La Niña tornado touchdown point density. Where density values are positive, the ENSO Neutral point density value exceeds the La Niña point density value. Where density values are negative, the ENSO Neutral point density value is less than the La Niña point density value.

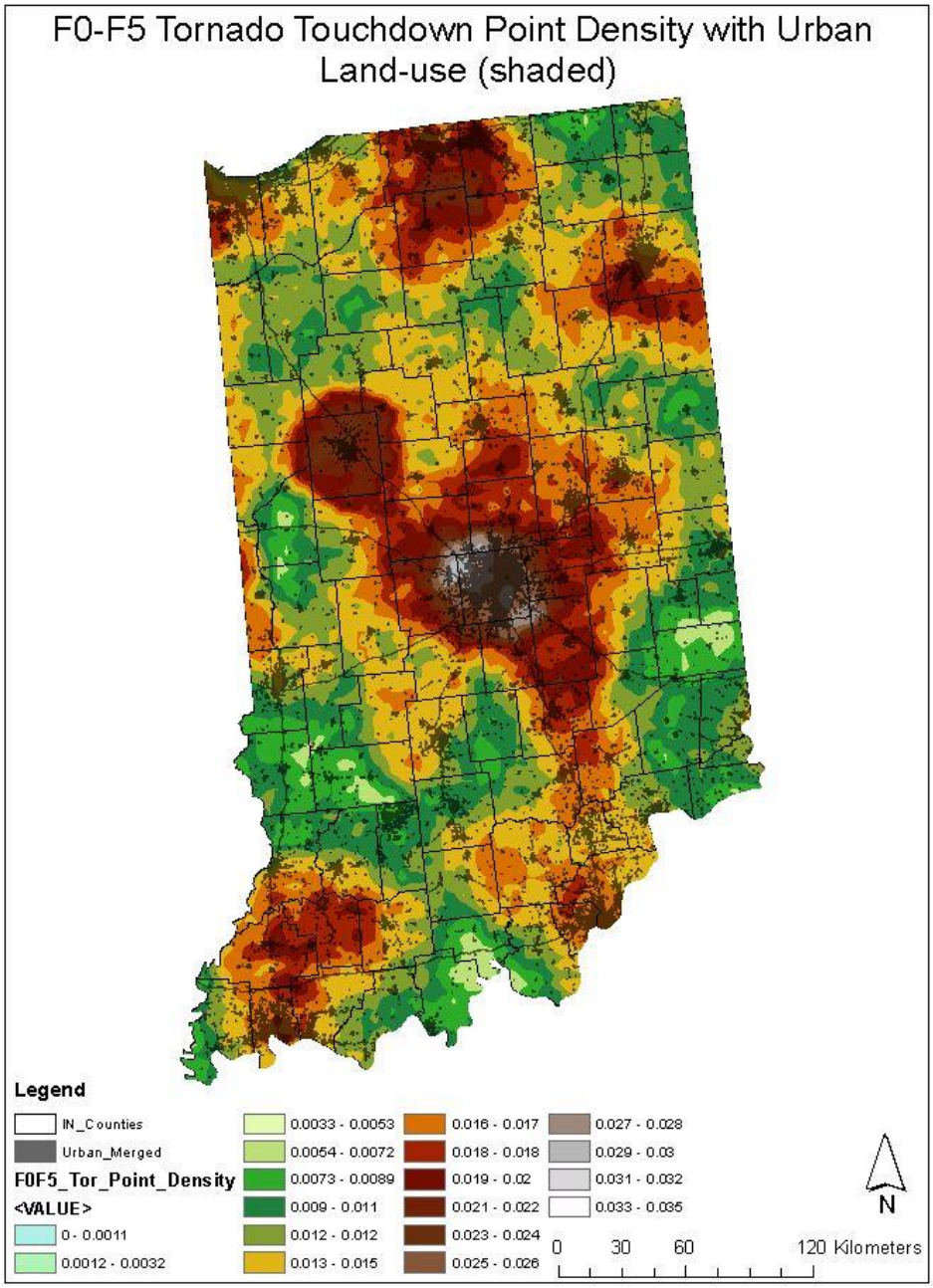

Figure 10: F0-F5 tornado touchdown point density with urban LULC categories as designated by the USGS land cover classification.

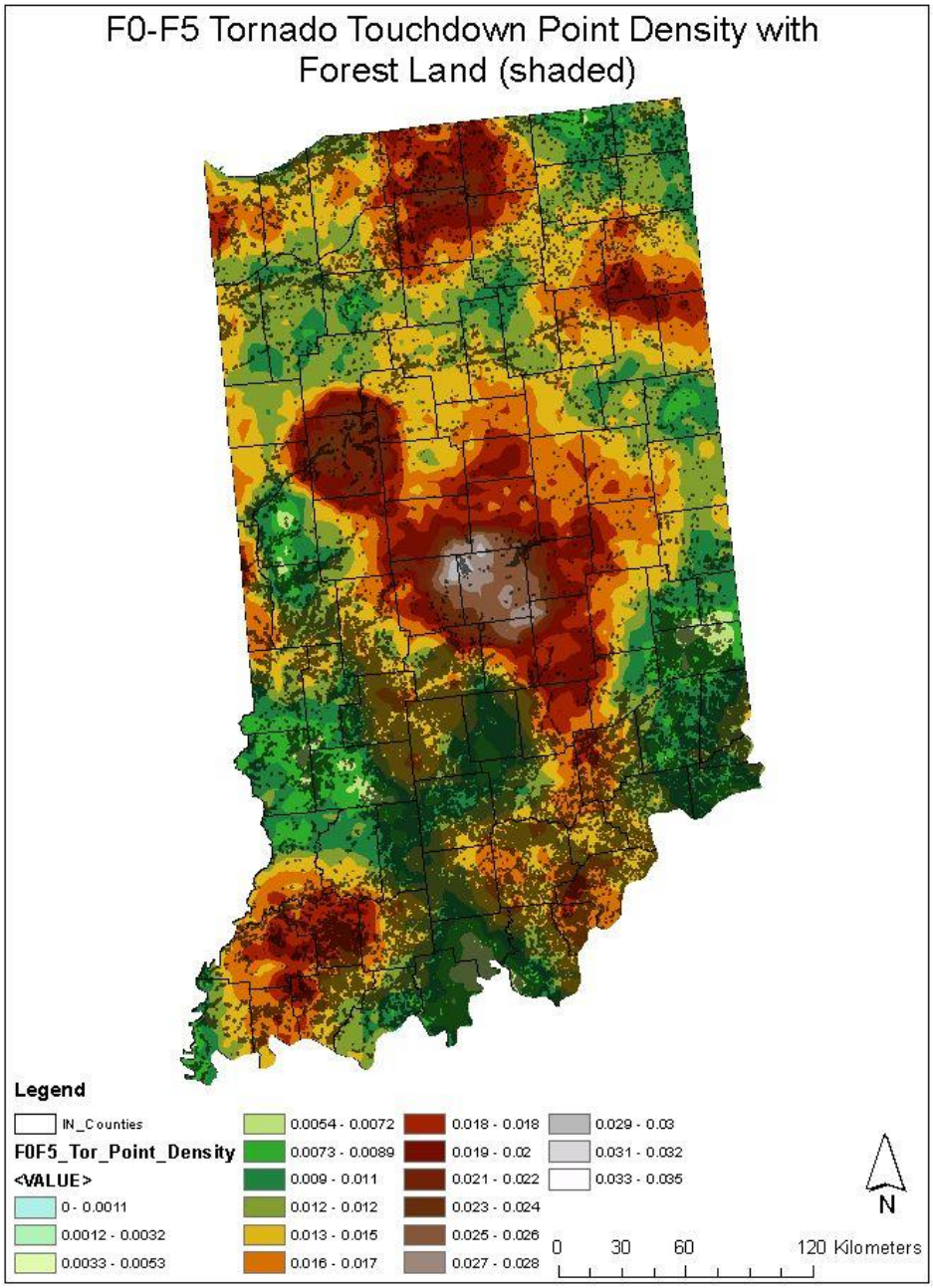

Figure 11: F0-F5 tornado touchdown point density with forest land as designated by the USGS land cover classification.

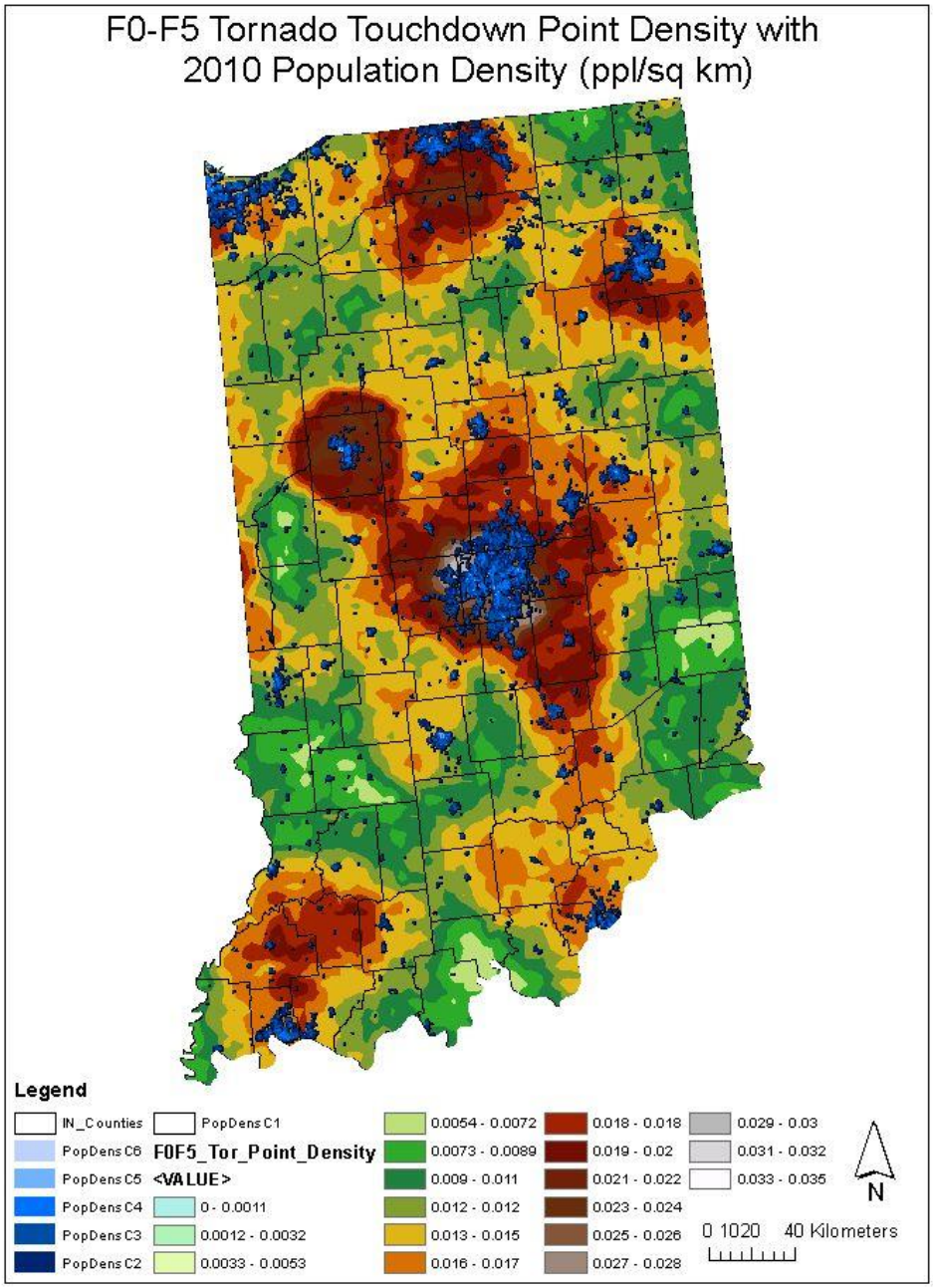

Figure 12: F0-F5 tornado touchdown point density with the 2010 U.S. Census population density of people per square km. While the densest regions (higher count in a given area) of tornado touchdown points in Indiana lie in close proximity to regions of high population, the statistical signal is not significant enough to dismiss land-surface feedbacks to the storm environment.

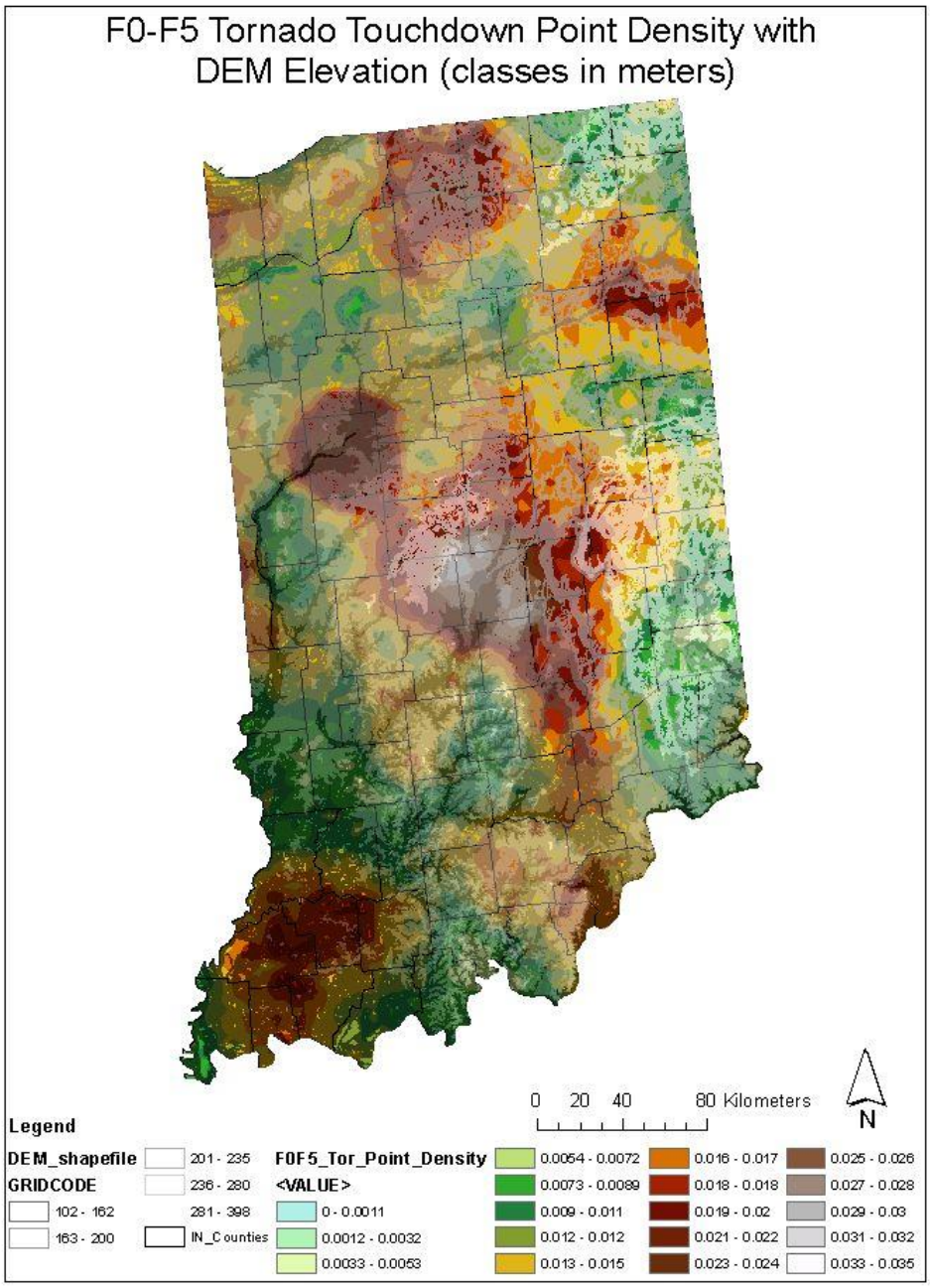

Figure 13: F0-F5 tornado touchdown point density with DEM elevation contours (lines of equal elevation) displayed in gradient color so that lower elevations are dark grey lines and highest elevations are white lines.

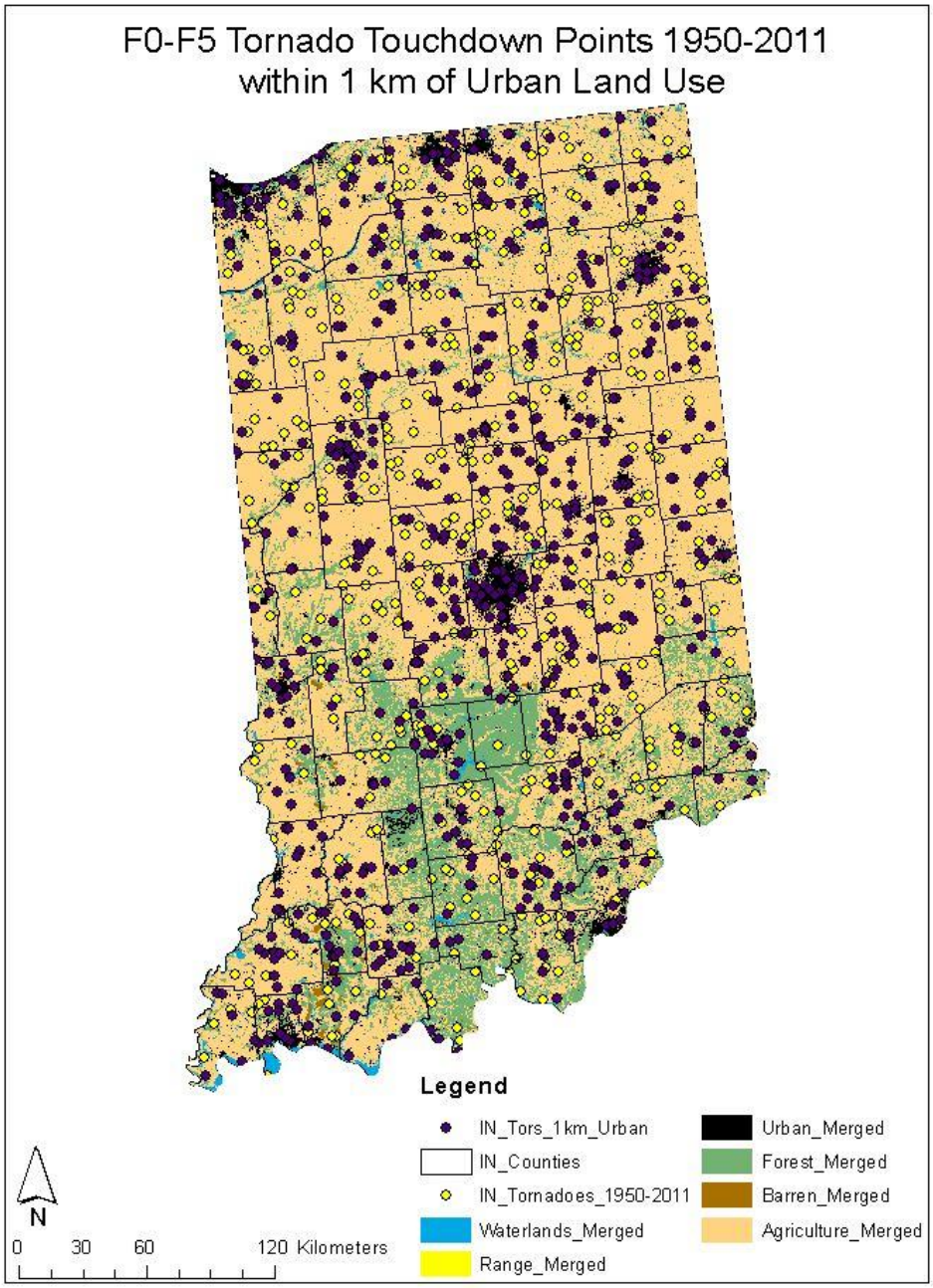

Figure 14: Map of Indiana showing USGS land cover classifications of wetlands/water bodies, range land, urban areas, barren land, and agriculture. Tornado touchdown points within 1 mile of an urban land use classification are in purple. Yellow points represent those tornado touchdown points not within a mile of an urban land cover classification.

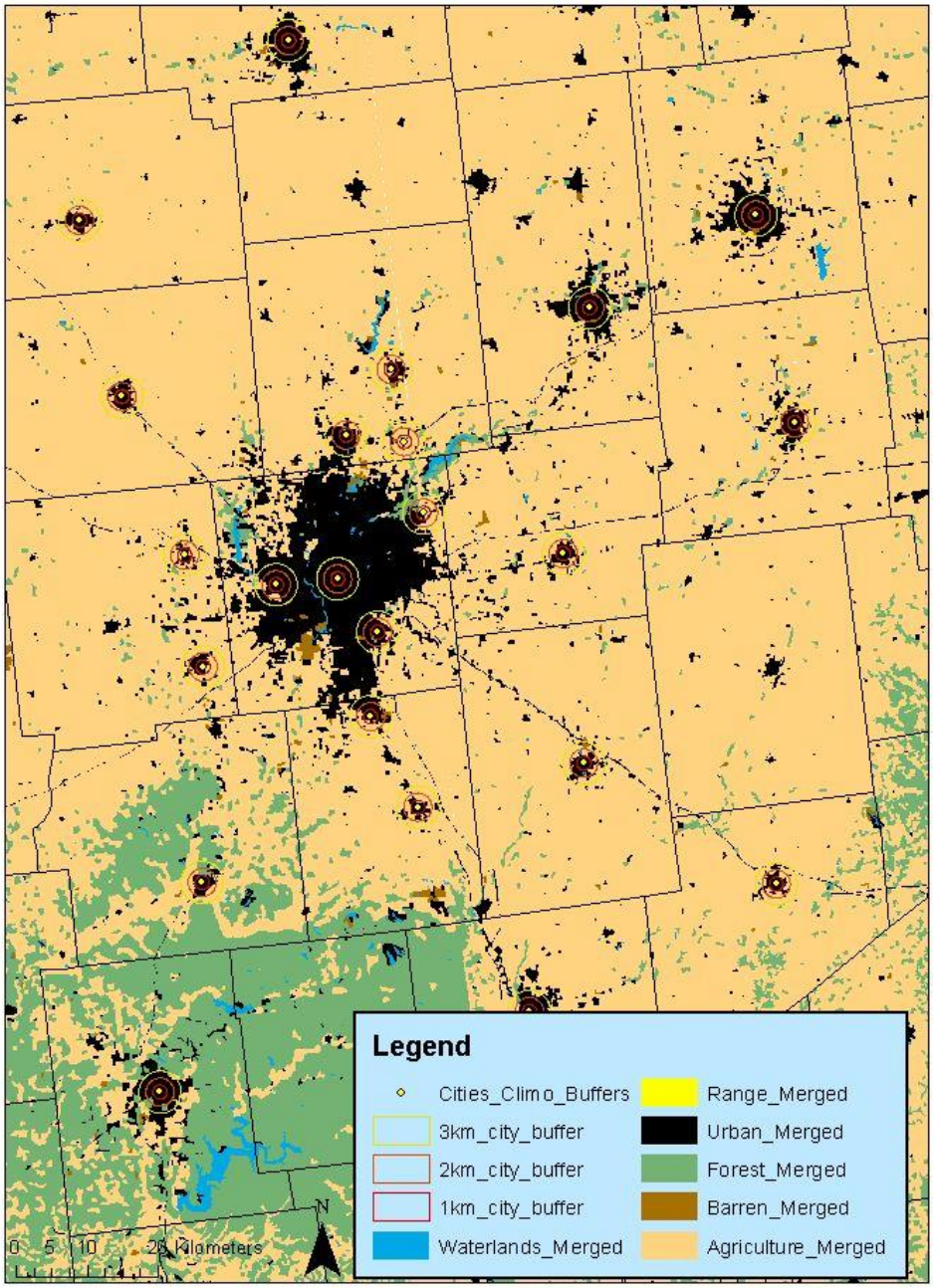

Figure 15: Zoomed-in map of land use classifications, city centriods (yellow points) and 1, 2, and 3 mile buffers. Tornado touchdown points are in purple. This image corresponds to Indianapolis, the largest area of urban to rural heteorogeneity in Indiana.

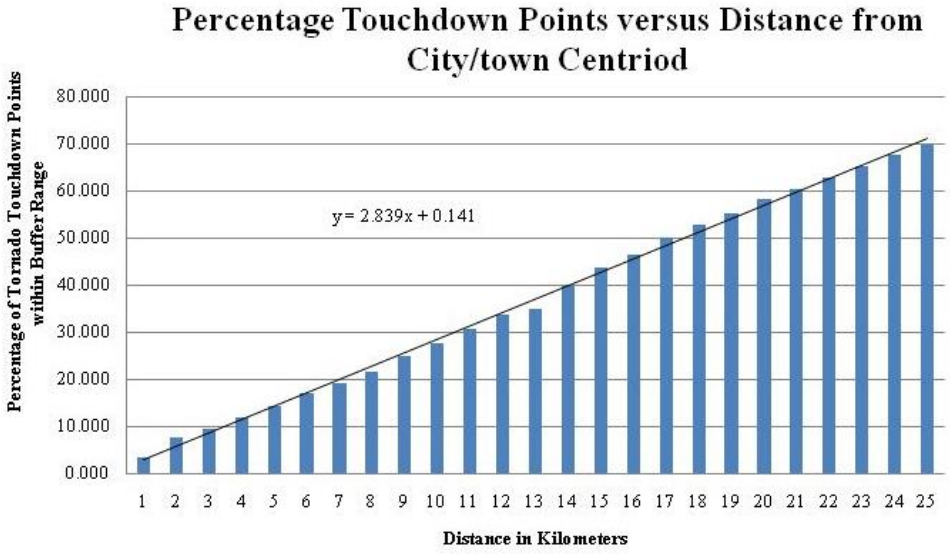

Figure 16: Regression plot of city centriod buffer distance and the percentage of F0-F5 tornadoes occuring within the specified distance. A near geometric relationship exists between the two, showing that a small amount of tornado touchdown points are close to city centers and increase in number with distance from the city.

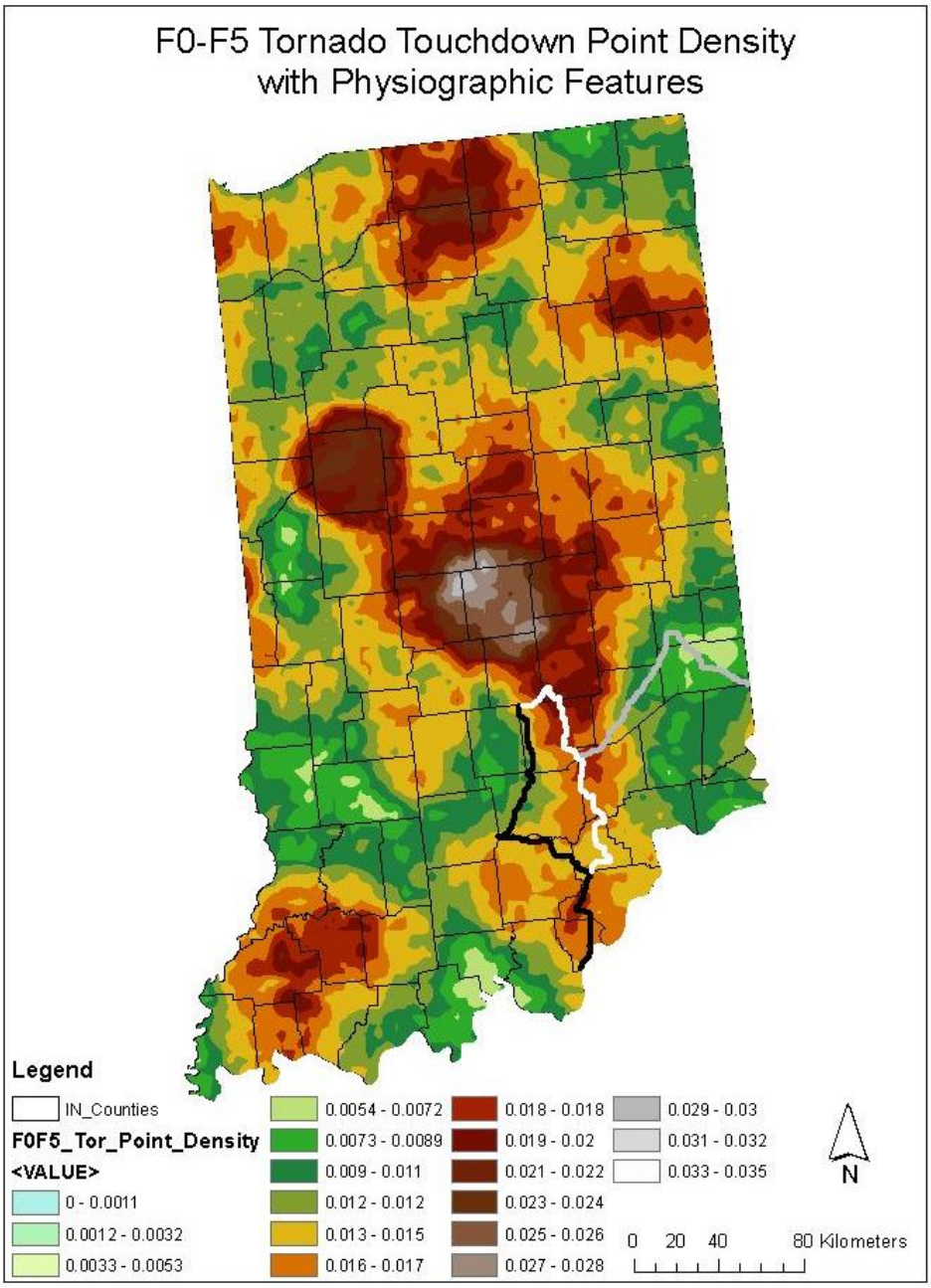

Figure 17: F0-F5 tornado touchdown point density map with region of increased tornado touchdown points (circled in yellow) east of the Knobstone Escarpment (thick black line) where the Scottsburg Lowlands (east of black line and west of white line) rise to the Muscatatuck Plateau and Dearborn Uplands (east of white line and south of grey line).

Supplemental Material

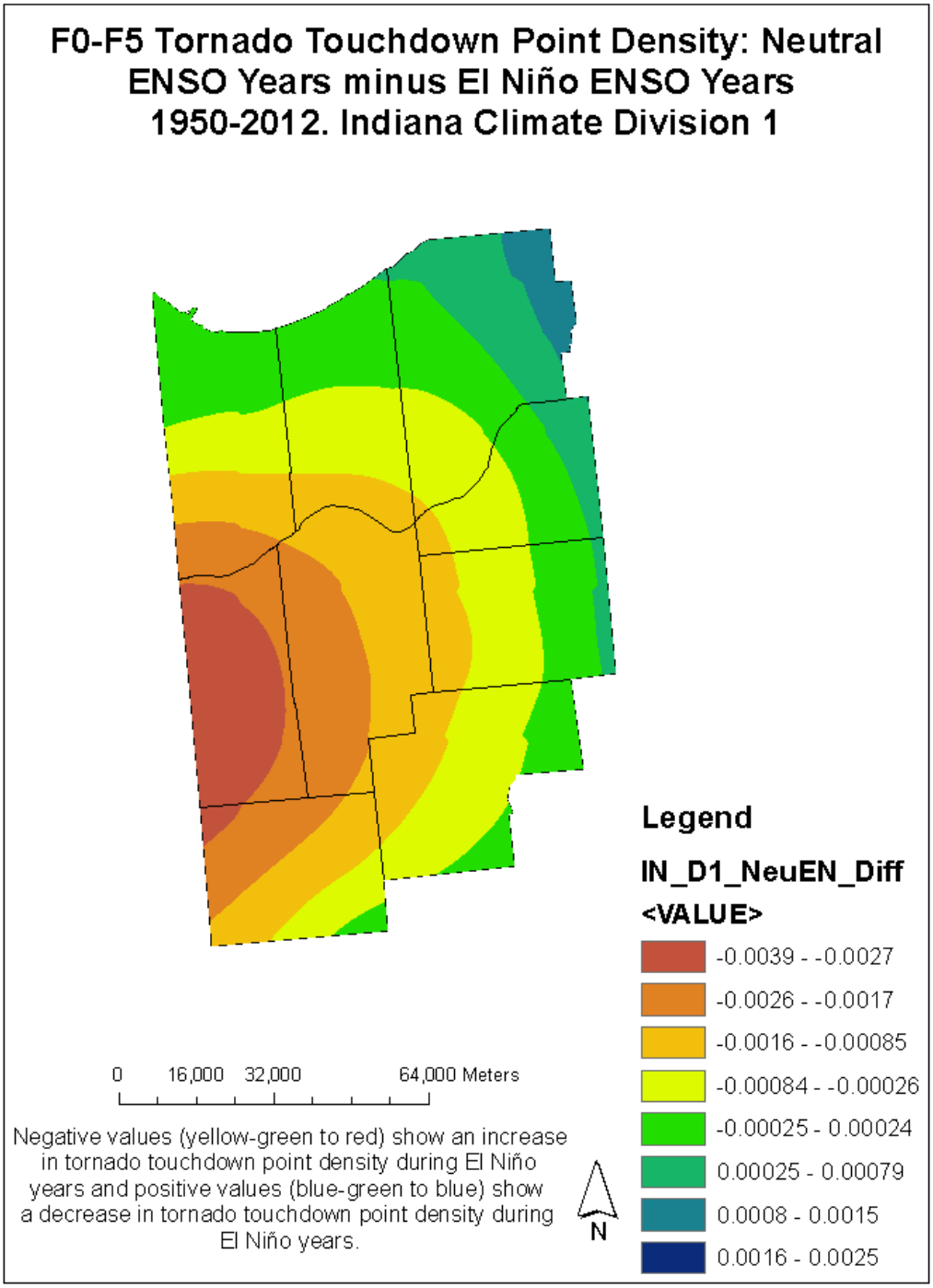

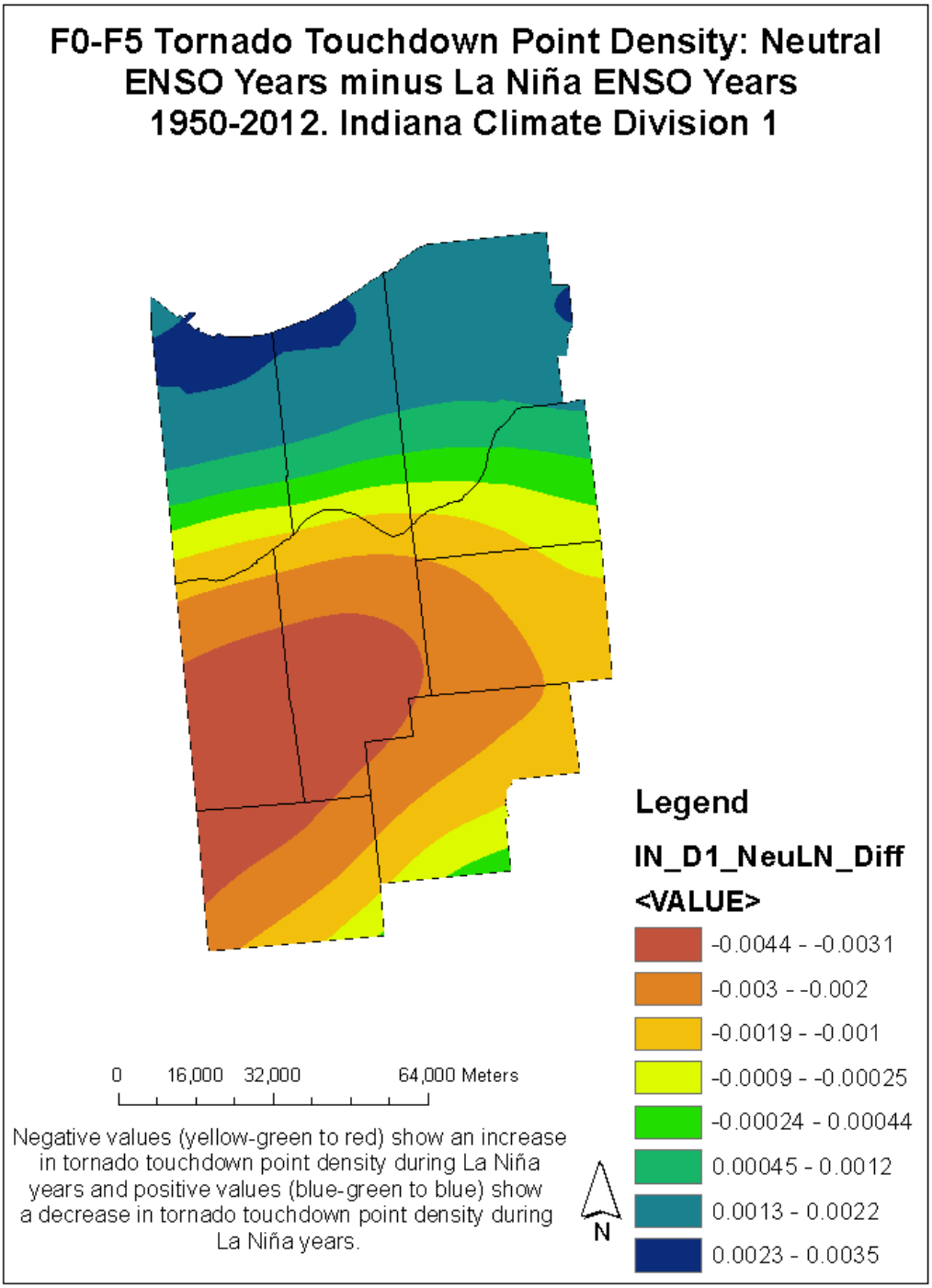
F0-F5 Tornado Touchdown Point Density: Neutral ENSO Years minus La Niña ENSO Years 1950-2012. Indiana Climate Division 1
0
16,000
32,000
64,000 Meters
Negative values (yellow-green to red) show an increase in tornado touchdown point density during La Niña years and positive values (blue-green to blue) show a decrease in tornado touchdown point density during La Niña years.
N
Legend
IN_D1_NeuLN_Diff
<VALUE>
-0.0044 - -0.0031
-0.003 - -0.002
-0.0019 - -0.001
-0.0009 - -0.00025
-0.00024 - 0.00044
0.00045 - 0.0012
0.0013 - 0.0022
0.0023 - 0.0035

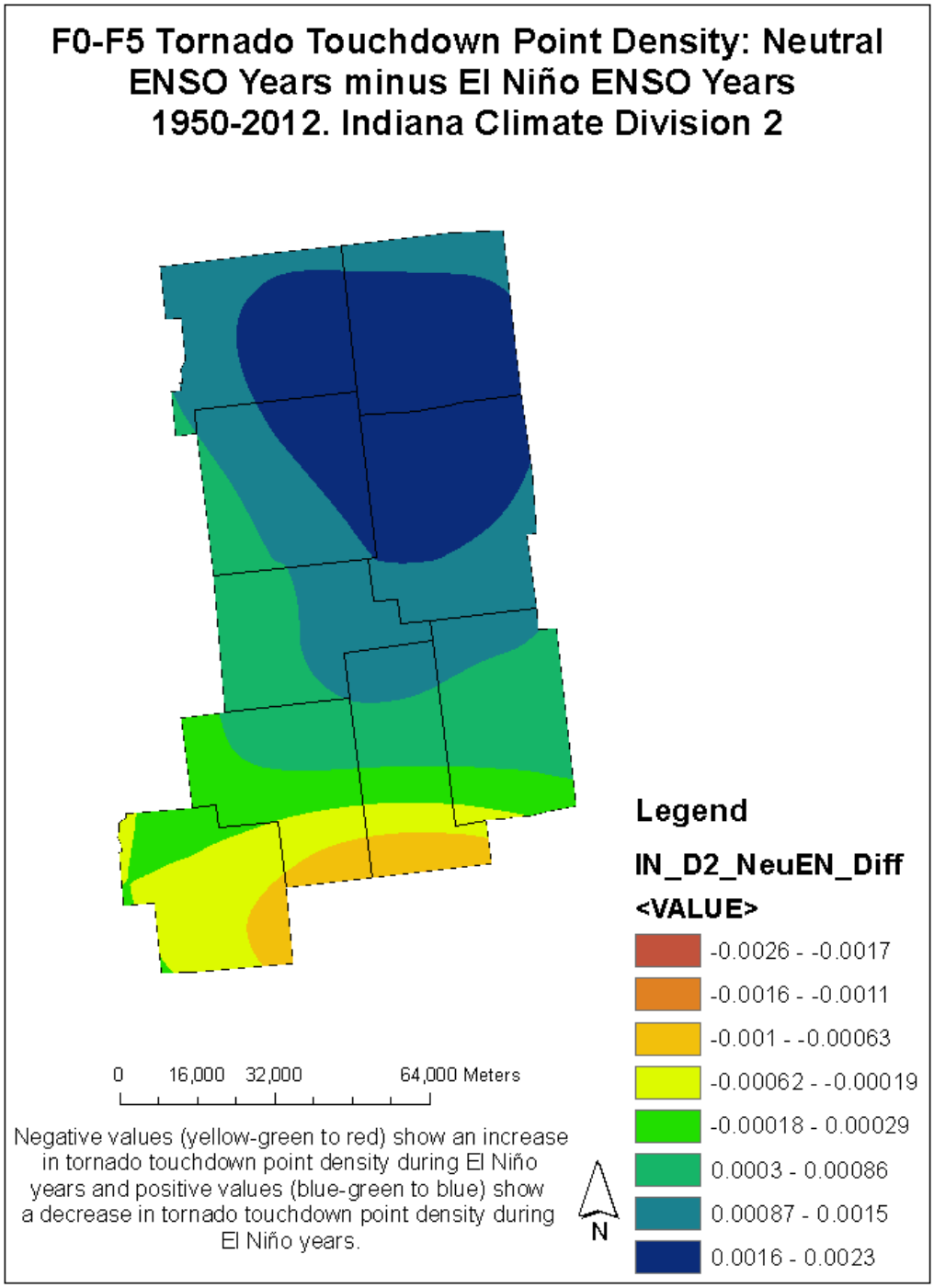
F0-F5 Tornado Touchdown Point Density: Neutral ENSO Years minus El Niño ENSO Years 1950-2012. Indiana Climate Division 2
0
16,000
32,000
64,000 Meters
Negative values (yellow-green to red) show an increase in tornado touchdown point density during El Niño years and positive values (blue-green to blue) show a decrease in tornado touchdown point density during El Niño years.
N
Legend
IN_D2_NeuEN_Diff
<VALUE>
-0.0026 - -0.0017
-0.0016 - -0.0011
-0.001 - -0.00063
-0.00062 - -0.00019
-0.00018 - 0.00029
0.0003 - 0.00086
0.00087 - 0.0015
0.0016 - 0.0023

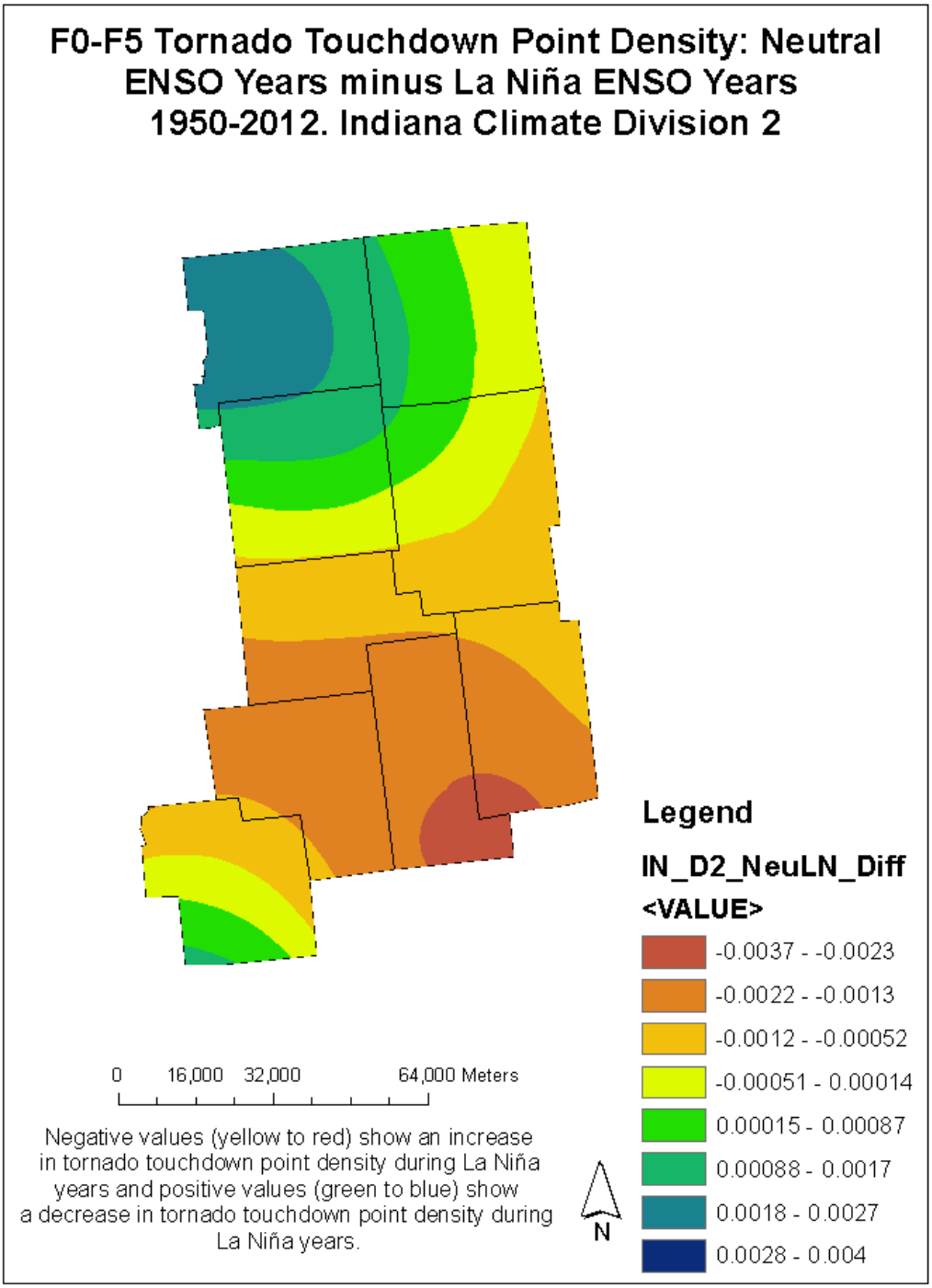
F0-F5 Tornado Touchdown Point Density: Neutral ENSO Years minus La Niña ENSO Years 1950-2012. Indiana Climate Division 2
0
16,000
32,000
64,000 Meters
Negative values (yellow to red) show an increase in tornado touchdown point density during La Niña years and positive values (green to blue) show a decrease in tornado touchdown point density during La Niña years.
N
Legend
IN_D2_NeuLN_Diff
<VALUE>
-0.0037 - -0.0023
-0.0022 - -0.0013
-0.0012 - -0.00052
-0.00051 - 0.00014
0.00015 - 0.00087
0.00088 - 0.0017
0.0018 - 0.0027
0.0028 - 0.004

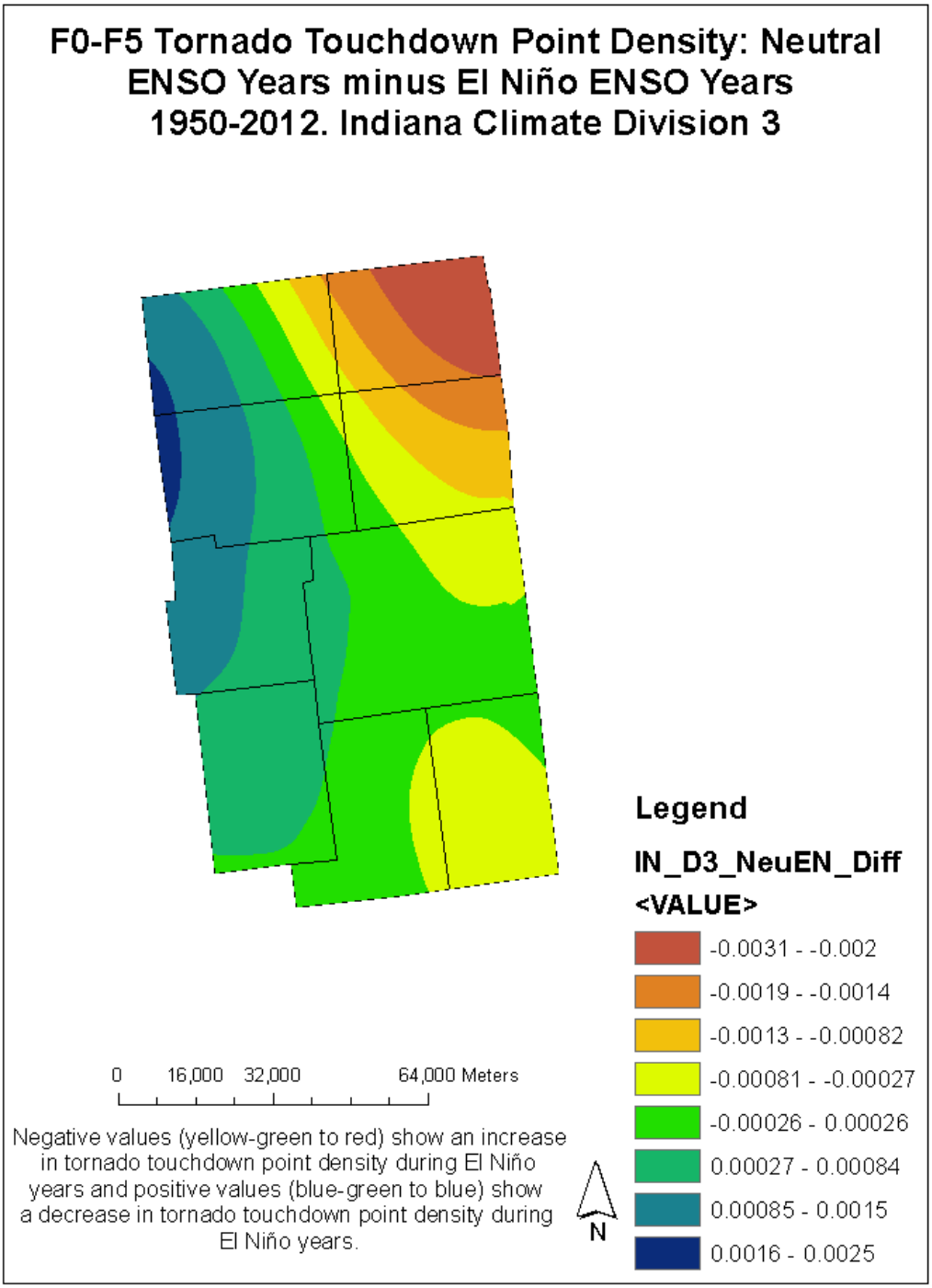
F0-F5 Tornado Touchdown Point Density: Neutral ENSO Years minus El Niño ENSO Years 1950-2012. Indiana Climate Division 3
Legend
IN_D3_NeuEN_Diff
<VALUE>
-0.0031 - -0.002
-0.0019 - -0.0014
-0.0013 - -0.00082
-0.00081 - -0.00027
-0.00026 - 0.00026
0.00027 - 0.00084
0.00085 - 0.0015
0.0016 - 0.0025
0
16,000
32,000
64,000 Meters
N
Negative values (yellow-green to red) show an increase in tornado touchdown point density during El Niño years and positive values (blue-green to blue) show a decrease in tornado touchdown point density during El Niño years.

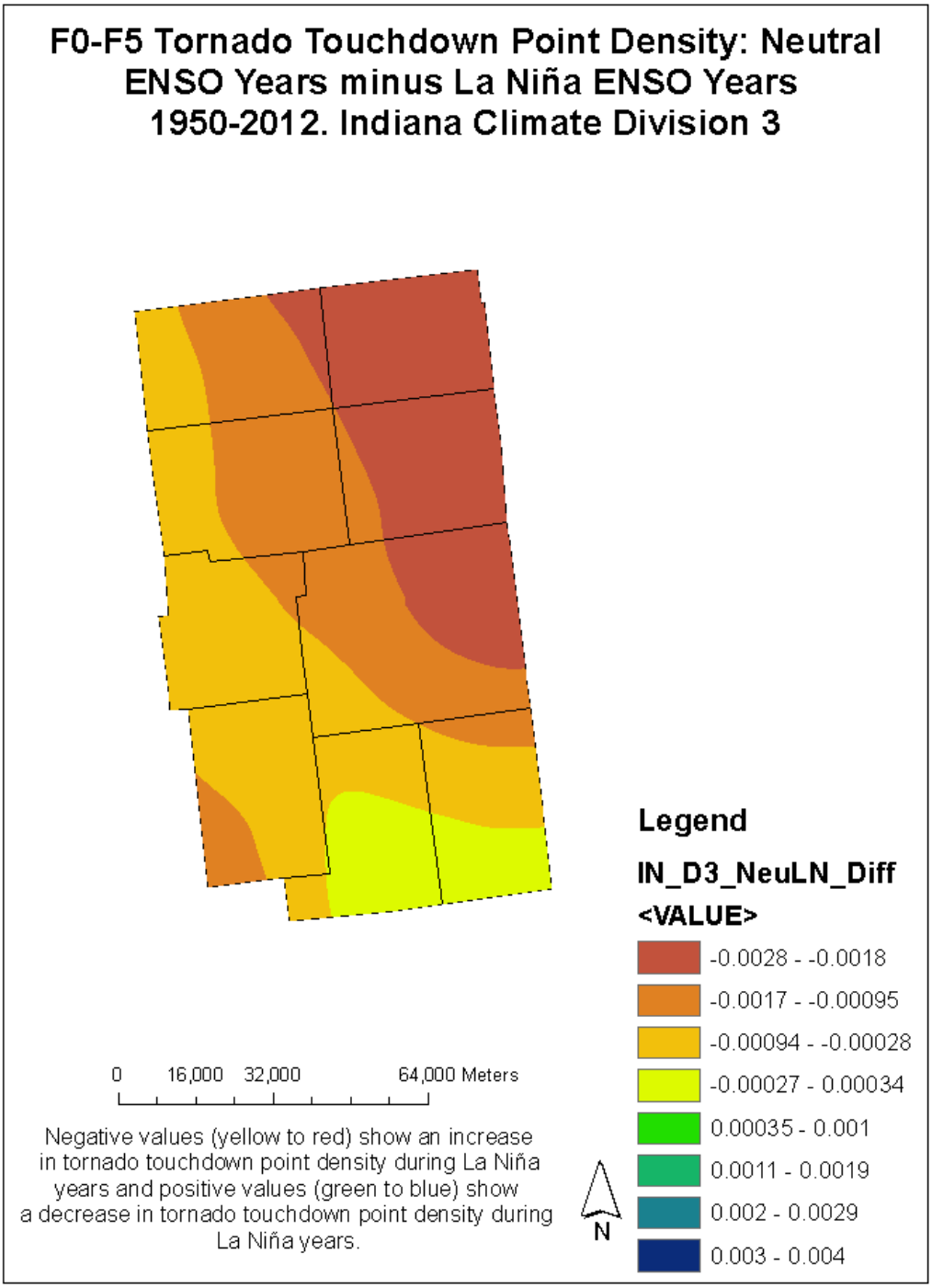
F0-F5 Tornado Touchdown Point Density: Neutral ENSO Years minus La Niña ENSO Years 1950-2012. Indiana Climate Division 3
0
16,000
32,000
64,000 Meters
Negative values (yellow to red) show an increase in tornado touchdown point density during La Niña years and positive values (green to blue) show a decrease in tornado touchdown point density during La Niña years.
N
Legend
IN_D3_NeuLN_Diff
<VALUE>
-0.0028 - -0.0018
-0.0017 - -0.00095
-0.00094 - -0.00028
-0.00027 - 0.00034
0.00035 - 0.001
0.0011 - 0.0019
0.002 - 0.0029
0.003 - 0.004

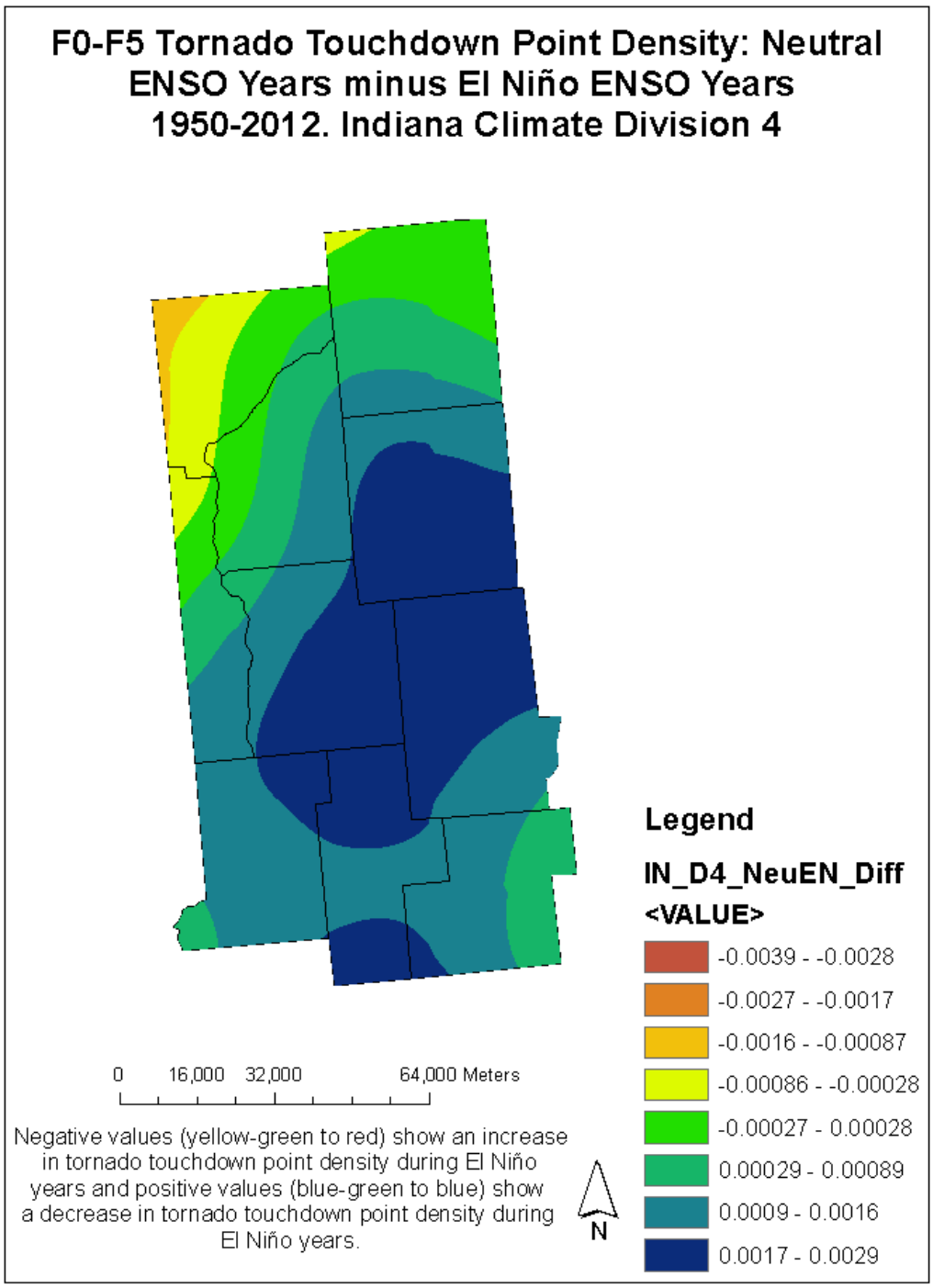
F0-F5 Tornado Touchdown Point Density: Neutral ENSO Years minus El Niño ENSO Years 1950-2012. Indiana Climate Division 4
0
16,000
32,000
64,000 Meters
Negative values (yellow-green to red) show an increase in tornado touchdown point density during El Niño years and positive values (blue-green to blue) show a decrease in tornado touchdown point density during El Niño years.
N
Legend
IN_D4_NeuEN_Diff
<VALUE>
-0.0039 - -0.0028
-0.0027 - -0.0017
-0.0016 - -0.00087
-0.00086 - -0.00028
-0.00027 - 0.00028
0.00029 - 0.00089
0.0009 - 0.0016
0.0017 - 0.0029

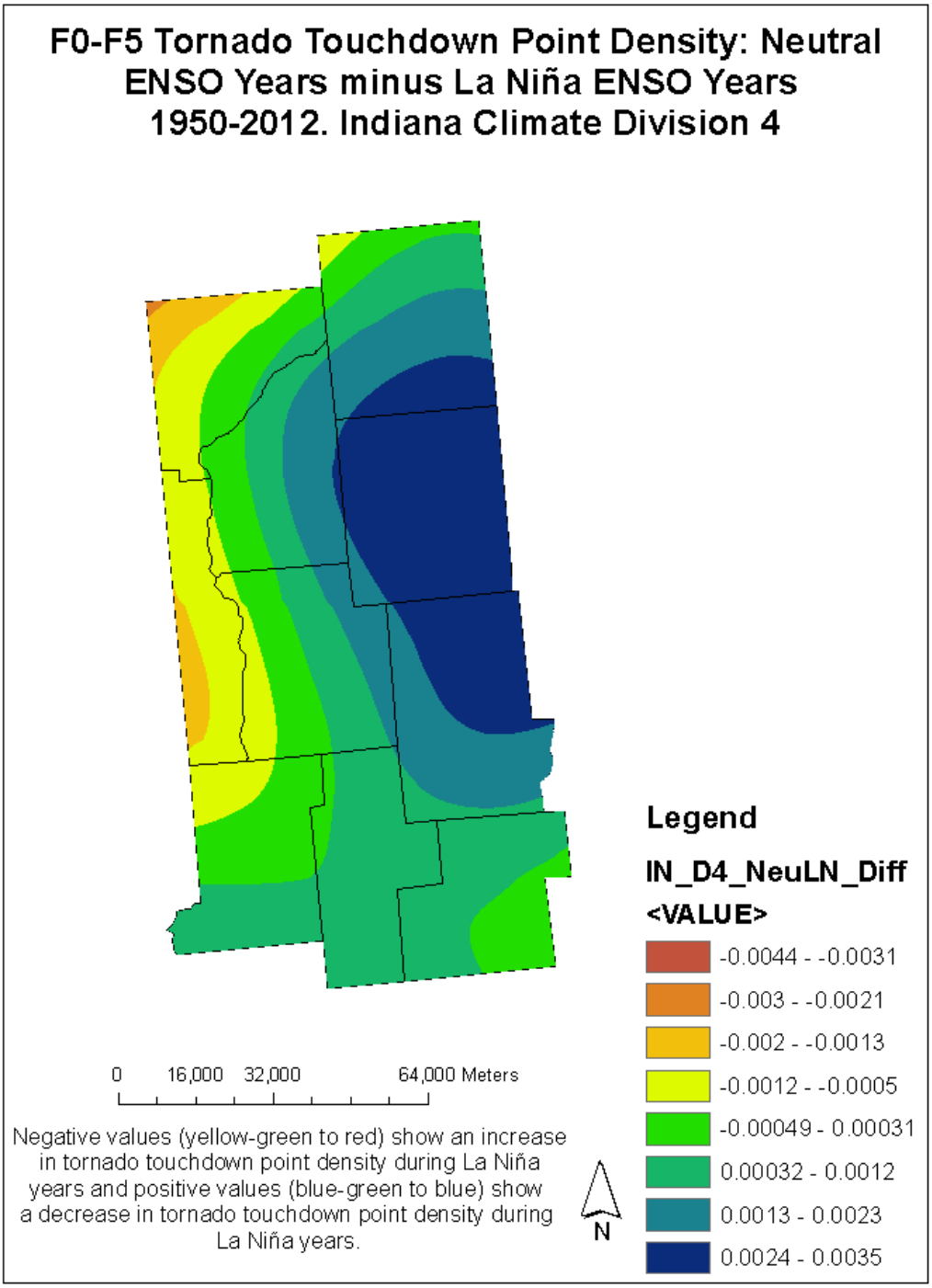
F0-F5 Tornado Touchdown Point Density: Neutral ENSO Years minus La Niña ENSO Years 1950-2012. Indiana Climate Division 4
0
16,000
32,000
64,000 Meters
Negative values (yellow-green to red) show an increase in tornado touchdown point density during La Niña years and positive values (blue-green to blue) show a decrease in tornado touchdown point density during La Niña years.
N
Legend
IN_D4_NeuLN_Diff
<VALUE>
-0.0044 - -0.0031
-0.003 - -0.0021
-0.002 - -0.0013
-0.0012 - -0.0005
-0.00049 - 0.00031
0.00032 - 0.0012
0.0013 - 0.0023
0.0024 - 0.0035

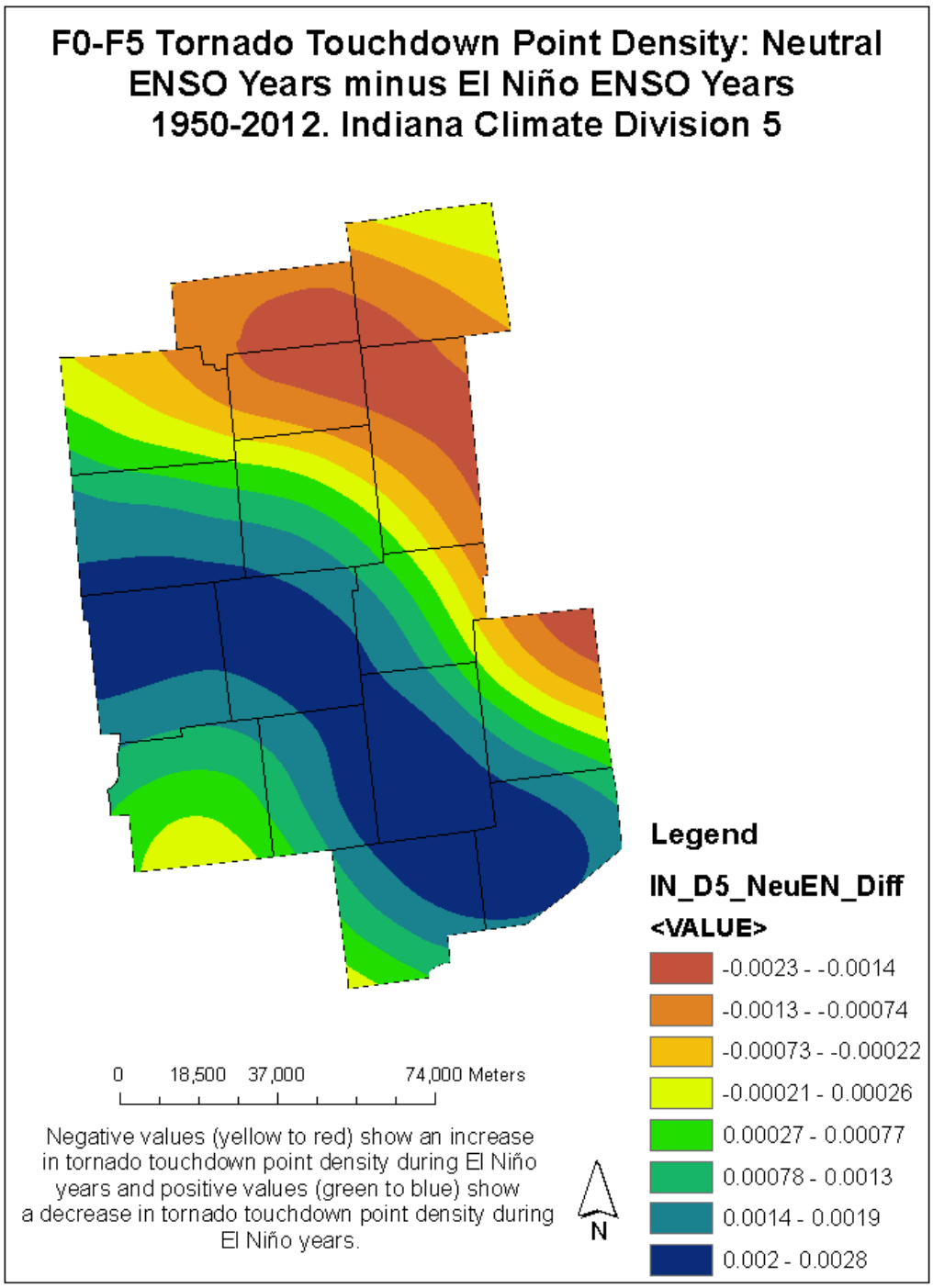
F0-F5 Tornado Touchdown Point Density: Neutral ENSO Years minus El Niño ENSO Years 1950-2012. Indiana Climate Division 5
Legend
IN_D5_NeuEN_Diff
<VALUE>
-0.0023 - -0.0014
-0.0013 - -0.00074
-0.00073 - -0.00022
-0.00021 - 0.00026
0.00027 - 0.00077
0.00078 - 0.0013
0.0014 - 0.0019
0.002 - 0.0028
0 18,500 37,000 74,000 Meters
N
Negative values (yellow to red) show an increase in tornado touchdown point density during El Niño years and positive values (green to blue) show a decrease in tornado touchdown point density during El Niño years.

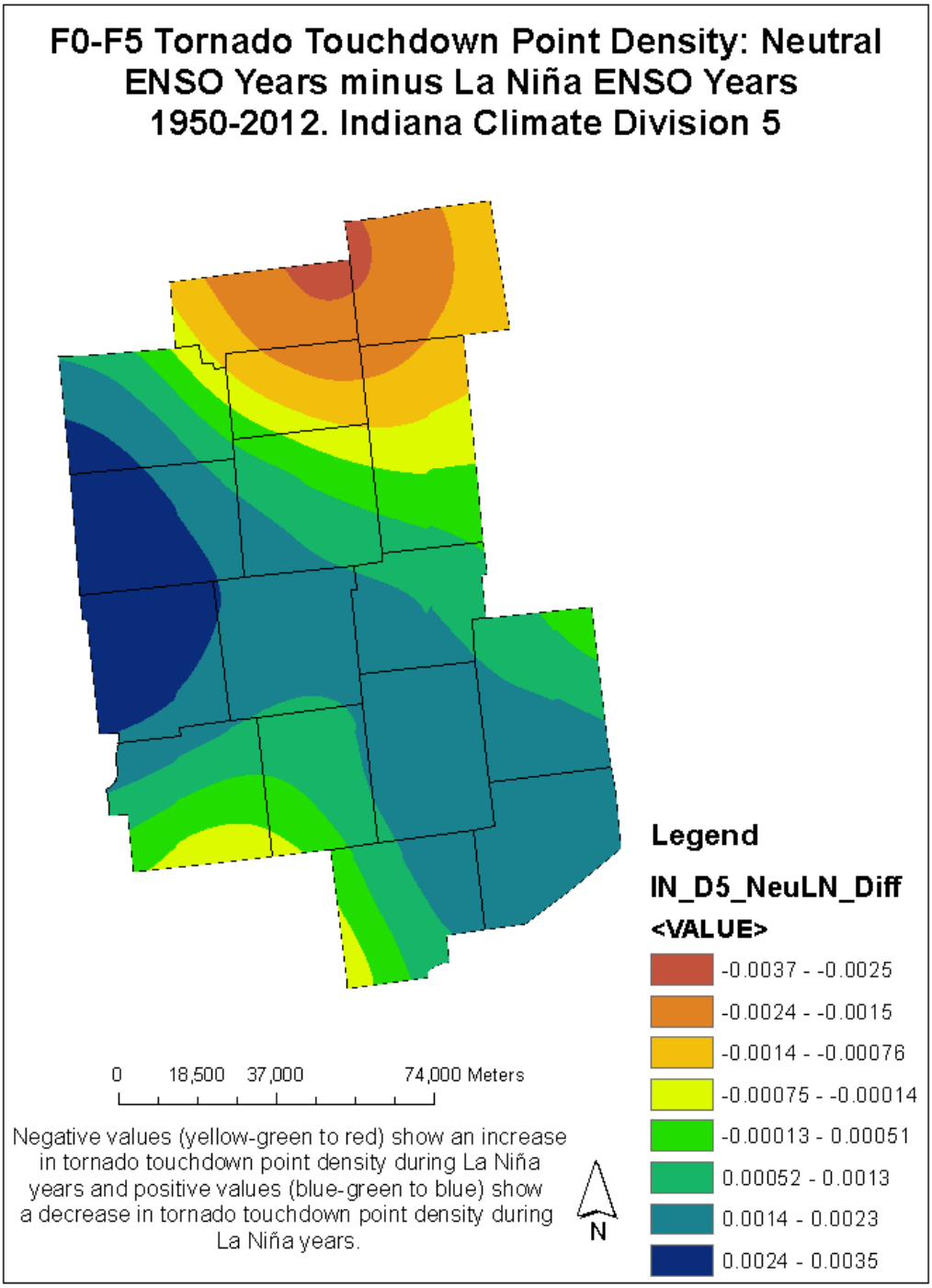
F0-F5 Tornado Touchdown Point Density: Neutral ENSO Years minus La Niña ENSO Years 1950-2012. Indiana Climate Division 5
0
18,500
37,000
74,000 Meters
Negative values (yellow-green to red) show an increase in tornado touchdown point density during La Niña years and positive values (blue-green to blue) show a decrease in tornado touchdown point density during La Niña years.
N
Legend
IN_D5_NeuLN_Diff
<VALUE>
-0.0037 - -0.0025
-0.0024 - -0.0015
-0.0014 - -0.00076
-0.00075 - -0.00014
-0.00013 - 0.00051
0.00052 - 0.0013
0.0014 - 0.0023
0.0024 - 0.0035

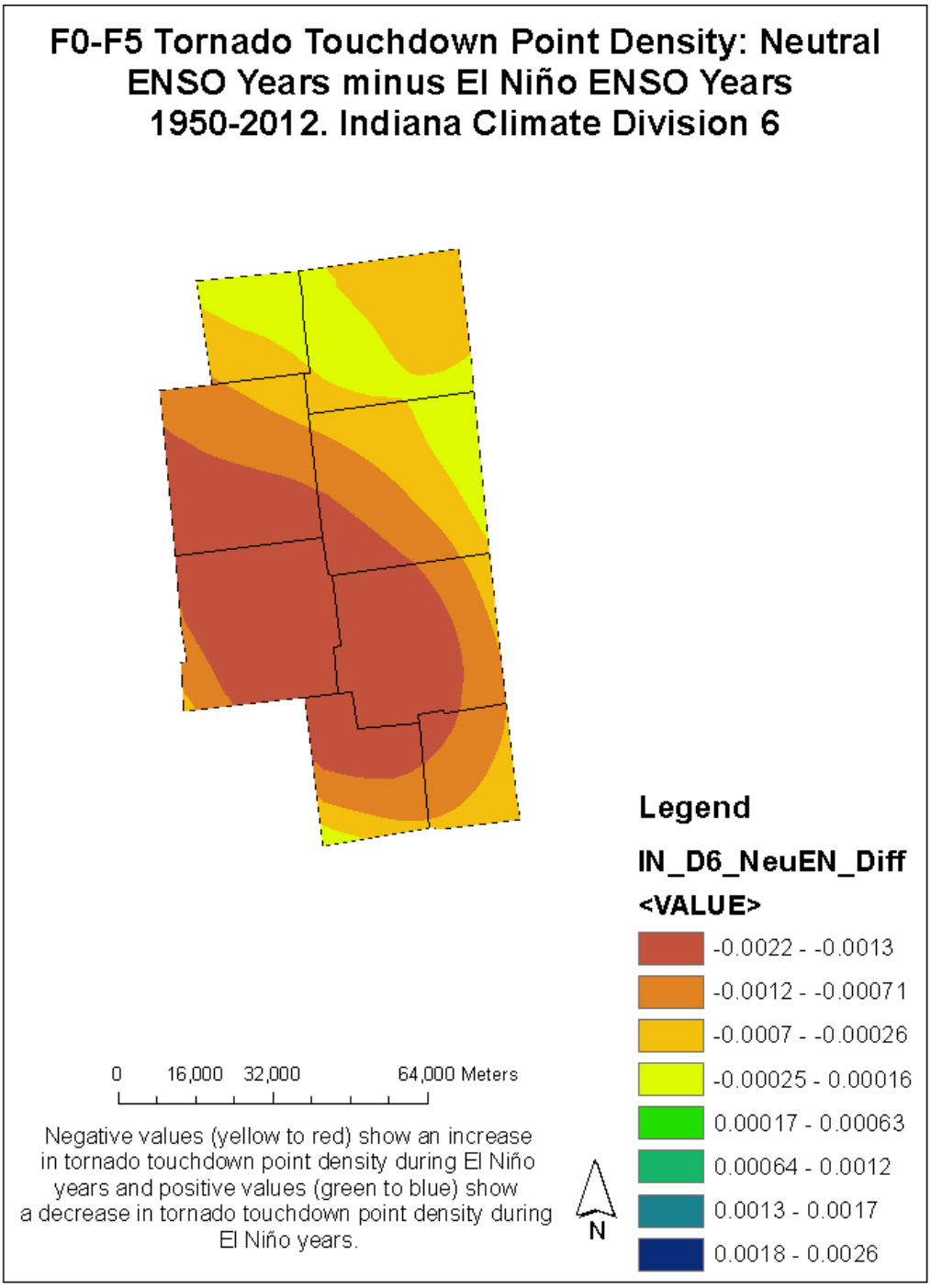
F0-F5 Tornado Touchdown Point Density: Neutral ENSO Years minus El Niño ENSO Years 1950-2012. Indiana Climate Division 6
Legend
IN_D6_NeuEN_Diff
<VALUE>
-0.0022 - -0.0013
-0.0012 - -0.00071
-0.0007 - -0.00026
-0.00025 - 0.00016
0.00017 - 0.00063
0.00064 - 0.0012
0.0013 - 0.0017
0.0018 - 0.0026
0
16,000
32,000
64,000 Meters
N
Negative values (yellow to red) show an increase in tornado touchdown point density during El Niño years and positive values (green to blue) show a decrease in tornado touchdown point density during El Niño years.

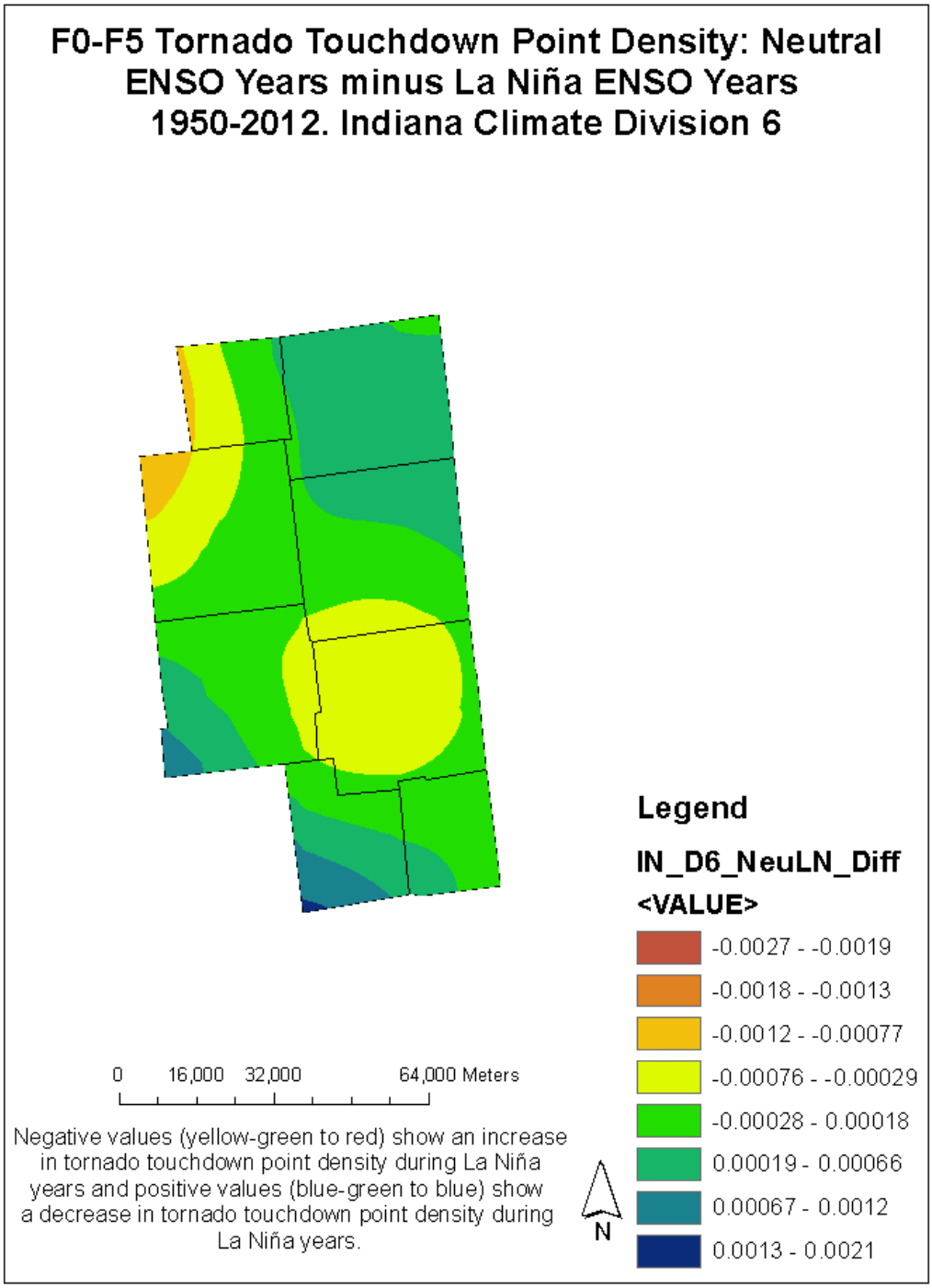
F0-F5 Tornado Touchdown Point Density: Neutral ENSO Years minus La Niña ENSO Years 1950-2012. Indiana Climate Division 6
0
16,000
32,000
64,000 Meters
Negative values (yellow-green to red) show an increase in tornado touchdown point density during La Niña years and positive values (blue-green to blue) show a decrease in tornado touchdown point density during La Niña years.
N
Legend
IN_D6_NeuLN_Diff
<VALUE>
-0.0027 - -0.0019
-0.0018 - -0.0013
-0.0012 - -0.00077
-0.00076 - -0.00029
-0.00028 - 0.00018
0.00019 - 0.00066
0.00067 - 0.0012
0.0013 - 0.0021

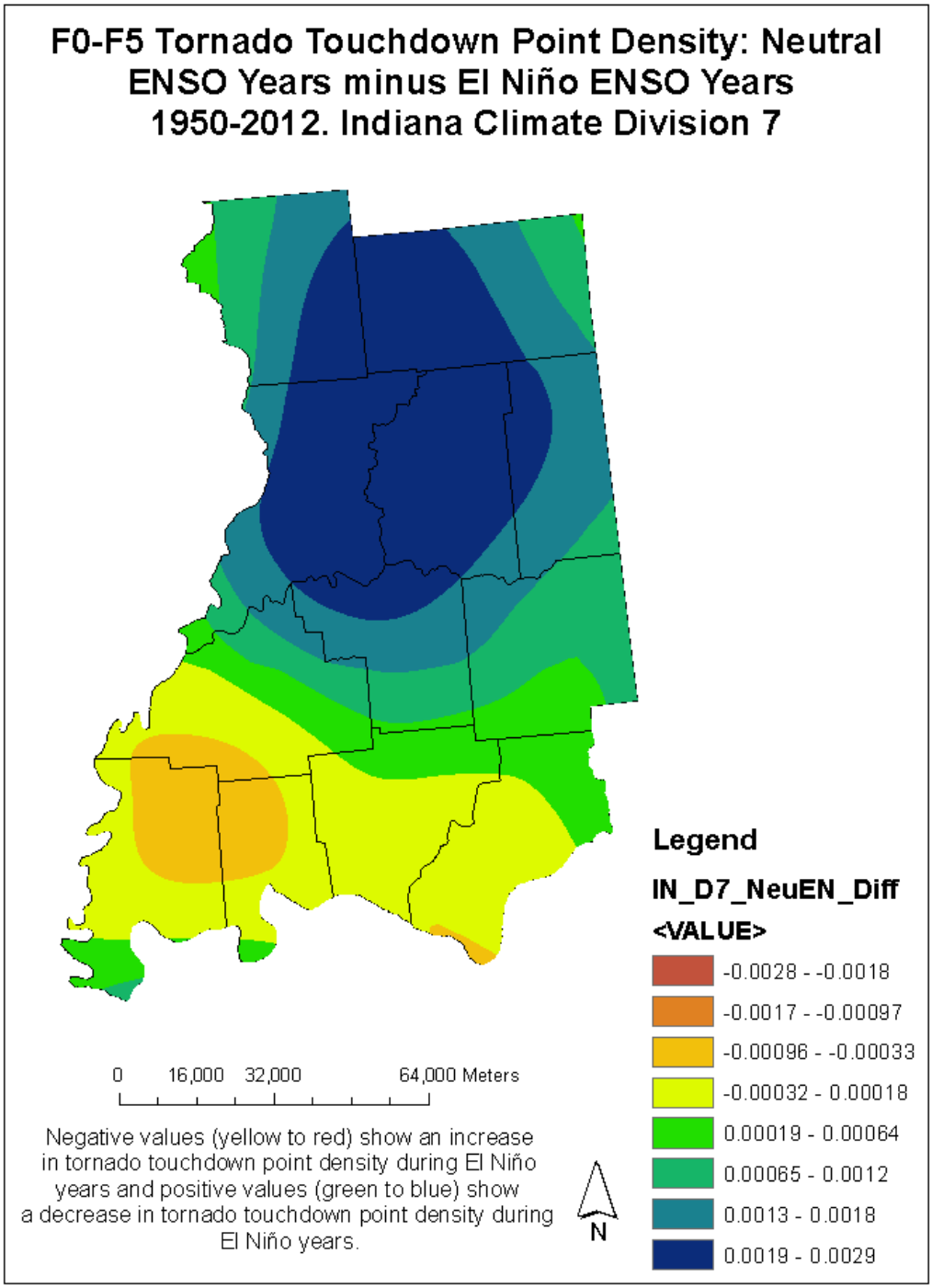
F0-F5 Tornado Touchdown Point Density: Neutral ENSO Years minus El Niño ENSO Years 1950-2012. Indiana Climate Division 7
0
16,000
32,000
64,000 Meters
Negative values (yellow to red) show an increase in tornado touchdown point density during El Niño years and positive values (green to blue) show a decrease in tornado touchdown point density during El Niño years.
N
Legend
IN_D7_NeuEN_Diff
<VALUE>
-0.0028 - -0.0018
-0.0017 - -0.00097
-0.00096 - -0.00033
-0.00032 - 0.00018
0.00019 - 0.00064
0.00065 - 0.0012
0.0013 - 0.0018
0.0019 - 0.0029

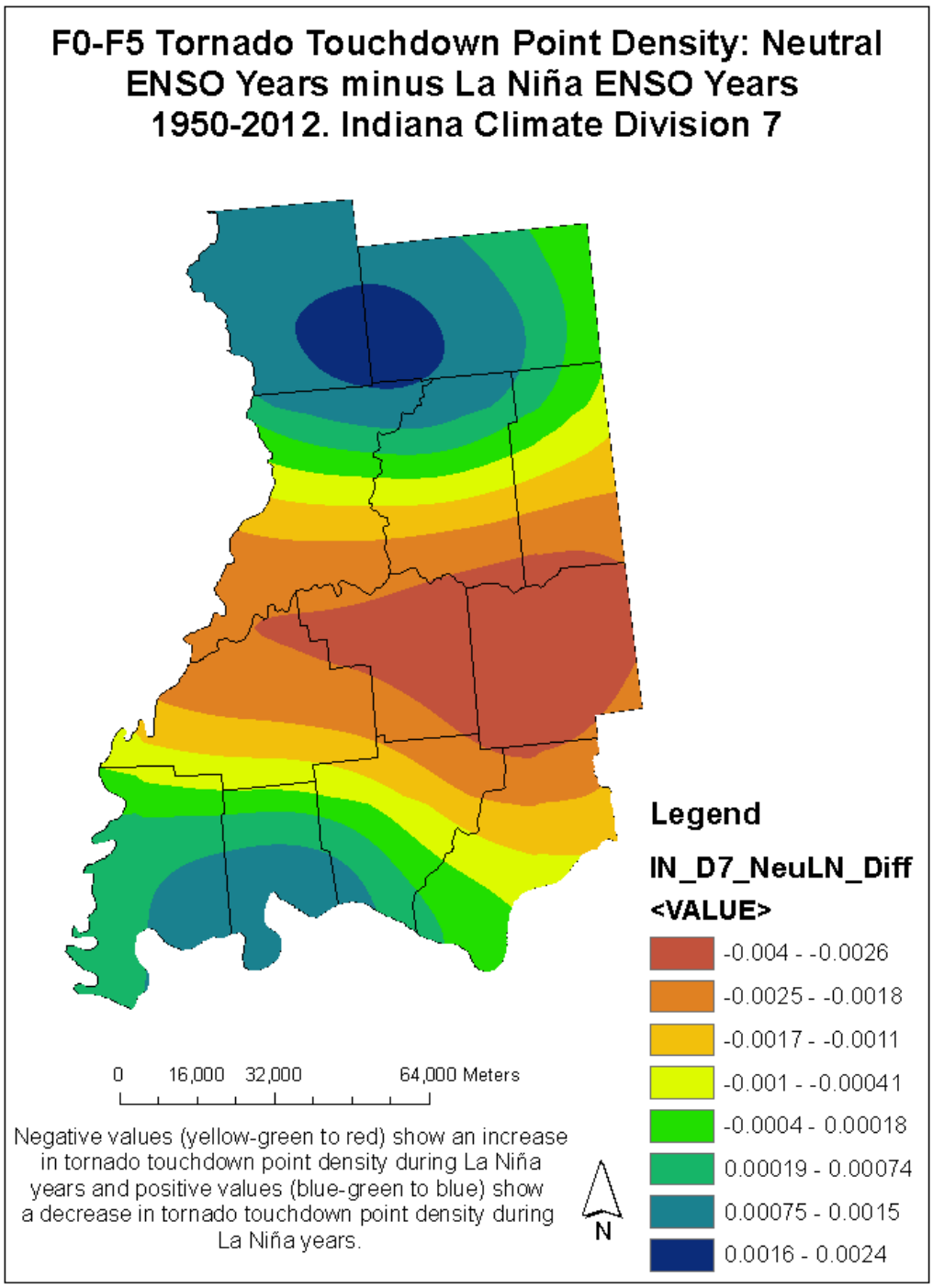
F0-F5 Tornado Touchdown Point Density: Neutral ENSO Years minus La Niña ENSO Years 1950-2012. Indiana Climate Division 7
Legend
IN_D7_NeuLN_Diff
<VALUE>
-0.004 - -0.0026
-0.0025 - -0.0018
-0.0017 - -0.0011
-0.001 - -0.00041
-0.0004 - 0.00018
0.00019 - 0.00074
0.00075 - 0.0015
0.0016 - 0.0024
0 16,000 32,000 64,000 Meters
Negative values (yellow-green to red) show an increase in tornado touchdown point density during La Niña years and positive values (blue-green to blue) show a decrease in tornado touchdown point density during La Niña years.
N

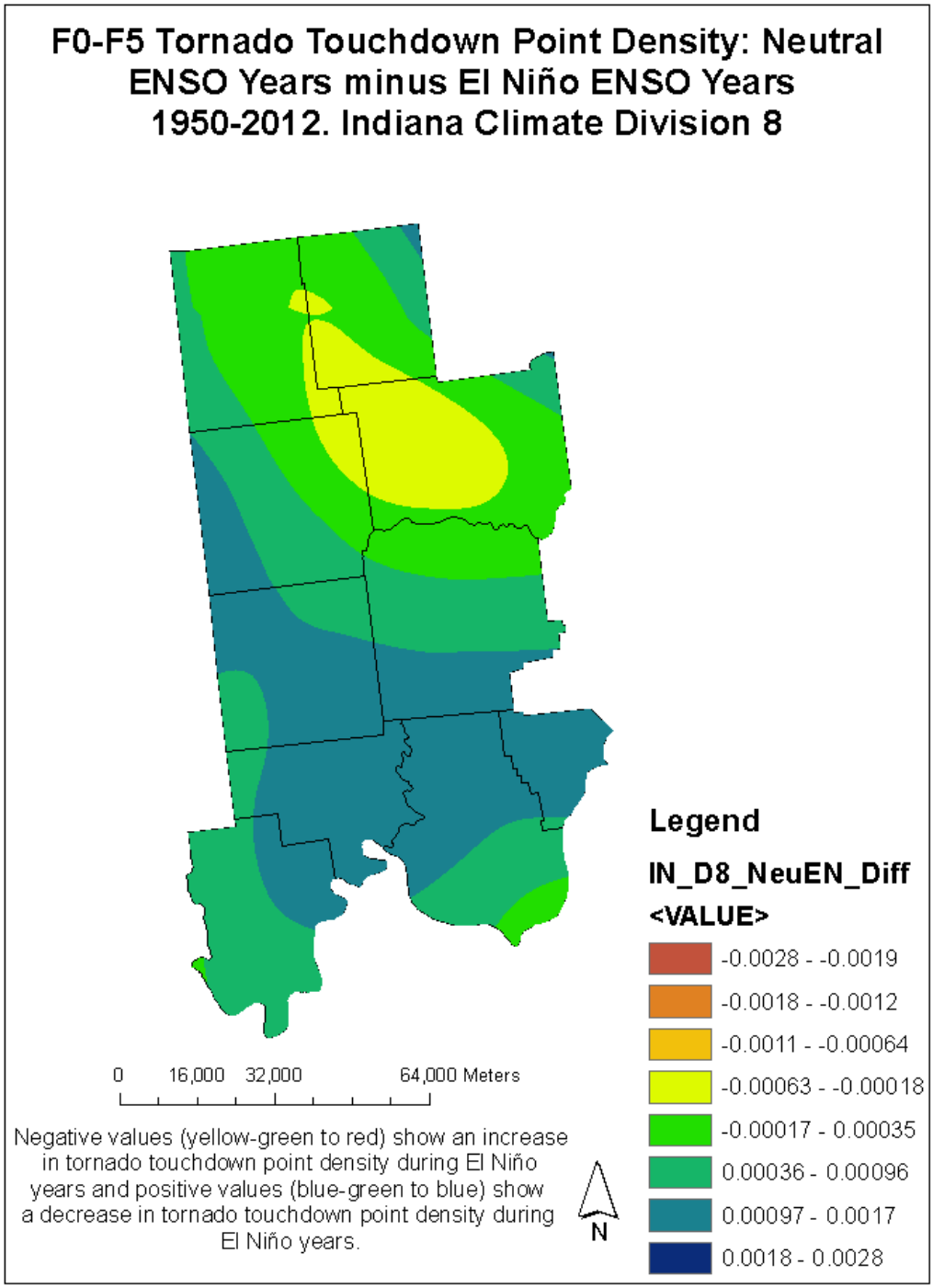
F0-F5 Tornado Touchdown Point Density: Neutral ENSO Years minus El Niño ENSO Years 1950-2012. Indiana Climate Division 8
0
16,000
32,000
64,000 Meters
Negative values (yellow-green to red) show an increase in tornado touchdown point density during El Niño years and positive values (blue-green to blue) show a decrease in tornado touchdown point density during El Niño years.
N
Legend
IN_D8_NeuEN_Diff
<VALUE>
-0.0028 - -0.0019
-0.0018 - -0.0012
-0.0011 - -0.00064
-0.00063 - -0.00018
-0.00017 - 0.00035
0.00036 - 0.00096
0.00097 - 0.0017
0.0018 - 0.0028

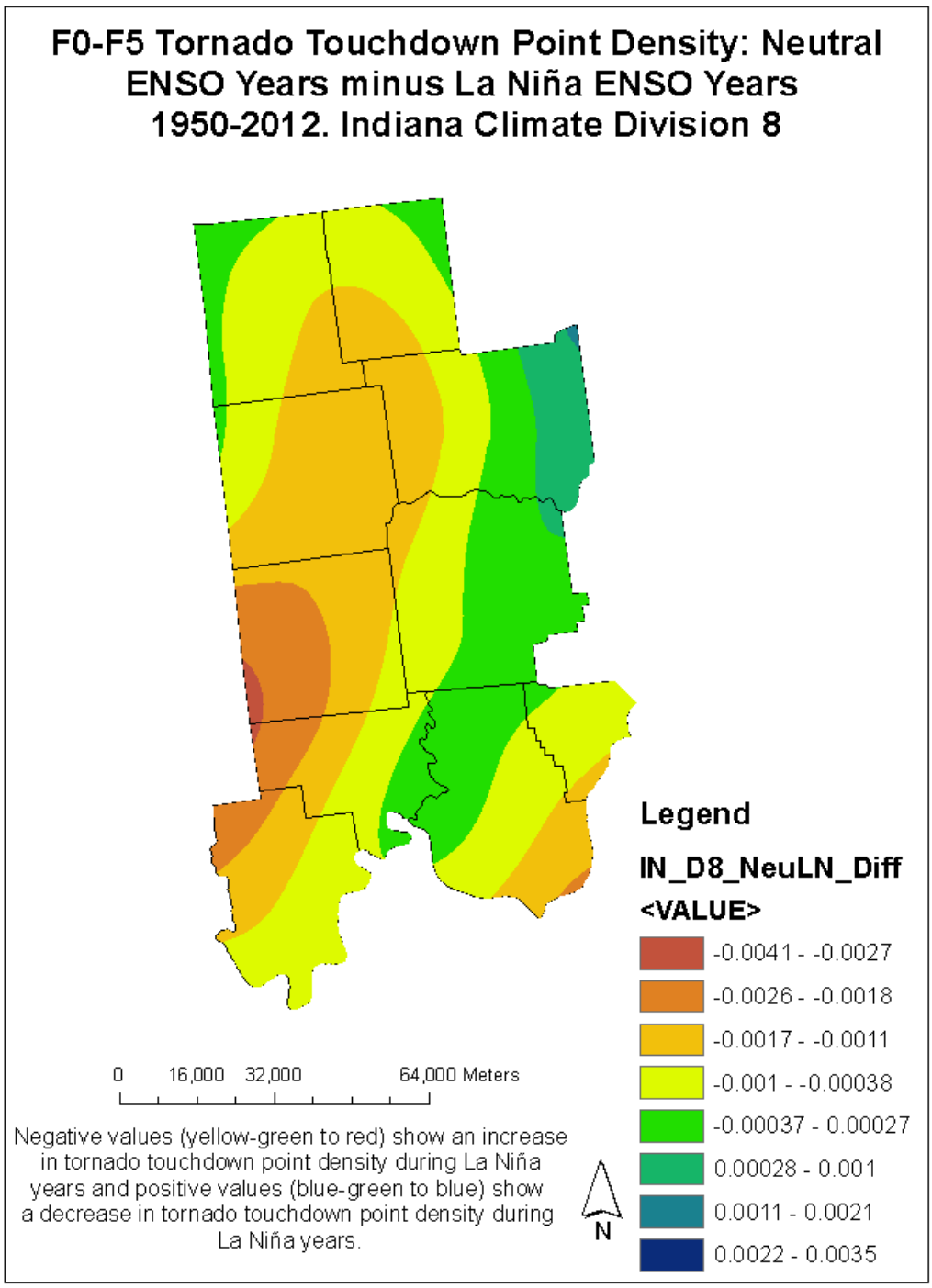
F0-F5 Tornado Touchdown Point Density: Neutral ENSO Years minus La Niña ENSO Years 1950-2012. Indiana Climate Division 8
Legend
IN_D8_NeuLN_Diff
<VALUE>
-0.0041 - -0.0027
-0.0026 - -0.0018
-0.0017 - -0.0011
-0.001 - -0.00038
-0.00037 - 0.00027
0.00028 - 0.001
0.0011 - 0.0021
0.0022 - 0.0035
0
16,000
32,000
64,000 Meters
N
Negative values (yellow-green to red) show an increase in tornado touchdown point density during La Niña years and positive values (blue-green to blue) show a decrease in tornado touchdown point density during La Niña years.

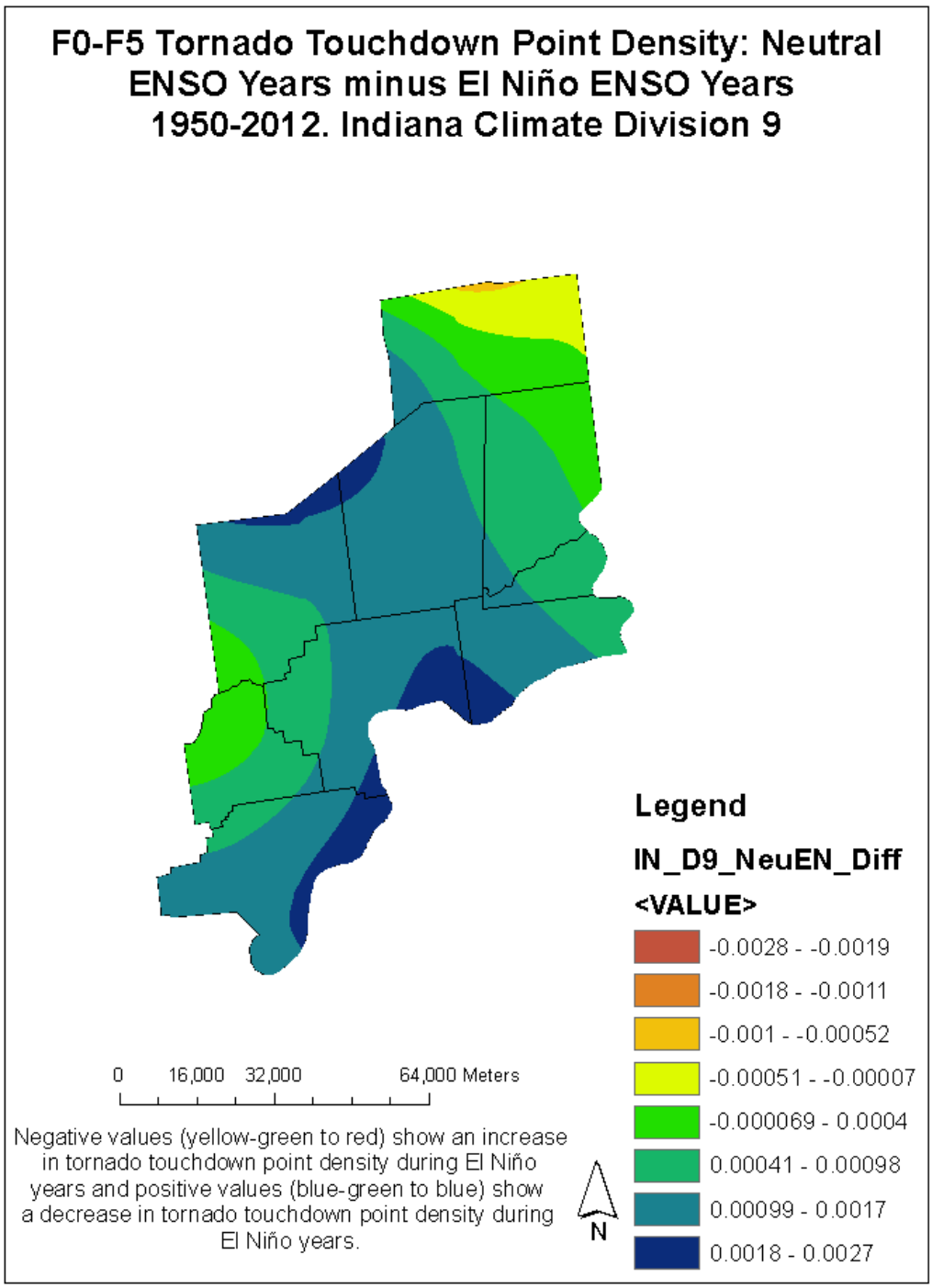
F0-F5 Tornado Touchdown Point Density: Neutral ENSO Years minus El Niño ENSO Years 1950-2012. Indiana Climate Division 9
Legend
IN_D9_NeuEN_Diff
<VALUE>
-0.0028 - -0.0019
-0.0018 - -0.0011
-0.001 - -0.00052
-0.00051 - -0.00007
-0.000069 - 0.0004
0.00041 - 0.00098
0.00099 - 0.0017
0.0018 - 0.0027
0
16,000
32,000
64,000 Meters
N
Negative values (yellow-green to red) show an increase in tornado touchdown point density during El Niño years and positive values (blue-green to blue) show a decrease in tornado touchdown point density during El Niño years.

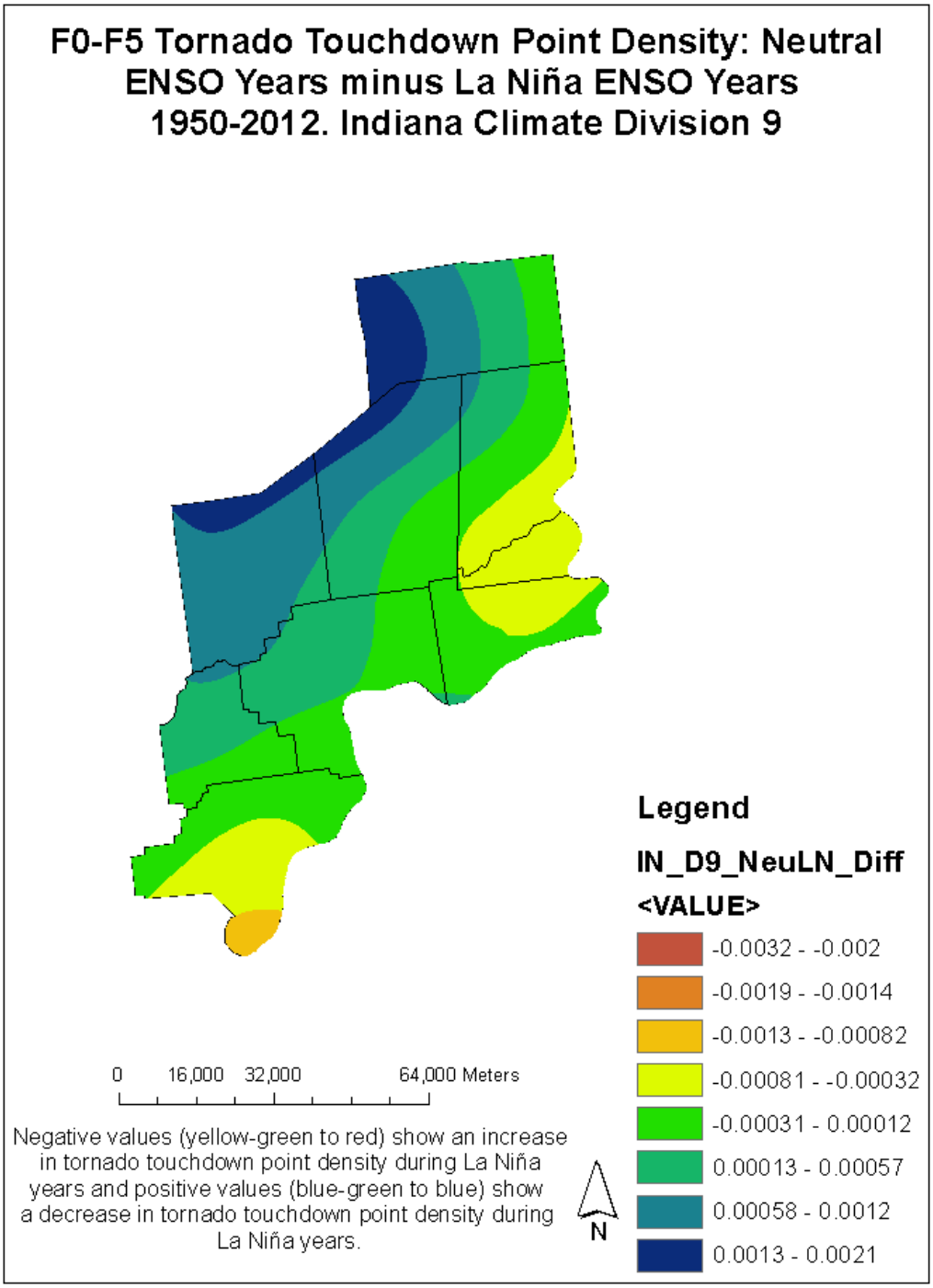
F0-F5 Tornado Touchdown Point Density: Neutral ENSO Years minus La Niña ENSO Years 1950-2012. Indiana Climate Division 9
0
16,000
32,000
64,000 Meters
Negative values (yellow-green to red) show an increase in tornado touchdown point density during La Niña years and positive values (blue-green to blue) show a decrease in tornado touchdown point density during La Niña years.
N
Legend
IN_D9_NeuLN_Diff
<VALUE>
-0.0032 - -0.002
-0.0019 - -0.0014
-0.0013 - -0.00082
-0.00081 - -0.00032
-0.00031 - 0.00012
0.00013 - 0.00057
0.00058 - 0.0012
0.0013 - 0.0021

VITA

VITA

Olivia Kellner
Graduate School, Purdue University

EDUCATION

Purdue University, West Lafayette, IN
Ph.D. Department of Earth, Atmospheric, and Planetary Sciences 2015
Research: Land surface interactions and the feedback to extreme weather and climate, land-surface interactions, hydroclimatology, and applied climatology.
Dissertation: "A Hydroclimatic Assessment across the U.S. Corn Belt across Spatial and Temporal Scales"

Purdue University, West Lafayette, IN
M.S. Department of Earth and Atmospheric Sciences August 2011
Research: Land surface interactions on tropical systems - anomalous soil moisture feedbacks to land-falling tropical systems.
Thesis: "The Role of Anomalous Soil Moisture on the Inland Reintensification of Tropical Storm Erin (2007)"

Ball State University, Muncie, IN
B.S. Geography December 2008
Operational Meteorology and Climatology, Professional Track
GIS Science and Cartography

AWARDS

NASA Earth and Space Science Fellowship 2010 – 2014

AMS Student Member Committee on Applied Climatology 2013 – 2015

NOAA Student Career Experience Program (SCEP) Student 2010 – 2011

Ball State University Presidential Scholarship Recipient 2004 – 2008

James C. Fidler Undergraduate Award for Excellence in Meteorology and Climatology 2006

Hurlburt-Leak Memorial Scholarship/Award 2006

TEACHING EXPERIENCE

Purdue University, West Lafayette, IN 2009-2010

Capstone in Environmental Science for Elementary Education

Teaching Assistant: conducted labs covering environmental education topics such as water quality and pollution, climate change, waste disposal and recycling, topographic map reading, biodiversity, population growth and effects, and fuel/energy source management. Administered grades for lab course, led study and review sessions, and helped to proctor exams.

Community School Corporation of Southern Hancock County 2009

New Palestine, IN

Substitute Teacher: All grade levels, mainly middle and high school math and science courses.

RELATED EXPERIENCE

Midwest Regional Climate Center, Champaign, IL

Climatologist 2014 - Present

American Meteorological Society

Student Member, Committee on Applied Climatology 2013-2015

Indiana State Climate Office, West Lafayette, Indiana

Climate Specialist 2009-2014

Lee and Ryan Environmental Consulting, Inc. Greenfield, Indiana

Staff Scientist April 2012 – August 2012

NOAA National Weather Service, Indianapolis and Milwaukee
SCEP and Meteorologist Intern June 2010 – April 2012
Delaware County Indiana GIS Office, Muncie, Indiana
GIS Technician 2008

PRESENTATIONS

- "*NOAA's National Weather Service: Meteorological Careers and Forecasting Operations*." University of Wisconsin, Milwaukee. February 10th, 2012.
- "*A Change in the Air: View from the State Climatologist on the Past and Upcoming Season."* ADM Grain, Logansport, IN. March 22, 2013.
- "*Beyond Ball State: Careers in the NWS and Graduate School*." Ball State University Department of Geography. April 16th, 2013.
- "*A Change in the Air: View from the State Climatologist on the Past and Upcoming Season*." Tippecanoe County Master Gardener Expo, Tippecanoe County Fairgrounds. April 27, 2013.
- "*Climate Data, Variability, and Change*." Dynamics of Climate Conference, Purdue University. May 16, 2013.
- "*Impacts of Climate Change on Global Agriculture*." Presentation to Syngenta Brazilian groups visiting Purdue University. August 8, 2013.
- "*Dynamics of Climate*". Climate Clinic for Educators. Indiana Dunes National Lakeshore Douglas Center for Environmental Education. November 23, 2013.
- "*White House Event: Roundtable Discussion on Climate Preparedness and Resiliency*" Carmel, IN. December 19th, 2013. Proxy panel member/attendee for Dr. Dev Niyogi. Members David Agnew and Nancy Sutley of President Obama's Task Force on Climate Preparedness and Resiliency were in attendance. Recognition for participation in the event highlighted on Purdue University's Graduate School Facebook and Google+ pages on January 17, 2014. http://on.fb.me/18WdcZU and Google+ http://bit.ly/15jIJb9

- "*Weather and Climate*" presented and taught at Greenfield Middle School, Greenfield, IN February 10th, 2014.
- "*Twister Tracking: Analysis of Weather Events in Indiana*." 2014 Indiana GIS Conference, Indiana Geographic Information Council. May 7-8th, 2014 Sheraton, Keystone at the Crossing, Indianapolis, IN.
- "*Climatological Analysis of ENSO and AO Impacts on Temperature and Precipitation across the U.S. Corn Belt 1980-2010*." AMS 21st Conference on Applied Climatology, Westmintser, CO, June 9-13, 2014.
- "*Dynamics of Climate*" toolkit for the city of Carmel, Indiana. September 27, 2014.
- "*Climate Change and Its Impacts: Past, Present, and Future for Galena, IL*." 27th Roundtable hosted by the Galena, IL Rotary Club. January 14, 2015.
- "*Agro-Climatic Variability and Change across the Midwest: What to Expect in the Future and Tools Available to Adapt."* Litchfield, IL Agronomy Field Day hosted by University of Illinois Extension. February 19, 2015.

GRANTS AND FELLOWSHIPS

- "Useful to Usable: Transforming Climate Variability and Change Information for Cereal Crop Producers." National Institute of Food and Agriculture. Grant NO. 2011-68002-30220. Ph.D. researcher and tool development team member, Objective 1 Team: Crop and Climate Modeler Group. Primary focus on development of the Climate Patterns Viewer tool. 2012-present.
- "Dynamics of Climate: A Toolkit for Informal and Formal Educators." National Science Foundation. NSF Grants GEO-1034821 and DRL 0822181. Toolkit development team and conference planning. 2010-summer 2014.
- NASA Earth and Space Science Fellowship Recipient 2010-2014. Grant NNX10AN70H

PUBLICATIONS

PUBLICATIONS

Kellner, Olivia, and D. Niyogi, 2014: Climate variability and the U.S. Corn Belt: ENSO and AO phase-dependent hydroclimatic feedbacks to corn production at regional and local scales. Accepted April 2015, Earth Interactions.

Niyogi, D., X. Liu, J. Andresen, Y. Song, A. Jain, O. Kellner, E.S. Takle, and O.C. Doering, 2014: Crop models can capture the impacts of climate variability on corn yield. Accepted April 2015, *Geophys. Res. Letters*.

Kellner, Olivia, D. Niyogi, and F.D. Marks, 2015: Land-falling Tropical System Contribution to the hydroclimate of the Eastern U.S. Corn Belt. Wea. and Cli. Extremes, Submitted Feb. 2015.

Kellner, O., 2015: From Too Much to Too Little: How the central U.S. drought of 2012 evolved out of one of the most devastating floods on record in 2011: Section 3.3. Fuchs, B.A., D.A. Wood, and D. Ebbeka (Editors). National Drought Mitigation Center and National Integrated Drought Information System, http://drought.unl.edu/Portals/0/docs/CentralUSDroughtAssessment2012.pdf.

Kellner, Olivia and D. Niyogi, 2014: Assessing Drought Vulnerability in Agricultural Production Systems in the Context of the 2012 Drought. Journal of Animal Science, DOI:10.2527/jas.2013-7496.

Kellner, Olivia, and D. Niyogi, 2014: Land-surface Heterogeneity Signature in Tornado Climatology? An Illustrative Analysis over Indiana 1950-2012. 18.10. Earth Interactions. DOI: 10.1175/2013EI000548.1.

O. Kellner and D. Niyogi, 2014: Agroclimatology. Encyclopedia of Natural Resources: Air. Doi: 10.1081-ENRA-120047622 <http://www.tandfonline.com/doi/full/10.1081/E-ENRA-120047622#.VFKEn_ldXTo>.

O. Kellner, D. Niyogi, M. Lei, A. Kumar, 2011: The Role of Anomalous Soil Moisture on the Inland Reintensification of Tropical Storm Erin (2007), Natural Hazards – Tropical Cyclones of 21st Century Special Issue, DOI: 10.1007/s11069-011-0015-2.

Kishtawal C. M., D. Niyogi, A. Kumar, M. Laureano, O. Kellner, 2011: Observed sensitivity of inland decay of tropical cyclones to soil surface characteristics, Natural Hazards- Tropical Cyclones of 21st Century Special Issue, DOI: 10.1007/s11069-011-0015-2.